AD_____

Award Number: DAMD17-01-1-0411

TITLE: The Role of Nuclear β_{II}-Tubulin in Breast Cancer Cells

PRINCIPAL INVESTIGATOR: Richard F. Luduena, Ph.D.

CONTRACTING ORGANIZATION: The University of Texas
Health Science Center at San Antonio
San Antonio, Texas 78229-3900

REPORT DATE: May 2002

TYPE OF REPORT: Annual

PREPARED FOR: U.S. Army Medical Research and Materiel Command
Fort Detrick, Maryland 21702-5012

DISTRIBUTION STATEMENT: Approved for Public Release;
Distribution Unlimited

REPORT DOCUMENTATION PAGE

Form Approved
OMB No. 074-0188

1. AGENCY USE ONLY (Leave blank)	2. REPORT DATE	3. REPORT TYPE AND DATES COVERED
	May 2002	Annual (23 Apr 01 - 22 Apr 02)

4. TITLE AND SUBTITLE

The Role of Nuclear β_{II}-Tubulin in Breast Cancer Cells

5. FUNDING NUNUMBER
DAMD17-01-1-0411

6. AUTHOR(S)

Richard F. Luduena, Ph.D.

7. PERFORMING ORGANIZATION NAME(S) AND ADDRESS(ES)

The University of Texas
Health Science Center at San Antonio
San Antonio, Texas 78229-3900
email - luduena@uthscsa.edu

8. PERFORMING ORGANIZATION REPORT NUMBER

9. SPONSORING / MONITORING AGENCY NAME(S) AND ADDRESS(ES)

U.S. Army Medical Research and Materiel Command
Fort Detrick, Maryland 21702-5012

10. SPONSORING / MONITORING AGENCY REPORT NUMBER

11. SUPPLEMENTARY NOTES
Report contains color

12a. DISTRIBUTION / AVAILABILITY STATEMENT
Approved for Public Release; Distribution Unlimited

12b. DISTRIBUTION CODE

13. ABSTRACT *(Maximum 200 Words)*

The research is based on our finding that many cancers, including breast cancers, contain the β_{II} isotype of tubulin in their cell nuclei. Our overall goal is to elucidate the function of nuclear β_{II}-tubulin. We have begun by testing the hypothesis that the kinetochores of microtubules have a preferential interaction with β_{II}. We are also exploring alternate hypotheses and defining the tubulin isotypes in breast cancer cells. We have found that these cells contain the β_{I}, β_{II}, β_{III} and β_{IVb} isotypes. The β_{II} isotype is located preferentially in the nucleoli of breast cancer cells. The β_{IVb} isotype which, in other cells, interacts with actin, appears to do so less in breast cancer cells. The β_{I} isotype regulates the actin-tubulin interaction in these cells. The β_{III} isotype appears to protect the microtubules in breast cancer cells from oxidative damage. Breast cancer cells cause nearby normal cells to develop nuclear β_{II}. This latter finding could shed light on the function of nuclear β_{II} and also be useful in the diagnosis of breast cancer. We are currently pursuing these various avenues to elucidate the physiological function of nuclear β_{II} in breast cancer cells.

14. SUBJECT TERMS	15. NUMBER OF PAGES
breast cancer, tubulin isotypes, cell nucleus	248
	16. PRICE CODE

17. SECURITY CLASSIFICATION OF REPORT	18. SECURITY CLASSIFICATION OF THIS PAGE	19. SECURITY CLASSIFICATION OF ABSTRACT	20. LIMITATION OF ABSTRACT
Unclassified	Unclassified	Unclassified	Unlimited

Table of Contents

INTRODUCTION

This research is based on the observation that the β_{II} isotype of tubulin is located in the nuclei of many breast cancer cells. In contrast, it is significantly less abundant in the nuclei of normal cells. Our aim in this research is to understand the functional significance of the nuclear localization of β_{II} in breast cancer cells. We are exploring this question by testing hypotheses, one of which is that β_{II} has a specific interaction with the kinetochores and facilitates the binding of spindle microtubules to these structures. We are also approaching this issue by putting the β_{II} isotype of tubulin in a larger context, namely, examining the functional roles of the other tubulin isotypes, analyzing the sub-nuclear distribution of β_{II}, and determining the occurrence of nuclear β_{II} in a variety of cancers.

BODY

Task 1. Immunohistochemical analysis of tubulin isotypes in the mitotic spindle of breast cancer cells.

The aim of this task is to localize the different isotypes in the mitotic spindle of breast cancer cells. We have decided to begin this task by using RT-PCR to measure the expression of the different beta isotypes in MCF-7 breast cancer cells. We used primers specific for the β_I, β_{II}, β_{III}, β_{IVa}, and β_{IVb} isotypes. We found that all of these isotypes, except for β_{IVa}, are expressed in breast cancer cells (Figure 1). The overall thrust of the proposed research is to elucidate the function of nuclear β_{II} in breast cancer cells. It is clear that it must function in a context that includes the β_I, β_{III} and β_{IVb} isotypes. That conclusion plays a role in framing the rest of this research.

Task 2. Development of method of purifying kinetochores from breast cancer and normal cells.

We have been following various procedures for chromosomes from MCF-7 breast cancer cells. This took considerably longer than anticipated, but we appear to have finally accomplished this. We have adapted the procedure of Wordeman et al. (1). The purified chromosomes are now beginning to be used for the experiments for Tasks 3 and 4.

Task 3. Immunohistochemical analysis of tubulin associated with kinetochores.

We have begun by treating the purified chromosomes with antibodies specific for the different isotypes and then examining them by immunofluorescence microscopy. Our preliminary results suggest that the tubulin that is most likely to bind to kinetochores is β_{III}. This is actually in contradiction with the hypothesis underlying Tasks 3-6. We intend to pursue diligently the experiments in Tasks 3 and 4 and undertake some rigorous testing of the hypothesis. Nevertheless, our preliminary results raise the possibility that our hypothesis may require alteration. Consequently, we are also doing some experiments to collect data that would allow us to refine the underlying hypothesis or even to frame alternative hypotheses. We are using three different approaches to attain this end.

The first approach is to re-examine more carefully the intra-nuclear localization of β_{II} in breast cancer cells. We had earlier stated that nuclear β_{II} was concentrated in the nucleoli of rat kidney mesangial cells and MCF-7 breast cancer cells, but this was based on the morphology of the nuclear staining and not on rigorous co-localization experiments. This has now been remedied. Using two kinds of breast cancer cells, MCF-7 and MDA-MB-435, we have shown that β_{II} co-localizes with both RNA and nucleolin (2,3). RNA is concentrated in nucleoli and nucleolin is a nucleolar-specific antigen. Thus, the concentration of nuclear β_{II} in the nucleoli has now been rigorously demonstrated.

The second approach is to examine the roles of the other isotypes in MCF-7 cells, specifically, the β_I, β_{III} and β_{IVb} isotypes. This has led to some very clear results that are described below:

1. β_{IVb}. We have previously reported that β_{IV} is involved in interactions with actin filaments. We have seen this very clearly in cultured rat kidney mesangial cells (4) and also in A10 smooth muscle cells. When we investigated this in MCF-7 breast cancer cells, we found that there was relatively little overlap between actin and β_{IV} in interphase cells although there was considerable overlap in the mitotic spindle (Figure 2). There was little overlap between actin and β_{II} (Figure 3). This suggests that the tight coordination between actin and microtubules, mediated by β_{IV}, present in other cell types, might be diminished in breast cancer cells. This may be a fruitful avenue of exploration in the future.

2. β_I. We have previously reported that transfection of β_I into MDCK cells inhibits cell adhesion as a result of blocking the actin-microtubule interaction (5). We have now transfected the β_I isotype into MCF-7 breast cancer cells and measured adhesion, using mock-transfected cells as a control. In each case, β_I transfection inhibits adhesion by up to 76% (Figure 4). We previously hypothesized that β_I works by inhibiting the β_{IV}-actin interaction. Since MCF-7 cells have relatively little of this interaction, our results raise the possibility that β_I has a direct effect on adhesion, that need not involve β_{IV} or perhaps even microtubules. We also examined the effect of combretastatin A-4 phosphate on the β_I effect. We previously observed, using endothelial cells, that β_I is considerably more sensitive to this drug than is β_{IV}. As one would predict, combretastatin A-4- phospahte partially blocks the inhibition of adhesion due to β_I transfection (Figure 5).

3. β_{III}. This isotype lacks the cysteine residue at position 239 that is present in the other β isotypes. This particular residue is very easily oxidized and, when it is oxidized, microtubule assembly is blocked (6,7). β_{III} differs from the other isotypes in that it has a very narrow distribution (8). It is particularly concentrated in neurons (8). Interestingly, it is also found in many tumor cells. We have hypothesized that its role in tumors may be to protect microtubule assembly inhibition from oxidizing agents. To see if this is a reasonable hypothesis, we measured the levels of free radicals in three different cell lines: A10 smooth muscle cells, that do not express β_{III}, MDA-MB-435 breast cancer cells that have low levels of β_{III} and BT5492 breast cancer cells, that have very high levels of β_{III} and, incidentally, are resistant to a variety of anti-mitotic drugs. As a probe, we used 2,7-dichlorofluorescein diacetate, that fluoresces in the presence of H_2O_2; although H_2O_2 is not itself a free radical, it is highly reactive and is also produced from the superoxide free radical by the action of superoxide dismutase (9). The results show clearly that the levels of free radicals are higher in cells that are also rich in β_{III} (Figure 6). It may be that breast cancer cells express β_{III} in order to protect their microtubules from free radicals. It is also conceivable that these cells place β_{II} in the nucleus to protect it from oxidation.

Our third approach is to widen our search for nuclear β_{II} in cancer excisions from actual patients. Using the immunoperoxidase staining procedure, we have examined a total of 204 excisions from patients and have found β_{II} in the nuclei of 74% of them. In general, nuclear β_{II} is more common in tumors of epithelial origin. About 86% of breast tumors have nuclear β_{II}. This is in contrast to colon tumors, where 100% have nuclear β_{II}, and to lymphomas, where none have nuclear β_{II}. Perhaps one of the most striking findings that we have made is that, in breast cancer metastases, the metastatic cancer cells influence the nearby lymphocytes to produce nuclear β_{II} (Figure 7). This implies the existence of a factor produced by the cancer cells that affects the nearby cells. We are considering using a microarray approach to identify the pathways involved in localizing β_{II} to the nuclei; it is likely that an understanding of this localization mechanism would also explain the function of nuclear β_{II}.

The following tasks were originally planned to be undertaken in the last two years. They have not yet been commenced.

Task 4. Measurement of tubulin isotype binding to kinetochores.

Task 5. Measurement of ability of chromosomes to nucleate assembly of tubulin isotypes.

Task 6. Determination of the ability of chromosomes to capture microtubules made of isotypically purified tubulin.

Task 7. To determine the effect of inhibitors of tyrosine kinase on nuclear localization of tubulin.

KEY RESEARCH ACCOMPLISHMENTS

- The β-tubulin isotypes that are expressed in MCF-7 breast cancer cells are β_I, β_{II}, β_{III}, and β_{IVb},
- In MCF-7 breast cancer cells and MDA-MB-435 breast cancer cells, β_{II} is specifically concentrated in the nucleoli as shown by co-localization with RNA and a nucleolar antigen.
- The β_{IV} isotype does not interact with actin filaments as strongly in MCF-7 breast cancer cells as it does in other cell types.
- β_I transfection into MCF-7 breast cancer cells inhibits cell adhesion.
- β_{III} expression in breast cancer cells may be correlated with free radical levels in the cells.
- 74% of cancers have nuclear β_{II}; 86% of breast cancers have nuclear β_{II}.
- Breast cancer cells stimulate nearby, otherwise normal, cells to generate nuclear β_{II}.

REPORTABLE OUTCOMES

1. Manuscripts, abstracts, presentations, degrees obtained:

Manuscripts:

Walss-Bass, C., Xu, K., David, S., Fellous, A. and Ludueña, R.F. (2002) Occurrence of nuclear β_{II}-tubulin in cultured cells. *Cell and Tissue Research*, in press **(Appendix 1)**.

Xu, K. and Ludueña, R.F. (2002) Characterization of nuclear β_{II}-tubulin in tumor cells: a possible novel target for taxol. *Cell Motility and the Cytoskeleton*, in press **(Appendix 2)**.

Woo, K., Jensen-Smith, H.C., Ludueña, R.F. and Hallworth, R. Differential expression of β tubulin isotypes in gerbil nasal epithelia. *Cell and Tissue Research*, in press **(Appendix 3)**.

Khan, I.A. and Ludueña, R.F. Different effects of vinblastine on the polymerization of isotypically purified tubulins from bovine brain. *Investigational New Drugs*, submitted for publication **(Appendix 4)**.

Walss-Bass, C., Kreisberg, J.I. and Ludueña, R.F. Effect of the anti-tumor drug vinblastine on nuclear β_{II}-tubulin cultured rat kidney mesangial cells. *Investigational New Drugs*, submitted for publication **(Appendix 5)**.

Perry, B., Jensen-Smith, H.C., Ludueña, R.F. and Hallworth, R. Differential expression of β tubulin isotypes in gerbil vestibular end organs. *Journal of the Association for Research in Otorhinolaryngology*, submitted for publication **(Appendix 6)**.

Yeh, I.-T. and Ludueña, R.F. The β_{II} isotype of tubulin is present in the cell nuclei of a variety of cancers. To be submitted **(Appendix 7)**.

Abstracts (Appendix 8):

Chaudhuri, A.R., Natarajan, M., Herman, T.S. and Thomas, C.R. (2001) Ionizing radiation generates drug resistance to tubulin-directed antiproliferative agents in MCF-7 human adenocarcinoma breast cancer cells. Submitted to American Society for Therapeutic Radiology and Oncology.

Woo, K., Ludueña, R.F. and Hallworth, R. (2001) Localization of β-tubulin isotypes in nasal epithelia. *Association for Research in Otorhinolaryngology*, p. 17.

Perry, B., Ludueña, R.F. and Hallworth, R. (2001) Localization of β-tubulin isotypes in vestibular tissues. *Association for Research in Otorhinolaryngology*, p. 17.

Ludueña, R.F., Perez, G.T. and Yeh, I-T. (2001) Occurrence of the β_{II} isotype of tubulin in the nuclei of cancer cells. *Mol. Biol. Cell* **12**, 430a.

Xu, K. and Ludueña, R.F. (2001) Nuclear β_{II}-tubulin in cultured cancer cells: subnuclear localization and the effects of anti-tubulin drugs. *Mol. Biol. Cell* **12**, 431a.

Chaudhuri, A.R., Schwarz, P.M., Carrizales, G.R., Mooberry, S.L. and Luduena, R.F. (2001) Elevated βIII tubulin in cancer and drug-resistant cells and selective conformational effect of phomopsin A on the αβIII tubulin dimer. *Mol. Biol. Cell* **12**, 431a.

Prasad, V., Kasinath, V., Clements, R.B., Leal, R., Mooberry, S.L. and Luduena, R.F. (2001) Interaction of actin and the βIV isotype of tubulin in normal and transformed cells. *Mol. Biol. Cell* **12**, 431a.

Presentations:

Chaudhuri, A.R., Natarajan, M., Herman, T.S. and Thomas, C.R. Ionizing radiation generates drug resistance to tubulin-directed antiproliferative agents in MCF-7 human adenocarcinoma breast cancer cells. *American Society for Therapeutic Radiology and Oncology*, San Francisco, November 4-8, 2001. (poster).

Ludueña, R.F., Perez, G.T. and Yeh, I-T. Occurrence of the β_{II} isotype of tubulin in the nuclei of cancer cells. *American Society for Cell Biology*, Washington, DC, December 8-12, 2001. (poster)

Xu, K. and Ludueña, R.F. Nuclear β_{II}-tubulin in cultured cancer cells: subnuclear localization and the effects of anti-tubulin drugs. *American Society for Cell Biology*, Washington, DC, December 8-12, 2001. (poster)

Chaudhuri, A.R., Schwarz, P.M., Carrizales, G.R., Mooberry, S.L. and Luduena, R.F. Elevated βIII tubulin in cancer and drug-resistant cells and selective conformational effect of phomopsin A on the αβIII tubulin dimer. *American Society for Cell Biology*, Washington, DC, December 8-12, 2001. (poster)

Prasad, V., Kasinath, V., Clements, R.B., Leal, R., Mooberry, S.L. and Luduena, R.F. Interaction of actin and the βIV isotype of tubulin in normal and transformed cells. *American Society for Cell Biology*, Washington, DC, December 8-12, 2001. (poster)

Ludueña, R.F. Occurrence of the β_{II} isotype of tubulin in the nuclei of cancer cells. *Second Iberoamerican Forum on Cytoskeleton*, Valdivia, Chile, January 21-24,

2002 (symposium talk).

Degrees Obtained:

Keliang Xu, Investigations of Nuclear β_{II}-Tubulin in Tumor Cells. M.S. Thesis, defended in July, 2001. Degree awarded May 23, 2002. Mentor: Richard F. Ludueña, Ph.D.

2. Funding Applied for Based on Work Supported by this Award

Applied for and Funded:

Title: The Role of the β_{II} Isotype of Tubulin in the Diagnosis and Development of Prostate Cancer
Funding Agency: US Army Prostate Cancer Research Program
PI: Richard F. Ludueña
Dates: November 1, 2001-October 31, 2004 **Amount of Funding**: $199,215

Title: The Cysteine Residues of Tubulin Isotypes
Funding Agency: Welch Foundation
PI: Richard F. Ludueña
Dates: June 1, 2002-May 31, 2005 **Amount of Funding**: $165,000

Title: Epothilones and Tubulin Isotypes
Funding Agency: Schering AG, Berlin, Germany
PI: Richard F. Ludueña
Dates: July 1, 2001-June 30, 2002 **Amount of Funding**: $64,834

Applied for and Not Funded:

Title: What are the Physiological Roles of the Tubulin Isotypes?
Funding Agency: Texas Advanced Research Program
PI: Richard F. Ludueña
Dates: January 1, 2002-December 31, 2002 **Amount of Funding:** $300,000

Pending:

Title: The Multiple Forms of Tubulin: What are Their Functions?
Funding Agency: National Institutes of Health
PI: Richard F. Ludueña **Dates:** April 1, 2003-March 31, 2008
Amount of Funding: $1,000,000 (direct costs)

3. Personnel Receiving Salary from this Grant:

Richard F. Ludueña, Ph.D., Professor, Principal Investigator
Veena Prasad, Senior Research Associate
Asish R. Chaudhuri, Ph.D., Research Instructor
Mohua Banerjee, Research Assistant
Patricia Schwarz, Senior Research Associate
Phyllis Trcka Smith, Senior Research Assistant

CONCLUSIONS

We have found that, in addition to β_{II}, MCF-7 breast cancer cells also express the β_I, β_{III}, and β_{IVb} isotypes of tubulin. The β_{II} isotype is particularly concentrated in the nucleoli of these cells. Nuclear β_{II} is found in 74% of all cancers examined, and in 86% of breast cancers. The β_{IV} isotype, that normally interacts with actin filaments in other cells, does not appear to do so to the same extent in MCF-7 cells. The β_I isotype appears to inhibit actin-microtubule interactions in these cells, however. β_{III} expression in breast cancer cells may be correlated with free radical levels in these cells and may be involved in protecting the microtubules from oxidizing reagents. We have also found that breast cancer cells stimulate nearby, otherwise normal, cells to generate nuclear β_{II}.

Our results have some potential implications with respect to cancers. First, the differences we have observed between normal and cancerous cells (less β_{IV}-actin interaction in cancer cells, nuclear localization of β_{II} in cancer cells) open new avenues to better understanding of the unique biology of cancer cells that could in turn allow the development of novel therapeutic modalities. Second, the possible role played by the β_{III} isotype in protecting the microtubules of cancer cells from oxidation highlights the importance of designing a β_{III}-specific drug as an anti-tumor agent. Third, the finding that cancer cells can stimulate otherwise normal nearby cells to generate nuclear β_{II} has great implications for cancer diagnosis. For example, a biopsy might miss the cancer itself, but if it detects these alterations in adjacent cells, it may detect the cancer indirectly.

REFERENCES

1. Wordeman L, Steuer ER, Shetz MP & Mitchison T (1991) Chemical subdomains within the kinetochore domain of isolated CHO mitotic chromosomes. *J. Cell Biol.* **114**, 285-294.
2. Walss-Bass C, Xu K, David S, Fellous A & Ludueña RF (2002) Occurrence of nuclear β_{II}-tubulin in cultured cells. *Cell and Tissue Research*, in press.
3. Xu K & Ludueña RF (2002) Characterization of nuclear β_{II}-tubulin in tumor cells: a possible novel target for taxol. *Cell Motility and the Cytoskeleton*, in press
4. Walss-Bass C, Prasad V, Kreisberg JI & Ludueña RF (2001) Interaction of the β_{IV}-tubulin isotype with actin stress fibers in cultured rat kidney mesangial cells. *Cell Motil. Cytoskeleton* **49**, 200-207.
5. Lezama R, Castillo A, Ludueña RF & Meza I (2001) Over-expression of βI tubulin in MDCK cells and incorporation of exogenous βI tubulin into microtubules interferes with adhesion and spreading. *Cell Motil. Cytoskeleton* **50**, 147-160.
6. Ludueña RF, Roach MC, Trcka PP, Little M, Palanivelu P, Binkley P & Prasad V (1982) β_2-tubulin, a form of chordate brain tubulin with lesser reactivity toward an assembly-inhibiting sulfhydryl-directed cross-linking reagent. *Biochemistry* **21**, 4787-4794.
7. Bai RL, Lin CM, Nguyen NY, Liu TY & Hamel E (1989) Identification of the cysteine residue of beta-tubulin affected by the antimitotic agent 2,4-dichlorobenzyl thiocyanate, facilitated by separation of the protein subunits of tubulin by hydrophobic column chromatography. *Biochemistry* **28**, 5606-5612.
8. Ludueña RF (1998) The multiple forms of tubulin: different gene products and covalent modifications. *Int. Rev. Cytol.* **178**, 207-275.
9. LeBel CP, Ischiropoulos H & Bondy SC (1992) Evaluation of the probe 2',7'-dichlorofluorescin as an indicator of reactive oxygen species formation and oxidative stress. *Chem. Res. Toxicol.* **5**, 227-231.

Appendix 1

Occurrence of Nuclear β_{II}-Tubulin in Cultured Cells[1]

Consuelo Walss-Bass[a], Keliang Xu[a], Sebastien David[b], Arlette Fellous[b] and Richard F. Ludueña[a,2]

[a]*Department of Biochemistry, University of Texas Health Science Center, San Antonio, Texas 78284, USA.*

[b]*Laboratoire de Pharmacologie Experimentale et Clinique, 27 Rue Juliette Dodu, 75010 Paris, France.*

Key words: tubulin, nuclear tubulin, tubulin isotypes, cell proliferation, immunofluorescence

Footnotes:

[1]This research has been supported by grants CA26376 from the National Institutes of Health, AQ-0726 from the Welch Foundation, and DAMD17-98-1-8246 and DAMD17-01-1-0411 from the U.S. Army Breast Cancer Research Program to R.F.L. as well as by grant P30 CA54174 from the National Cancer Institute to the San Antonio Cancer Institute.

[2]Send correspondence to: Dr. Richard F. Ludueña, Department of Biochemistry, University of Texas Health Science Center San Antonio, Texas 78284-7760. Tel: 210-5673732, FAX: 210-5676595; e-mail: luduena@uthscsa.edu

In Press: Cell and Tissue Research

[3]The abbreviations used are: PBS, phosphate-buffered NaCl solution; DAPI, 4',6-diamidino-2-phenylindole, dihydrochloride; LNCaP, lymph node carcinoma of the prostate; EGTA, ethyleneglycol-bis-(β-aminoethylether)*N,N,N,N'*-tetraacetic acid; PIPES, piperazine-*N,N'*-bis(2-ethanesulfonic acid); PMSF, phenylmethyl sulfonyl fluoride; PDGF, platelet-derived growth factor; IL-1, interleukin-1.

ABSTRACT

Microtubules are cylindrical organelles that play critical roles in cell division. Their subunit protein, tubulin, is a target for various anti-tumor drugs. Tubulin exists as various forms, known as isotypes. In most normal cells, tubulin occurs only in the cytosol and not in the nucleus. However, we have recently reported the finding of the β_{II} isotype of tubulin in the nuclei of cultured rat kidney mesangial cells (Walss, C., Kreisberg, J.I. and Ludueña, R.F. Cell Motil. Cytoskeleton. *42*: 274-284, 1999). Mesangial cells, unlike most normal cell lines, have the ability to proliferate rapidly in culture. In efforts to determine if nuclear β_{II}-tubulin occurred in other cell lines, we examined the distribution of the β_I, β_{II} and β_{IV} mammalian tubulin isotypes in a variety of normal and cancer human cell lines by immunofluorescence microscopy. We have found that, in the normal cell lines, all three isotypes are present only in the cytoplasm. However, the β_{II} isotype of tubulin is located, not only in the cytoplasm, but also in the nuclei of the following cell lines: LNCaP prostate carcinoma, MCF-7, MDA and Calc18 breast carcinoma, C6 and T98G glioma, and HeLa cells. In contrast, the β_I and β_{IV}-isotypes, which are also synthesized in cancer cells, are not localized to the nucleus but are restricted to the cytoplasm. We have also seen β_{II} in breast cancer excisions. In most of these cells, β_{II} appears to be concentrated in the nucleoli. These results suggest that transformation may lead to localization of β_{II}-tubulin in cell nuclei, serving an as yet unknown function, and that nuclear β_{II} may be a useful marker for detection of tumor cells.

INTRODUCTION

A fundamental fact about cancer is that cancer cells are our own cells misbehaving. They are not really alien cells. Most anti-cancer drugs target cell division, a process that is faster in cancer cells than in most normal cells. The problem, however, is that certain normal cells, such as those of the bone marrow, also divide fairly rapidly. Hence, the agents of chemotherapy have serious side effects, which limit their use. Therefore, the challenge for cancer chemotherapy is to find a drug that attacks cancer cells but not normal cells.

Microtubules, made of the protein tubulin, are organelles that play a critical role in mitosis; they attach to chromosomes as they line up in metaphase and help move them into the daughter cells (Hyams and Lloyd 1994). For this reason, the protein tubulin is a major target for anti-tumor drugs such as vinblastine and taxol (Wilson and Jordan 1994). Nevertheless, these drugs do not discriminate between normal and cancer cells, both of which contain tubulin, and therefore have serious side effects and limitations.

The tubulin protein is made of two subunits, α and β (Hyams and Lloyd 1994). These subunits exist as numerous isotypes, which differ in their tissue and subcellular localization, as well as in their interaction with anti-tumor drugs (Ludueña 1998). We have previously found that the β_{II} isotype of tubulin is present in the nuclei of rat kidney mesangial cells (Walss et al. 1999). In order to determine whether this finding was an isolated incident, or occurred in other cell types, we have now examined the intracellular distribution of the vertebrate β-tubulin isotypes β_I, β_{II} and β_{IV} in several cultured human cell lines, both normal and cancerous. We have found that the β_{II}-isotype of tubulin is present in the nuclei of all the cancer cells investigated, but is absent from the nuclei of

most of the normal cells. In the nuclei β_{II} is particularly concentrated in the nucleoli. These results suggest that transformation may lead to localization of β_{II} in cell nuclei, serving an as yet unknown function. Furthermore, nuclear β_{II} may be a useful marker for detection of tumor cells and may serve as a target for anti-tumor drugs, such as taxol and vinblastine, to selectively attack cancer cells. Despite the fact that microtubules are generally considered to be purely cytoplasmic organelles, there have been a few previous reports of tubulin in the nucleus (Menko and Tan 1980; Armbruster et al. 1983; Ranganathan et al. 1997), although no function has been proposed for such tubulin. Our results raise the possibility that nuclear tubulin may lend itself to proliferation or transformation.

MATERIALS AND METHODS

Source of cells and antibodies. The HDF human dermal fibroblasts were a kind gift from Dr. Eugene Sprague (University of Texas Health Science Center at San Antonio (UTHSCSA), San Antonio, TX). The 506 smooth muscle cells from human colon and the HSK fibroblasts from baby foreskin were a kind gift from Dr. Mary Pat Moyer. (UTHSCSA). The osteoblasts were a kind gift from Dr. John Lee (UTHSCSA). The MCF-10F breast epithelial cells, the LNCaP prostate carcinoma cells, as well as the MCF-7, and MDA breast carcinoma cells were a kind gift from Dr. Nandini Chaudhuri (UTHSCSA). The Calc 18 breast carcinoma cell line was a kind gift from Dr. Jean-François Riou, Rhône-Poulenc, Paris, France. MDA cells used in confocal microscopy experiments were a kind gift from Dr. Susan Mooberry, Southwest Foundation for Biomedical Research, who also gave us the HeLa cells. C6 and T98G glioma cells were kindly provided to us by Dr. Martin Adamo of the Department of Biochemistry, University of Texas Health Science Center, San Antonio, TX. Fluorescein-colchicine, fluorescein and acridine orange were from Molecular Probes, Eugene, OR.

Excisions of mammary adenocarcinomas were provided by the Department of Anapathology, Hôpital St. Louis, Paris, France.

The monoclonal antibodies SAP.4G5, JDR.3B8, and ONS.1A6 specific, respectively, for the β_I, β_{II}, and β_{IV} isotypes of tubulin were prepared as previously described (Banerjee et al. 1988, 1992; Roach et al. 1998).

Immunofluorescence microscopy. All cells were grown to near confluency on glass coverslips at 37 °C and 5% CO_2. Cells were then washed twice with PBS[3] (0.15M NaCl, 0.0027 M KCl, 0.00147M KH_2PO_4, 0.01M $NaHPO_4$, pH 7.2), fixed for 15 min

with 3.7 % paraformaldehyde at room temperature and permeabilized for 1 min with 0.5% Triton X-100 in PBS. Cells were then incubated at 4 °C overnight with the respective isotype-specific monoclonal IgG mouse antibody (anti-β_I, 0.05 mg/ml; anti-β_{II}, 0.03 mg/ml; anti-β_{IV}, 0.08) diluted in PBS containing 10% normal goat serum (Jackson Immunoresearch, West Grove, PA). Cells were rinsed in PBS and labeled with Cy3-conjugated goat anti-mouse antibody (1:100, Jackson Immunoresearch) for 1 hr at room temperature. Cells were then rinsed three times with PBS. For DNA detection, cells were stained with DAPI[3], (Molecular Probes, Eugene OR.), (2 µl/ml in PBS) during the last wash with PBS after incubation with the secondary antibody. Coverslips were mounted on glass slides and examined with a Zeiss epifluorescence photomicroscope using a Plan-Neufluar 63x oil objective. In experiments involving fluorescein-colchicine or fluorescein, cells were incubated in the dark with the reagent for 2 hours, then mounted on glass slides and examined. If co-localization with RNA was to be examined, the cells were incubated immediately after fluorescein-colchicine treatment with acridine orange (10 mg/ml) in PBS at roome temperature for 5 min. Cells were then washed with PBS and mounted on a glass slide for examination. Immunofluorescence microcopy was performed either on an Olympus Fluoview laser scanning confocal microscope or on a Zeiss epifluoresncence photomicroscope.

Immunoperoxidase staining. Tumors were fixed in formol and embedded in paraffin. Sections (60 µ) were obtained, placed on slides and treated with xylene to remove paraffin and with ethanol solutions from 100% to 70% to rehydrate the sections. The epitopes were restored in a microwave oven set at 680W by the method of Cattoretti et al (1993) (3 x 5-minutes in 1 M Na citrate, pH 6.8. Endogenous peroxidases were

inhibited by treatment with 3% H_2O_2 for 30 minutes. Phosphate-buffered saline containing 10% fetal calf serum was used as both the blocking buffer and the antibody dilution buffer. Slides were incubated with anti-β_{II} (1:2000) overnight at 4 °C followed by incubation with biotinylated secondary antibody for 40 minutes at room temperature. Signal amplification was provided by treatment with streptavidin-peroxidase complex (Strept ABC kit, DAKO, Trappes, France). The signal was detected by a colorimetric method using AminoEthylCarbazol (Sigma Aldrich, St. Quentin Falavier, France). Samples were photographed with a tri-CCD camera (LH750 RC3, Lhesa Electronic Systems).

***In situ* cell fractionation.** LNCaP[3] cells, grown on glass coverslips, were washed twice with ice-cold PBS and incubated on ice for 5 min with cold cytoskeleton buffer (10 mM PIPES[3], pH 6.8, 300 mM sucrose, 100 mM NaCl, 3 mM $MgCl_2$, 1 mM EGTA[3], 1% Triton X-100, 1.2 mM PMSF[3], 0.1% aprotinin, 0.1% pepstatin A, 1% vanadyl ribonucleoside complex). This procedure removes all soluble cytoplasmic and nucleoplasmic proteins. This was followed by 5 min incubation on ice with double detergent buffer (10 mM Tris-HCl, pH 7.4, 10 mM NaCl, 3 mM $MgCl_2$, 0.5% deoxycholate, 1% Tween-40, 1.2 mM PMSF, 0.1% aprotinin, 0.1% pepstatin A, 1% vanadyl ribonucleoside complex), which removes all cytoskeletal proteins, except the intermediate filaments that remain tightly associated with the nucleus. Cells prepared this way are the cytosol-extracted cells. For nuclear matrix preparations, these cells were further incubated at room temperature for 1 hr in cytoskeleton-50 buffer (same as above except with 50 mM NaCl instead of 100 mM) containing 100 μg/ml of DNAse I (Sigma Chemical Co., St. Louis, MO.). The chromatin was then removed by adding 2M

$(NH_4)_2SO_4$ dropwise to a final concentration of 0.25 M. What is left behind is the nuclear matrix structure and the intermediate filaments (Fey et al. 1984). Cells were then fixed with 3.7% paraformaldehyde in cytoskeleton buffer and treated as in. the regular immunofluorescence procedure. For DNA detection, cells were stained with DAPI, (2 μl/ml in PBS) during the last wash with PBS after incubation with the secondary antibody. Removal of chromatin in the nuclear matrix preparations was monitored in this way. For blocking experiments, primary antibodies were incubated with a 200-fold excess of the respective peptide for 30 min at room temperature, prior to incubation with fixed and permeabilized cells.

RESULTS

We have examined the intracellular distribution of the β_I, β_{II} and β_{IV} tubulin isotypes by indirect immunofluorescence on 5 different cultured normal human cell lines: HDF human dermal fibroblasts, HSK fibroblasts from baby foreskin, MCF-10F breast endothelial cells, osteoblasts, and 506 smooth muscle cells. In each case, the β_I- and β_{IV} -tubulin isotypes were found in the cytosol, as part of the microtubule network (Fig. 1*A*, *D*, *G*, *J*, *M* for β_I and *C*, *F*, *I*, *L*, *O* for β_{IV}). The same was seen for β_{II}-tubulin in these cell lines (Fig. 1*B*, *E*, *H*, *K*, *N*). In addition, in the smooth muscle cells, β_{II}-tubulin appeared to be present in the centrosomes (Fig. 1*N*). In no case were any of the isotypes, including β_{II}, found in the nuclei, as no nuclear fluorescence was observed in any of the cell lines investigated.

The presence of β_{II}-tubulin in the nuclei was detected by labeling with anti-β_{II} in all the cancer cell lines investigated. These include LNCaP prostate carcinoma and three types of breast carcinoma: MCF-7, MDA and Calc 18 cell lines (Fig. 2*B*, *E*, *H*, *J*). In the LNCaP, MCF-7 and MDA cells, the nucleus was almost indistinguishable from the cytosol; the whole cell appeared to be stained equally with anti-β_{II} (Fig. 2*B*, *E*, *H*). Comparison of the nuclear staining by anti-β_{II} in these cells with that of DAPI, which shows the position of the nuclei, reveals that anti-β_{II} does in fact stain the nucleus in LNCaP, MCF-7 and MDA cells (not shown). In contrast, in the Calc 18 cells, the cytosol was labeled only weakly by anti-β_{II}, while the nuclear labeling was very strong (Fig. 2 *J*). The intra-nuclear distribution of β_{II}-tubulin appeared to be the same in all the cancer cells. The pattern of nuclear fluorescence was homogenous within the nucleus, except for the Calc 18 cells, in which there appeared to be no β_{II} staining in the nucleoli (Fig. 2*J*).

Some of the MCF-7 cells may also have had less staining in the nucleoli than in the rest of the nuclei (Fig. 2*E*). The β_I- and β_{IV} -isotypes were found only in the cytosol, as part of the interphase microtubule network, of each of the cancer cells investigated (Fig. 2*A*, *D*, *G* for β_I and *C*, *F*, *I* for β_{IV}).

To determine the sub-nuclear localization of β_{II}-tubulin, *in situ* cell fractionation was performed in LNCaP cells. Removal of the soluble cytoplasmic and nucleoplasmic proteins by detergent extraction did not cause the nuclear fluorescence, obtained by staining with anti-β_{II}, to disappear (Fig. 3*A*). Furthermore, nuclear fluorescence was still detected after chromatin and chromatin-associated proteins were removed by DNAse digestion (Fig. 3*C*). In these cells, β_{II} appeared to accumulate in the nucleolar remnants. These results suggest that β_{II}-tubulin is part of the nuclear matrix in LNCaP cells. Pre-incubation of anti-β_{II} with its peptide epitope inhibited the nuclear fluorescence in both the cytosol-extracted and the nuclear matrix preparations, indicating that nuclear fluorescence obtained in these cells was due to specific binding of the antibody to β_{II}-tubulin (Fig. 3*E*, *G*).

The results obtained with LNCaP cells suggested that β_{II}-tubulin is concentrated in their nucleoli. Although the morphology of the β_{II}-containing structures suggested that they were nucleoli, independent evidence for this was desirable. Since nucleoli are rich in RNA, we used acridine orange, a stain for RNA, to see if the β_{II}-tubulin co-localized with RNA in a variety of cancer cells (Fig. 4). These included C6 glioma (Fig. 4*A*,*B*,*C*), T98G glioma (Fig. 4*D*, *E*, *F*), MCF-7 breast cancer (Fig. 4*G*, *H*, *I*), MDA breast cancer (Fig. 4*J*, *K*, *L*), and HeLa cells (Fig. 4*M*, *N*, *O*). We used confocal microscopy to have a

clearer picture of the putative nucleoli. The results indicate that β_{II}-tubulin co-localizes almost perfectly with the RNA clusters in the nucleoli.

The above results imply that β_{II}-tubulin is located in the nucleoli of a variety of cultured cancer cells, but they do not address the question of whether β_{II} is in a functional state. One way to address this possibility, as was previously done with β_{II}-tubulin in cultured rat kidney mesangial cells (Walss et al. 1999), is to see if it binds to colchicine. Accordingly, the same panel of cancer cells used in Fig. 4 was incubated with fluorescein-colchicine and then stained with acridine orange to identify the RNA. As seen in Fig. 5, the fluorescein-colchicine and acridine orange consistently co-localize. In order to eliminate the possibility that fluorescein-colchicine somehow has a particular affinity for nuclei and/or nucleoli, fetal rat calvaria cells, known to lack β_{II}-tubulin, were incubated with fluorescein-colchicine; no nuclear accumulation of fluorescence was seen (not shown). The results in Fig. 5 indicate that the nucleolar β_{II}-tubulin is in its native state, capable of binding colchicine, and is presumably in the form of an $\alpha\beta_{II}$ dimer.

In this study we have examined a variety of cultured cells, some transformed and some not. The transformed cells we have examined contains nuclear β_{II}, whereas few of the non-transformed do. Although based on a small sample, our results raise the possibility that cancer cells are more likely to contain nuclear β_{II}. It is possible, however, that nuclear β_{II} is some kind of artifact arising from growing cells in culture, an artifact conceivably more likely to occur with transformed cells. In order to see if β_{II}-tubulin can occur in the nuclei of cancer cells *in situ*, we examined mammary adenocarcinomas from two patients with breast cancer (Fig. 6). Immunoperoxidase staining reveals that β_{II}

occurs in the nuclei of the cancer cells; higher magnification shows that β_{II} appears to be concentrated in small intra-nuclear bodies that may be nucleoli (Fig. 6).

DISCUSSION

In the work described here, we have examined a total of seven cancer cell lines, all of which appear to contain the β_{II} isotype of tubulin in their nuclei. We also see β_{II} in the nuclei of adenocarcinoma cells in breast cancer excisions. We examined five non-transformed cell lines and found that none of them contain nuclear β_{II}. In previous work, however, we found that the non-transformed rat kidney mesangial cells contained nuclear β_{II} (Walss et al., 1999) as do Rat-1 fibroblasts (Prasad and Ludueña, unpublished results) but not MDCK epithelial cells (Modig and Ludueña, unpublished results). Similarly, Ranganathan et al. (1997) have found β_{II}-tubulin in the nuclei of prostate carcinoma as well as in adjacent areas of benign prostate hypertrophy. There have also been some early reports of nuclear tubulin that were not followed up. Menko and Tan (1980) purified tubulin from the nuclei of 3T3 cells and showed that it bound to colchicine, while Armbruster et al. (1983) demonstrated its presence in the nuclei of Chinese hamster ovary cells by immunogold staining. In brief, the results presented here as well as those of Ranganathan et al. (1997) raise the possibility that localization of tubulin in the nucleus may be a phenomenon that is more likely to occur in cancer cells.

Our initial discovery of nuclear β_{II}-tubulin was in rat kidney mesangial cells, obtained from a non-transformed primary cell line. Although these cells are not cancerous, they grow very quickly in culture. Mesangial cells are known to maintain a basal proliferation rate *in vitro*, even in the absence of exogenous mitogens (Floege et al. 1990). This is most likely due to the fact that these cells self-produce growth factors such as PDGF[3], (Abboud et al.1987), and IL-1[3], (Mene et al. 1989), and in this way undergo autocrine-mediated proliferation *in vitro* (Floege et al. 1991a). Furthermore, cultured

mesangial cells are commonly maintained in the presence of 20% fetal calf serum, of which PDGF is the principal mitogen (Floege et al. 1991b). PDGF is known to be the most potent mitogen for cultured mesangial cells, as it has been shown to increase the thymidine incorporation rate in these cells by 10-15 fold (Floege et al. 1991b). This explains the rapid proliferation of mesangial cells *in vitro*, in contrast to normal mesangial cells *in vivo*, which are almost non-proliferative (Pabst and Sterzel, 1983), and have been shown to proliferate rapidly only in cases of renal glomerular injury or disease (Schocklmann et al. 1999). Considering these facts, together with our present finding of β_{II}-tubulin in the nuclei of cultured cancer cells, we hypothesize that nuclear β_{II}-tubulin may play a role in assisting rapid cell proliferation. This would explain the finding of β_{II} inside the nuclei of cancer cells but not normal cells. It is possible that other normal cells that proliferate rapidly may also contain β_{II} in their nuclei.

The β_{II} isotype of tubulin has been found to be part of the nuclear matrix in mesangial cells and also has been shown to accumulate in the nucleolus. We now show that this is also the case for β_{II}-tubulin in various cancer cells; nuclear fluorescence due to anti-β_{II} staining was detected in the nuclear matrix and the nucleolar remnants after chromatin digestion. The fact that tubulin has been reported to interact with chromatin *in vitro* (Mithieux et al. 1984,1986) could be related to the functions of β_{II} in the nucleolus and the nuclear matrix. In the former case, β_{II} could be binding to the DNA regions, which contain the ribosomal RNA genes, whereas in the latter situation it could be functioning as a chromosomal scaffold. Interestingly, it is known that the anti-tubulin drug vinblastine affects biochemical processes that are seemingly unrelated to tubulin, such as DNA and RNA synthesis (Creasey 1968; Bernstam et al. 1980). It is possible

that its effects on these processes could occur through an interaction with nuclear β_{II}-tubulin.

We have shown that β_{II}-tubulin accumulates preferentially in the nuclei of cancer cells. Perhaps its role in the nucleus is to accelerate DNA and RNA synthesis and therefore facilitate proliferation. Alternatively, nuclear β_{II} may have no specific nuclear function, but rather a unique and as yet unknown function in the mitotic spindle; its location in the nucleus, therefore, may allow it to act quickly when mitosis begins. If either hypothesis were correct, it makes sense that nuclear β_{II} would be needed more in cancer cells, to assist rapid cell proliferation. In conclusion, one may speculate that nuclear β_{II} may become an interesting and novel target for cancer chemotherapy; a tubulin-specific drug whose major effects are on cancer cells would be very exciting.

Although our results suggest, as argued above, that there is a correlation between transformation and the presence of nuclear β_{II}, there is another correlation that needs to be considered. Of the seven cancer cell lines, used in this study, four were from tumors of epithelial origin. Of the non-transformed cell lines we have used here, as well as those used by Menko and Tan (1980), Armbruster et al. (1983), and Walss et al. (1999), seven were of epithelial origin. Grouping the results according to epithelial origin, we find that 7 out of 8 cell lines of epithelial origin have nuclear β_{II}, whereas that is true for only 4 out of 9 cell lines of non-epithelial origin. This is comparable to the presence of nuclear β_{II} in 7 out of 7 transformed cell lines and 4 out of 10 non-transformed cell lines. It is quite possible that nuclear localization of β_{II} is more likely to occur in transformed cells, particularly if they are of epithelial origin. Further investigation may clarify these relationships.

ACKNOWLEDGMENTS

We thank Dr. Eugene Sprague for providing the human dermal fibroblasts, Dr. Mary Pat Moyer for providing the 506 smooth muscle cells and the HSK fibroblasts, Dr. John Lee for providing the osteoblasts, Dr. Nandini Chaudhuri for providing the LNCaP, MCF-7 and MDA cells, Dr. Jean-François Riou for providing the Calc 18 cells, Dr. Susan Mooberry for.the gift of MDA and HeLa cells and Dr. Martin Adamo for the C6 and T98G glioma. We also thank Phyllis Smith for preparation of the monoclonal antibodies used in these experiments and Dr. Victoria Centonze for invaluable assistance with confocal microscopy.

REFERENCES

Abboud HE, Poptic E, Dicorleto PE (1987) Production of platelet–derived growth factor-like protein by rat mesangial cells in culture. J Clin Invest 80: 675-683.

Armbruster BL, Wunderli H, Turner BM, Raska I, Kellenberger E (1983) Immunocytochemical localization of cytoskeletal proteins and histone 2B in isolated membrane-depleted nuclei, metaphase chromatin, and whole Chinese hamster ovary cells. J Histochem Cytochem 31: 1385-1393.

Banerjee A, Roach MC, Wall KA, Lopata MA, Cleveland DW, Ludueña RF (1988) A monoclonal antibody against the type II isotype of β-tubulin. Preparation of isotypically altered tubulin. J Biol Chem 263: 3019-3034.

Banerjee A, Roach MC, Trcka P, Ludueña RF (1992) Preparation of a monoclonal antibody specific for the class IV isotype of β-tubulin. Purification and assembly of $\alpha\beta_{II}$, $\alpha\beta_{III}$, and $\alpha\beta_{IV}$ tubulin dimers from bovine brain. J Biol Chem 267: 5625-5630.

Bernstam VA, Gray RH, Bernstein IA (1980) Effect of microtubule-disrupting drugs on protein and RNA synthesis in *Physarum polycephalum* Amoebae. Arch Microbiol 128: 34-40.

Cattoretti G, Pileri S, Parravicini C, Becker MH, Poggi S, Bifulco C, Key G, D'Amato L, Sabattini E, Feudale E (1993) Antigen unmasking on formalin-fixed, paraffin-embedded tissue sections. Journal of Pathology 171: 83-98.

Creasey WA (1968) Modifications in biochemical pathways produced by the *Vinca* alkaloids. Cancer Chemother Res 52: 501-507.

Fey EG, Wan KM, Penman S (1984) Epithelial cytoskeletal framework and nuclear matrix-intermediate filament scaffold: three dimensional organization and protein composition. J Cell Biol 98: 1973-1984.

Floege J, Topley N, Wessel K, Kaever V, Radeke HH, Hoppe J, Kishimoto T, Resch K (1990) Monokines and platelet-derived growth factor modulate prostanoid production in growth arrested human mesangial cells. Kidney Int 37: 859-869.

Floege J, Topley N, Resch K (1991a) Regulation of mesangial cell proliferation. Am J Kidney Diseases 17: 673-676.

Floege J, Topley N, Hoppe J, Barrett TB, Resch K (1991b) Mitogenic effect of platelet-derived growth factor in human glomerular mesangial cells: modulation and/or suppression by inflammatory cytokines. Clin Exp Immunol 86: 334-341.

Hyams JS, Lloyd CW (eds.) (1994) Microtubules. Wiley-Liss, New York.

Ludueña RF (1998) Multiple forms of tubulin: different gene products and covalent modifications. Int Rev Cytol 178: 207-275.

Mene P, Simonson MS, Dunn MJ (1989) Physiology of the mesangial cell. Physiol Rev 69: 1347-1424.

Menko AS, Tan KB (1980) Nuclear tubulin of tissue cultured cells. Biochim Biophys Acta 629:359-370.

Mithieux G, Alquier C, Roux B, Rousset B (1984) Interaction of tubulin with chromatin proteins. H1 and core histones. J Biol Chemi 259:15523-15531.

Mithieux G, Roux B, Rousset B (1986) Tubulin-chromatin interactions: evidence for tubulin-binding sites on chromatin and isolated oligonucleosomes. Biochim Biophys Acta, 888: 49-61.

Pabst R, Sterzel RB (1983) Cell renewal of glomerular cell types in normal rats. An autoradiographic study. Kidney Int 24: 626-631.

Ranganathan S, Salazar H, Benetatos CA, Hudes GR (1997) Immunohistochemical analysis of β-tubulin isotypes in human prostate carcinoma and benign prostate hypertrophy. Prostate 30: 263-268.

Roach MC, Boucher VL, Walss C, Ravdin P, Ludueña RF (1998) Preparation of a monoclonal antibody specific for the class I isotype of β-tubulin: the β isotypes of tubulin differ in their cellular distributions within human tissues. Cell Motil Cytoskeleton 39: 273-285.

Schocklmann HO, Lang S, Sterzel RB (1999) Regulation of mesangial cell proliferation. Kidney Int 56: 1199-1207.

Walss C, Kreisberg JI, Ludueña RF (1999) Presence of the β_{II} isotype of tubulin in the nuclei of cultured mesangial cells from rat kidney. Cell Motil Cytoskeleton 42: 274-284.

Wilson L, Jordan MA (1994) Pharmacological probes of microtubule function. In: Hyams JS, Lloyd CW (eds) Microtubules. Wiley-Liss, New York, pp 59-83.

FIGURE LEGENDS

Fig. 1. Detection of the tubulin β-isotypes, β_I, β_{II} and β_{IV} in cultured normal human cells. (*A, D, G, J, M*), Cells treated with anti-β_I by indirect immunfluorescence. (*B, E, H, K, N*), Cells treated with anti-β_{II} by indirect immunofluorescence. (*C, F, I, L, O*), Cells treated with anti-β_{IV} by indirect immunfluorescence. (*A-C*), Human dermal fibroblasts. (*D-F*), HSK fibroblasts. (*G-I*), MCF-10F breast endothelial cells. (*J-L*), Osteoblasts. (*M-O*), 506 smooth muscle cells. Bar = 28 μ. The one cell in panel K where β_{II} appears to be concentrated in the area of the nucleus is actually a mitotic cell in prophase.

Fig. 2. Occurrence of β_{II}-tubulin in the nuclei of cultured human cancer cells. (*A, D, G*), Cells treated with anti-β_I by indirect immunfluorescence. (*B, E, H, J*), Cells treated with anti-β_{II} by indirect immunofluorescence. (*C, F, I*), Cells treated with anti-β_{IV} by indirect immunofluorescence. (*A-C*), LNCaP prostate carcinoma cells. (*D-F*), MCF-7 breast carcinoma cells. (*G-I*), MDA breast carcinoma cells. (*J*), Calc 18 breast carcinoma cells. Bar = 28 μ.

Fig. 3. Subcellular localization of β_{II}-tubulin in LNCaP cells. (*A*), Cytosol-extracted cells treated with anti-β_{II}. (*B*), Same cells as in A, stained with DAPI. (*C*), Cytosol- and chromatin-extracted cells treated with anti-β_{II}. (*D*), Same cells as in C, stained with DAPI. The almost complete absence of fluorescence indicates that most of the chromatin was successfully removed. (*E*), Cytosol-extracted cells treated with anti-β_{II} that had been blocked with its peptide epitope. (*F*), Same cells as in E, stained with DAPI to show position of nuclei. (*G*), Cytosol- and chromatin-extracted cells treated with anti-β_{II} that had been previously blocked with its peptide epitope. Note the absence of fluorescence. Bar = 28 μ.

Fig. 4. Co-localization of β_{II}-tubulin and RNA in the nucleoli of several carcinoma cells. Cells were treated to extract the chromatin as in Fig. 3. Cells were then treated with anti-β_{II} and acridine orange. β_{II} staining is shown in *A, D, G, J,* and *M.* Acridine orange staining of the corresponding cells is shown in *B, E., H, K,* and *N.* The superimposed images of β_{II} and acridine orange staining are shown in *C, F, I, L,* and *O.* Cells are as follows: C6 glioma (*A,B,C*); T98G glioma (*D, E, F*); MCF-7 breast cancer *(G, H, I*); MDA breast cancer (*J, K, L*); HeLa cells (*M, N, O*). Note co-localization of RNA and β_{II}-tubulin. Bar = 20 μ.

Fig. 5. Presence of functional tubulin in the nucleoli of several carcinoma cells. Cells were treated to extract the chromatin as in Fig. 3. Cells were then treated with fluorescein-colchicine and acridine orange. Fluorescein-colchicine staining is shown in *A, D, G, J,* and *M.* Acridine orange staining of the corresponding cells is shown in *B, E., H, K,* and *N.* The superimposed images of fluorescein-colchicine and acridine orange staining are shown in *C, F, I, L,* and *O.* Cells are as follows: C6 glioma (*A,B,C*); T98G glioma (*D, E, F*); MCF-7 breast cancer *(G, H, I*); MDA breast cancer (*J, K, L*); HeLa cells (*M, N, O*). Acridine orange stains RNA; note co-localization of RNA and colchicine. Bar = 20 μ.

Fig. 6. Presence of β_{II}-tubulin in nuclei of human breast cancer tissue. Immunoperoxidase staining of two different breast tumors (A and B) was performed as described in Materials and Methods. Tumors are shown at two different magnifications: (a) bar = 200 μ); (b) bar = 50 μ). Note widespread presence of β_{II} in the nuclei and slightly more intense staining in what appear to be nucleoli.

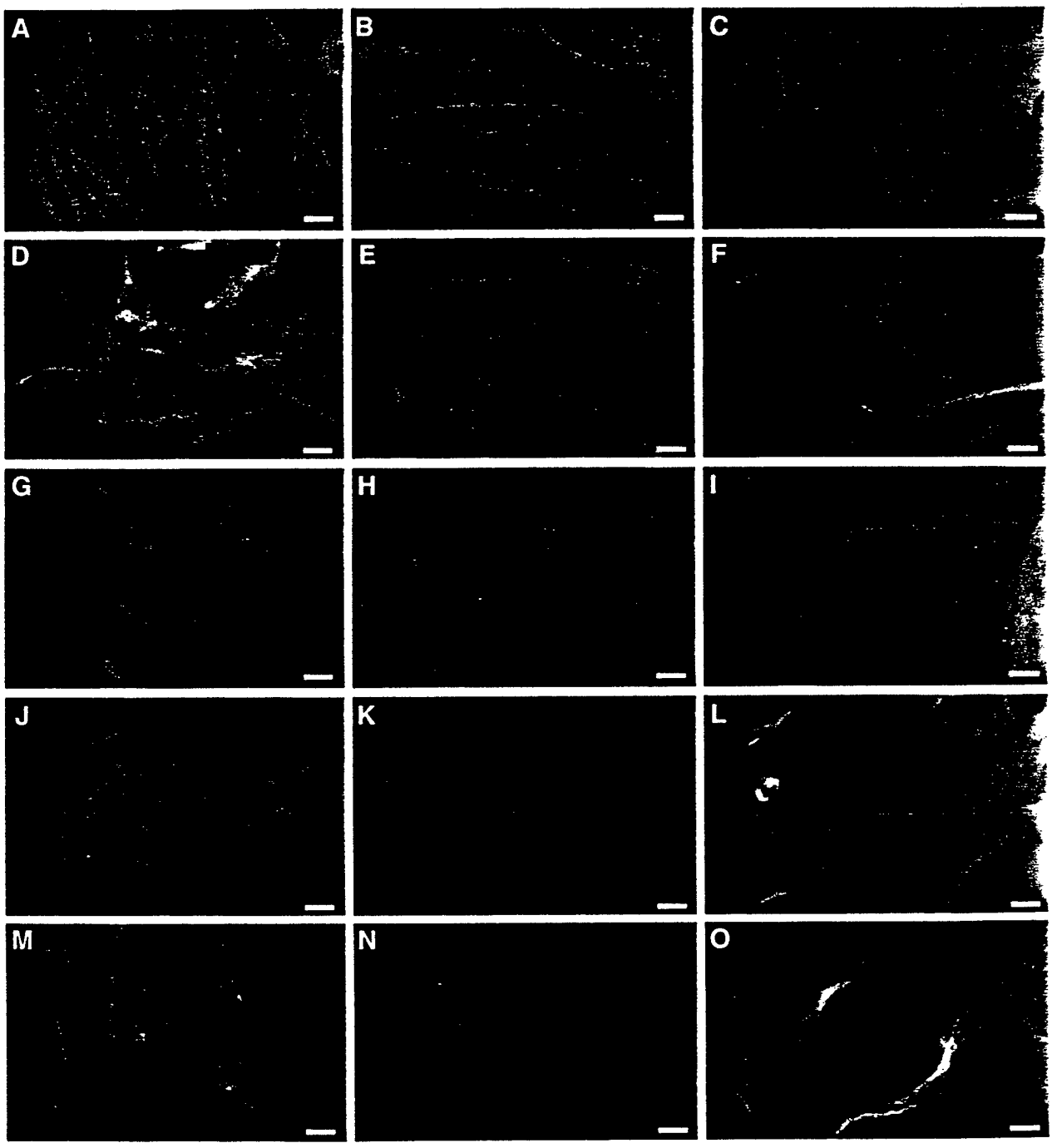

Figure 1

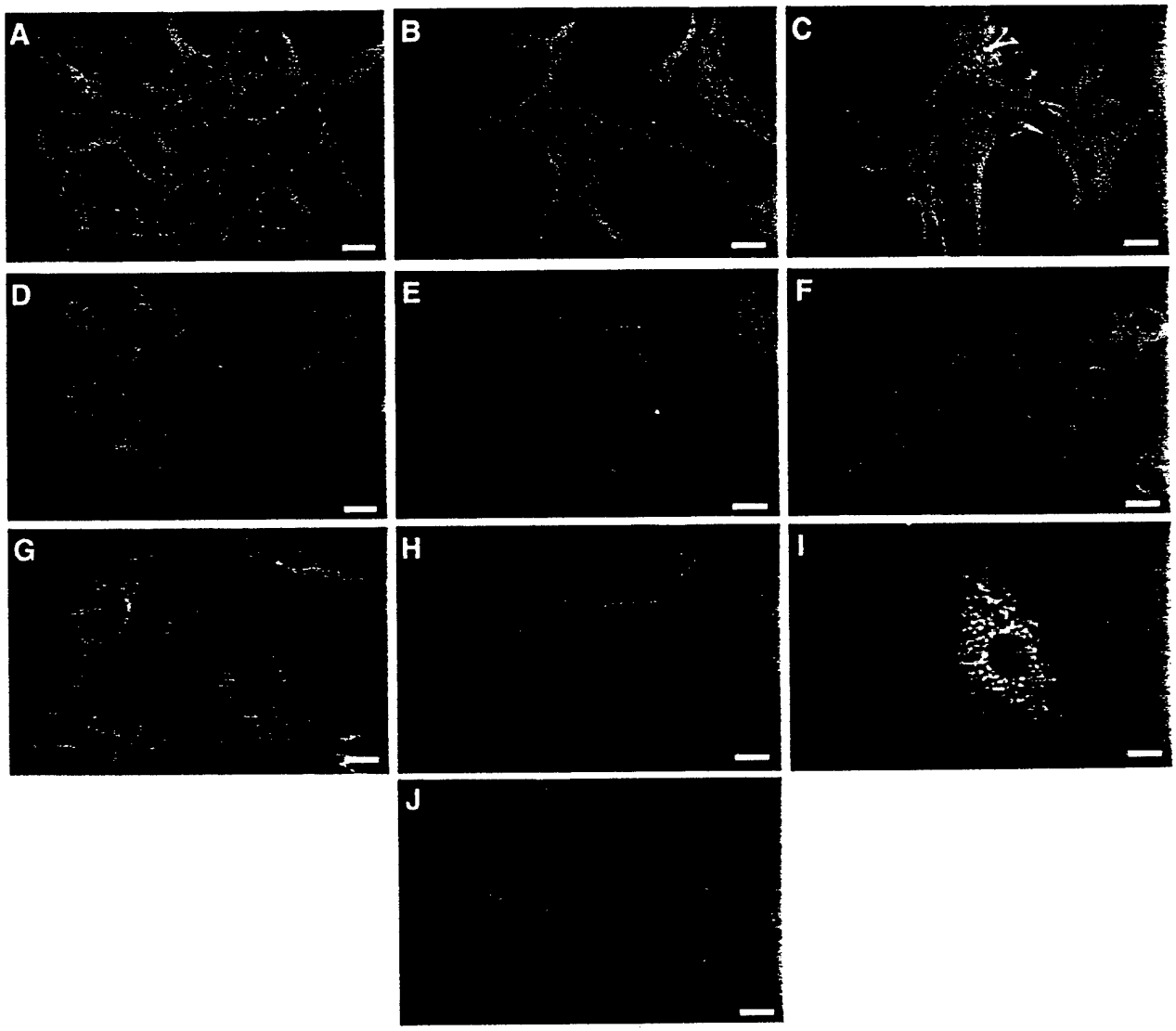

Figure 2

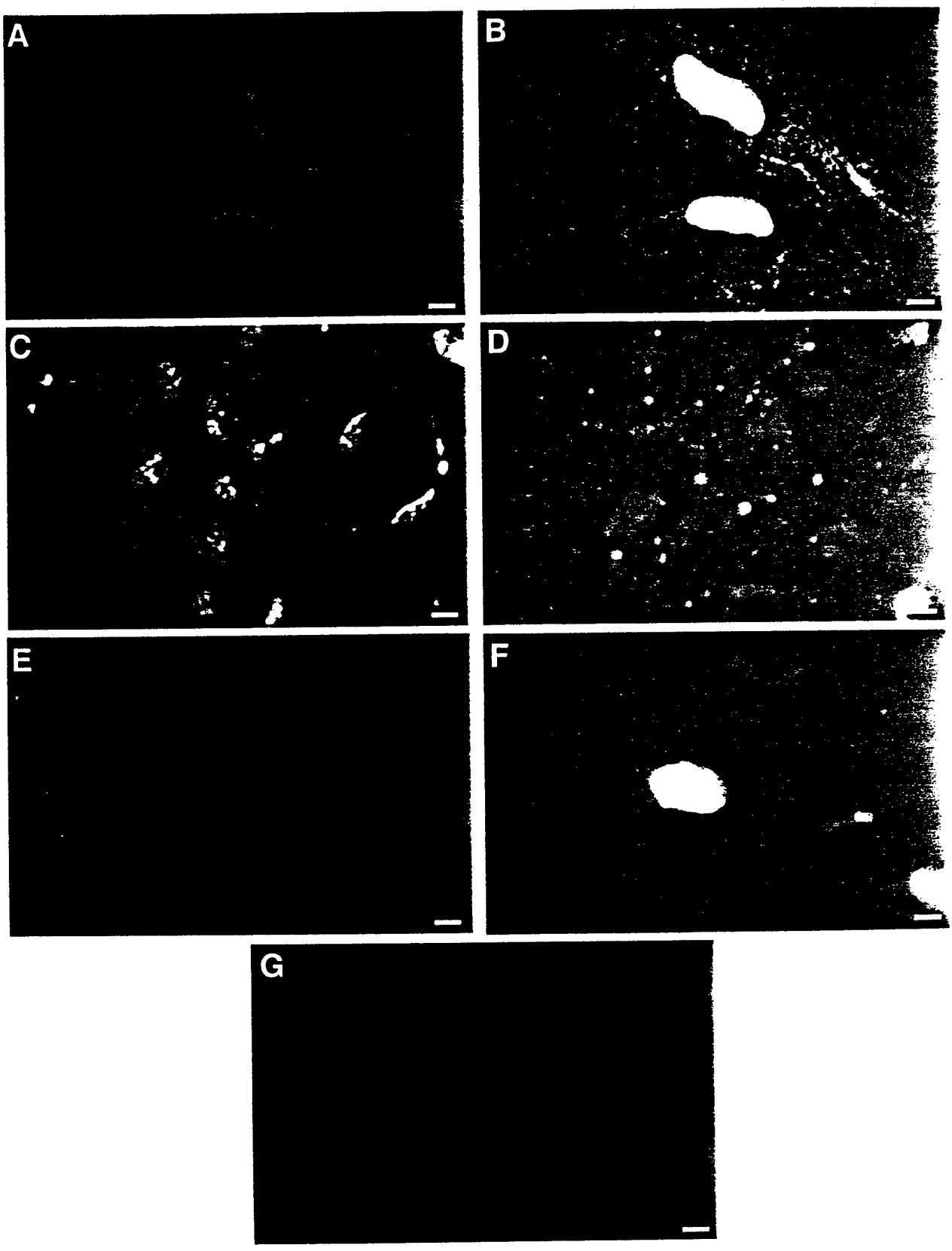

Figure 3

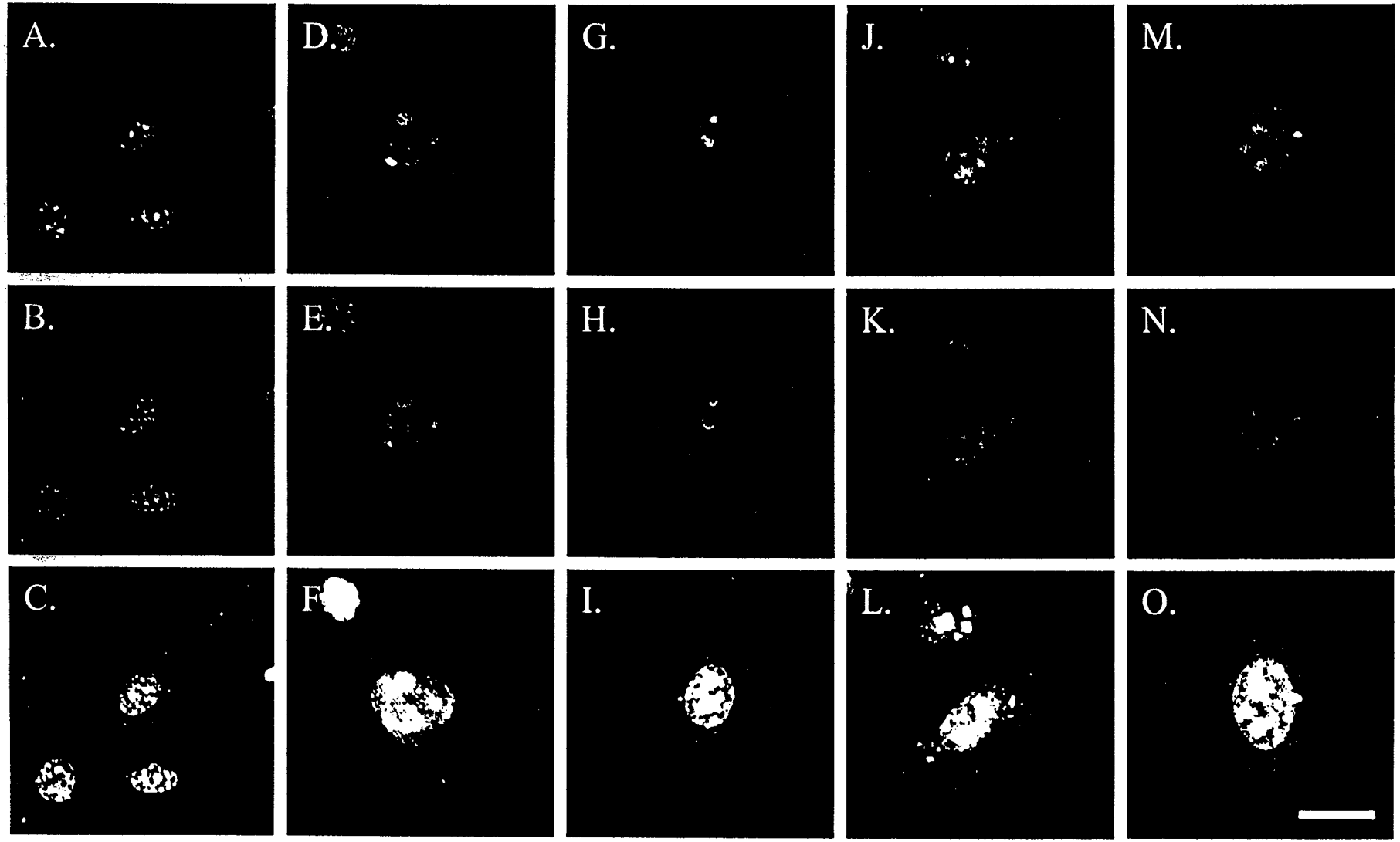

Figure 4

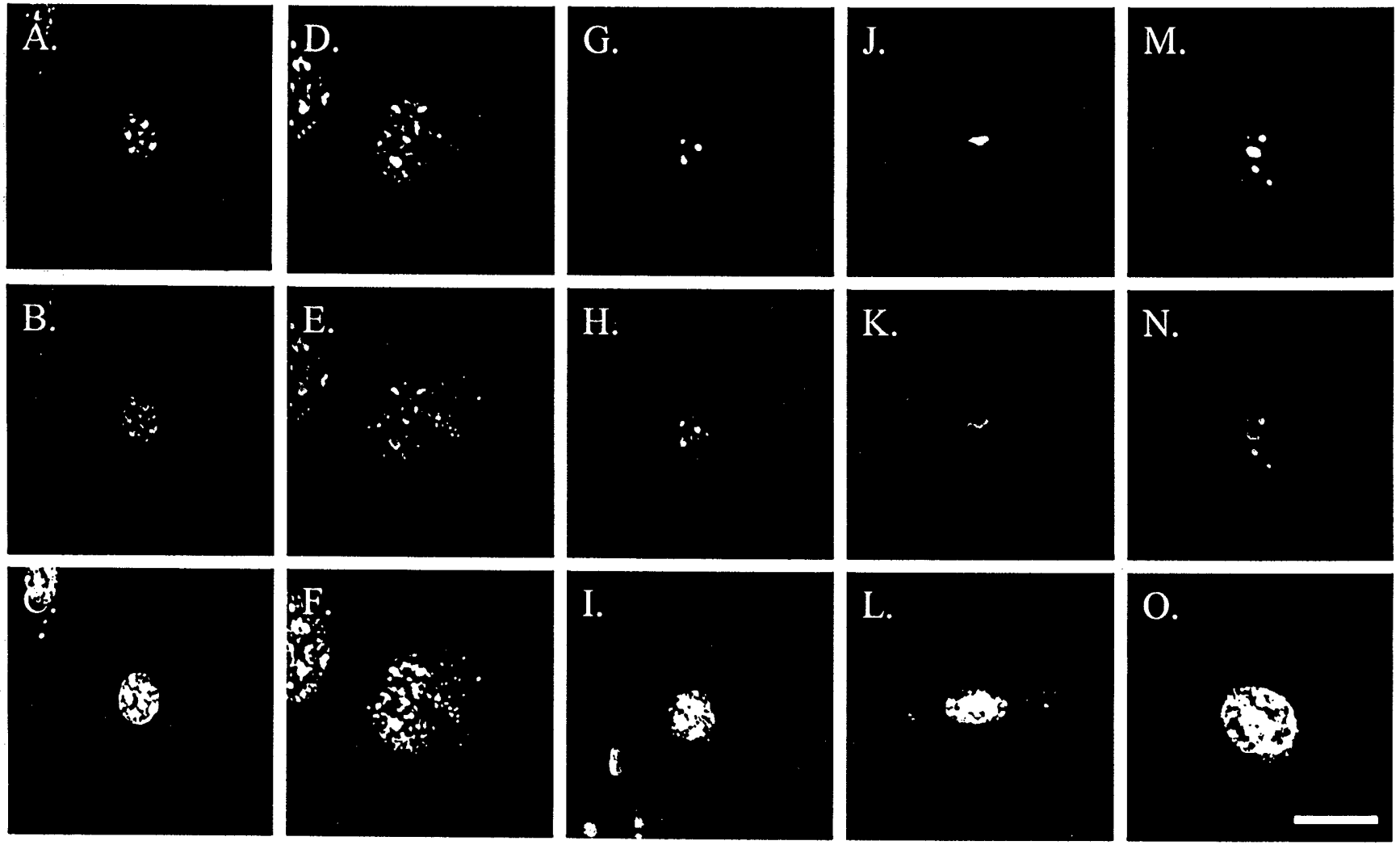

Figure 5

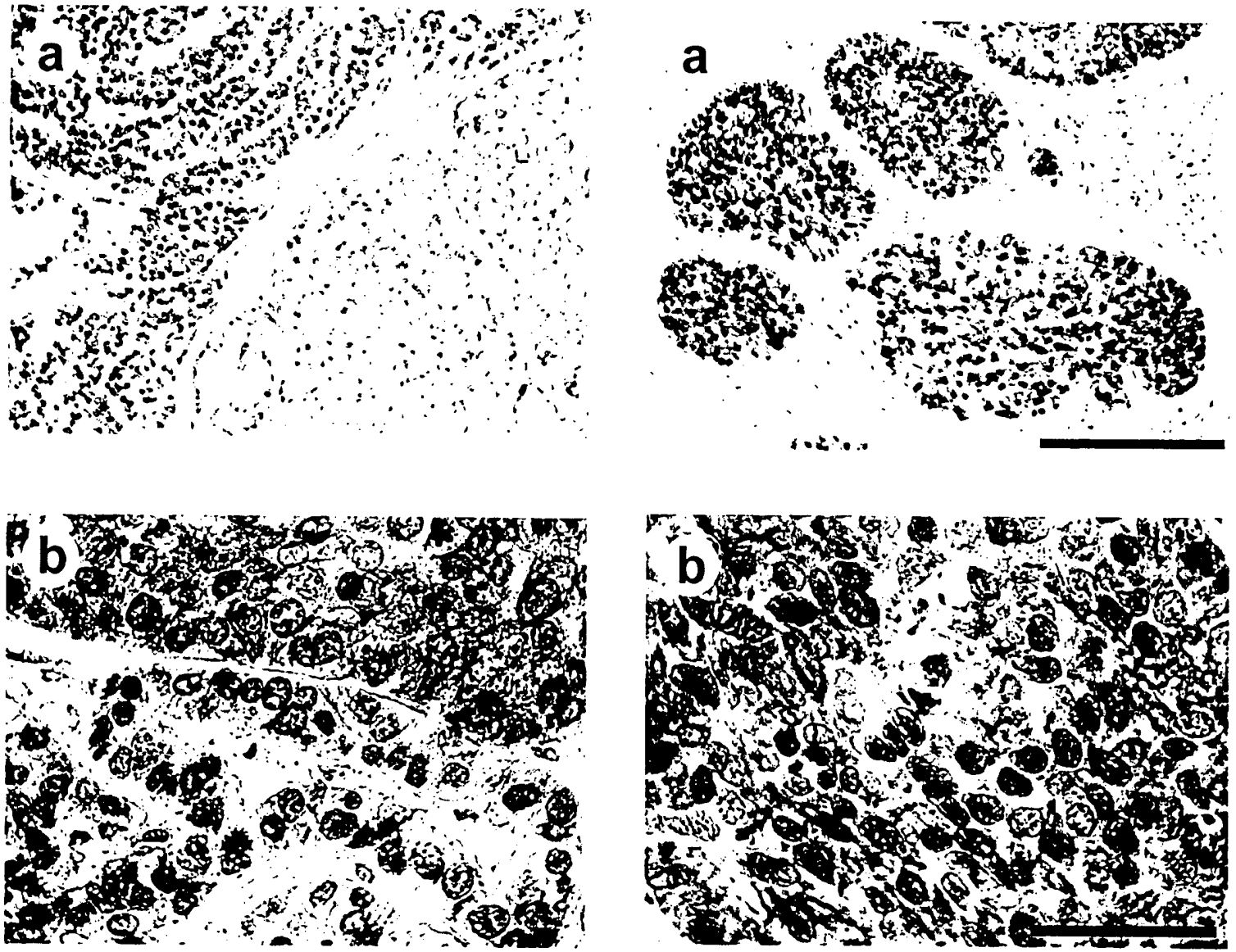

Figure 6

Appendix 2

Characterization of Nuclear β_{II}-Tubulin in Tumor Cells: A Possible Novel Target for Taxol

Keliang Xu and Richard F. Ludueña

Department of Biochemistry, The University of Texas Health Science Center at San Antonio, San Antonio, Texas, 78229-3900

Running Title: Taxol Depletes Nuclear β_{II}-tubulin

Address Correspondence to:

Dr. Richard F. Ludueña

Department of Biochemistry, Mail Code 7760

The University of Texas Health Science Center at San Antonio

7703 Floyd Curl Drive

San Antonio, Texas 78229-3900

210-567-3731

Fax: 210-567-6595

E-mail: luduena@uthscsa.edu

In Press: Cell Motility and the Cytoskeleton

ABSTRACT

As the subunits of microtubules, α- and β-tubulins have been thought to only exist in the cytoplasm where they are incorporated into microtubules. However, the β_{II} isotype of tubulin has recently been observed in the nuclei of rat kidney mesangial cells (Walss C, Kreisberg JI, Ludueña RF. 1999. Cell Motil. Cytoskeleton 42:274-284). In this study we detected nuclear β_{II}-tubulin in rat C6 glioma cells, human T98G glioma cells, human MCF-7 breast carcinoma cells, human MDA-MB-435 breast carcinoma cells, and human Hela cervix carcinoma cells. In addition, nuclear β_{II}-tubulin in these cells was found to exist as $\alpha\beta_{II}$ dimers instead of assembled microtubules and appeared to be particularly concentrated in the nucleoli. Several anti-tubulin drugs were used to treat C6 cells to determine their influence on nuclear β_{II}-tubulin. Taxol, a tubulin drug with higher specificity for β_{II}-tubulin than for other β-tubulin isotypes, irreversibly decreased nuclear β_{II} content in a concentration-dependent manner in C6 cells. Meanwhile, cells were found to be apoptotic as was suggested by the presence of multiple micronuclei and DNA fragmentation. On the other hand, no depletion of nuclear β_{II}-tubulin was observed when C6 cells were incubated with colchicine or nocodazole, two anti-tubulin drugs with higher specificity for the $\alpha\beta_{IV}$ isotype, supporting the hypothesis that drugs with higher specificity for β_{II}-tubulin deplete nuclear β_{II}-tubulin.

Keywords: Nuclear structure, Tubulin, Apoptosis, Taxol, Isotypes

INTRODUCTION

The structural subunit of microtubules, the 100-kDa protein tubulin, is a heterodimer of two polypeptide chains designated α and β (Bryan and Wilson, 1971; Ludueña et al. 1977). Both α- and β-tubulin exist as numerous isotypes encoded by different genes, among which β isotypes exhibit more complex and variable tissue distributions than do the α isotypes (Ludueña, 1998). It has been previously reported that the β_{II} isotype of tubulin, which was thought to be normally present only in the cytoplasm where it participates in microtubule formation, is present in the nuclei of a prostate tumor (Ranganathan et al., 1997) and a breast tumor (Walss et al., 2000) as well as cultured rat kidney mesangial cells, a non-transformed cell line (Walss et al., 1999). In contrast, biopsy samples of several normal human tissues using immunoperoxidase staining did not show any evidence for the existence of nuclear β_{II}-tubulin (Roach et al., 1998). These results raise the possibility that nuclear β_{II}-tubulin may be correlated with the cancerous state. In this study, we searched for β_{II}-tubulin in the nuclei of several cancer cells. We found that nuclear β_{II}-tubulin exists in the nuclear matrix and is often concentrated in the nucleolus. In addition, the depletion of nuclear β_{II}-tubulin after taxol treatment was observed as well as cell apoptosis in rat C6 glioma cells. As a successful anti-tumor drug with higher specificity for β_{II}-tubulin than for other β-tubulin isotypes (Derry et al., 1997), taxol has been known to target polymerized microtubules, presumably in the cytoplasm of cells (Schiff and Horwitz, 1981; Parness and Horwitz, 1981; Wilson and Jordan, 1994). Our results suggest the possibility that nuclear β_{II}-tubulin in cancer cells

may constitute a novel target for taxol.

MATERIALS AND METHODS

Cell Culture

Rat C6 glioma cells, human T98G glioma cells (kind gifts from Dr. Martin Adamo, Department of Biochemistry, University of Texas Health Science Center at San Antonio (UTHSCSA)), human MCF-7 breast carcinoma cells (a kind gift from Dr. Robert Klebe, Department of Cellular and Structural Biology, UTHSCSA), human MDA-MB-435 breast carcinoma cells, and Hela cells (kind gifts from Dr. Susan Mooberry, Southwest Foundation for Biomedical Research) were cultured in Ham's F-12 (Gibco/BRL, Rockville, MD) with 1 mM glutamine, Minimum Essential Medium (Gibco/BRL) with Earle's salts and L-glutamine, HyQ DME/F-12 (Hyclone, Logan, UT) with 2.5 mM L-glutamine, Improved MEM Zinc Option (Gibco/BRL) with 2 mg/L L-glutamine, L-proline, and 50 μg/ml gentamicin sulfate, and Basal Medium Eagle (Gibco/BRL) with Earle's salts and L-glutamine, respectively. All media contained 100 IU/ml penicillin, 100 μg/ml streptomycin, and 10% fetal bovine serum (FBS) (Gibco/BRL). For each cell line, an equivalent number of cells were plated onto each coverslip in six-well plates or 100 mm tissue culture dishes and incubated for 24-48 hr at 37 °C in 5% CO_2. For drug treatment, cells were incubated in appropriate medium with either taxol (provided by the National Cancer Institute), colchicine (Sigma Chemical Corp., St Louis, MO), or nocodazole (Sigma Chemical Corp.) at the indicated concentrations and for the indicated times as described below. Cells were used between the 4^{th} and 30^{th} passages in this study.

Antibodies and Peptides

The monoclonal antibodies SAP.4G5, JDR.3B8, SDL.3D10, and ONS.1A6 specific, respectively, for the β_I, β_{II}, β_{III}, and β_{IV} isotypes of tubulin were prepared as previously described (Banerjee et al., 1988, 1990, 1992; Roach et al., 1998). The sequences of the peptides (Bio-Search Corp., San Rafael, CA) used as immunogens to raise these antibodies were CEEAEEEA, CEGEEDEA, CESESQGPK, and CEAEEEVA, respectively. Each sequence is identical to the C-terminal sequence of the corresponding isotype of tubulin except for the N-terminal cysteine. The monoclonal primary nucleolin antibody (C23) was obtained from Santa Cruz Biotechnology (Santa Cruz, CA). The monoclonal antibody AYN.6D10, specific for the tyrosinated forms of the Mα1, Mα3, and Mα4 mammalian α-tubulin isotypes was a kind gift from Dr. Asok Banerjee (Department of Biochemistry, UTHSCSA). The rhodamine-labeled anti-β_{II} was generated as described (Walss et al., 1999). Cy3-conjugated goat anti-mouse IgG and fluorescein-conjugated goat anti-mouse IgG were both obtained from Jackson Immunoresearch (West Grove, PA).

Immunofluorescence Microscopy

Cultured cells on coverslips were rinsed twice with phosphate-buffered saline (PBS), fixed with 3.7% paraformaldehyde at room temperature for 15 min, and permeabilized with 0.5% Triton X-100 in PBS for 1 min. Cells were then incubated overnight with the respective isotype-specific monoclonal IgG mouse antibody (anti-β_I, 0.17 mg/ml; anti-β_{II}, 0.03 mg/ml; anti-β_{III}, 0.08 mg/ml; anti-β_{IV}, 0.17 mg/ml; anti-α, 0.02-0.03 mg/ml) diluted in PBS containing 10% normal goat serum (Jackson Immunoresearch). Cells were rinsed

with PBS and incubated with Cy3-conjugated goat anti-mouse IgG (1:50) for 1 hr at room temperature. Cells were then stained with 4', 6-diamidino-2-phenylindole, dihydrochloride (DAPI) (Molecular Probes, Eugene, OR) to visualize the nucleus. Coverslips were mounted on glass slides and examined with a Zeiss epifluorescence photomicroscope using a Plan-Neufluar 60x oil objective or an Olympus Fluoview laser scanning confocal microscope. For blocking experiments, primary antibodies were incubated with a 200-fold excess of the respective peptide for 30 min at room temperature prior to incubation with cells. In the experiments using fluorescein-colchicine (Molecular Probes), fixed and permeabilized cells were incubated with fluorescein-colchicine (0.1 mg/ml) or fluorescein in the dark at room temperature for 2 hr. Coverslips were then mounted on glass slides for visualization.

For the double immunofluorescence experiments, cytosol- and chromatin-extracted cells were incubated with anti-α (0.02-0.03 mg/ml) or anti-nucleolin (0.01 mg/ml) at 4 °C overnight, rinsed with PBS and incubated with fluorescein-conjugated goat anti-mouse IgG (1:50). Cells were rinsed and further incubated with rhodamine-labeled anti-β_{II} (0.1 mg/ml) at 4 °C overnight.

In situ Cell Fractionation

Cells grown to 50% confluence on glass coverslips were washed twice with ice-cold PBS and incubated on ice for 5 min with cold CSK-100 buffer (10 mM Pipes, PH 6.8, 300 mM sucrose, 100 mM NaCl, 3 mM $MgCl_2$, 1 mM EGTA, 1% Triton X-100, 1.2 mM PMSF, 0.1% aprotinin, 0.1% pepstatin A, and 1% vanadyl ribonucleoside complex) to

remove all soluble cytoplasmic and nucleoplasmic proteins. These cells were further incubated at room temperature for 1 hr in CSK-50 buffer (same as CSK-100 except with 50 mM NaCl instead of 100 mM) containing 100 μg/ml of DNase I (Sigma Chemical Corp.). The chromatin was then removed by addition of 2 M $(NH_4)_2SO_4$ dropwise to a final concentration of 0.25 M. What was left behind consisted of the nuclear matrix and the intermediate filaments (Fey et al., 1984). Cells were then fixed with 3.7% paraformaldehyde in CSK-100 buffer and stained using the regular immunofluorescence procedure.

DNA Fragmentation

C6 cells were grown on 100 mm tissue culture dishes to confluence and treated with taxol or vehicle (DMSO) at 37 °C for 72 hr. Cells in each dish were then harvested by trypsinization and spun down at 1,000 g for 5 min. The cell pellet was then lysed in 300 μl of 0.5% Triton X-100 TE buffer (pH 8.0) at room temperature for 15 min, followed by two extractions with phenol/chloroform. Genomic DNA was then precipitated in ethanol at –20 °C overnight. DNA was then collected and treated with 50 μg/ml RNase A (Sigma) in 20 μl TE (pH 8.0) at 37 °C for 1 hr. Ten percent glycerol was added to the sample, and DNA fragments were separated on a 1.8% agarose gel and visualized under an ultra-violet light (Sabbatini and McCormick, 1999).

RESULTS

Subcellular Localization of Tubulin Isotypes in Tumor Cells

The subcellular localization of the tubulin isotypes β_I, β_{II}, β_{III}, and β_{IV} in rat C6 glioma cells, human T98G glioma cells, human MCF-7 breast carcinoma cells, human MDA-MB-435 breast carcinoma cells, and human Hela cervix carcinoma cells was determined by indirect immunofluorescence microscopy using mouse monoclonal antibodies specific for each isotype. As shown in the confocal micrographs, all of these tumor cells express the four β-tubulin isotypes (Fig. 1). β_I, β_{III}, and β_{IV} only appeared in the cytoplasm (Fig. 1), while β_{II} was localized in both the nucleus and the cytoplasm. Compared to the cytoplasmic microtubule network, nuclear β_{II} was more evenly distributed, suggesting that it is probably not in microtubule form. Pre-incubation of the β_{II} antibody with a 200-fold excess of β_{II} peptide blocked the fluorescence (data not shown), while pre-incubation of the β_{II} antibody with a 200-fold excess of the β_I, β_{III}, or β_{IV} peptides did not affect the fluorescence, demonstrating that the β_{II} antibody is specific for β_{II}-tubulin.

Nuclear β_{II}-Tubulin Exists as $\alpha\beta_{II}$ Dimers

The fact that tubulin molecules usually exist in the αβ heterodimer form raises the possibility that α-tubulin is associated with nuclear β_{II}-tubulin. Hence, we determined whether α-tubulin occurs in the nuclei of these cells; indirect immunofluorescence was

performed using a monoclonal antibody specific for tyrosinated α-tubulin. While the cytoplasmic microtubule networks were stained by the antibody, the nuclei did not appear to be fluorescent (data not shown). It is possible that the α-tubulin epitope was masked by chromatin and therefore could only be observed after chromatin was removed. Indeed, after the cytosol and the chromatin were removed, leaving only the nuclear matrix, small fluorescent bodies were observed (not shown). These results suggest that α-tubulin also localizes to the nuclear matrix. In order to confirm the colocalization of α- and β_{II}-tubulin, double immunofluorescence microscopy was performed after *in situ* cell fractionation. The fluorescent patterns of α-tubulin were indeed same as those of β_{II}-tubulin in the same cells (not shown). These results suggest that α-tubulin associates with β_{II}-tubulin in the nuclei of C6, T98G, MCF-7, MDA and Hela cells.

To determine whether nuclear β_{II}-tubulin exists in the form of tubulin dimers in their native state rather than assembled microtubules or denatured tubulin, fluorescein-colchicine was used as a fluorescent probe since colchicine is known to only bind to soluble native tubulin dimers, but not the tubulin in microtubules (Banerjee and Ludueña, 1992). The nuclei of all these tumor cells were stained extensively by fluorescein-colchicine as shown in Fig. 2, suggesting that nuclear β_{II}-tubulin exists in the form of soluble dimers rather than microtubules and that these dimers are functional. No nuclear fluorescence was observed in control experiments in which cells were treated with fluorescein rather than fluorescein-colchicine (data not shown), demonstrating that the nuclear fluorescence obtained with fluorescein-colchicine was due to the binding of colchicine rather than that of the fluorescein moiety.

Nuclear β_{II}-Tubulin Concentrates in the Nucleolus

In order to determine the subnuclear localization of β_{II}-tubulin, *in situ* cell fractionation was performed. We removed the cytosol and the chromatin from these five tumor cells while the nuclear matrix was kept intact. As shown in Fig. 3, nuclear matrix was stained by fluorescein-colchicine. Small bodies apparently corresponding to the nucleoli in the phase contrast pictures were extensively stained, suggesting that tubulin dimers accumulate in the nucleoli of these cells. In order to confirm that β_{II}-tubulin accumulates in the nucleolus, the nuclear matrix of these cells was stained with rhodamine-conjugated β_{II} antibody as well as a monoclonal antibody specific for nucleolin, a nucleolar marker. The fluorescent pattern of β_{II}-tubulin in these cells (Fig. 4, *A*, *D*, *G*, *J*, and *M*) resembles that of fluorescein-colchicine staining (Fig. 3, *A*, *C*, *E*, *G*, and *H)*. Superimposing the confocal micrographs of β_{II}-tubulin staining (red) and nucleoli staining (green) shows that β_{II}-tubulin colocalizes with nucleolin in the nucleolus (yellow spots), while the rest of the nucleus was stained with a light red color (Fig. 4, *C*, *F*, *I*, *L*, and *O*). These results confirmed that β_{II}-tubulin localizes in the nuclear matrix and concentrates in the nucleoli of C6, T98G, MCF-7, MDA, and Hela cells.

The Effects of Taxol on Nuclear β_{II}-Tubulin in C6 cells

When C6 cells were treated with taxol at a concentration as low as 20 nM, nuclear β_{II}-tubulin began to rearrange into aggregated forms (Fig. 5*C*), and multiple micronuclei were observed in the same cells (Fig. 5*D*). Since micronucleation is a marker for apoptosis (Hoshino et al., 2001), our results suggested that these cells were undergoing

apoptosis. When C6 cells were treated with 1 μM taxol, nuclear β_{II}-tubulin began to diminish (Fig. 5*E*), and the cytoplasmic microtubules were strongly bundled, which is one of taxol's known effects (Schiff and Horwitz, 1980; Turner and Margolis, 1984; Roberts et al., 1989). Confocal microscopy confirmed the depletion of nuclear β_{II}-tubulin caused by taxol treatment (not shown). Meanwhile, the appearance of the micronuclei in certain cells in Fig. 5*F* suggest that these cells were apoptotic. Though taxol binds specifically and reversibly to the β-tubulin subunit in the microtubules *in vitro* (Caplow et al., 1994), the uptake of taxol into cells is not easily reversible (Jordan et al., 1993, 1996). To determine whether the effect of taxol on C6 cells is reversible, we incubated C6 cells with taxol for 24 hr; the cells were then washed and kept in normal growth medium for 48 hr. It turned out that the rearrangement and depletion of nuclear β_{II}-tubulin were not reversed (data not shown), suggesting an irreversible effect of taxol on C6 cells. Numbers of C6 cells lacking nuclear β_{II} or showing micronuclei treated with or without taxol were counted and plotted against the concentration of taxol. As shown in Figure 6*A*, nuclear β_{II} was depleted in a concentration-dependent manner in response to taxol treatment. Meanwhile, the percentage of apoptotic cells increased with increasing concentrations of taxol up to 5 μM but remained almost the same with higher concentrations (Fig. 6*B*), suggesting that mechanism(s) other than nuclear β_{II} depletion are involved in the apoptotic pathway in C6 cells at very high taxol concentrations. The effect of taxol on C6 cell apoptosis was confirmed by DNA fragmentation analysis. A DNA ladder was observed when C6 cells were treated with 5 μM, 20 μM, or 50 μM taxol, while the genomic DNA of the untreated C6 cells was intact, indicated by the single band in the agarose gel.

To visualize the localization of taxol inside cells, 1 μM 7-O-[N-(2,7-difluoro-4'-fluoresceincarbonyl)-L-alanyl]taxol (flutax-2) was used to treat C6 cells at 37 °C for 3 hr. As shown in Fig. 7, flutax-2 stained the cytoplasm, which was probably due to the binding of taxol to the cytoplasmic microtubules since taxol has been found to bind directly to microtubules in cells (Manfredi et al., 1982). In addition, the nucleoli were stained by flutax-2, suggesting that tubulin binding to flutax-2 was enriched in the nucleoli though taxol binds to soluble tubulin dimers with a reduced affinity (Parness and Horwitz, 1981, Takoudju et al., 1988; Diaz et al., 1993; Sengupta et al., 1995). This result is consistent with the fluorescein-colchicine staining of the nuclear matrix in C6 cells, in which an accumulation of tubulin dimers in the nucleolus was observed (Fig. 3). As a control, incubation with fluorescein did not show any fluorescence of C6 cells (data not shown). Since taxol has higher specificity for β_{II}-tubulin (Derry et al., 1997) and only β_{II} localizes in the nucleoli of C6 cells (Figs. 2 and 3), these results support the hypothesis that taxol can indeed bind to nuclear β_{II} *in vivo* though with low affinity.

As shown in Figure 5, taxol induces disappearance of nuclear β_{II}-tubulin; this is accompanied by the concomitant appearance of β_{II} in what appear to be bundles of microtubules in the cytoplasm. It is natural to hypothesize that taxol induces β_{II} to migrate from the nucleus into the cytoplasm. However, one could imagine a different model, one in which taxol somehow causes the nuclear β_{II} to be degraded or masked and at the same time, more β_{II} is synthesized de novo in the cytoplasm. By this model, there would be no migration of β_{II} from the nucleus into the cytoplasm. In order to test this second hypothesis, we treated C6 cells with cycloheximide, a protein synthesis inhibitor,

for 1 hr prior to taxol treatment. No nuclear β_{II} depletion was observed when cells were treated only with cycloheximide (Fig. 8). However, the percentage of cells lacking nuclear β_{II}-tubulin pretreated with cycloheximide was higher than that of cells only treated with taxol. These results suggest that ongoing new protein synthesis is not required by taxol to deplete nuclear β_{II}-tubulin. Moreover, inhibition of ongoing protein synthesis potentiates the depletion of nuclear β_{II}-tubulin caused by taxol in C6 cells, yet the depletion is initiated by taxol.

The Effects of Other Anti-Tubulin Drugs on Nuclear β_{II}-Tubulin in C6 Cells

C6 cells were treated with different concentrations of colchicine or nocodazole for 24 hr. As shown in Fig. 9, *A* and *C*, neither 10 μM colchicine nor 10 μM nocodazole affected nuclear β_{II}-tubulin content while the cytoplasmic microtubule networks were totally disrupted. Moreover, no nuclear β_{II} depletion was observed at colchicine or nocodazole concentrations of 10 nM, 100 nM, 1 μM, and 100 μM (data not shown). Since colchicine (Banerjee et al., 1992) and nocodazole (Xu et al., 2001) have been found to have higher specificity for $\alpha\beta_{IV}$ while taxol has higher specificity for $\alpha\beta_{II}$ than for other tubulins (Derry et al., 1997), these results support the hypothesis that anti-tubulin drugs with lower relative affinity for β_{II}-tubulin are less effective in depleting nuclear β_{II}-tubulin. Multiple nuclei were observed in cells treated with either colchicine or nocodazole (Fig. 9, *B* and *D*), suggesting that colchicine and nocodazole can cause apoptosis in C6 cells by affecting cytoplasmic microtubules.

DISCUSSION

We investigated the subcellular localization of β_I-, β_{II}-, β_{III}-, and β_{IV}-tubulin in five different tumor cell types, including C6 glioma cells, T98G glioma cells, MCF-7 breast carcinoma cells, MDA-MB-435 breast carcinoma cells, and Hela cervix carcinoma cells. In all these cells, only β_{II}-tubulin was localized in both the nucleus and the cytoplasm, while the other isotypes were only observed in the cytoplasm. Although its function is not yet known, nuclear β_{II}-tubulin has been observed previously. Ranganathan et al (1997) reported that β_{II}-tubulin was expressed to a greater extent in malignant compared to benign prostate glands, and that some nuclei of the neoplastic prostate glands showed intense β_{II} isotype staining. The existence of nuclear β_{II}-tubulin was also observed in a breast tumor in situ as well as in cultured rat kidney mesangial cells (Walss et al., 1999, 2000; Walss-Bass et al., 2002). In contrast, biopsy samples of several normal human tissues using immunoperoxidase staining did not show any evidence for the existence of nuclear β_{II} (Roach et al., 1998). Collectively, the nuclear localization of β_{II}-tubulin seems to be a unique feature of tumor cells. Since it has been observed that β_{II}-tubulin forms part of the spindle and the midbody during mitosis, and re-enters the nucleus at the end of telophase (Walss et al., 1999), it is possible that β_{II}-tubulin is stored in the nucleus during interphase to be readily available for use during mitosis, where it may conceivably play a role in regulating the process. In other words, nuclear tubulin could be a "passenger: protein, a nuclear protein that has no nuclear function per se but whose nuclear location positions it appropriately to perform some function during mitosis. Other proteins have been suggested to be "passenger" proteins; these include mitosin, NuMA and p62 as has

been proposed for other proteins (Zhu et al., 1997; Saredi *et al.*, 1996; Warner and Sloboda, 1999). However, the hypothesis that nuclear tubulin is a passenger protein remains to be tested; it will also be interesting to understand why it is β_{II}, rather than the other isotypes, that occurs in the nuclei of tumor cells.

Nuclear β_{II} did not appear to be in the form of microtubule networks (Fig. 1, *B, F, J, N,* and *R*), but rather as an $\alpha\beta_{II}$-heterodimer, demonstrated by fluorescein-colchicine staining (Figs. 2 and 3) and double immuno-staining of α- and β_{II}-tubulin (not shown). Our results also suggest that the $\alpha\beta_{II}$-heterodimer is a component of the nuclear matrix and accumulates in the nucleoli of C6, T98G, MCF-7, MDA, and Hela cells (Figs. 3 and 4). Nucleolar loclization of β_{II}-tubulin was shown by co-localization with the nucleolar marker nucleolin (Fig. 4). We have shown elsehwere that β_{II}-tubulin co-localizes with RNA in the nucleus, also consistent with nucleolar localization (Walss-Bass et al., 2002). Another cytoskeleton protein, F-actin, has been found in the nuclei of a variety of cell types (Clark and Merriam, 1977; Fukui, 1978; Fukui and Katsumaru, 1979; Clark and Rosenbaum, 1979; Osborn and Weber, 1980; Welch and Suhan, 1985; De Boni, 1994; Yan et al., 1997) and has been suggested to play a role in RNA export or other intranuclear transport phenomena (Pederson, 1998). The accumulation of $\alpha\beta_{II}$-tubulin in the nucleolus raises the possibility that $\alpha\beta_{II}$-tubulin is involved in certain functions in the nucleolar area, possibly RNA export or transcription. On the other hand, as a component of the nuclear matrix, the skeleton of the nucleus, nuclear $\alpha\beta_{II}$-tubulin may play a role in maintaining nuclear shape.

Being synthesized in the cytoplasm, β_{II}-tubulin does not contain any known nuclear localization signal (NLS) (Kalderon et al., 1984), suggesting other mechanism(s) may be involved in localizing β_{II}-tubulin in the nucleus. Earnshaw and Bernat (1991) found that the INCENP's and other proteins could enter the nucleus by binding to chromosomes during mitosis. Thus, we hypothesize that β_{II}-tubulin localizes in the nucleus by remaining attached to chromatin after cell division. This hypothesis is supported by the findings that tubulin interacts with chromatin *in vitro* (Mithieux et al., 1986), and that cell division may be necessary for β_{II}-tubulin to enter the nucleus (Walss-Bass et al., 2001).

Since of the four β isotypes we are able to study, β_{II} is the only one present in the nucleus, we examined the effect on nuclear β_{II}-tubulin of anti-tubulin drugs of known isotype specificity. We first characterized the effect on nuclear β_{II} of taxol, which has higher specificity for the $\alpha\beta_{II}$ dimers than for the other isotypes (Derry et al.,1997). Our results suggest that, depending on the concentration, taxol has two effects on C6 cells. At nanomolar concentrations, taxol affects the cytoplasmic microtubules and causes the rearrangement of nuclear β_{II}-tubulin as well as cell apoptosis (Fig. 5, *C* and *D*); at micromolar concentrations, taxol additionally depletes nuclear β_{II}-tubulin (Figs. 5, *E* and *F*, 7, 8, and 9). As an anti-tumor drug, taxol is known to freeze microtubule dynamics and induce cell apoptosis at low concentrations (<10 nM) (Jordan et al., 1993). This is probably the mechanism by which nanomolar concentrations of taxol affect the cytoskeleton and apoptosis in C6 cells though other possibilities cannot be excluded. To the best of our knowledge, the depletion of nuclear β_{II}-tubulin caused by micromolar concentrations of taxol is a novel finding. Based on its potential function(s) involved in

tumor cell proliferation, nuclear β_{II} may be a novel target for taxol in the anti-tumor process. Multiple nuclei were observed even at 20 nM taxol treatment when nuclear β_{II} was not depleted (Fig. 5*D*), suggesting that the depletion of nuclear β_{II}-tubulin may not be essential for C6 cell apoptosis. However, this does not exclude the possibility that nuclear β_{II} depletion may lead to apoptosis.

Pretreatment with cycloheximide increased the percentage of nuclear β_{II} depletion in C6 cells (Fig. 8), suggesting that the inhibition of ongoing new protein synthesis can potentiate the depletion of nuclear β_{II}-tubulin caused by taxol. A possible model for the depletion of nuclear β_{II} is that there is an equilibrium between nuclear β_{II} and cytoplasmic β_{II}, and that taxol treatment lowers the concentration of cytoplasmic β_{II} thus driving the equilibrium toward the direction of cytoplasmic β_{II}. Cycloheximide treatment may further lower the concentration of cytoplasmic β_{II}, while taxol seems to be essential to initiate nuclear β_{II} depletion since cycloheximide alone cannot cause this effect (data not shown). The proteins involved in the translocation of β_{II} are still unknown. One of the candidates can be Ran, a small nuclear GTPase, because of its identified roles in both regulating microtubules (Desai and Hyman, 1999) and nuclear protein transport (Melchior and Gerace, 1995; Azuma and Dasso, 2000; Moore, 2001). However, this possibility remains to be tested.

If the effect of taxol on nuclear β_{II}-tubulin is due to the higher specificity of taxol for $\alpha\beta_{II}$-tubulin, one would expect that the effect would be less with drugs of lower specificity for $\alpha\beta_{II}$. Two anti-tubulin drugs, colchicine (Banerjee and Ludueña, 1992)

and nocodazole (Xu et al., 2002), both binding best to $\alpha\beta_{IV}$, were used to treat C6 cells. No nuclear β_{II} depletion was observed in C6 cells treated with either colchicine or nocodazole (Fig. 9, *A* and *C*). This supports the hypothesis that drugs with lower specificity for $\alpha\beta_{II}$-tubulin are less effective in altering nuclear β_{II}-tubulin content. On the other hand, multiple nuclei were also observed when C6 cells were treated with either colchicine or nocodazole (Fig. 9, *B* and *D*), which is probably due to the known effect of these drugs on cytoplasmic microtubules.

Our results raise the possibility that nuclear β_{II}-tubulin may be widespread in cancer cells. They also suggest that nuclear β_{II}-tubulin represents a separate population of tubulin with a unique set of properties; such a population may constitute a novel target for anti-tumor drugs.

ACKNOWLEDGMENTS

We thank Dr. Martin Adamo for C6 and T98G cells, Dr. Robert Klebe for MCF-7 cells, Dr. Susan Mooberry for MDA and Hela cells, and Dr. Matthew Suffness for taxol. We appreciate technical instruction in confocal microscopy from Dr. Victoria Centonze Frohlich. We also thank Dr. Asok Banerjee, Dr. Asish Chaudhuri, Veena Prasad, Consuelo Walss-Bass, Patricia Schwarz and Mohua Banerjee for technical support and helpful advice. We are grateful to Dr. Larry Barnes, Dr. Jean Jiang, and Dr. Jeffrey Kreisberg for helpful discussion and advice. This study was supported by grants to R.F.L. from the NIH (CA26376), US Army BCRP (DAMD17-01-1-0411), and the Welch Foundation (AQ-0726) as well as grant P30 CA54174 from the NIH to the San Antonio Cancer Institute.

REFERENCES

Azuma Y, Dasso M. 2000. The role of Ran in nuclear function. Curr. Opin. Cell Biol. 12:302-307.

Banerjee A, Ludueña RF. 1992. Kinetics of colchicine binding to purified β-tubulin isotypes from bovine brain. J. Biol. Chem. 267:13335-13339.

Banerjee A, Roach MC, Wall KA, Lopata MA, Cleveland DW, Ludueña RF. 1988. A monoclonal antibody against the type II isotype of β-tubulin. Preparation of isotypically altered tubulin. J. Biol. Chem. 263:3029-3034.

Banerjee A, Roach MC, Trcka P, Ludueña RF. 1990. Increased microtubule assembly in bovine brain tubulin lacking the type III isotype of β-tubulin. J. Biol. Chem. 265:1794-1799.

Banerjee A, Roach MC, Trcka P, Ludueña RF. 1992. Preparation of a monoclonal antibody specific for the class IV isotype of β-tubulin. Purification and assembly of $\alpha\beta_{II}$, $\alpha\beta_{III}$, and $\alpha\beta_{IV}$ tubulin dimers from bovine brain. J. Biol. Chem. 267:5625-5630.

Bryan J, Wilson L. 1971. Are cytoplasmic microtubules heteropolymers? Proc. Natl. Acad. Sci. USA 68:1762-1766.

Caplow M, Shanks J, Ruhlen R. 1994. How taxol modulates microtubule disassembly. J. Biol. Chem. 269:23399-23402.

Clark TG, Merriam RW. 1977. Diffusible and bound actin nuclei of Xenopus laevis oocytes. Cell 12:883-891.

Clark TG, Rosenbaum JL. 1979. An actin filament matrix in hand-isolated nuclei of X. laevis oocytes. Cell 18:1101-1108.

De Boni U. 1994. The interphase nucleus as a dynamic structure. Int. Rev. Cytol. 150:149-171.

Derry WB, Wilson L, Khan IA, Ludueña RF, Jordan MA. 1997. Taxol differentially modulates the dynamics of microtubules assembled from unfractionated and purified β-tubulin isotypes. Biochemistry 36:3554-3562.

Desai A, Hyman A. 1999. Microtubule cytoskeleton: No longer an also Ran. Curr. Biol. 9:704-707.

Diaz JF, Menendez M, Andreu JM. 1993. Thermodynamics of ligand-induced assembly of tubulin. Biochemistry 32:10067-10077.

Earnshaw WC, Bernat RL. 1991. Chromosomal passengers: toward an integrated view of mitosis. Chromosoma 100:139-146.

Fey EG, Wan KM, Penman S. 1984. Epithelial cytoskeletal framework and nuclear matrix-intermediate filament scaffold: three-dimensional organization and protein composition. J. Cell Biol. 98:1973-1984.

Fukui Y. 1978. Intranuclear actin bundles induced by dimethyl sulfoxide in interphase nucleus of Dictyostelium. J. Cell Biol. 76:146-157.

Fukui Y, Katsumaru H. 1979. Nuclear actin bundles in Amoeba, Dictyostelium and human HeLa cells induced by dimethyl sulfoxide. Exp. Cell Res. 120:451-455.

Hoshino R, Tanimura S, Watanabe K, Kataoka T, Kohno M. 2001. Blockade of the extracellular signal-regulated kinase pathway induces marked G1 cell cycle arrest and apoptosis in tumor cells in which the pathway is constitutively activated. J. Biol. Chem. 276:2686-2692.

Jordan MA, Toso RJ, Thrower D, Wilson L. 1993. Mechanism of mitotic block and inhibition of cell proliferation by taxol at low concentrations. Proc. Natl. Acad. Sci. USA 90:9552-9556.

Jordan MA, Wendell K, Gardiner S, Derry WB, Copp H, Wilson L. 1996. Mitotic block induced in HeLa cells by low concentrations of paclitaxel (Taxol) results in abnormal mitotic exit and apoptotic cell death. Cancer Res. 56:816-825.

Kalderon D, Richardson WD, Markham AF, Smith AE. 1984. Sequence requirements for nuclear location of simian virus 40 large-T antigen. Nature (Lond.) 311:33-38.

Ludueña RF. 1998 Multiple forms of tubulin: different gene products and covalent modifications. Int. Rev. Cytol. 178:207-275.

Ludueña RF, Shooter EM, Wilson L. 1977. Structure of the tubulin dimer. J. Biol. Chem. 252:7006-7014.

Manfredi JJ, Parness J, Horwitz SB. 1982. Taxol binds to cell microtubules. J. Cell Biol. 94:688-696.

Melchior F, Gerace L. 1995. Mechanisms of nuclear protein import. Curr. Opin. Cell Biol. 7:310-318.

Mithieux G, Roux B, Rousset B. 1986. Tubulin-chromatin interactions: evidence for tubulin-binding sites on chromatin and isolated oligonucleosomes. Biochim. Biophys. Acta 888:49-61.

Moore J. 2001. The Ran-GTPase and cell-cycle control. BioEssays 23:77-85.

Osborn M, Weber K. 1980. Dimethylsulfoxide and the ionophore A23187 affect the arrangement of actin and induce nuclear actin paracrystals in PtK2 cells. Exp. Cell Res. 129:103-114.

Parness J, Horwitz SB. 1981. Taxol binds to polymerized tubulin in vitro. J. Cell Biol. 91:479-487.

Pederson T. 1998. Thinking about a nuclear matrix. J. Mol. Biol. 277:147-159.

Ranganathan S, Salazar H, Benetatos CA, Hudes GR. 1997. Immunohistochemical analysis of β-tubulin isotypes in human prostate carcinoma and benign prostatic hypertrophy. Prostate 30:263-268.

Roach MC, Boucher VL, Walss C, Ravdin PM, Ludueña RF. 1998. Preparation of a monoclonal antibody specific for the class I isotype of β-tubulin: the β isotypes of tubulin differ in their cellular distributions within human tissues. Cell Motil. Cytoskel. 39:273-285.

Roberts JR, Rowinsky EK, Donehower RC, Robertson J, Allison, D. C. 1989. Demonstration of the cell cycle positions of taxol-induced "asters" and "bundles" by sequential measurements of tubulin immunofluorescence, DNA content, and

autoradiographic labeling of taxol-sensitive and -resistant cells. J. Histochem. Cytochem. 37:1659-1665.

Sabbatini P, McCormick F. 1999. Phosphoinositide 3-OH kinase (PI3K) and PKB/Akt delay the onset of p53-mediated, transcriptionally dependent apoptosis. J. Biol. Chem. 274:24263-24269.

Saredi A, Howard L, Compton DA. 1996. NuMA assembles into an extensive filamentous structure when expressed in the cell cytoplasm. J. Cell Sci. 109:619-630.

Schiff PB, Horwitz SB. 1980. Taxol stabilizes microtubules in mouse fibroblast cells. Proc. Natl. Acad. Sci. USA 77:1561-1565.

Schiff PB, Horwitz SB. 1981. Taxol assembles tubulin in the absence of exogenous guanosine 5'-triphosphate or microtubule-associated proteins. Biochemistry 20:3247-3252.

Sengupta S, Boge TC, George GI, Himes RH. 1995. Interaction of a fluorescent paclitaxel analogue with tubulin. Biochemistry 34:11889-11894.

Takoudju M, Wright M, Chenu J, Gueritte-Voegelein F, Guenard D. 1988, Absence of 7-acetyl taxol binding to unassembled brain tubulin. FEBS Lett. 227:96-98.

Turner PF, Margolis RL. 1984. Taxol-induced bundling of brain-derived microtubules. J. Cell Biol. 99:940-946.

Walss C, Kreisberg JI, Ludueña RF. 1999. Presence of the β_{II} isotype of tubulin in the nuclei of cultured mesangial cells from rat kidney. Cell Motil. Cytoskeleton 42:274-284.

Walss C, Barbier P, Banerjee M, Bissery MC, Ludueña RF, Fellous A. 2000. Nuclear tubulin as a possible marker for breast cancer cells. Proc. Amer. Assoc. Cancer Res. 41:553.

Walss-Bass C, Kreisberg JI., Ludueña RF. 2001. Mechanism of localization of β_{II}-tubulin in the nuclei of cultured rat kidney mesangial cells. Cell Motil. Cytoskeleton 49:208-217.

Walss-Bass C, Xu K, David S, Fellous A, Ludueña RF. 2002. Occurrence of nuclear β_{II}-tubulin in cultured cells. Cell Tissue Res., in press.

Warner AK, Sloboda RD. 1999. C-terminal domain of the mitotic apparatus protein p62 targets the protein to the nucleolus during interphase. Cell Motil Cytoskeleton 44:68-80.

Welch WJ, Suhan JP. 1985. Morphological study of the mammalian stress response: characterization of changes in cytoplasmic organelles, cytoskeleton, and nucleoli, and appearance of intranuclear actin filaments in rat fibroblasts after heat-shock treatment. J. Cell Biol. 101:1198-1211.

Wilson L, Jordan MA. 1994. Pharmacological probes in microtubule function. In: Hyams JS and Lloyd CW, editors. Microtubules, New York: Wiley-Liss, p 59-83.

Wilson L, Jordan MA, Morse A, Margolis RL. 1982. Interaction of vinblastine with steady-state microtubules in vitro. J. Mol. Biol. 159:125-149.

Xu K, Schwarz PM, Ludueña RF. 2002. Interaction of nocodazole with tubulin isotypes. Drug Development Res., in press.

Yan C, Leibowitz, N, Melese T. 1997. A role for the divergent actin gene, ACT2, in nuclear pore structure and function. EMBO J. 16:3572-3586.

Zhu X, Ding L, Pei G. 1997. Carboxyl-terminus of mitosin is sufficient to confer spindle pole localization. J Cell Biochem 66:441-449.

FIGURE LEGENDS

Figure 1. Subcellular localizations of tubulin β_I, β_{II}, β_{III}, β_{IV} in several carcinoma cells. Indirect immunofluorescence was performed using monoclonal anti-β_I, anti-β_{II}, anti-β_{III}, and anti-β_{IV} followed by confocal microscopy. C6 cells are shown in *A*, *B*, *C*, and *D*; T98G cells are shown in *E*, *F*, *G*, and *H*; MCF-7 cells are shown in *I*, *J*, *K*, and *L*; MDA-MB-435 cells are shown in *M*, *N*, *O*, and *P*; Hela cells are shown in *Q*, *R*, *S*, and *T*. *A*, *E*, *I*, *M*, and *Q*: localization of β_I; *B*, *F*, *J*, *N*, and *R*: localization of β_{II}; *C*, *G*, *K*, *O*, and *S*: localization of β_{III}; *D*, *H*, *L*, *P*, and *T*: localization of β_{IV}. Bar = 10 μ.

Figure 2. Localization of tubulin dimer in several carcinoma cells. Cells were stained with 0.1 mg/ml fluorescein-colchicine and visualized by confocal microscopy. *A*: C6 cells; *B*: T98G cells; *C*: MCF-7 cells; *D*: MDA-MB-435 cells; *E*: Hela cells. Bar = 10 μ.

Figure 3. Localization of tubulin dimer in the nuclear matrix of several carcinoma cells. Cells were grown on glass coverslips, and nuclear matrix was prepared as described in Materials and Methods. The extracted cells were then fixed and incubated with 0.1 mg/ml fluorescein-colchicine. Confocal micrographs showing the localization of tubulin dimer are shown in *A*, *C*, *E*, *G*, and *I*; Phase contrast micrographs showing the nuclei and the nucleoli in the same cells are shown in *B*, *D*, *F*, *H*, and *J*. *A* and *B*: C6

cells; *C* and *D*: T98G cells; *E* and *F*: MCF-7 cells; *G* and *H*: MDA-MB-435 cells; *I* and *J*: Hela cells. Bar = 10 μ.

Figure 4. Accumulation of β_{II}-tubulin in the nucleoli of several carcinoma cells. Cells were extracted as described in Materials and Methods and incubated with the monoclonal anti-nucleolin primary antibody followed by with fluorescein-conjugated secondary antibody. The same cells were then incubated with rhodamine-conjugated anti-β_{II} primary antibody. Confocal micrographs showing the localization of β_{II}-tubulin (red) were superimposed on those showing the localization of nucleoli (green) in the same cells. *A*, *D*, *G*, *J*, and *M*: β_{II}-tubulin staining in the nuclear matrix of C6 cells, T98G cells, MCF-7 cells, MDA-MB-435 cells, and Hela cells, respectively; *B*, *E*, *H*, *K*, and *N*: nucleolin staining in the nuclear matrix of C6 cells, T98G cells, MCF-7 cells, MDA-MB-435 cells, and Hela cells, respectively; *C*, *F*, *I*, *L*, and *O*: superimposed micrographs of *A* and *B*, *D* and *E*, *G* and *H*, *J* and *K*, and *M* and *N*, respectively. Bar = 10 μ.

Figure 5. The effects of taxol on nuclear β_{II}-tubulin in C6 cells. Cells were treated with indicated concentration of taxol for 24 hr. Cells stained with anti-β_{II} are shown in *A*, *C*, and *E*; the same cells stained with DAPI are shown in *B*, *D*, and *F*. *A* and *B*: C6 cells in the absence of taxol. *C* and *D*: C6 cells incubated with 20 nM taxol. *E* and *F*: C6 cells incubated with 1 μM taxol. Arrows point to the cells depleted of nuclear β_{II}-tubulin but clearly containing bundles of microtubules in the cytoplasm. Other cells still retain some nuclear β_{II}. Bar = 10 μ.

Figure 6. The effects of taxol on nuclear β_{II}-tubulin depletion and micronucleation in C6 cells. Cells were treated with increasing concentrations of taxol for 24 hr followed by immunofluorescence. About 500 cells were counted for each treatment. Results are presented as mean ± SEM for three separate experiments.

Figure 7. Flutax-2 stains both the cytoplasm and the nucleoli of C6 cells. A concentration of 1 μM for flutax-2 was chosen for the 3 hr incubation with C6 cells. Then cells were fixed by 3.7% paraformaldehyde. The fixed cells were then washed with PBS and mounted on glass slides prior to confocal microscopy. At this concentration, taxol causes considerable diminution of nuclear β_{II}, but even after 24 hr of treatment with 1 μM taxol, certain cells still retain some nuclear β_{II} (Fig. 6*E*). Bar = 10 μ.

Figure 8. The effect of cycloheximide on taxol-induced nuclear β_{II} depletion in C6 cells. Cells were incubated with 1 μg/ml cycloheximide for 1 hr, followed by treatment with taxol for 24 hr. Cells were then stained with β_{II} antibody. About 500 cells were counted for each treatment. Results are presented as mean ± SEM for three separate experiments.

Figure 9. The effects of colchicine and nocodazole on nuclear β_{II}-tubulin in C6 cells. Cells were treated with colchicine or nocodazole for 24 hr followed by immunostaining with β_{II} antibody and DAPI. β_{II} staining is shown in *A* and *C*; DAPI staining is shown in *B* and *D*. *A* and *B*: cells treated with 10 μM colchicine. *C* and *D*: cells treated with 10 μM nocodazole. Bar = 10 μ.

Figure 1

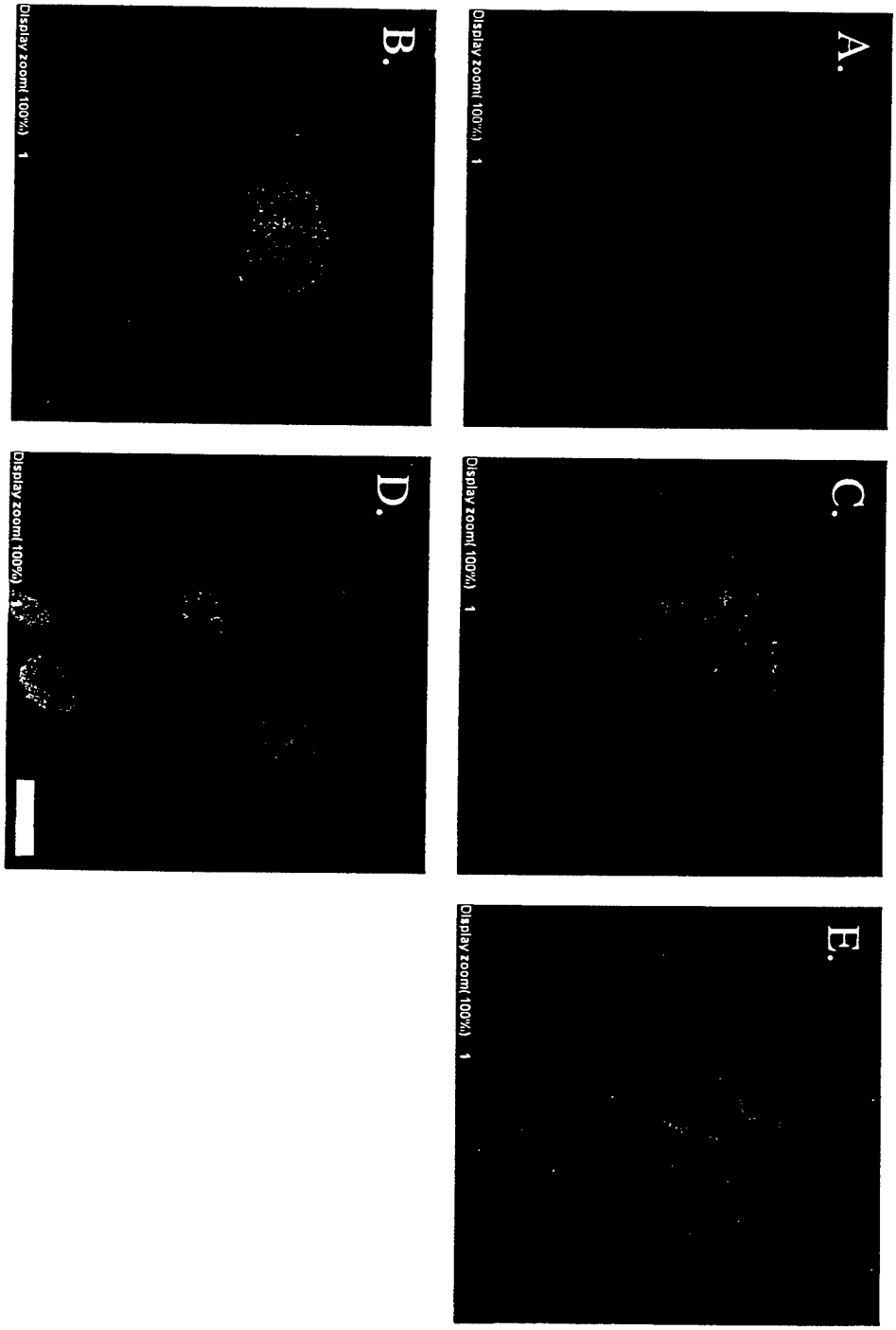
A.
Display zoom(100%) 1
B.
Display zoom(100%) 1
C.
Display zoom(100%) 1
D.
Display zoom(100%) 1
E.
Display zoom(100%) 1

Figure 2

Figure 3

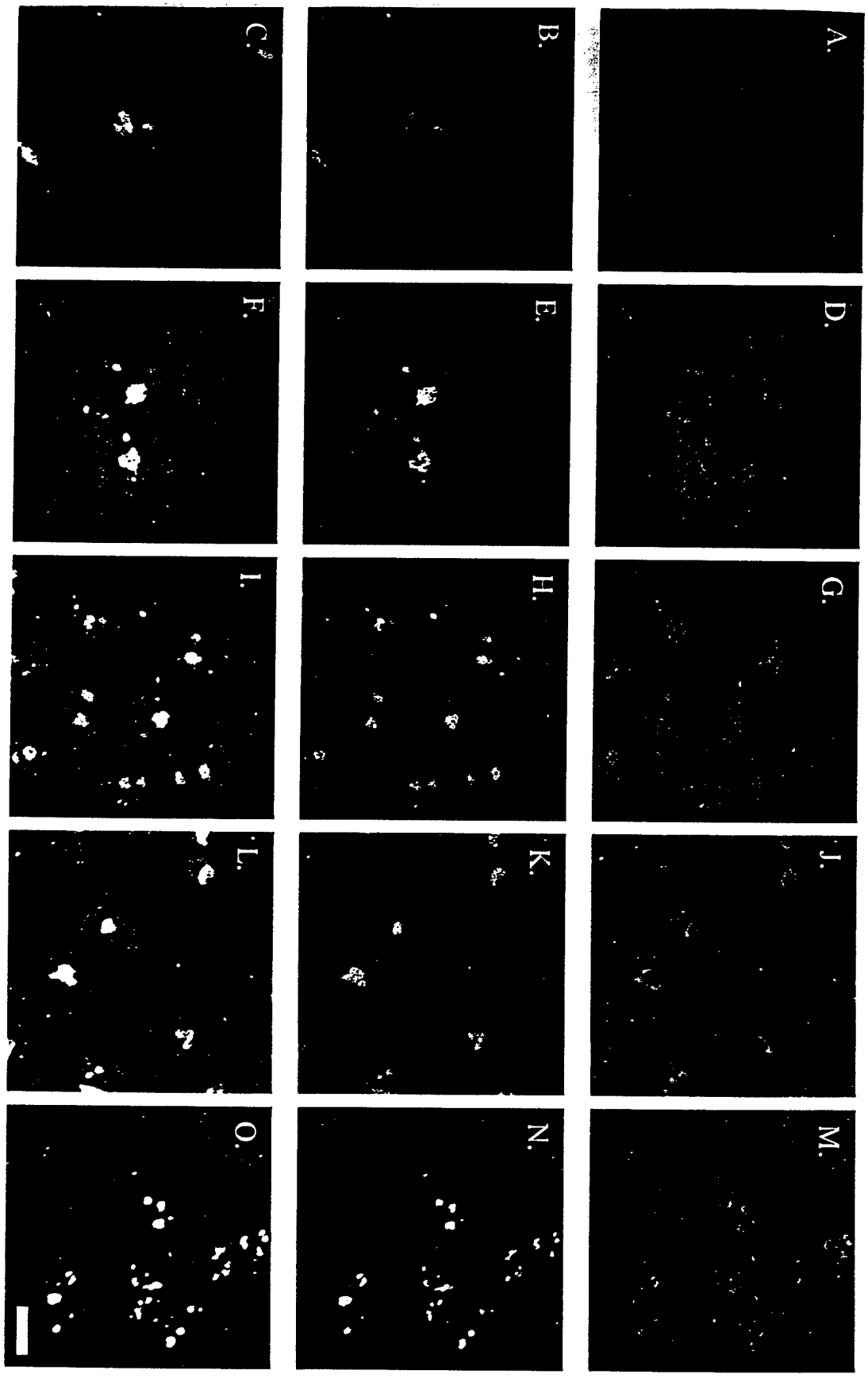

Figure 4

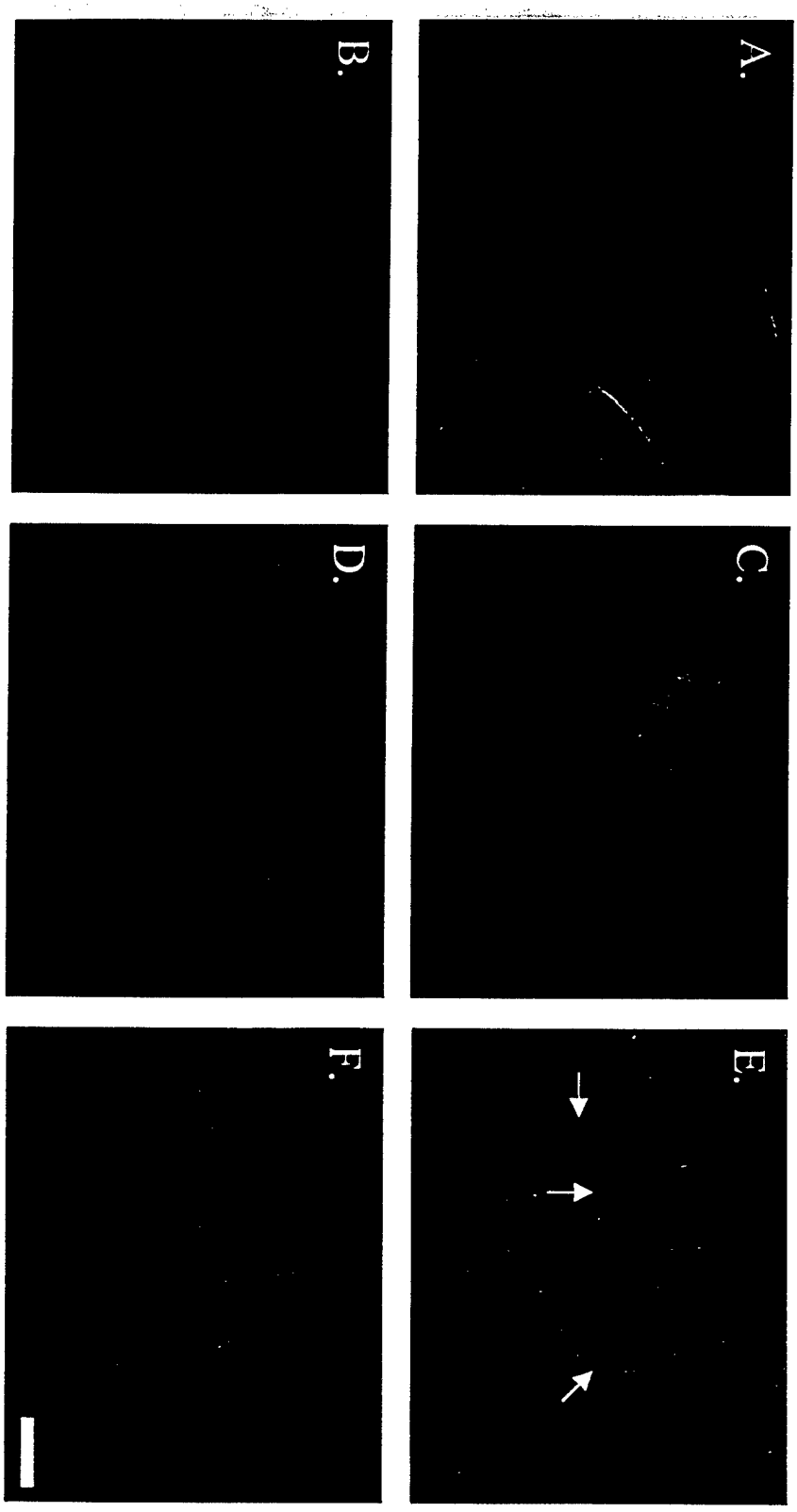

Figure 5

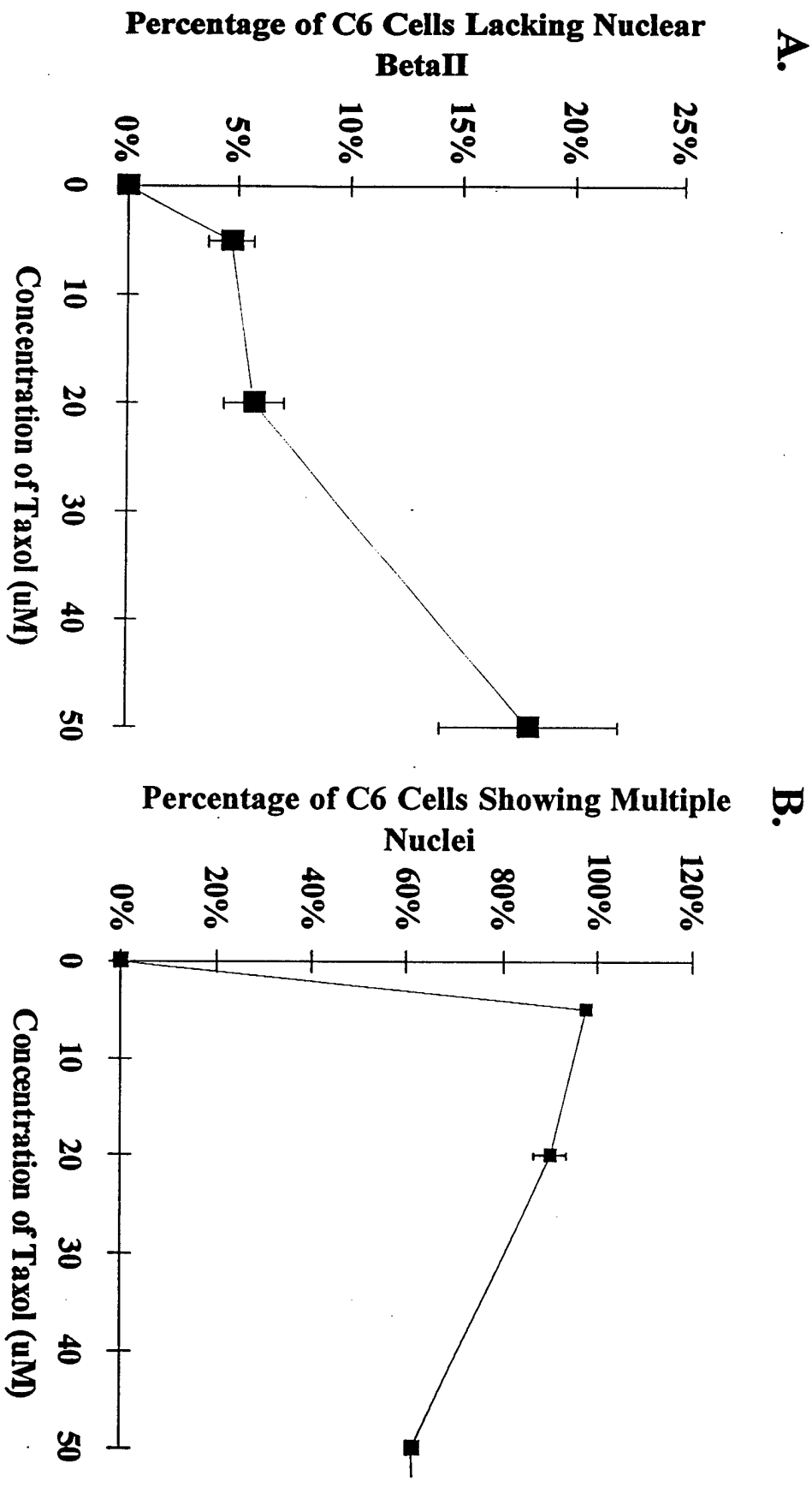
A.
Percentage of C6 Cells Lacking Nuclear BetaII
0%
5%
10%
15%
20%
25%
0
10
20
30
40
50
Concentration of Taxol (uM)
B.
Percentage of C6 Cells Showing Multiple Nuclei
0%
20%
40%
60%
80%
100%
120%
0
10
20
30
40
50
Concentration of Taxol (uM)

Figure 6

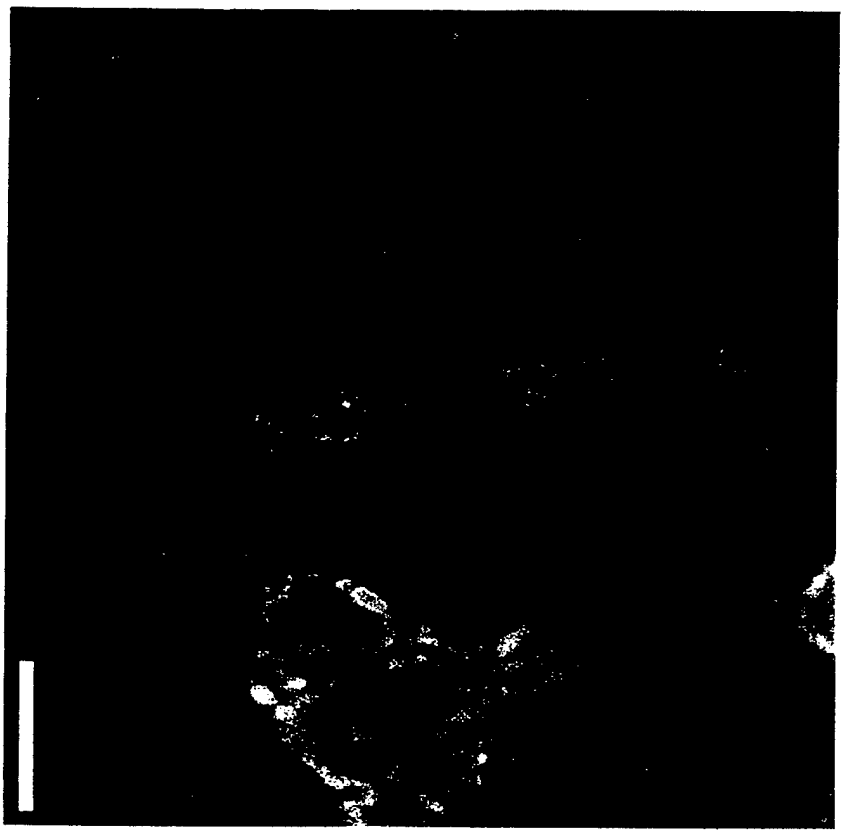

Figure 7

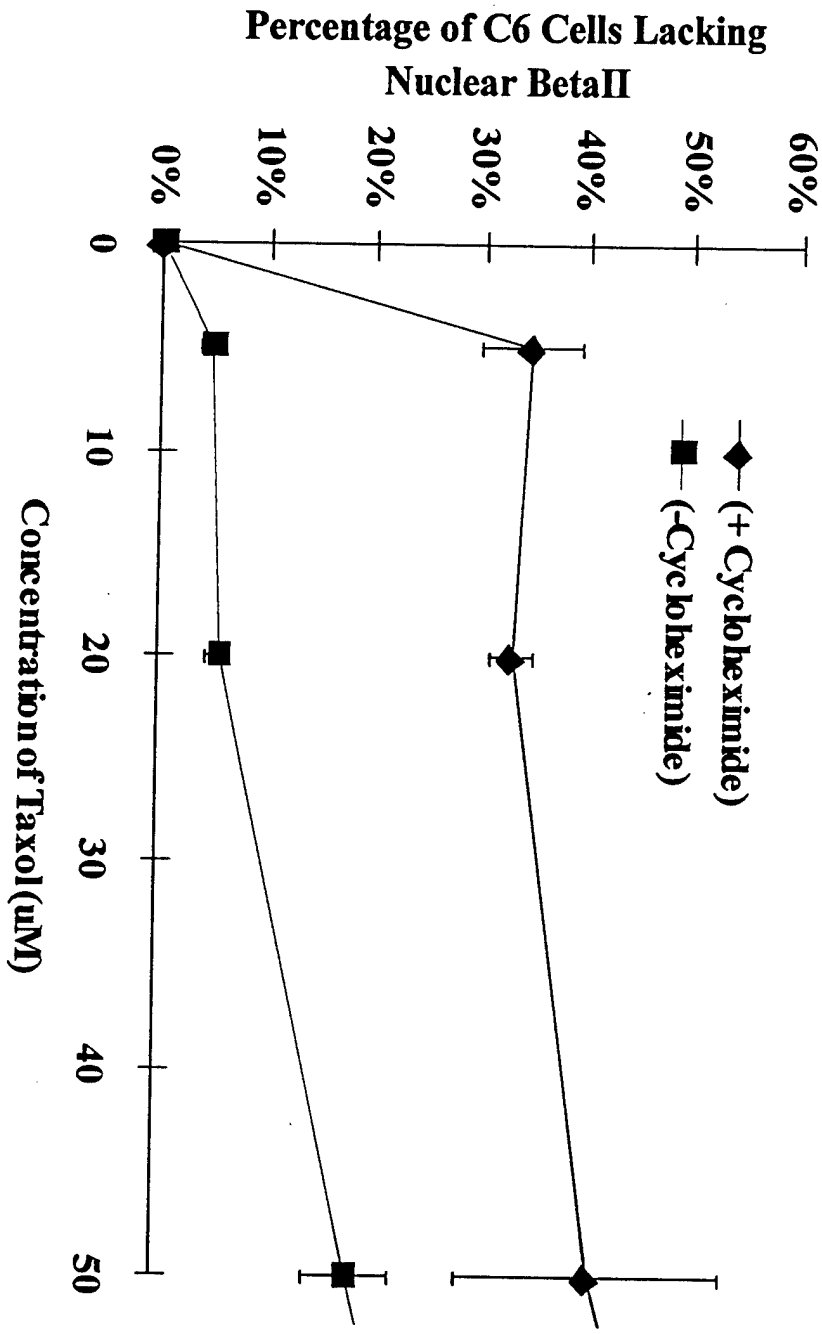
Percentage of C6 Cells Lacking Nuclear BetaII
0%
10%
20%
30%
40%
50%
60%
0
10
20
30
40
50
Concentration of Taxol (uM)
(+ Cycloheximide)
(-Cycloheximide)

Figure 8

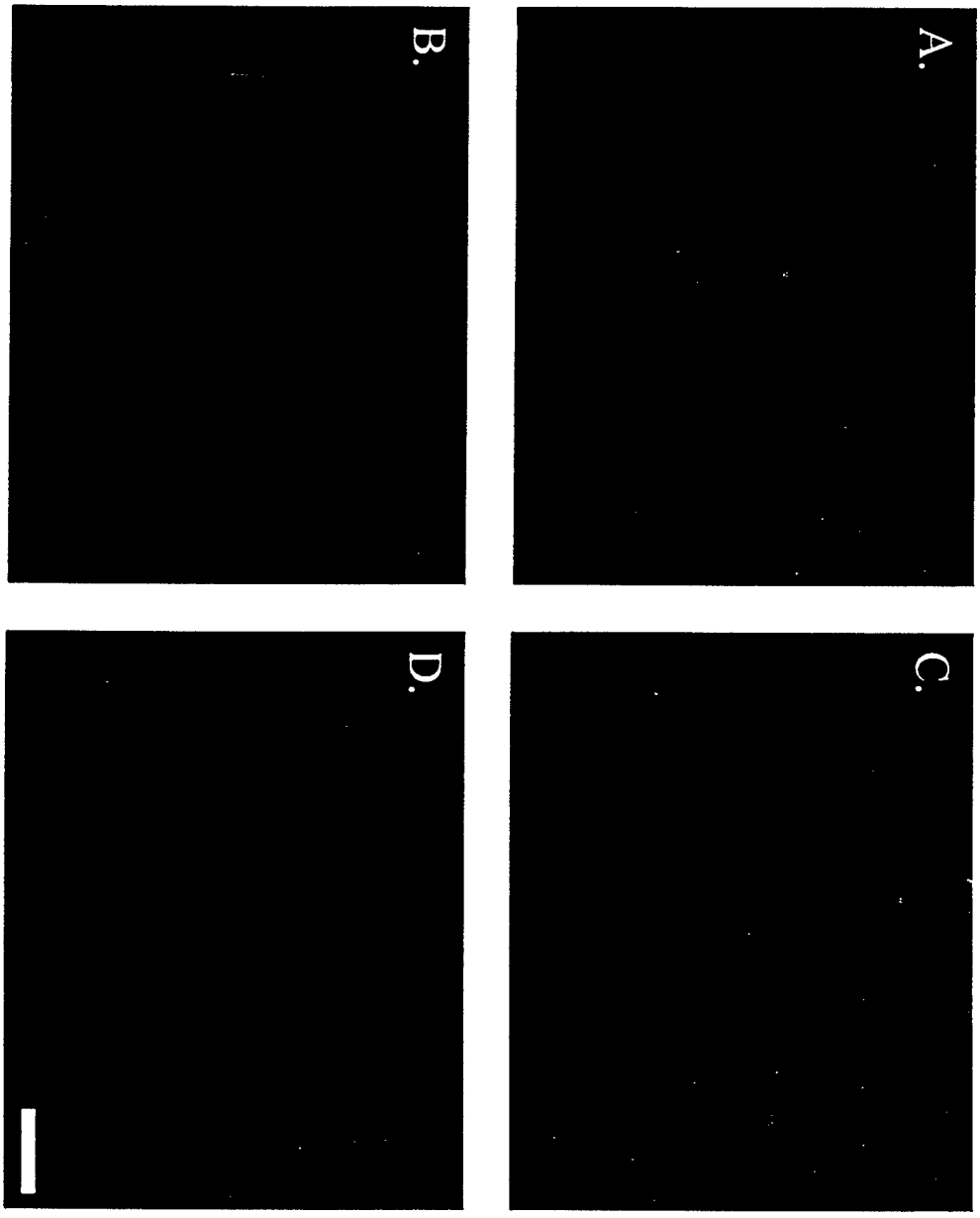

Figure 9

Appendix 3

Differential Expression of β Tubulin Isotypes In Gerbil Nasal Epithelia

KAREN WOO[1], HEATHER C. JENSEN-SMITH[2], RICHARD F. LUDUEÑA[3], RICHARD HALLWORTH[2]

[1]The Medical School and [3]Department of Biochemistry, University of Texas Health Science Center at San Antonio, San Antonio, Texas 78229-3900, and [2]Department of Biomedical Sciences, Creighton University, Omaha, Nebraska 68178.

In Press: Cell and Tissue Research

Running Head: β Tubulin in the Nose
Target Journal: Cell and Tissue Research
Corresponding Author:
Richard Hallworth
Department of Biomedical Sciences
Creighton University
2500 California Plaza
Omaha, NE 68178
Ph: (402) 280-3057
FAX: (402) 280-2690
Email: hallw@creighton.edu

Summary

The mammalian β isoform of the microtubule protein tubulin has seven remarkably similar isotypes. If β tubulin isotypes have separate functions, it should be reflected in cell-specific isotype expression or by sorting of isotypes into different pools within the same cell. The nasal cavity offers two epithelia, the sensory olfactory epithelium and the respiratory epithelium, containing cells that bear on their apical surfaces microtubule-containing organelles called kinocilia, a possible cellular compartment for isotypic sorting of tubulin. We have characterized the expression of β tubulin isotypes in gerbil olfactory and respiratory epithelia using specific antibodies to four β tubulin isotypes (β_I, β_{II}, β_{III} and β_{IV}). We found evidence of cell-specific isotype expression but found no evidence of compartmentalization of isotypes in nasal epithelia. All four isotypes were expressed in the kinocilia, dendrites, soma and axons of olfactory sensory neurons. The kinocilia and somas of respiratory epithelial cells expressed only β_I and β_{IV}. The β_{IV} isotype was absent from globose cells, the stem cells of olfactory neurons, which suggests that a phenotypic change in β tubulin isotype expression occurs in olfactory neurons during development. A population of nerve endings, presumed to be sensory, was detected in the respiratory epithelium with the antibody to β_{III}. Our results suggest that β tubulin isotype expression is controlled by both functional and developmental considerations.

Key Words: *Tubulin isotypes, β tubulin, olfactory neuron, respiratory epithelium, kinocilia*

Introduction

Microtubules perform a variety of functions in the eukaryotic cell, ranging from providing cell form and rigidity to controlling movement of organelles within the cell. Microtubules consist of heterodimers of α and β tubulin, both of which exist as numerous isotypes. Seven isotypes of mammalian β tubulin have been characterized, termed β_I, β_{II}, β_{III}, β_{IVa}, β_{IVb}, β_V and β_{VI} (Ludueña 1998). The β-tubulin isotypes are among the most highly conserved proteins known.

Nonetheless, the isotypic sequence differences are also highly conserved (Ludueña 1998). Thus It has been proposed that the isotypes have specific functional roles (Fulton and Simpson 1976). Consistent with this idea, it has been found that cells express different isotypes even in the same tissue (Roach et al. 1998; Hallworth and Ludueña 2000). However, little is known about the functional significance of the seven isotypes, except that the β_{IVb} isotype appears to be associated with axonemal microtubules and with actin stress fibers (Renthal et al. 1993; Lu et al. 1998; Roach et al. 1998; Walss-Bass et al. 2001).

A consequence of the hypothesis is that β tubulin isotypes have specific functional roles is that they may be be sequestered to different compartments in the same cell. In olfactory epithelia, microtubules exist in discreet populations (Burton 1992). For example, olfactory neurons have four identifiable compartments (kinocilia, dendrite, soma and axon), that may have microtubules with different functions. Olfactory kinocilia, which extend from the dendritic bulb at the external surface, contain the 9+2 arrangement of microtubules typical of an axoneme, but are not motile. Within the dendrite, microtubules are longitudinally arranged (Graziadei 1973). The soma of the olfactory neuron represents a distinct compartment for microtubules and the axon may contain yet another population of microtubules. In addition, bordering the olfactory sensory epithelia is respiratory

epithelium, whose cells contain a population of motile kinocilia, with the same fundamental structure as those in olfactory neuron kinocilia but an entirely different function.

The variety of microtubule populations in olfactory and respiratory epithelia therefore offers a rich opportunity to investigate the multi-tubulin hypothesis. This study was designed to determine if any of the potential pools of microtubules in nasal epithelia contain different β tubulin isotypes. We found that olfactory sensory neurons and respiratory epithelial cells express different β tubulin isotypes. However, neither sensory neurons nor respiratory epithelial cells segregate isotypes to within cell pools. We show evidence for a change in isotype expression during development of sensory neurons from globose cells. The implication of these findings is that β tubulin isotypes may have specific functional roles but that the isotypes expressed may also be linked to developmental programs.

Materials and Methods

The expression of β tubulin isotypes was examined in gerbil nasal epithelium using indirect immunofluorescence in sections of sensory and respiratory epithelium. Adult gerbils (22 days old or older) were anesthetized with Nembutal and cardiac-perfused with 4% paraformaldehyde in phosphate buffered saline (PBS). Dorso-posterior nasal epithelium was then dissected away from the septum, rinsed in PBS and equilibrated in 30% sucrose in PBS as a cryoprotectant. Strips of epithelium were frozen in O.C.T (Tissue-Tek, Miles Laboratories) and transverse sections, 10 μm thick, were cut on a cryostat. Sections were blocked and permeabilized in PBS containing 1% bovine serum albumin (BSA), 0.25% Triton-X100 and 1% normal goat serum and then rinsed in PBS plus 0.1% BSA. Sections were then labeled with primary monoclonal antibodies specific for β tubulin isotypes, raised in mouse, and were rinsed in PBS plus 0.1% BSA and labeled with secondary antibody (goat anti-mouse IgG coupled to fluorescein isothiocyanate (Sigma) or to Alexa 488 (Molecular Probes)). Rinsed sections were then sealed under cover slips on glass slides in 50% PBS:50% glycerol containing 1% *n*-propylgallate. All sections were examined using a Zeiss Axioskop II microscope equipped for epifluorescence with 40x and 100x oil-immersion objectives. Images were acquired digitally using a Spot RT cooled digital camera and were analyzed and prepared for presentation using Adobe Photoshop. Confocal images of sections were obtained on a Radiance 2000 confocal microscope (Bio-Rad, Hercules, CA) attached to a Nikon Eclipse 800 upright microscope equipped for epifluorescence.

The isotype-specific antibodies were prepared and tested as previously described (Banerjee et al. 1988, 1990, 1992; Roach et al. 1998). Each antibody was prepared to an epitope unique to the C-terminus of that isotype. Since the C-termini of β_{IVa} and β_{IVb} are virtually identical, the anti-β_{IV}

antibody was unable to discriminate between them. Negative controls were performed by omitting the primary antibody.

For immunoblotting, nasal epithelium were removed from anesthetized and decapitated gerbils and was homogenized in SDS sample buffer. Approximately 18 μg protein were loaded onto each lane of a 10% poly-acrylamide Tris-glycine gel (Gradipore Ltd., French's Forest, N.S.W., Australia) and was run at 150 V for 90 m in SDS electrophoresis buffer. The proteins were then transferred to nitrocellulose sheets after soaking in chilled Tris/glycine/methanol transfer buffer. Lanes were cut into strips for labeling with the different β tubulin isotype antibodies and with an antibody against β tubulin (Sigma). The strips were rinsed in Tris-buffered saline (TBS) with 0.1% Tween, then were blocked in 2% powdered milk in TBS for 1 h. Fresh blocking buffer was added to each primary antibody solution and the nitrocellulose sheets were exposed to one of the five primary antibodies overnight at 4 °C. After rinsing in TBS with 0.1% Tween, the protein strips were incubated in anti-mouse IgG conjugated with biotin coupled to horseradish peroxidase (Cell Signaling Technology, Beverly, MA) in 2% milk/TBS blocking buffer for 1 h at room temperature. All protein strips were rinsed again in TBS with 0.1% Tween and treated for 10 m with Luminol reagent (Santa Cruz Biotechnology, Santa Cruz, CA). After one final rinse in TBS with 0.1% Tween, the protein strips were wrapped in plastic and exposed to XAR5 scientific imaging film (Kodak, Rochester, N.Y.).

Animal care and handling was performed in conformance with approved protocols of the University of Texas Health Science Center at San Antonio and Creighton University School of Medicine Institutional Animal Care and Use Committees.

Results

The sensory epithelium of the nose consists of a pseudo-stratified layer of round cell bodies. The lowest layer of cell bodies consists of basal (globose) cells, which are the stem cells for olfactory neurons. The middle layer is the somas of mature sensory neurons. Each neuron sends a dendritic process to the epithelial surface, and an axonal process away from the epithelium to the olfactory bulb. The long sensory kinocilia arise from a small swelling at the apical surface of the dendrite, termed the dendritic bulb. Above the neuronal somas are the cell bodies of supporting cells, whose processes span the epithelium and intercalate between neurons. The adjacent respiratory epithelium consists of a thin uniform layer of epithelial cells bearing multiple short kinocilia.

We found that preservation of sensory kinocilia in frozen sections was achieved only with great difficulty, while the more robust kinocilia of the respiratory epithelium were usually well preserved. Usually the sensory kinocilia were seen only in truncated form. As a supplementary approach to identify the isotypes expressed in olfactory sensory kinocilia, we obtained confocal microscopic images of labeled sections at high magnification. The images obtained demonstrated clear, albeit shortened, processes emanating from dendritic knobs at the apical surface of sensory epithelial regions.

Immunoblots

Western blots of olfactory and sensory epithelia indicated that labeling for β tubulin isotypes is restricted to a single band of molecular at or near 50 kDaltons (Figure 1). This is close to the molecular weight of β tubulin. Labeling for β_{IV} tubulin was faint in all experiments, which is consistent with the results described below.

{insert Figure 1 near here}

I don't see "b" anywhere in the figure.

β_I

In the sensory portion of the nasal epithelium, label for β_I tubulin was found in the olfactory neurons and basal cells (Figure 2A). The label consisted of, first, a bright, slightly irregular strip along the free surface of the olfactory epithelium, apparently representing the sensory kinocilia (*kc*). Fine strands of label were also seen to be running perpendicular to the kinocilia layer, likely representing the dendrites of the sensory neurons. Deeper in the epithelium, labeling was evident in the somas of the olfactory neurons (*n*) and basal cells (*b*). The perikarya of the supporting cells, the most superficial layer of somas, were unlabeled. Irregularly shaped bundles of bright label, likely representing the axons of olfactory neurons, were present in scattered locations deep in the epithelium (*ax*). In the confocal microscope, fine processes could be seen to emanate from the knobs of sensory neurons (Figure 2B). These appeared to be olfactory kinocilia, likely truncated. In the respiratory portion of the epithelium (Figure 2C, *r*), labeling for β_I was strongest in the kinocilia layer (*kc*). Essentially no label was seen in most of the respiratory epithelium (*r*).

{insert Figure 2 near here}

Where is "b"

β_{II}

Inspection of the labeling pattern for β_{II} in the sensory epithelium (Figure 3A) revealed strong label at the epithelial surface, which suggested that β_{II} was present in olfactory kinocilia. Fine strands of dendritic labeling ran from the superficial aspect of the epithelium to the deeper layers and terminated in the neuronal soma layer (*n*), similar to the pattern of β_I tubulin. Deeper in the epithelium, label in the basal cells (*b*) also resembled that observed with β_I. As with β_I, no label was observed in the perikarya of the supporting cells. Beneath the epithelium, bright labeling in the axon bundles was found (*ax*). In the confocal microscope, fine processes (*arrow*) could be seen to emanate from the knobs at the end of dendrites (*d*) of sensory neurons (Figure 2B).

In the respiratory epithelium (Figure 3C), no labeling with antibodies to β_{II} tubulin was detected. The figure illustrates the abrupt transition from the label present in the thicker sensory epithelium (*s*) to the relative absence of label in the thinner respiratory epithelium (*r*).

{insert Figure 3 near here}

β_{III}

In the sensory epithelium (Figure 4A), β_{III} tubulin was found in the sensory kinocilia layer (*kc*). The somas (*s*) and dendrites of the sensory neurons, and the basal cells (*g*), were labeled in a pattern identical to that of β_I and β_{II}. No label was seen in the perikarya of the supporting cells. The axon bundles (*ax*) deep in the sub-epithelial tissue contained bright speckles of label. Confocal images of epithelial sections showed beading and tufts close to the knobs at the end of the dendrites (*d*) of olfactory neurons (Figure 4B).

β_{III} was absent from the somas and kinocilia of the respiratory epithelium (Figure 4C). Label appeared to stop abruptly at the junction between olfactory sensory epithelium (*s*) and the respiratory epithelium (*r*). However, as shown in Figure 4D, some fine processes (*arrow*), presumed to be unmyelinated axons, were seen in the respiratory epithelium. These processes often extended more that halfway into the epithelium, and were occasionally seen to extend laterally for many cell widths.

{insert Figure 4 near here}

β_{IV}

β_{IV} was prominent in the kinocilia layer of the sensory epithelium (Figure 5A). Weaker label was observed in the remainder of the sensory epithelium (*n*), and in the axons (*ax*), except in the perikarya of cells in the globose cell layer (*g*), from which it was strikingly absent. Confocal microscope revealed similar kinocilia label to that described for the other isotypes (Figure 5B,

arrow). In the respiratory epithelium (*r*), β_{IV} was found strongly in the kinocilia but not in the somas. The label in respiratory kinocilia was very bright compared to that in sensory kinocilia.

{insert Figure 5 near here}

Discussion

β Tubulin isotypes in cells of the nasal epithelium

The results of this study are summarized in Table 1. Olfactory neurons were found to express all four isotypes studied (β_I, β_{II}, β_{III} and β_{IV}) in all compartments. This suggests that olfactory neurons do not selectively express β tubulin isotypes nor sort them into different cellular compartments. In contrast, in the respiratory epithelium, the kinocilia layer contained β_I and β_{IV}. This suggests that respiratory epithelial cells selectively express two β tubulin isotypes of the four examined.

INSERT #1

{Insert Table 1 near here}

All isotypes found in sensory neuron soma were also found in basal cells, which are neuronal stem cells, except one, β_{IV}. The expression of β_{IV} in olfactory neurons is in itself remarkable in that β_{IV} is found in only small amounts in brain, especially when compared with the other isotypes. β_{IV} appears to be a common but not unique feature of kinocilia. In the kinocilium of photoreceptors, β_{IV} was found but not β_{II} or β_{III} (β_I was not tested) (Renthal et al. 1993). In vestibular hair cells, both β_I and β_{IV} are found in kinocilia (Perry et al. 2001). β_{IV} expression in olfactory sensory neurons appears to coincide approximately with the appearance of kinocilia. Thus it may be that β_{IV} expression is required for kinocilia, but that the other isotypes are optional. Thus β_{IV} expression may be initiated only when it is needed for the synthesis of kinocilia, although this idea needs further study.

The label in the kinocilia layer of sensory neurons appears to be in the kinocilia themselves rather than in the dendritic bulbs. Each olfactory neuron bears 10-25 fine kinocilia that together appear as a dense mat (Morrison and Costanzo 1992). If label were present only in the dendritic bulbs, we would expect the label to have a more punctate appearance. In the confocal microscope,

we see small pints and filaments of label clustered around dendritic knobs, ~~cosistent~~ consistent with the expected appearance of (possibly truncated) kinocilia. We also do not believe that the label in the kinocilia layer represents non-specific binding due to contamination by olfactory mucus. The sharp transition between labeled sensory kinocilia and unlabeled respiratory kinocilia in Figure 3C and Figure 4C argues strongly against the existence of non-specific label in the kinocilia layer.

We did not see label for any β tubulin isotypes in the supporting cells of the sensory epithelium. Undoubtedly these cells have at least some microtubules, although they may be few in number. It is possible that faint label from one of our antibodies may have been obscured by the relatively bright label in other cells, or that other isotypes may be present. → INSERT #2

We did see fine fibers delineated by β_{III} tubulin in the respiratory epithelium (Figure 4D). These fibers, which appear to be unmeyelinated, may be mechanosensory or temperature sensing fibers of trigeminal origin. Touch and temperature sensitivity have been described in human nasal epithelia but its origin is not well described (Cauna 1982). It is possible that such fibers are also present in the sensory epithelium but were undetected amid the denser label of the sensory neurons.

β Tubulin Isotypes in Kinocilia

The variety of isotypes expressed in a single organelle type, the kinocilium, is most intriguing. It is not surprising that β_{IV} should be so prominent in kinocilia since, of all the vertebrate β tubulin isotypes, β_{IV} is the one that presently comes closest to having a functional assignment, as the β isotype of axonemes. β_{IV} has been localized by immuno-electronmicroscopy to the axonemal microtubules of bovine retinal rod cells and bovine tracheal cilia (Renthal et al. 1993). It is also the only one of the four isotypes found in oviduct epithelial cilia (Roach et al. 1998) and mouse sperm flagella (Lu et al. 1998). The presence of β_{IV} in axonemes is also consistent with the prediction of Raff et al. (1997) who postulated that, for a β isotype to be in an axonemal microtubule, it must have

the sequence EGEFEEE near its C-terminus. β_{IV} (both β_{IVa} and β_{IVb}) is the only vertebrate isotype that contains this sequence (Ludueña 1998). However, olfactory sensory kinocilia are here shown to contain β_I, β_{II}, β_{III} and β_{IV}, and nasal respiratory epithelial kinocilia to contain β_I and β_{IV}. The underlying structure of the two kinocilia types is similar – each contains the familiar 9+2 arrangement of axonemal microtubules – but the functions of the kinocilia are nonetheless altogether different. The long, thin kinocilia of olfactory sensory neurons are flexible and provide a surface for olfactory receptor molecules. In contrast the short, motile kinocilia of nasal respiratory epithelial cells function to move mucous around the organ. Common to all kinocilia so far described is the presence of the β_{IV} isotype. While it remains to be seen what might be the function of each isotype, or combination of isotypes, it is clear from these studies that cells can exquisitely tailor the isotype composition of even such a stereotypical structure as the axoneme in order to meet their needs.

The Multi-Tubulin Hypothesis

In its original formulation, the multi-tubulin hypothesis (Fulton and Simpson 1976) envisaged specific functions for each isotype. The complexity of the isotype expressions patterns that have so far been observed, in which even neighboring cells of apparently similar function in the same organ express different isotype panels (Roach et al. 1998, Hallworth and Ludueña 2000, Perry et al. 2001), seemingly refutes this form of the hypothesis. In the cochlea, for example, it is almost the case that no two cell types express the same panel of isotypes (Hallworth and Ludueña 2000). Only the adjacent inner and outer pillar cells in the cochlea express the same isotypes (β_{II} and β_{IV}); even inner and outer hair cells express different isotypes (β_I and β_{II} versus β_I and β_{IV}, respectively). In vestibular hair cells, β_I and β_{IV} are found in hair cell somas, while in the adjacent supporting cells the isotypes seen are β_I, β_{II} and β_{IV} (Perry et al. 2001). Thus ascribing a single function to a single isotype has proved impossible, at least at our present level of understanding about function. The fact

remains, however, that cells select a panel of β tubulin isotypes to express from the seven available isotypes. The function of this selectivity remains obscure but intriguing.

Developmental Changes in the Expression of β Tubulin Isotypes

We here show that the globose cells, the stem cell of olfactory sensory neurons, do not express the β_{IV} isotype. This isotype, which is apparently essential for cilia and flagella, is presumed to be expressed only when the globose cell matures into a sensory neuron, by extending a dendrite to the receptor surface and synthesizing kinocilia. It is likely that during the developmental program, the expression of β_{IV} is induced when it is required, to make olfactory kinocilia. The β_{IV} isotype could therefore function as a marker for the globose cell to sensory neuron transition, just as the olfactory marker protein does now (Margolis et al. 1983), albeit perhaps a later one. The β_{IV} isotype appears in all compartments of the neuron, not just in the kinocilia. Our observations could be an example of a cell synthesizing a specific isotype for a specific function, even if that isotype then becomes widely distributed within the cell.

Acknowledgments

Supported by N.I.H. grant CA26376, U.S. Army grant DAMD17-98-1-8246, and Welch Foundation grant AQ-0726 to R.F.L., and N.I.H. grant DC02053 to R.H. We thank Joseph Kaeller for early technical assistance, Tom Adrian, Xinquan Li and Xianzhong Ding for assistance with the Western blots, and Don Leopold and Laurence Dryer for sage advice. Purchase of the confocal microscope used in this study was made possible by a grant from the Taub Foundation.

References

BANERJEE A, ROACH MC, WALL KA, LOPATA MA, CLEVELAND DW, LUDUEÑA RF. A monoclonal antibody against the type II isotype of β-tubulin. Preparation of isotypically altered tubulin. J. Biol. Chem. 263:3029-3034, 1988.

BANERJEE A, ROACH MC, TRCKA P, LUDUEÑA RF. Increased microtubule assembly in bovine brain tubulin lacking the type III isotype of β-tubulin. J. Biol. Chem. 265:1794-1799, 1990.

BANERJEE A, ROACH MC, TRCKA P, LUDUEÑA RF. Preparation of a monoclonal antibody specific for the class IV isotype of β-tubulin. Purification and assembly of $\alpha\beta_{II}$, $\alpha\beta_{III}$, and $\alpha\beta_{IV}$ tubulin dimers from bovine brain. J. Biol. Chem. 267:5625-5630, 1992.

BURTON PR. Ultrastructural studies of microtubules and microtubule organizing centers of the vertebrate olfactory neuron. Micros. Res. and Tech. 23:142-156, 1992.

CAUNA N. Blood and nerve supply of the nasal lining. In: Proctor DF, Andersen I (eds). The Nose: Upper Airway Physiology and The Atmospheric environment.Elsevier Biomedical Press NY pp. 63-65, 1982.

FULTON C, SIMPSON PA. Selective synthesis and utilization of flagellar tubulin. The multi-tubulin hypothesis. In: Goldman R, Pollard T, Rosenbaum J (eds) Cell Motility, vol. 3. Cold Spring Harbor Laboratory Press, New York, NY, pp. 987-1005, 1976.

GRAZIADEI PPC. The ultrastructure of vertebrates olfactory mucosa. In Friedmann I (ed) The Ultrastructure of Sensory Organs. North Holland, Amsterdam, pp 267-305, 1973.

HALLWORTH R, LUDUEÑA RF. Differential expression of β tubulin isotypes in the adult gerbil organ of Corti. Hear. Res. 148:161-172, 2000.

LU Q, MOORE GD, WALSS C, LUDUEÑA RF. Structural and functional properties of tubulin isotypes. Adv. Struct. Biol. 5:203-227, 1998.

LUDUEÑA RF. The multiple forms of tubulin: Different gene products and covalent modifications. Int. Rev. Cytol. 178:207-275, 1998.

MARGOLIS F. A brain protein unique to the olfactory bulb. P.N.A.S. 69:1221-1224, 1972.

MORRISON EE, COSTANZO RM. Morphology of olfactory epithelium in human and other vertebrates. Microsc. Res. and Tech. 23:49-61, 1992.

PERRY B, JENSEN H, LUDUEÑA RF, HALLWORTH R. Differential expression of β tubulin isotypes in gerbil vestibular end organs. *Submitted*, 2001.

RAFF EC, FACKENTHAL JD, HUTCHENS JA, HOYLE HD, TURNER FR. Microtubule architecture specified by a β-tubulin isoform. Science 275:70-73, 1997.

RENTHAL R, SCHNEIDER BG, MILLER MA, LUDUEÑA RF. β_{IV} is the major β-tubulin isotype in bovine cilia. Cell Motil. Cytoskeleton 25:19-29, 1993.

ROACH MC, BOUCHER VL, WALSS C, RAVDIN PM, LUDUEÑA RF. Preparation of a monoclonal antibody specific for the class I isotype of β-tubulin: The β isotypes of tubulin differ in their cellular distributions within human tissues. Cell Motil. Cytoskel. 39:273-285, 1998.

WALSS-BASS C, PRASAD V, KREISBERG JI, LUDUEÑA RF. Interaction of the β_{IV}-tubulin isotype with actin stress fibers in cultured rat kidney mesangeal cells. Cell Motil. Cytoskel. 49:200-207, 2001.

Figures

Figure 1. Western blots showing immunolabeling of gerbil nasal epithelial tissue with an antibody to beta tubulin (second lane from left) and the isotype-specific antibodies used in this study (lanes 3 through 6). ~~A protein ladder~~ a sample of protein standards with the molecular weights indicated is in the leftmost lane.

Figure 2. A) Section of olfactory sensory epithelium stained for β_I tubulin, showing label in the somas (*n*) of sensory neurons, in basal cells (*b*), in the axons of sensory neurons (*ax*), and in the kinocilia (*kc*), but not in support cells (*s*). B) Confocal view of a section of sensory epithelium at the level of the kinocilia, showing label in kinocilia (*arrow*) and in a dendrite (*d*). C) Section of respiratory epithelium (*r*) stained for β_I tubulin, showing label in the kinocilia only (*kc*). Scale bar = 20 μm for A and C, 5 μm for B.

Figure 3. A) Section of olfactory sensory epithelium stained for β_{II} tubulin, showing label in the somas (*n*) of sensory neurons, in basal cells (*b*), in the axons of sensory neurons (*ax*), and in the kinocilia (*kc*). B) Confocal view of a section of sensory epithelium stained for β_{II} tubulin at the level of the kinocilia, showing label in kinocilia (*arrow*) and in a dendrite (*d*). C) Section of a transition region between sensory (*s*) and respiratory epithelium (*r*) stained for β_{II} tubulin, showing complete loss of label in the respiratory epithelium. Scale bar = 20 μm for A and C, 5 μm for B.

Figure 3. A) Section of olfactory sensory epithelium stained for β_{III} tubulin, showing label in the somas (*n*) of sensory neurons, in basal cells (*b*), in the axons of sensory neurons (*ax*), and in the kinocilia (*kc*). B) Confocal view of a section of sensory epithelium stained for β_{III} tubulin at the level of the kinocilia, showing label in kinocilia (*arrow*) and in a dendrite (*d*). C) Section of a transition region between sensory (*s*) and respiratory epithelium (*r*) stained for β_{III} tubulin, showing complete loss of label in the respiratory epithelium. D) Section of respiratory epithelium showing fine nerve fibers (*arrow*). Scale bar = 20 μm for A, C and D, 5 μm for B.

Figure 5. A) Section of olfactory sensory epithelium stained for β_{IV} tubulin, showing label in the neurons (*n*), and the kinocilia (*kc*), but not the basal cells (*g*). B) Confocal view of a section of sensory epithelium stained for β_{IV} tubulin at the level of the kinocilia, showing label in kinocilia (*arrow*) and in a dendrite (*d*). C) Section of the transition region between sensory (*s*) and respiratory epithelium (*r*) stained for β_{IV} tubulin, showing label in the kinocilia of the respiratory epithelium (*kc*). Scale bar = 20 μm for A and C, 5 μm for B.

Table 1. Summary of the results of this study.

Sensory Epithelium

	β_I	β_{II}	β_{III}	β_{IV}
Kinocilia	✓	✓	✓	✓
Dendrites	✓	✓	✓	✓
Somas	✓	✓	✓	✓
Axons	✓	✓	✓	✓
Globose cells	✓	✓	✓	x
Support cells	x	x	x	x

Respiratory Epithelium

	β_I	β_{II}	β_{III}	β_{IV}
Kinocilia	✓	x	x	✓
Epithelial cells	✓	x	x	✓

Figure 1


Biotin Marker
Beta Tubulin
Beta I
Beta II
Beta III
Beta IV
57.0
46.5

Figure 2

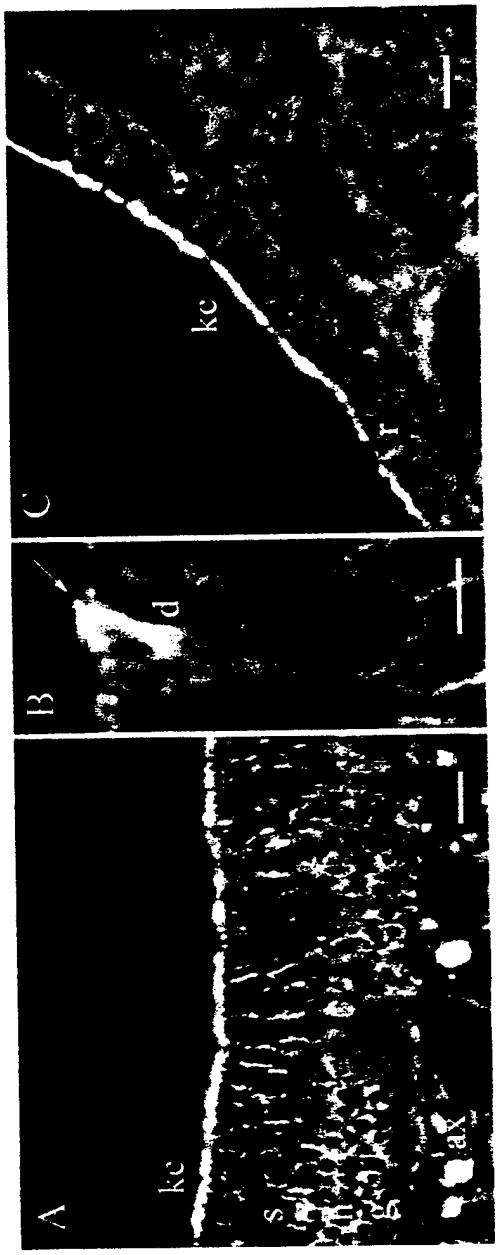

Figure 3

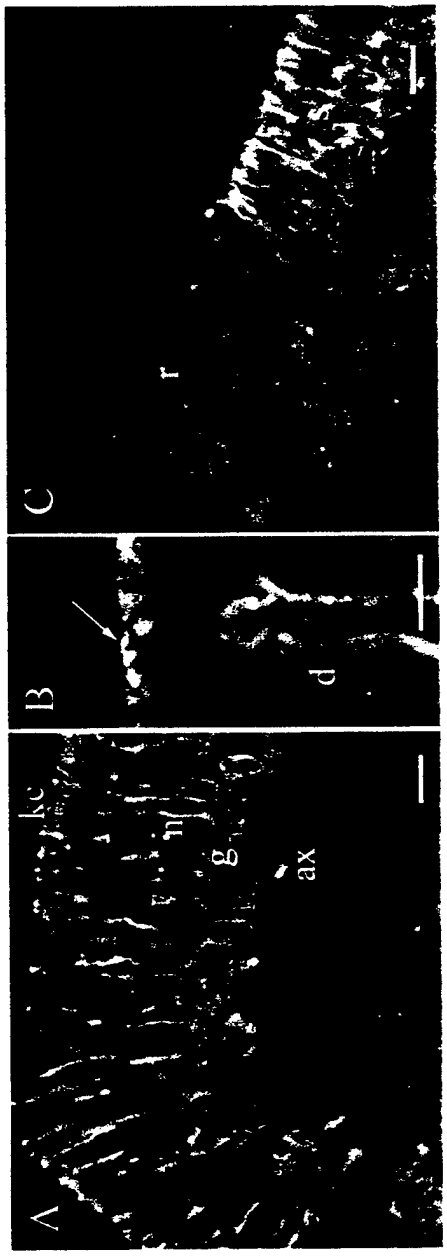

Figure 4

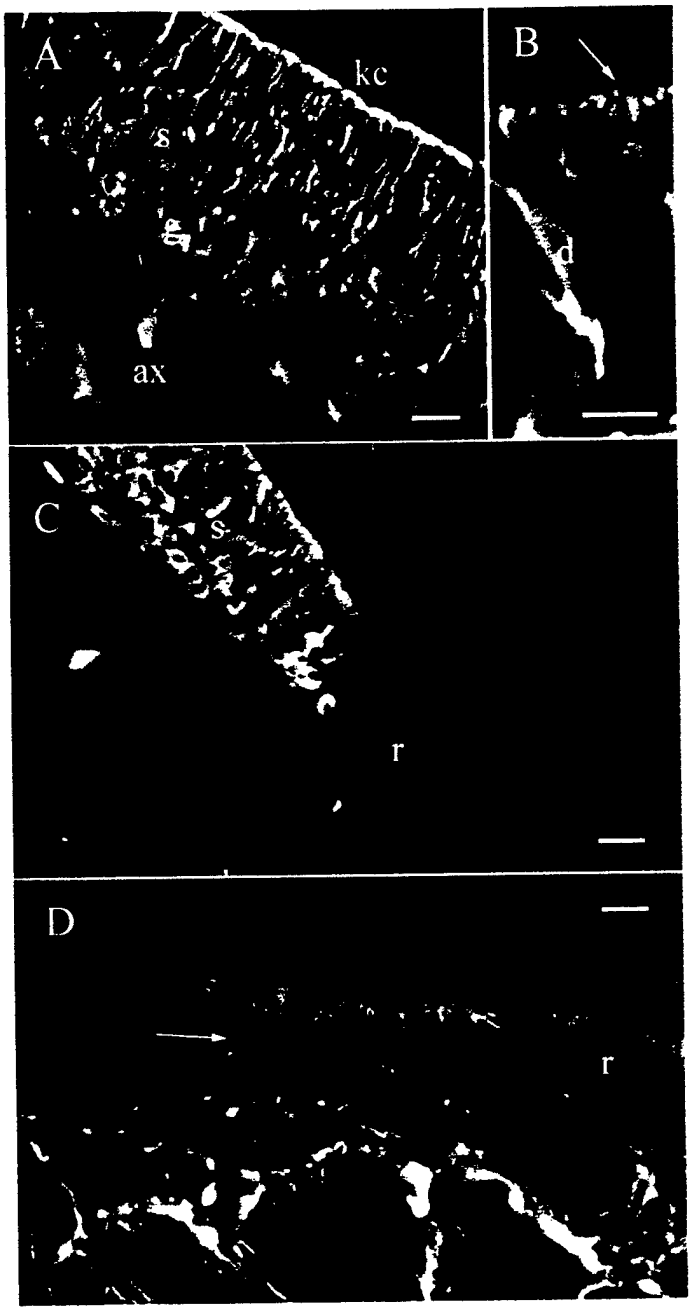

Figure 5

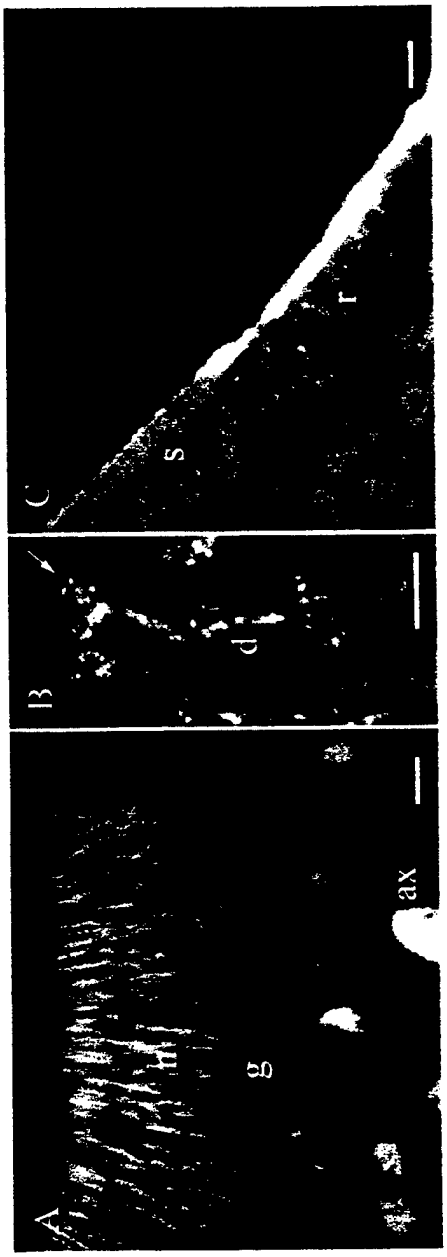

INSERT # 1

axonemes of rod outer segments

INSERT # 2

One such isotype may be β_V, to which a monoclonal antibody does not yet exist and whose distribution in mammalian cells is still unknown (Ludueña, 1998). Another possible explanation for why no tubulin was seen in these cells is that the particular isotypes may be present but their epitopes may be masked by some kind of post-translational modification or else by a microtubule-associated protein.

Appendix 4

DIFFERENT EFFECTS OF VINBLASTINE ON THE POLYMERIZATION OF ISOTYPICALLY PURIFIED TUBULINS FROM BOVINE BRAIN

Israr A. Khan[1] and Richard F. Ludueña*

Department of Biochemistry, University of Texas Health Science Center at San Antonio, TX 78229-3900.

**Address for Correspondence:*

Dr. Richard F. Ludueña

Department of Biochemistry: Mail Code 7760

U.T. Health Science Center

7703 Floyd Curl Drive

San Antonio, TX 78229-3900

Phone: (210) 567-3732 Fax: (210) 567-6595 E-mail: luduena@UTHSCSA.edu

[1]Present address: Alpha Diagnostics International, 5415 Lost Lane, San Antonio, TX 78238

Submitted to Investigational New Drugs

ABSTRACT

Vinblastine, a highly successful anti-tumor drug, targets the tubulin molecule. Tubulin, the subunit protein of microtubules, consists of an α- and a β-subunit, both of which consist of isotypes encoded by different genes. We have purified three isotypes of bovine brain tubulin, namely, $\alpha\beta_{II}$, $\alpha\beta_{III}$, and $\alpha\beta_{IV}$. Microtubule Associated Protein-2 (MAP2) and Tau-induced assembly of these isotypes were compared in the presence and absence of vinblastine. MAP2-induced assembly of unfractionated tubulin and all the isotypes except $\alpha\beta_{II}$ tubulin was resistant to 1 μM vinblastine. Vinblastine at low concentrations (<10 μM) progressively inhibited the assembly of all of the isotypes but the vinblastine concentration required for inhibition of MAP2 was minimal for $\alpha\beta_{II}$. The tau-induced assembly of unfractionated tubulin and $\alpha\beta_{III}$ were equally sensitive to 1 μM vinblastine whereas $\alpha\beta_{II}$ and $\alpha\beta_{IV}$ were much more sensitive to vinblastine. The microtubules obtained in the presence of tau from unfractionated tubulin, $\alpha\beta_{II}$, and $\alpha\beta_{IV}$ could be easily aggregated by 20 μM vinblastine whereas such an aggregation of microtubules obtained from $\alpha\beta_{III}$ and tau required approximately 40 μM vinblastine. Our results suggest that among the tubulin isotypes, $\alpha\beta_{II}$ is the most sensitive to vinblastine while $\alpha\beta_{III}$ is the most resistant and this intrinsic resistance of $\alpha\beta_{III}$ dimers persists in the polymeric form of $\alpha\beta_{III}$ tubulin as well. These results may be relevant to the therapeutic and toxic actions of vinblastine.

Keywords: Tubulin/ Tubulin Isotypes/ Microtubules/ Vinblastine/*Vinca* Alkaloids

INTRODUCTION

Microtubules are long cylindrical organelles playing critical roles in a variety of processes such as mitosis, axonal transport and axonemal motility [1]. The major constituent of microtubules is the 100 kDa protein tubulin, which is a heterodimer consisting of two polypeptide chains designated α and β, both of which exist in several isotypic forms [1-3]. Characterization of these dimers *in vitro* has indicated that properties of microtubules are strongly influenced by the isotypic composition of the constituent β-tubulin. For example, the intrinsic dynamicity of microtubules that is a critical regulator of their function both *in vivo* and *in vitro* [4,5] has been shown to be affected dramatically by the isotypic composition of tubulin [6]. Our previous studies have clearly demonstrated that shortening rates of microtubules composed of purified β–tubulin isotypes are less sensitive to taxol than the microtubules assembled from unfractionated tubulin [7]. The fact that different isotypes assemble into microtubules at different rates [8,9] could be one of the factors affecting the dynamic behavior of microtubules. However, it is not known how the dynamicity and the relative stability of microtubules composed of segregated isotypes are related *in vivo* but the stability of different microtubules is often reflected in their *in vitro* sensitivity to various tubulin/microtubule binding drugs [7,10-13]. Recently [10], we have demonstrated that the antimitotic compound IKP-104 inhibits the assembly of $\alpha\beta_{II}$ dimers more than that of $\alpha\beta_{III}$ and $\alpha\beta_{IV}$ dimers and that high concentrations of IKP-104 induce formation of spiral aggregates from $\alpha\beta_{II}$ and $\alpha\beta_{III}$ but not from $\alpha\beta_{IV}$. On the other hand, the $\alpha\beta_{III}$ dimer interacts much less strongly with colchicine, and taxol than do the $\alpha\beta_{II}$ and $\alpha\beta_{IV}$ dimers [7,14]. Also, the incorporation of estramustine into the $\alpha\beta_{III}$ isotype of tubulin occurs with a reduced efficiency compared to that of the other isotypes [12].

Among various anti-tubulin agents, vinblastine, a dimeric indole alkaloid derived from

Catharanthus (Vinca) roseus, is of special interest because of its widespread use as an antimitotic drug in cancer therapy. It is thought that vinblastine exerts its antimitotic activity by disrupting the functions of microtubules. The vinblastine-induced inhibition of microtubule-function requires a direct interaction of the drug with tubulin and/or the microtubules. At low concentrations (0.2-1 μM), vinblastine acts as a suppressor of microtubule dynamic instability by binding at both ends of microtubules and thus increasing the time spent in the attenuated state [15,16]. At intermediate concentrations, vinblastine acts as an inhibitor of microtubule assembly or promoter of disassembly both *in vitro* and in cells. At concentrations >1 μM it depolymerizes the microtubules by inducing the splaying and peeling of their protofilaments, presumably by interacting with low affinity sites along the microtubule surface [17,18]. At higher concentrations (>5-10 μM) vinblastine induces formation of paracrystals and other aggregates composed of tubulin complexed with vinblastine [19-25]. In previous studies the effect of vinblastine was tested on unfractionated tubulin which is a complex mixture of a number of isotypes. In the present study we have investigated the interaction of 1 to 20 μM vinblastine with isotypically pure tubulins, namely $\alpha\beta_{II}$, $\alpha\beta_{III}$ and $\alpha\beta_{IV}$. Furthermore we have used two different microtubule associated proteins (MAPs), namely, microtubule-associated protein 2 (MAP2) and tau, to dissect the responses of different isotypes to vinblastine in the presence of MAPs. Our results suggest that, of the various tubulin dimers, polymerization of $\alpha\beta_{II}$ is the most sensitive and that of $\alpha\beta_{III}$ the least sensitive to vinblastine.

MATERIALS AND METHODS

Purification of tubulin isotypes. Microtubules, MAP2 and tau were prepared from bovine cerebra and tubulin purified from the microtubules by phosphocellulose chromatography following the procedure of Fellous *et al.* [26]. The isotypically purified $\alpha\beta_{II}$, $\alpha\beta_{III}$ and $\alpha\beta_{IV}$ tubulin dimers were prepared as described previously [27]. All isotypically purified tubulins were stored at -80 °C until ready for use. The MAP2- or tau-induced assembly and electron microscopy of the polymers obtained were studied using the same batch of tubulin isotypes. The sedimentation and turbidimetric measurements on assembly of isotypically pure tubulins were performed using two different batches of tubulin isotypes. At a fixed tubulin concentration, the net amount of polymers obtained from several different batches of untreated isotypes varied from 0 to 20%.

Tubulin polymerization. Tubulin was thawed on ice water and spun at 18,000 x *g* for 6 minutes at 4 °C to remove any insoluble tubulin aggregates from the sample. Tubulin present in the supernatant was quantitated by the method of Lowry *et al.* [28] and mixed with vinblastine and MAP2 or tau in 0.1 M 2-(*N*-morpholino)ethanesulfonic acid, 1 mM GTP, 0.5 mM $MgCl_2$, 0.1 mM ethylenediaminetetraacetic acid, 1 mM ethylene glycol-bis(*β*–aminoethyl ether)-N',N',N',N'-tetraacetic acid, 1 mM β-mercaptoethanol, pH 6.4, at 4 °C. Unless otherwise mentioned, the final concentrations of tubulin, MAP2 and tau were 1.5, 0.3 and 0.15 mg/mL, respectively. The temperature of the samples was raised from 4 to 37 °C and the tubulin polymerization was followed by either of the following two methods [27]. (A) *Sedimentation.* Aliquots (100 µl) were withdrawn at various time intervals and centrifuged for 4 minutes in the Beckman airfuge at 175,000 x *g*. The polymer concentration in the pellets was measured by first

solubilizing the pellet in a final volume of 100 µl of 0.05 N NaOH and then quantitating the total protein in the sample by the method of Lowry et al. [28]. (B) *Turbidimetry*. The polymerization of tubulin was followed by measuring the change in turbidity at 350 nm on either a Beckman DU7400 or Gilford 250 spectrophotometer. The assembly profiles presented in this study are one of at least two representative experiments performed under identical conditions.

Electron microscopy. The mixtures of tubulin, MAP2 or tau were incubated for at least 30 minutes at 37 °C in the presence or absence of the indicated amount of vinblastine sulfate (Sigma Chemical Co., St. Louis, MO). Aliquots (50 µl) were withdrawn and treated with 1 % glutaraldehyde for 30 seconds, and then layered on 400-mesh carbon over formavar-coated copper grids. After 1 minute the grids were washed with 4 drops of water and stained with 1% uranyl acetate for 1 minute. Excess stain was removed and, after air-drying, grids were examined in a Phillips 300 electron microscope with an operating voltage of 60 kV [10].

RESULTS

Effect of vinblastine on the polymerization of tubulin isotypes in the presence of MAP2. The turbidimetric measurements on the MAP2-induced assembly of unfractionated tubulin and $\alpha\beta_{II}$ are shown in Figures 1A and B. Compared to unfractionated tubulin, which appeared to be insensitive to 1 μM vinblastine, $\alpha\beta_{II}$ tubulin lost almost one third of its ability to polymerize into microtubules (Table 1). However, the polymerization of $\alpha\beta_{III}$ and $\alpha\beta_{IV}$ was not significantly affected by 1 μM vinblastine. In fact, a slight increase of approximately 3% was observed in the case of unfractionated tubulin and $\alpha\beta_{IV}$ (Figures 1A and 1D). The morphology of the polymers obtained from various forms of tubulin in the presence and absence of 1 μM vinblastine is shown in Figs 2A-D. In the presence of 1 μM vinblastine, microtubules of apparently normal appearance were obtained from unfractionated tubulin and isotypically pure dimers (Figs. 2A2, 2B2 bottom, 2C2 and 2D2); however, in the case of $\alpha\beta_{II}$, polymers also included bundles of protofilaments (Fig. 2B2 top).

The addition of 20 μM of vinblastine to the assembly mixture prior to the initiation of assembly caused a gradual increase in the turbidity of the sample (Figs. 1A-D). Similarly, addition of 20 μM vinblastine to preformed microtubules resulted in the depolymerization of microtubules as reflected in a decrease in absorbance at 350 nm (Figures 1A-D). This greatly exceeded the decrease expected from the 6.7 % dilution of the sample. The turbidity obtained in the presence of vinblastine reflected formation of spirals in the case of unfractionated tubulin (Fig. 2A3) and $\alpha\beta_{IV}$ (Fig. 2D3); for $\alpha\beta_{II}$, addition of vinblastine led to formation of a protofilamentous structure resembling a spiral (Fig. 2B3). In the case of $\alpha\beta_{III}$, bundles of protofilaments were the dominant structures (Fig. 2C3).

It is evident from the above data that vinblastine at substoichiometric concentrations (1 μM) caused incomplete inhibition of microtubule assembly whereas at high concentrations (20 μM) it caused depolymerization of microtubules and complete inhibition of microtubule assembly. We measured the effect of a series of concentrations of vinblastine on the polymerization of various tubulin dimers and the results of this experiment are shown in Figures 3A-D. The effect of vinblastine on microtubule assembly could be dissected into two parts. First, at lower concentrations (<10 μM), vinblastine inhibited the MAP-induced formation of microtubules from unfractionated and isotypically pure tubulins. At a concentration of 5 μM vinblastine caused almost complete inhibition of the polymerization of $\alpha\beta_{III}$ tubulin. Second, at higher concentrations of the drug, depolymerization of microtubules (if any) and the aggregation of tubulin occurred. It should be noted that in the absence of vinblastine and irrespective of the method used to study the polymerization of tubulin, the extent of MAP-induced polymerization of unfractionated tubulin and the isotypes varied from each other. For example, the concentration of polymer mass, as measured by sedimentation, for $\alpha\beta_{II}$, unfractionated tubulin, $\alpha\beta_{III}$ and $\alpha\beta_{IV}$ were 0.41, 0.21, 0.19 and 0.11 mg/mL, respectively (Figures 3A-D). Similarly, the approximate absorbance values, obtained by turbidimetry, for the steady state microtubules obtained from for $\alpha\beta_{II}$, unfractionated tubulin, $\alpha\beta_{III}$ and $\alpha\beta_{IV}$ were 0.23, 0.15, 0.19 and 0.16, respectively (Figures 1A-D). From the above results, it is evident that polymerization of tubulin is more extensive in the case of $\alpha\beta_{II}$ than in either unfractionated tubulin or the other isotypes. It is therefore not surprising that in comparison to unfractionated tubulin or the other isotypes, $\alpha\beta_{II}$ is more sensitive to vinblastine. The maximal yield of polymer obtained in the presence of high concentrations of vinblastine varied greatly depending on the isotype composition of the tubulin. $\alpha\beta_{II}$ gave the highest yield (0.74 mg/mL) followed by unfractionated tubulin (0.38 mg/mL), $\alpha\beta_{III}$ (0.33 mg/mL)

and $\alpha\beta_{IV}$ (0.22 mg/mL), indicating that the aggregation is more extensive in the case of $\alpha\beta_{II}$ than in unfractionated tubulin or other isotypes. The apparent drug-induced aggregation of tubulin started in the range of vinblastine concentration where the drug caused maximum inhibition of tubulin polymerization (lowest point of the curves shown in Figures 3A-D. This result supports the data of Figure 1 that in comparison to unfractionated tubulin, $\alpha\beta_{III}$ and $\alpha\beta_{IV}$, $\alpha\beta_{II}$ is more sensitive to vinblastine. Analysis of the data in Figure 3 shows that, for unfractionated tubulin, $\alpha\beta_{II}$, $\alpha\beta_{III}$ and $\alpha\beta_{IV}$, half-maximal inhibition of microtubule assembly was obtained at vinblastine concentrations of 3.8, 0.5, 1.8 and 2 μM, respectively, while half-maximal enhancement of aggregation was obtained with vinblastine concentrations of 52, 17, 33 and 48 μM, respectively, suggesting that, in the presence of MAP2, $\alpha\beta_{II}$ is the most sensitive to vinblastine.

Effect of vinblastine on the polymerization of tubulin isotypes in the presence of tau. In contrast to MAP2-induced assembly of unfractionated tubulin, which was resistant to 1μM vinblastine, tau-induced assembly was inhibited by almost 32% (Figure 4A). The isotypically pure tubulins were more sensitive to 1μM vinblastine than was unfractionated tubulin, and, among the isotypes, the polymerization of $\alpha\beta_{II}$ tubulin was most sensitive to 1 μM vinblastine (Figures 4A-D and Table 1). Addition of 20 μM vinblastine to microtubules preformed from unfractionated tubulin, $\alpha\beta_{II}$ and $\alpha\beta_{IV}$ resulted in depolymerization of microtubules initially; followed by rapid aggregation (Figures 4A, 4B and 4D). This phenomenon of rapid aggregation was not observed with either unfractionated or isotypically pure tubulins when the assembly was induced by MAP2 (Figures 2A-D). The most striking difference among the isotypes was that $\alpha\beta_{III}$ did not aggregate even in the presence of 20 μM vinblastine (Figure 4C). However, aggregates of tau-induced microtubules appeared once the vinblastine concentration was raised to 40 μM or above

(Figure 5). A tremendous aggregation was observed when 20 μM vinblastine was included in the assembly mixture prior to initiation of the tau-induced polymerization of unfractionated tubulin, $\alpha\beta_{II}$ and $\alpha\beta_{IV}$ (Figures 4A, 4B and 4D). Again, in contrast, in the case of $\alpha\beta_{III}$, there was very little aggregation and the amount of aggregates was only 4% of the one produced in the presence of 50 μM vinblastine (Figures 4C and 5). Similar results were obtained when assembly was measured by sedimentation (Figure 7).

The morphology of the tau-induced polymers obtained from tubulin in the presence and absence of vinblastine are shown in Figure 6. The polymers of tubulin obtained in the presence of 1 μM vinblastine included microtubules combined with other protofilamentous structures in the cases of unfractionated tubulin (Fig.6A2), $\alpha\beta_{II}$ (Fig.6B2) and $\alpha\beta_{IV}$ (Fig.6D2, *top* and *bottom*). In contrast, in the case of $\alpha\beta_{III}$ only bundles of protofilaments were observed (Fig. 6C2, *top* and *bottom*). The inclusion of higher amounts of the drug, e.g., 20 μM vinblastine, in the assembly mixture led to formation of only protofilamentous spirals in $\alpha\beta_{IV}$ (Fig.6D3), linear bundles in unfractionated tubulin (Fig. 6A3) and $\alpha\beta_{II}$ (Fig. 6B3, *top*) or other aggregates perhaps resembling spirals in $\alpha\beta_{II}$ (Fig. 6B3, *bottom*) and $\alpha\beta_{III}$ (Fig. 6C3). As shown in Figs. 4 and 5, irrespective of the presence of vinblastine in the polymerization mixture, the resultant tau-induced polymers could be depolymerized by 20-40 μM vinblastine.

As seen in Figure 7, the inhibition of tau-induced polymerization of unfractionated and isotypically pure tubulin was observed in the lower concentration range of vinblastine. However, this range of vinblastine concentration for unfractionated tubulin, $\alpha\beta_{II}$ and $\alpha\beta_{IV}$ (1-5 μM vinblastine) was considerably lower than that required for $\alpha\beta_{III}$ (1-20 μM vinblastine). It is also interesting to note that, in the presence of 1 μM vinblastine, unfractionated tubulin, $\alpha\beta_{II}$, $\alpha\beta_{III}$

and $\alpha\beta_{IV}$ lost approximately 50%, 81%, 32% and 67%, respectively, of their ability to polymerize into microtubules (Figures 7A-D). This is consistent with the pattern of data obtained by turbidimetry (Table 1). Higher concentrations of vinblastine reveal a striking difference between $\alpha\beta_{III}$ on the one hand and $\alpha\beta_{II}$, $\alpha\beta_{IV}$ and unfractionated tubulin, on the other hand. For the latter three, the least polymer was obtained at 5 μM vinblastine, whereas for $\alpha\beta_{III}$, this occurred at 20 μM vinblastine. For the latter three, formation of non-microtubule aggregate in the presence of 20 μM vinblastine was much greater than microtubule assembly in the absence of vinblastine. In contrast, for $\alpha\beta_{III}$, this required 40 μM vinblastine. Analysis of the results of Figure 7 suggests that half-maximal inhibition of tau-induced microtubule assembly for unfractionated tubulin, $\alpha\beta_{II}$, $\alpha\beta_{III}$ and $\alpha\beta_{IV}$ was obtained at vinblastine concentrations of 1, 0.6, 2.1 and 0.6 μM, respectively. . In conjunction with the fact that MAP2-induced assembly of $\alpha\beta_{II}$ isotype is most sensitive to 1 μM vinblastine (Table 1), the data of Figures 2 and 7 suggest that sensitivity of polymerization of tubulin to vinblastine-induced inhibition is influenced by the type of the tubulin as well as the nature of microtubule associated proteins.

DISCUSSION

In the present study we found that vinblastine, at low concentrations, inhibited polymerization of tubulin and its isotypically pure forms into microtubules. At higher concentrations, the drug depolymerized microtubules and induced formation and aggregation of spirals. These observations are in agreement with the consensus on the presence of two types of vinblastine binding sites on tubulin. The first binding site is specific and strong, involving residues 175-213 on β-tubulin [29] and is probably responsible for the substoichiometric inhibition of microtubule assembly [30]. There are two additional vinblastine-binding sites on tubulin that are weak, nonspecific and responsible for aggregation [29,31]. Since MAPs are present *in vivo*, we considered it important to study the effect of vinblastine on tubulin in the presence of MAPs.

Our results indicate that the type of MAP used to induce tubulin polymerization affected the inhibition of this process by vinblastine. The inhibitory effect of vinblastine on MAP-induced assembly of tubulin may arise from a drug-induced conformational change in either tubulin itself or at the sites where the MAPs bind. Evidence for a structural change induced in tubulin by the drug has come from quenching of tubulin fluorescence, from changes in sulfhydryl reactivity and crosslinking, from altered proteolytic susceptibility, and from immunological reactivity [32-35]. A direct interaction between vinblastine and MAPs has not been documented. Since the sites of interaction of vinblastine and MAP(s) on the tubulin molecule are distinct, it is likely that the drug-induced conformational change in tubulin itself is responsible for the substoichiometric inhibition of assembly [31]. Since the binding of MAPs to the carboxyl terminal of tubulin influences and regulates both lateral and longitudinal interactions between subunits in tubulin polymers, the drug-induced conformational change in tubulin can be influenced by the nature of the MAPs present in the assembly mixture. It is not surprising, therefore, that at

substoichiometric concentrations of vinblastine, unfractionated tubulin was resistant to the drug when assembly was induced by MAP2. On the contrary, a 32% was observed when assembly was induced by tau instead of MAP2. This result is supported by previous findings that, in the presence of vinblastine, tau and MAP2 interact differently with tubulin [36]. This would imply that the regions in the tubulin dimer where the majority of the vinblastine-induced changes occur might alter the subunit-subunit interactions and that the latter is propagated differently to the site(s) within the tubulin molecule where MAP2 and tau bind. By this interpretation, the substoichiometric inhibition of tubulin polymerization by vinblastine should not vary among the isotypes of tubulin, provided the conformations of all the forms of tubulin are identical. As discussed below, however, our results from the experiments with isotypically pure tubulin dimers differ significantly from these expectations.

Vinblastine, at low concentrations, had a very strong inhibitory effect on MAP2-induced assembly of $\alpha\beta_{II}$ whereas the assembly of the other isotypes was affected much less. This suggests that tubulin isotypes are structurally different from each other and therefore that the magnitude and the propagation of vinblastine-induced conformational change differs among the isotypes. A tubulin isotype with a relatively rigid conformation would be expected to be more resistant to vinblastine-induced inhibition of assembly. This conclusion is also supported by our observation that among the isotypes, $\alpha\beta_{II}$ dimers were found to be most sensitive to vinblastine when assembly was induced by either tau or MAP2. It is worth emphasizing that $\alpha\beta_{III}$, which has a more rigid conformation than those of the other isotypes [37,38] was the least sensitive to low concentrations of vinblastine when assembly was induced by tau.

If the structural rigidity of tubulin isotypes is assumed to be directly related to their relative sensitivity to low concentrations of vinblastine, then polymers formed from a rigid isotype

are likely to be most resistant to depolymerization and subsequent aggregation by high concentrations of the drug. As expected, in contrast to unfractionated tubulin, $\alpha\beta_{II}$ and $\alpha\beta_{IV}$, the polymers obtained from $\alpha\beta_{III}$ could not be aggregated by 20 μM vinblastine indicating that $\alpha\beta_{III}$, both in its dimeric and polymeric forms, is most resistant to vinblastine. A much higher concentration of vinblastine (~40-50 μM) was required to induce depolymerization and subsequent aggregation. This further supports our earlier conclusion that conformational stability and thus relative sensitivity of tubulin varies among the isotypes.

Both MAP2 and tau stimulated the vinblastine-induced aggregation of unfractionated, $\alpha\beta_{II}$ and $\alpha\beta_{IV}$ tubulins, but the aggregation was more evident in the case of tau. Similar enhancement of aggregation has been reported after the removal of the carboxyl terminals of tubulin [31]. In the case of $\alpha\beta_{III}$, however, aggregation of tubulin dimers stimulated by tau in the presence of 20 μM vinblastine did not occur. This finding further substantiated our conclusion that among the isotypes, $\alpha\beta_{III}$ is most resistant to vinblastine.

Among all the forms of tubulin tested, only $\alpha\beta_{II}$ exhibited a significant loss in its ability to polymerize into microtubules when the assembly was stimulated by MAP2 in the presence of 1 μM vinblastine. The relatively higher sensitivity of $\alpha\beta_{II}$ was also evident from electron microscopy data. The polymers formed from $\alpha\beta_{II}$ included microtubules as well as a large population of other protofilament-based non-microtubule structures. In contrast, at this concentration of vinblastine, only microtubules were seen with unfractionated tubulin, $\alpha\beta_{III}$ or $\alpha\beta_{IV}$. Similar abnormal structures were obtained in the case of $\alpha\beta_{III}$ but higher (20 μM) vinblastine concentrations were required. At these concentrations, however, other forms of tubulin generated spirals and aggregates. Since the aggregation is induced by binding of

vinblastine to weak and nonspecific sites on tubulin, it appears that the affinity of these sites also varies among the isotypes. As described below, our results also provide evidence that isotypically pure tubulins are more sensitive to vinblastine than is unfractionated tubulin but at the same time are less prone to vinblastine-induced aggregation.

From the analysis of the morphology of the tau-induced polymers obtained in the presence of substoichiometric concentration of vinblastine it is clear that in the case of $\alpha\beta_{II}$ and $\alpha\beta_{IV}$, polymers include microtubules and other aggregates as well as spirals. In contrast, polymers obtained from $\alpha\beta_{III}$ include aggregates and bundles of protofilaments but not spirals. In the case of $\alpha\beta_{III}$ a small proportion of polymers included aggregates and spirals, but only at high (20 μM) concentrations of the drug, at which vinblastine interacts nonspecifically with weaker sites on the tubulin molecule.

Our results would appear to contradict those of Lobert *et al.* [11,39] who found no difference in the binding of vinblastine to the $\alpha\beta_{II}$ or $\alpha\beta_{III}$ dimers. They also observed that vinblastine promoted self-association of $\alpha\beta_{II}$ and $\alpha\beta_{III}$ to the same extent [11]. Interestingly, they also found that vincristine, which is structurally very similar to vinblastine, enhanced self-association of $\alpha\beta_{II}$ better than it did that of $\alpha\beta_{III}$ [11]. A major difference between the experiments of Lobert *et al.* [11,40] and ours, however, is that the self-association experiments described here were done in the presence of either MAP2 or tau while those of Lobert *et al.* [11,39] were performed in the absence of MAPs. It is quite reasonable to postulate that the real difference among the isotypes involves only the regions on the tubulin molecule which transduce conformational effects between the vinblastine and the MAP binding sites. We already know that this region is exquisitely sensitive to temperature, as well as to the nature and integrity of the MAP [37,40,41].

In summary, our results indicate that $\alpha\beta_{II}$ is the most sensitive to vinblastine and that $\alpha\beta_{III}$ is the least sensitive. Since vinblastine is a major anti-tumor drug, our results raise the possibility that sensitivity and resistance of tumors to this drug can be modulated by the tubulin isotype composition of the microtubules in the tumor cell, as was previously postulated by Lobert *et al.* [11] to be the case for vincristine and as is apparently the case with taxol and estramustine [42-44]. In the case of taxol, we have measured its effect on the dynamic behavior of microtubules formed from isotypically purified tubulin [7]. To choose one parameter, the shortening rate of microtubules made from $\alpha\beta_{II}$ is 4.6-4.7 times more sensitive to taxol than is the case for microtubules made from $\alpha\beta_{III}$ or $\alpha\beta_{IV}$ [7]. Consistent with this finding, tumors treated with taxol often respond by increasing their expression of $\alpha\beta_{III}$ and $\alpha\beta_{IV}$ [42,45]. Future investigation may reveal whether a similar pattern occurs in tumors treated with vinblastine.

Acknowledgments: We are grateful to Drs. Asok Banerjee and Asish R. Chaudhuri for their valuable suggestions. We thank Veena Prasad, Mohua Banerjee, Pat Schwarz and Alka Mittal for their help during the preparation of microtubules from bovine cerebra. This research was supported by grants CA26376 and HL07446 from the National Institutes of Health, DAMD17-98-1-8246 and DAMD17-01-1-0411 from the U.S. Army Medical Research and Materiel Command and AQ-0726 from the Welch Foundation.

REFERENCES

1. Dustin P: Microtubules, 2nd Ed. Springer-Verlag, Berlin, 1984

2. Ludueña RF, Shooter EM, Wilson :. Structure of the tubulin dimer. J Biol Chem 252: 7006-7014, 1977

3. Ludueña RF: Multiple forms of tubulin: different gene products and covalent modifications. Int Rev Cytol 178: 207-275, 1998

4. Wilson L, Jordan MA: In: Hyams JS, Lloyd CW (eds) Microtubules. New York: Wiley-Liss, New York, 1994, pp 59-83

5. Wordeman L, Mitchison T: In: Hyams JS, Lloyd CW (eds) Microtubules. New York: Wiley-Liss, New York, 1994, pp 287-301

6. Panda D, Miller HP, Banerjee A, Ludueña RF, Wilson L: Microtubule dynamics *in vitro* are regulated by the tubulin isotype composition. Proc Natl Acad Sci USA 91: 11358-11362, 1994

7. Derry WB, Wilson L, Khan IA, Ludueña RF, Jordan MA: Taxol differentially modulates the dynamics of microtubules assembled from unfractionated and purified β-tubulin isotypes. Biochemistry 36: 3554-3562, 1997

8. Banerjee A, Roach MC, Trcka P, Ludueña RF: Increased microtubule assembly in bovine brain tubulin lacking the type III isotype of β-tubulin. J Biol Chem 265: 1794-1799, 1990

9. Banerjee A, Roach MC, Trcka P, Ludueña RF: Preparation of a monoclonal antibody specific for the class IV isotype of β-tubulin. Purification and assembly of $\alpha\beta_{II}$, $\alpha\beta_{III}$, and $\alpha\beta_{IV}$ tubulin dimers from bovine brain. J Biol Chem 267: 5625-5630, 1992

10. Khan IA, Tomita I, Mizuhashi F, Ludueña RF: Differential interaction of tubulin isotypes

with the antimitotic compound IKP-104. Biochemistry 39: 9001-9009, 2000

11. Lobert S, Frankfurter A, Correia JJ: Energetics of Vinca alkaloid interactions with tubulin isotypes: implications for drug efficiency. Cell Motil Cytoskeleton 39: 107-121, 1998
12. Laing N, Dahllöf B, Hartley-Asp B, Ranganathan S, Tew KD: Interaction of estramustine with tubulin isotypes. Biochemistry 36: 871-878, 1997
13. Banerjee A, Ludueña RF: Distinct colchicine binding kinetics of bovine brain tubulin lacking

the type III isotype of β-tubulin. J Biol Chem 266: 1689-1691, 1991

14. Banerjee A, Ludueña RF: Kinetics of colchicine binding to purified β-tubulin isotypes from bovine brain. J Biol Chem 267: 13335-13339, 1992
15. Toso RJ, Jordan MA, Farrell KW, Matsumoto B, Wilson L: Kinetic stabilization of microtubule dynamic instability *in vitro* by vinblastine. Biochemistry 32: 1285-1293, 1993
16. Dhamodharan P, Jordan MA, Thrower D, Wilson L, Wadsworth P: Vinblastine suppresses dynamics of individual microtubules in living interphase cells. Mol Biol Cell 6: 1215-1229, 1995
17. Jordan MA, Margolis RL, Himes RH, Wilson L: Identification of a distinct class of vinblastine binding sites on microtubules. J Mol Biol 187: 61-73, 1986
18. Singer WD, Jordan MA, Wilson L, Himes RH: Binding of vinblastine to stabilized microtubules. Mol Pharmacol 36: 366-370, 1989
19. Wilson L, Jordan MA, Morse A, Margolis RL: Interaction of vinblastine with steady-state microtubules *in vitro*. J.Mol Biol 159: 125-149, 1982

20. Hamel E: Interactions of tubulin with small ligands. In: Avila J (ed) Microtubule Proteins, CRC Press, Boca Raton, 1990, pp 89-191

21. Bensch KG, Malawista SE: Microtubular crystals in mammalian cells. J Cell Biol 40: 95-107, 1969

21. Warfield RKN, Bouck GB: Microtubule-macrotubule transition: intermediates after exposure to the mitotic inhibitor vinblastine. Science 186: 1219-1220, 1974

23. Himes RH: Interaction of the catharanthus (*Vinca*) alkaloids with tubulin and microtubules. Pharmac Ther 51: 257-267, 1991

24. Schochet SS Jr, Lambert PW, Earle KM: Neuronal changes induced by intrathecal vincristine sulfate. J Neuropathol Exp Neurol 27: 645-658, 1968

25. Wilson L, Morse ANC, Bryan J: Characterization of *acetyl*-^{3}H-labeled vinblastine binding to vinblastine-tubulin crystals. J Mol Biol 121: 255-268, 1978

26. Fellous A, Francon J, Lennon AM, Nunez J: Microtubule assembly *in vitro*. Purification of assembly-promoting factor. Eur J Biochem 78: 167-174, 1977

27. Khan IA, Ludueña RF: Phosphorylation of β_{III}-tubulin. Biochemistry 35: 3704-3711, 1996

28. Lowry OH, Rosebrough NH, Farr AL, Randall RJ: Protein measurement with the Folin phenol reagent. J Biol Chem 193: 265-275, 1951

29. Rai SS, Wolff J: Localization of the vinblastine-binding site on β-tubulin. J Biol Chem 271: 14707-14711, 1996

30. Timasheff SN, Andreu JM, Na GC: Physical and spectroscopic methods for the evaluation of the interaction of antimitotic agents with tubulin. Pharmac Ther 52: 191-210, 1991

31. Correia JJ: Effects of antimitotic agents on tubulin-nucleotide interactions. Pharmac Ther52:

127-147, 1991

32. Ludueña RF, Roach MC: Tubulin sulfhydryl groups as probes and targets for antimitotic and antimicrotubule agents. Pharmac Ther 49: 13-152, 1991

33. Morgan JL, Spooner BS: Immunological detection of microtubule poison-induced conformational changes in tubulin. J Biol Chem 258: 13127-13133, 1983

33. Prakash V, Timasheff SN: The interaction of vincristine with calf brain tubulin. J Biol Chem 258: 1689-1697, 1983

35. Lee JC, Harrison D, Timasheff SN: Interaction of vinblastine with calf brain microtubule protein. J Biol Chem 250: 9276-9282, 1975

36. Ludueña RF, Fellous A, McManus L, Jordan MA, Nunez J: Contrasting roles of tau and microtubule-associated protein 2 in the vinblastine-induced aggregation of brain tubulin. J Biol Chem 259: 12890-12898, 1984

37. Schwarz PM, Liggins JR, Ludueña RF: β-Tubulin isotypes purified from bovine brain have different relative stabilities. Biochemistry 37: 4687-4692, 1998

38. Banerjee A, Ludueña RF: Kinetics of colchicine binding to purified β-tubulin isotypes from bovine brain. J Biol Chem 267: 13335-13339, 1992

39. Lobert S, Frankfurter A, Correia JJ: Binding of vinblastine to phosphocellulose-purified and αβ-class III tubulin: the role of nucleotides and β-tubulin isotypes. Biochemistry 34: 8050-8060, 1995

40. Prasad V, Jordan MA, Ludueña RF: Temperature sensitivity of vinblastine-induced tubulin polymerization in the presence of microtubule-associated proteins. J Prot Chem 11: 509-515, 1992

41. Fellous A, Prasad V, Ohayon R, Jordan MA, Ludueña RF: Removal of the projection domain of microtubule-associated protein 2 alters its interaction with tubulin. J Prot Chem 13: 381-391, 1994

42. Ranganathan S, Dexter DW, Benetatos CA, Chapman AE, Tew KD, Hudes GR: Increase of β_{III} - and β_{IVa}-tubulin isotypes in human prostate carcinoma cells as a result of estramustine resistance. Cancer Res 56: 2584-2589, 1996

43. Haber M, Burkhart CA, Regl DL, Madafiglio J, Norris MD, Horwitz SB: Altered expression of Mβ2, the class II β-tubulin isotype, in a murine J774.2 cell line with a high level of taxol resistance. J Biol Chem 270: 31269-31275, 1995

44. Dumontet C, Duran GE, Steger KA, Beketic-Oreskovic L, Sikic BI: Resistance mechanisms in human sarcoma mutants derived by single-step exposure to paclitaxel (taxol). Cancer Res 56: 1091-1097, 1996

45. Jaffrézou JP, Dumontet C, Derry WB, Durán G, Chen G, Tsuchiya E. Wilson L, Jordan MA, Sikic BI: Novel mechanism of resistance to paclitaxel (taxol) in human K562 leukemia cells by combined selection with PSC833. Oncol Res 7: 517-527, 1995

Table 1. Effect of vinblastine on the assembly of tubulin isotypes.

Tubulin	**% Inhibition**[a]		
	Tau	**MAP2**	
Unfractionated	31 ± 3 (5)	[1], [3]	
$\alpha\beta_{II}$	88 ± 4 (3)	29, 36	
$\alpha\beta_{III}$	29 ± 3 (4)	3, 4	
$\alpha\beta_{IV}$	65 ± 4 (3)	[3], [5]	

[a]Samples of tubulin (either unfractionated or else isotypically purified $\alpha\beta_{II}$, $\alpha\beta_{III}$, or $\alpha\beta_{IV}$) (1.0 mg/mL) were incubated at 37 °C in the presence of either tau (0.30 mg/mL) or MAP2 (1.5 mg/mL) and in the presence or absence of 1 μM vinblastine. Absorption of each sample at 350 nm was measured at 0, 10, 20 and 40 minutes (for samples containing tau) or at 0, 15, 30, 45 and 60 minutes (for samples containing MAP2). The net change in absorbance at 40 minutes (for tau) or 60 minutes (for MAP2) due to the presence of vinblastine was used to calculate the drug-induced inhibition of microtubule assembly. Incubations with MAP2 were done in duplicate, incubations with tau were done either 3, 4 or 5 times. For the duplicate MAP2 samples, both values of the inhibition are given. For the tau samples, the average inhibition is given, together with the standard deviation. Numbers in parentheses indicate the number of incubations. Numbers in brackets indicate enhancement rather than inhibition.

FIGURE LEGENDS

Fig. 1. Effect of vinblastine on MAP2-induced assembly of unfractionated and isotypically purified tubulin isotypes. In each sample, tubulin (1.5 mg/mL) was incubated with MAP 2 (0.3 mg/mL) in the absence (●) or in the presence of vinblastine concentrations of either 1 μM (○) or 20 μM (▲). Assembly was followed by turbidimetry. The arrows represent addition of vinblastine (final concentration 20 μM) to the assembly mixture. Conditions were as described in "Materials and Methods". Samples were as follows: unfractionated tubulin (A), $\alpha\beta_{II}$ (B), $\alpha\beta_{III}$ (C) and $\alpha\beta_{IV}$ (D).

Figure 2. Effect of vinblastine on the morphology of the tubulin polymers. The assembly mixtures containing MAP2 and unfractionated tubulin (A), $\alpha\beta_{II}$ (B), $\alpha\beta_{III}$ (C) or $\alpha\beta_{IV}$ (D) were mixed with the indicated amount of vinblastine at 0 °C (panels 1-3 in Figures A-D). Assembly was initiated by warming the samples to 37 °C and the polymers formed were processed for electron microscopy. The magnifications of electron micrographs were as follows: **2A (1),** 132000; **2A (2),** 264000; **2A (3),** 400000; **2B (1)**, 132000; **2B (2)** *top*, 264000; **2B (2)** *bottom*, 200000; **2B (3),** 400000; **2C (1)**, 400000; **2C (2),** 180180; **2C (3),** 132000; **2D (1)**, 132000; **2D (2)**, 264000; **2D (3)**, 200000.

Figure 3. Effect of 0-200 μM vinblastine on MAP2-induced assembly of unfractionated and isotypically pure tubulins. Assembly was followed by sedimentation. The arrows represent addition of vinblastine (final concentration 20 μM) to the assembly mixture. Samples were as follows: unfractionated tubulin (A), $\alpha\beta_{II}$ (B), $\alpha\beta_{III}$ (C) and $\alpha\beta_{IV}$ (D) tubulin.

Figure 4. Effect of vinblastine on tau-induced assembly of unfractionated and isotypically purified tubulins. In each sample, tubulin (1.5 mg/mL) was incubated with tau (0.15 mg/mL) in the absence (●) or in the presence of vinblastine concentrations of either 1 μM (○) or 20 μM (▲). Assembly was followed by turbidimetry. Samples were as follows: unfractionated tubulin (A), $\alpha\beta_{II}$ (B), $\alpha\beta_{III}$ (C) and $\alpha\beta_{IV}$ (D).

Figure 5. Effect of 40-50 μM vinblastine on the polymerization of $\alpha\beta_{III}$. Assembly was followed by turbidimetry and the depolymerization of microtubules at the steady state was induced by addition of vinblastine to a final concentration of either 40 μM (○) or 50 μM (●) (indicated by the arrows).

Figure 6. Effect of vinblastine on the morphology of tubulin polymers. The assembly mixtures containing tau and either unfractionated tubulin (A), $\alpha\beta_{II}$ (B), $\alpha\beta_{III}$ (C) or $\alpha\beta_{IV}$ (D) were mixed with indicated amount of vinblastine at 0 °C (panels 1-3 in Figures A-D). Assembly was initiated by warming the samples to 37 °C and the polymers formed were processed for electron microscopy. The magnifications of electron micrographs were as follows: **6A (1)**, 132000; **6A (2)**, 264000; **6A (3)**, 132000; **6B (1)**, 132000; **6B (2)**, 132000; **6B (3)**, 132000; **6C (1)**, 132000; **6C (2)**, *top* 520000; **6C (2)**, *bottom*, 264000; **6C (3)**, 520000; **6D (1)**, 99000; **6D (2)**, *top* 200000; **6D (2)**, *bottom*, 400000; **6D (3)**, 132000.

Figure 7. Effect of vinblastine on tau-induced assembly of unfractionated and isotypically

purified tubulins. Samples of tubulin (1.5 mg/mL) were incubated at 37 °C in the presence of tau (0.15 mg/mL) with the indicated concentrations of vinblastine. Samples were as follows: unfractionated tubulin (A), $\alpha\beta_{II}$ (B), $\alpha\beta_{III}$ (C) and $\alpha\beta_{IV}$ (D). Assembly was followed by sedimentation.

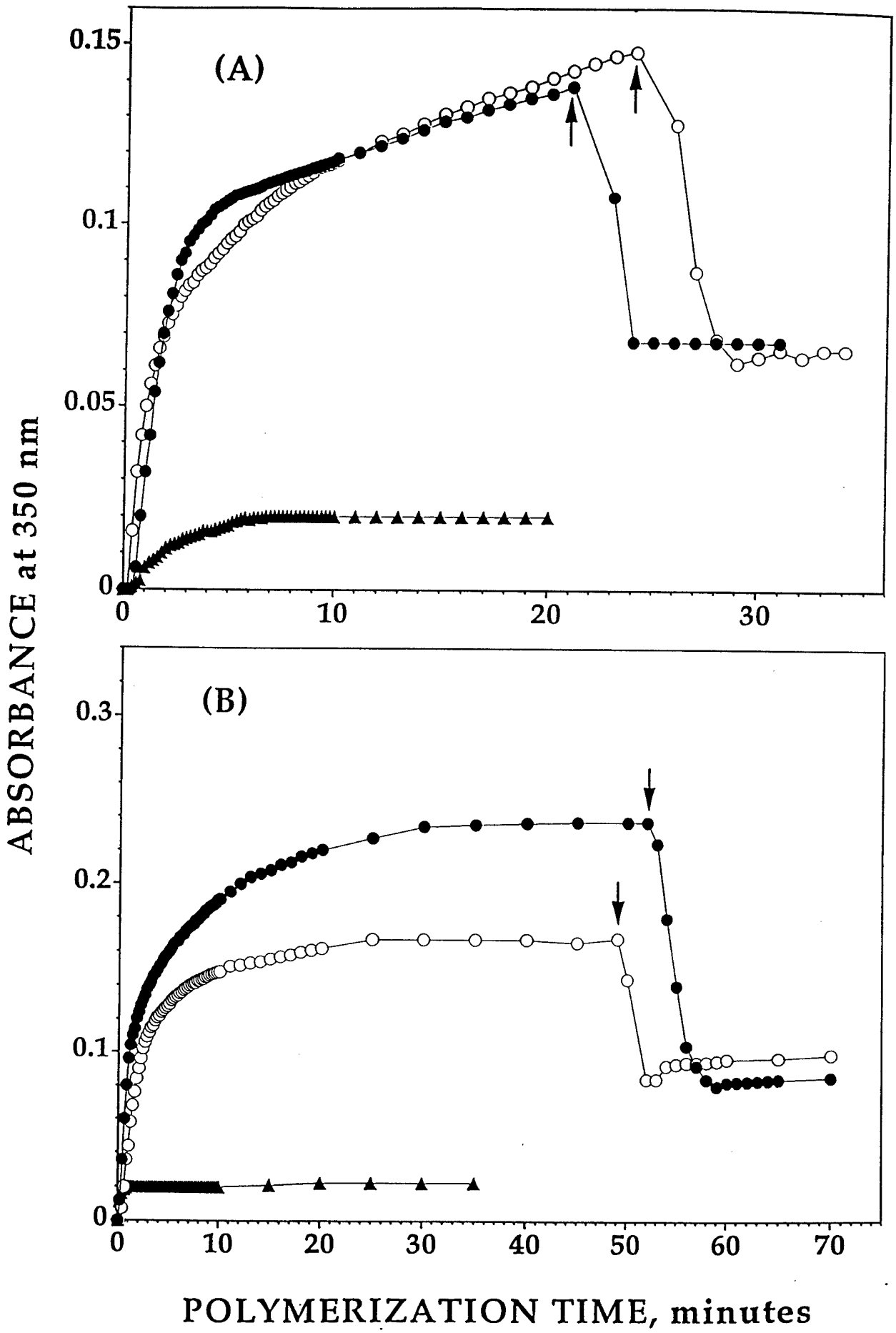

Figure 1a and 1b

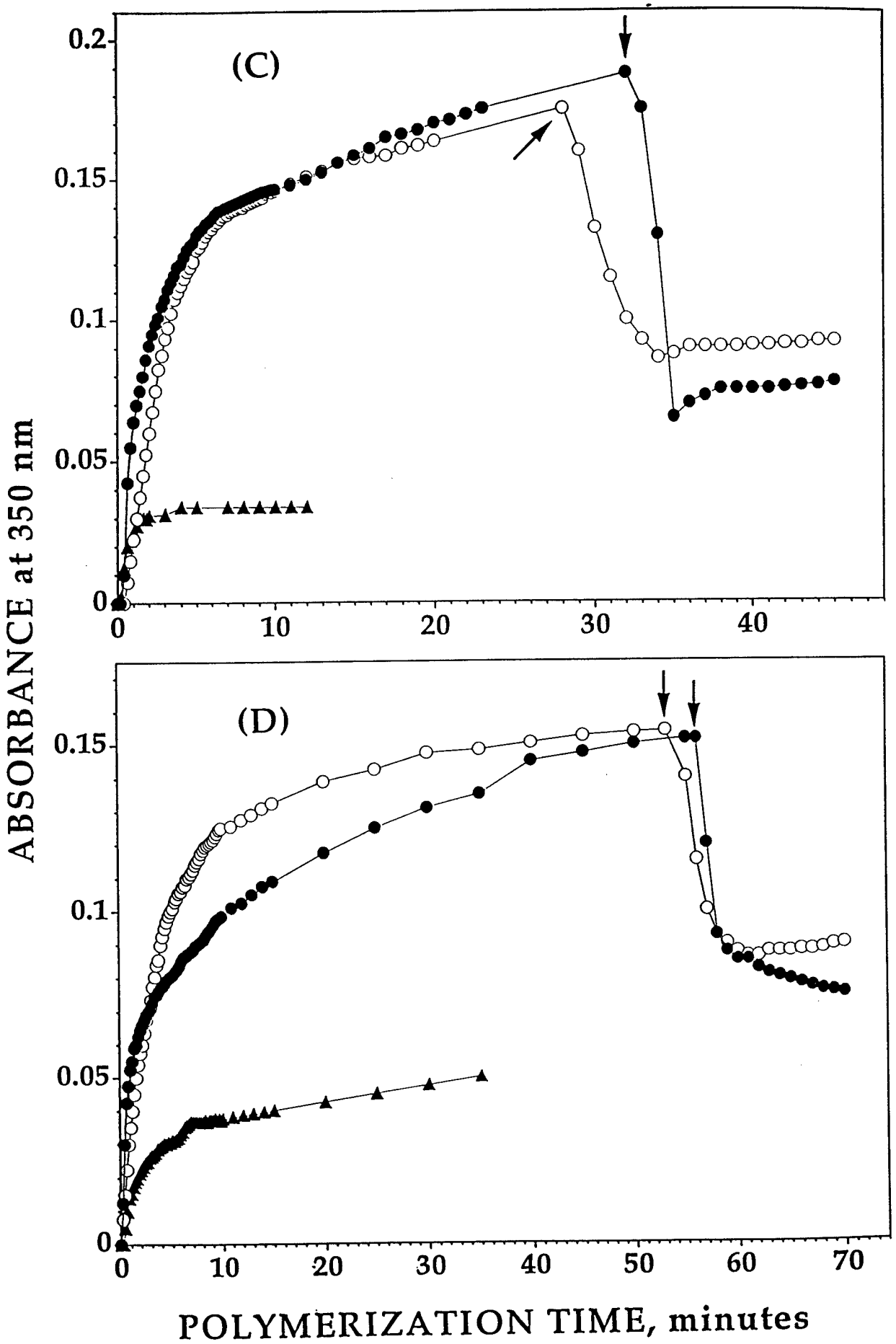

Figure 1c and 1d

(1). (PCT + 0 μM VBL + MAP2)

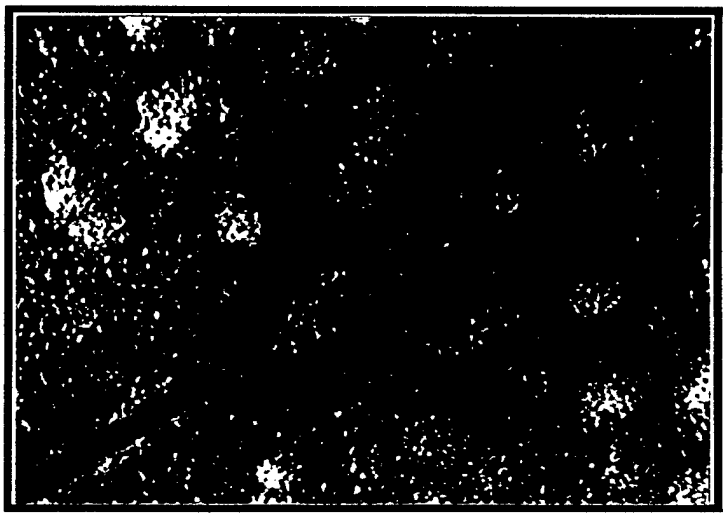

(2). (PCT + 1 μM VBL + MAP2)

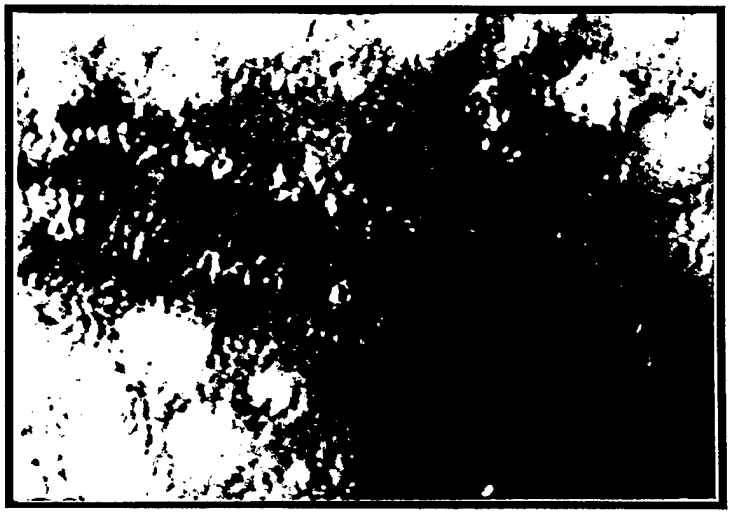

(3). (PCT + 20 μM VBL + MAP2)

Figure 2a

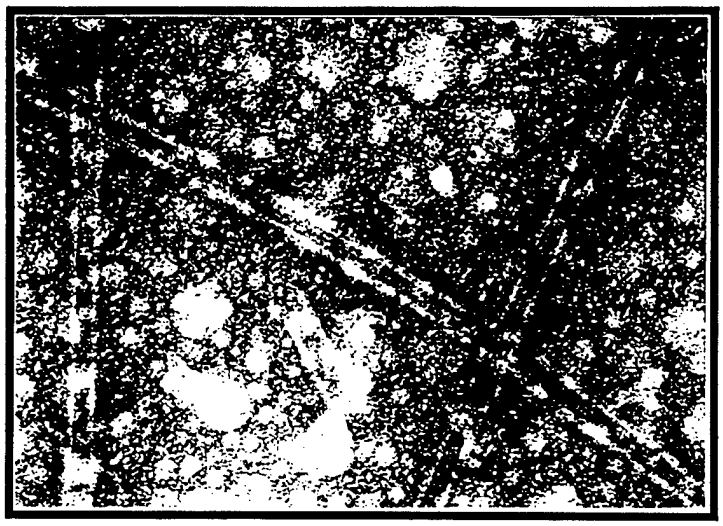

(1). ($\alpha\beta_{II}$ + 0 μM VBL + MAP2)

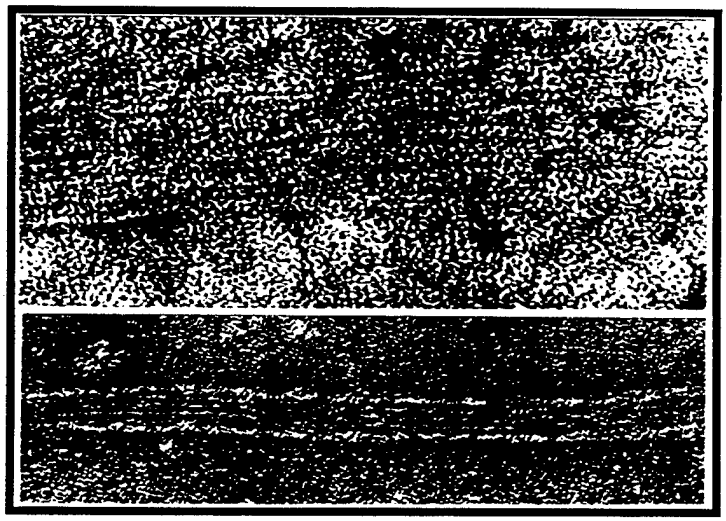

(2). ($\alpha\beta_{II}$ + 1 μM VBL + MAP2)

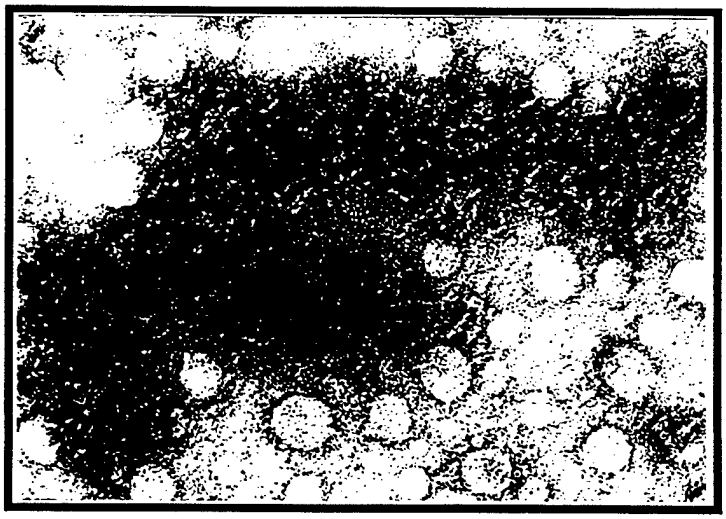

(3). ($\alpha\beta_{II}$ + 20 μM VBL + MAP2)

Figure 2b

(1). ($\alpha\beta_{III}$ + 0 μM VBL + MAP2)

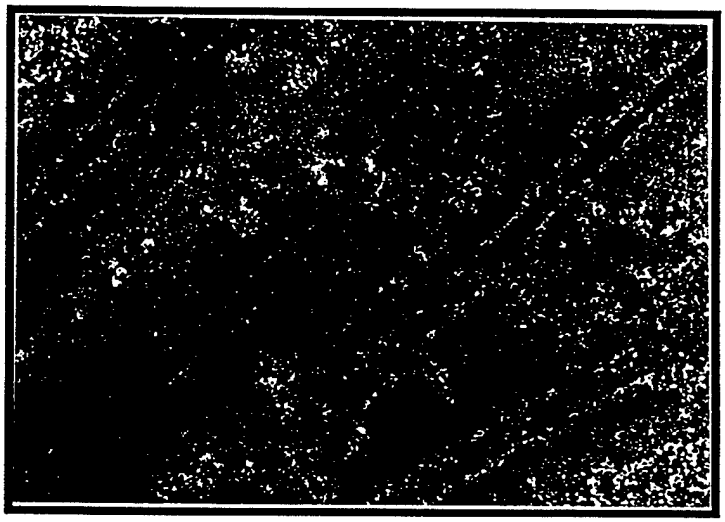

(2). ($\alpha\beta_{III}$ + 1 μM VBL + MAP2)

(3). ($\alpha\beta_{III}$ + 20 μM VBL + MAP2)

Figure 2c

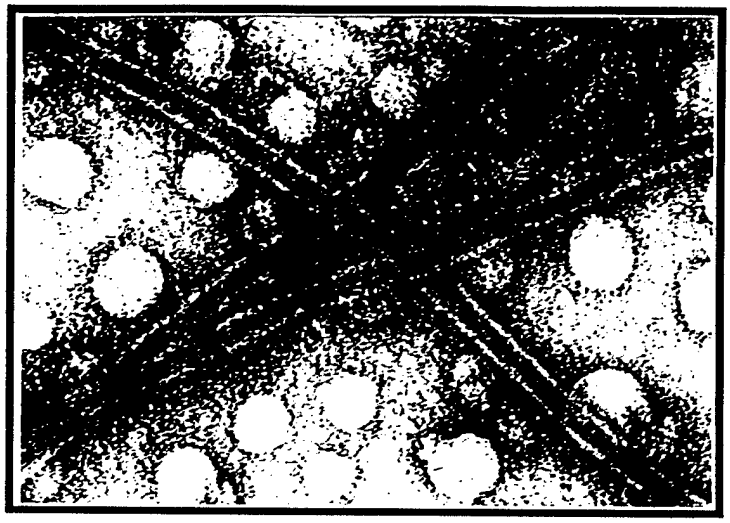

(1). ($\alpha\beta_{IV}$ + 0 μM VBL + MAP2)

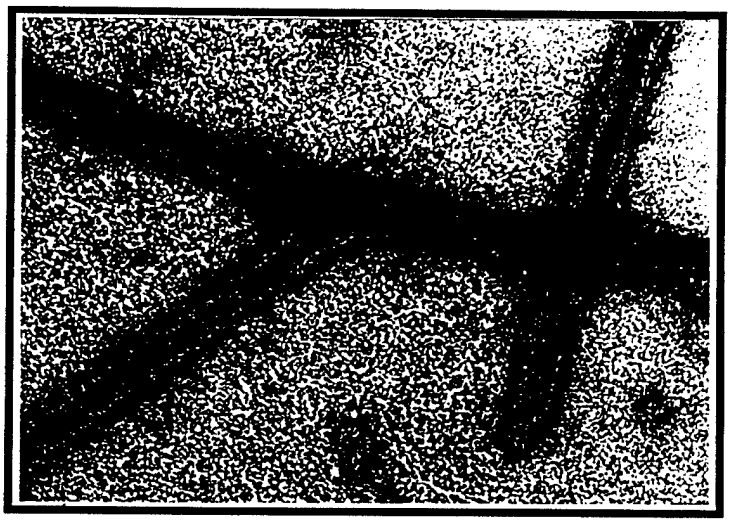

(2). ($\alpha\beta_{IV}$ + 1 μM VBL + MAP2)

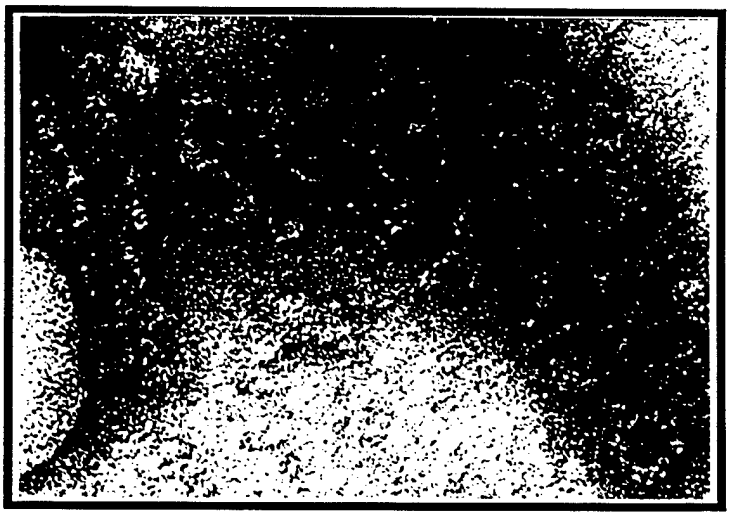

(3). ($\alpha\beta_{IV}$ + 20 μM VBL + MAP2)

Figure 2d

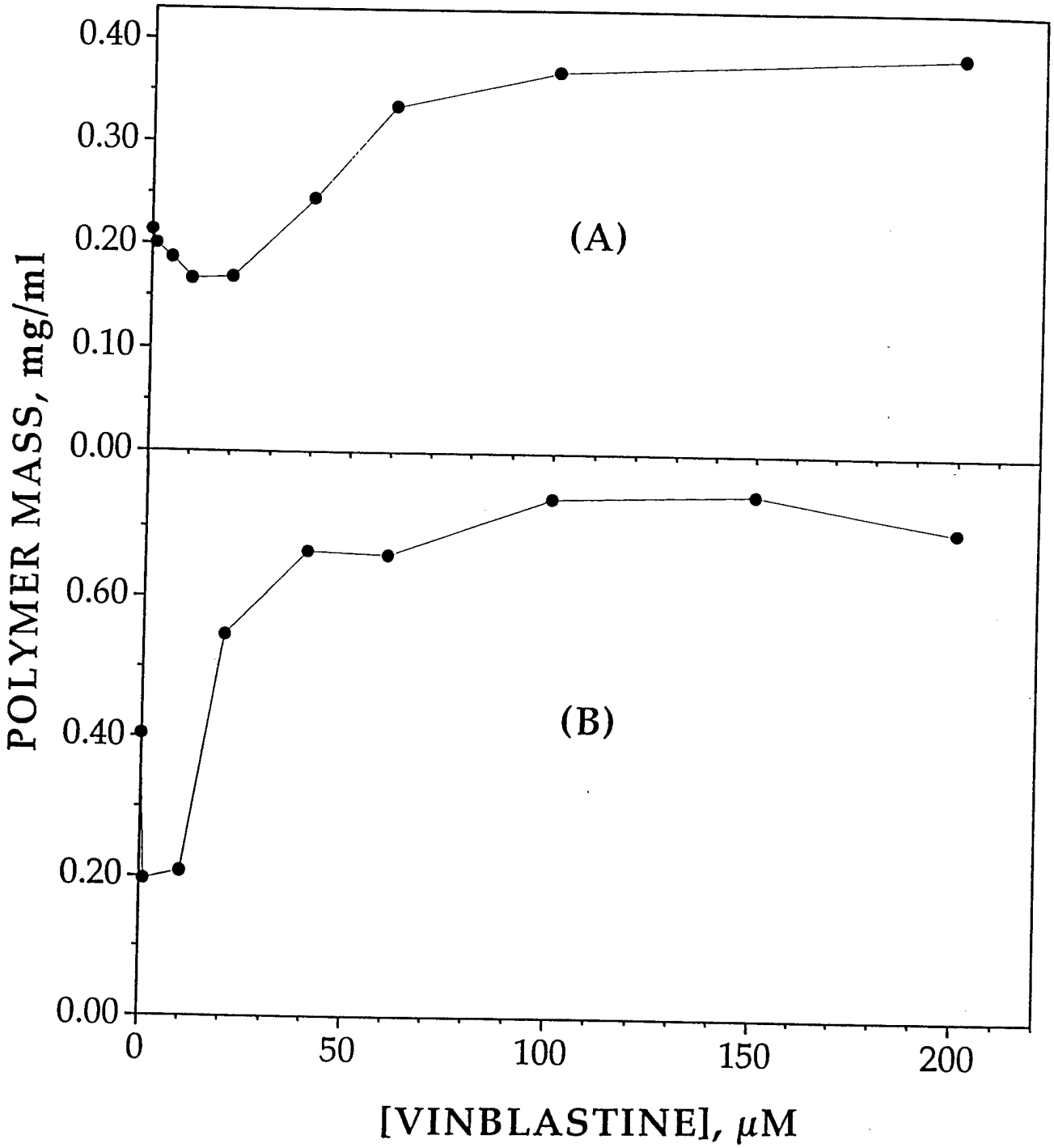

Figure 3a and 3b

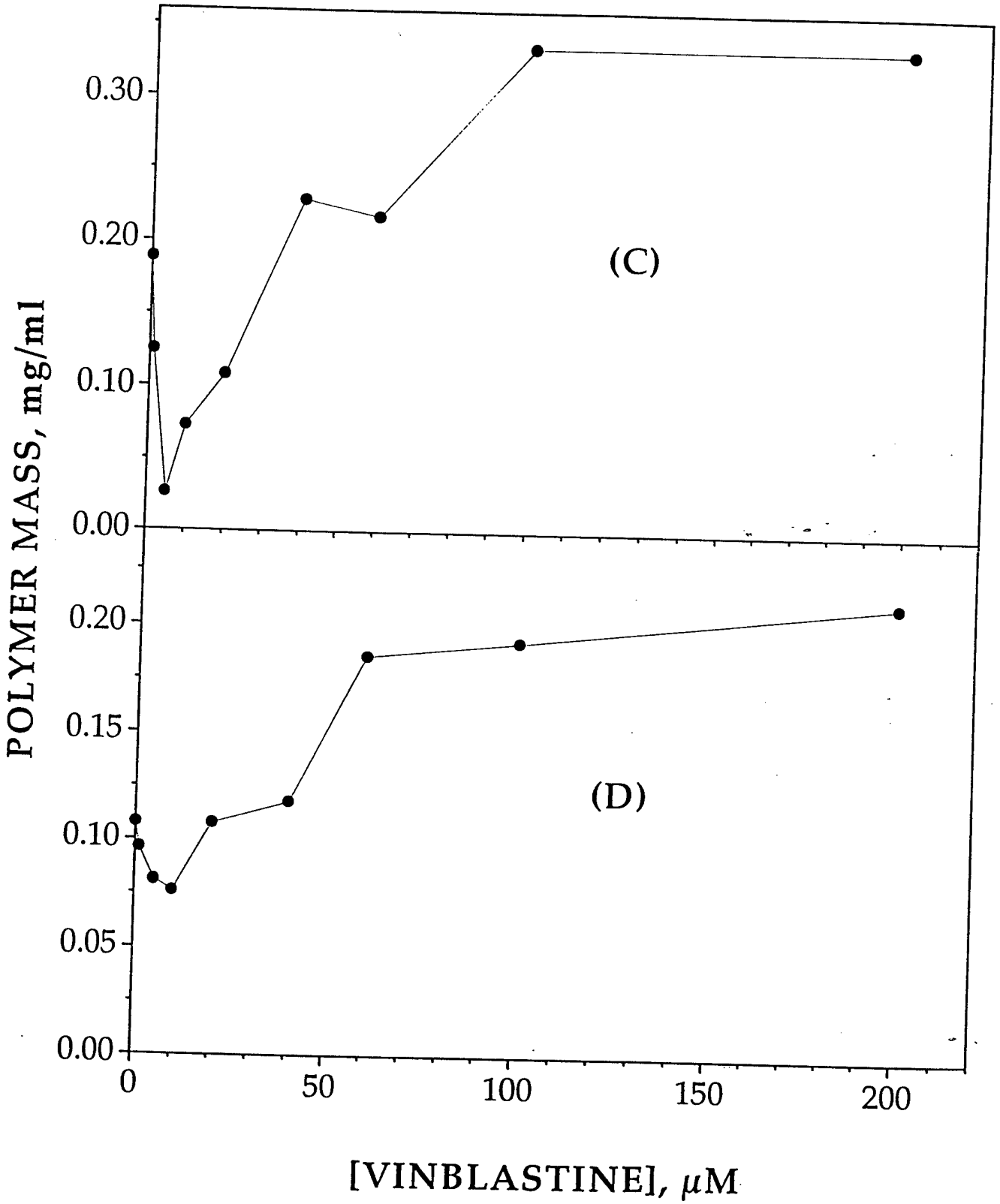

Figure 3c and 3d

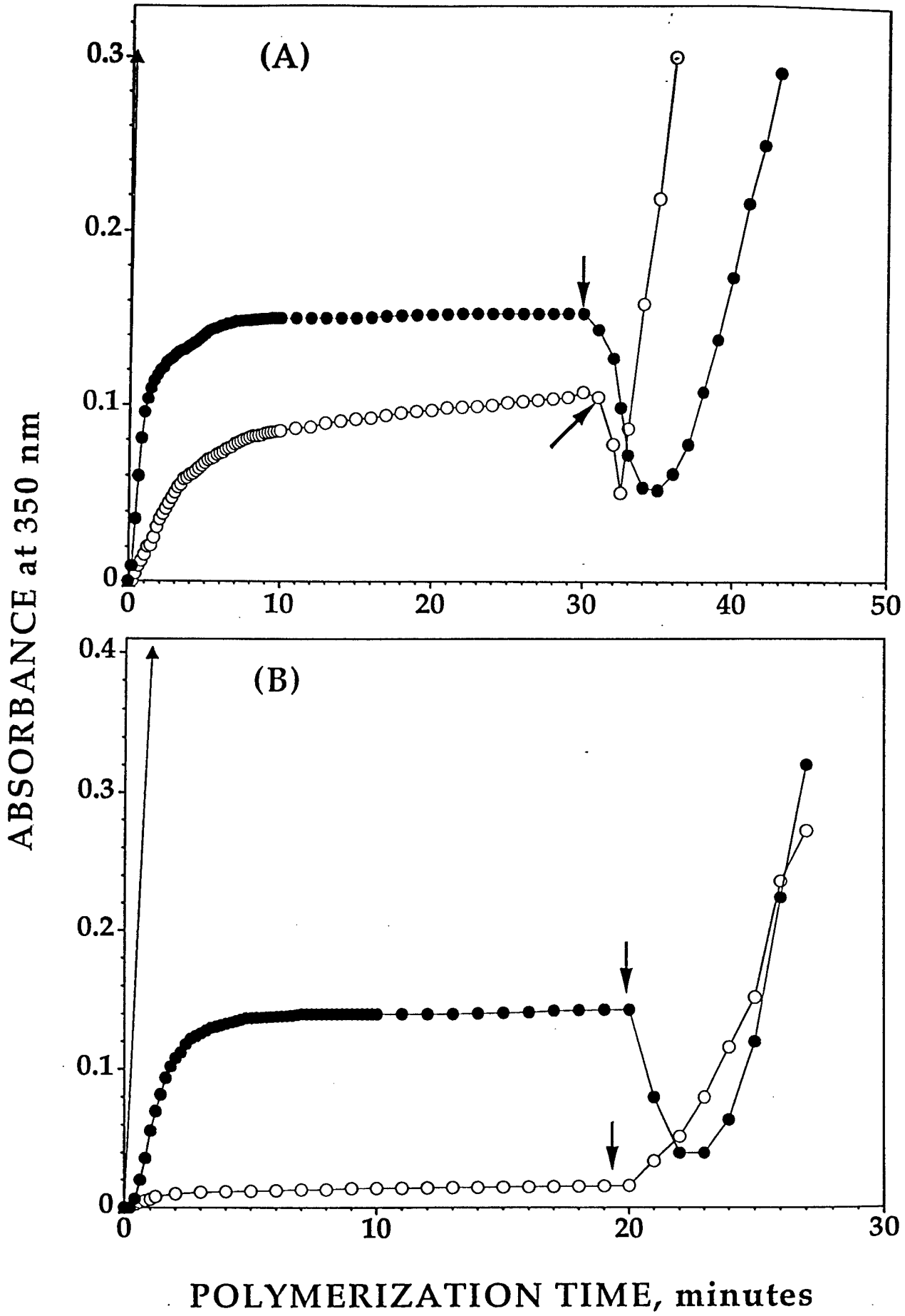

Figure 4a and 4b

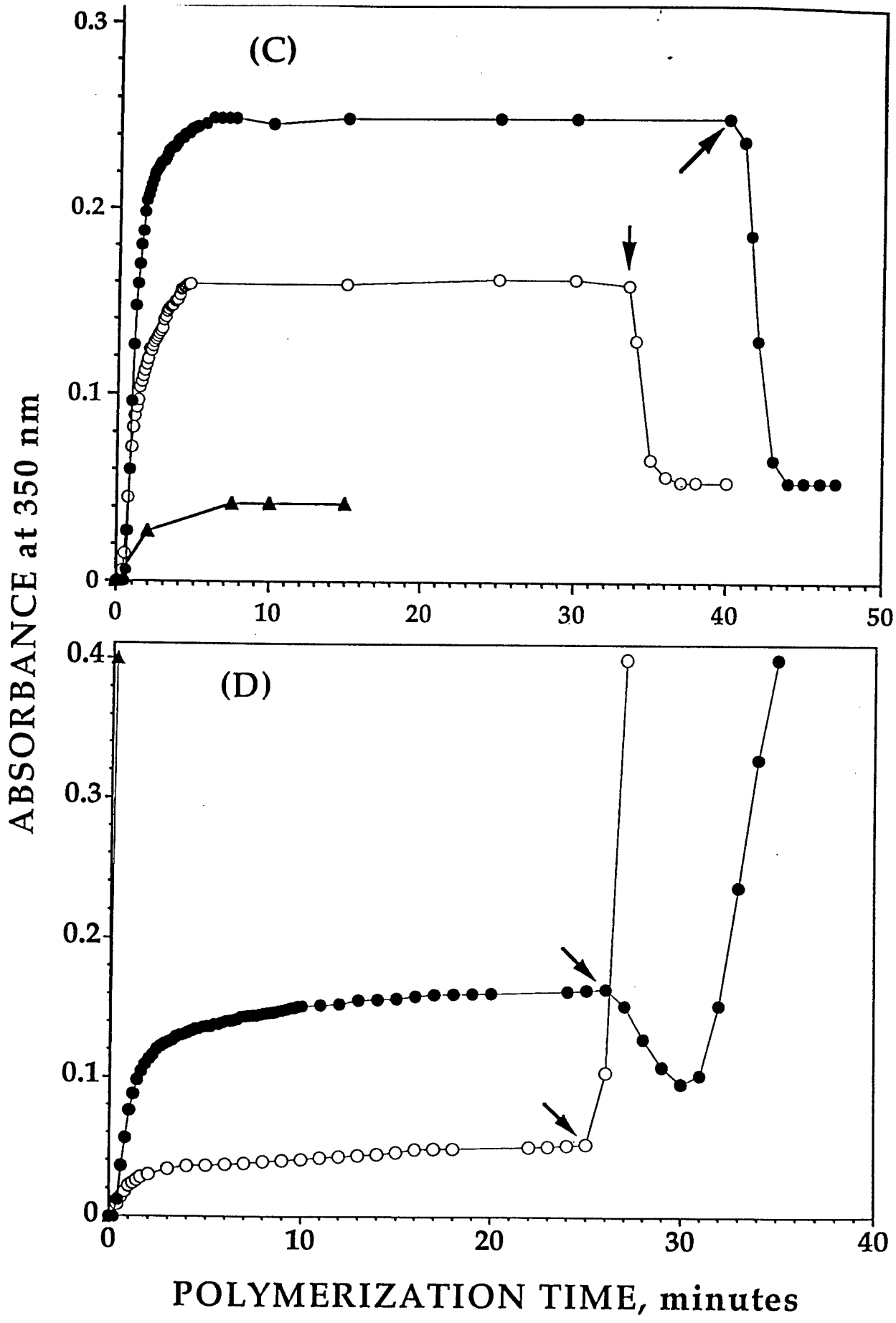

Figure 4c and 4d

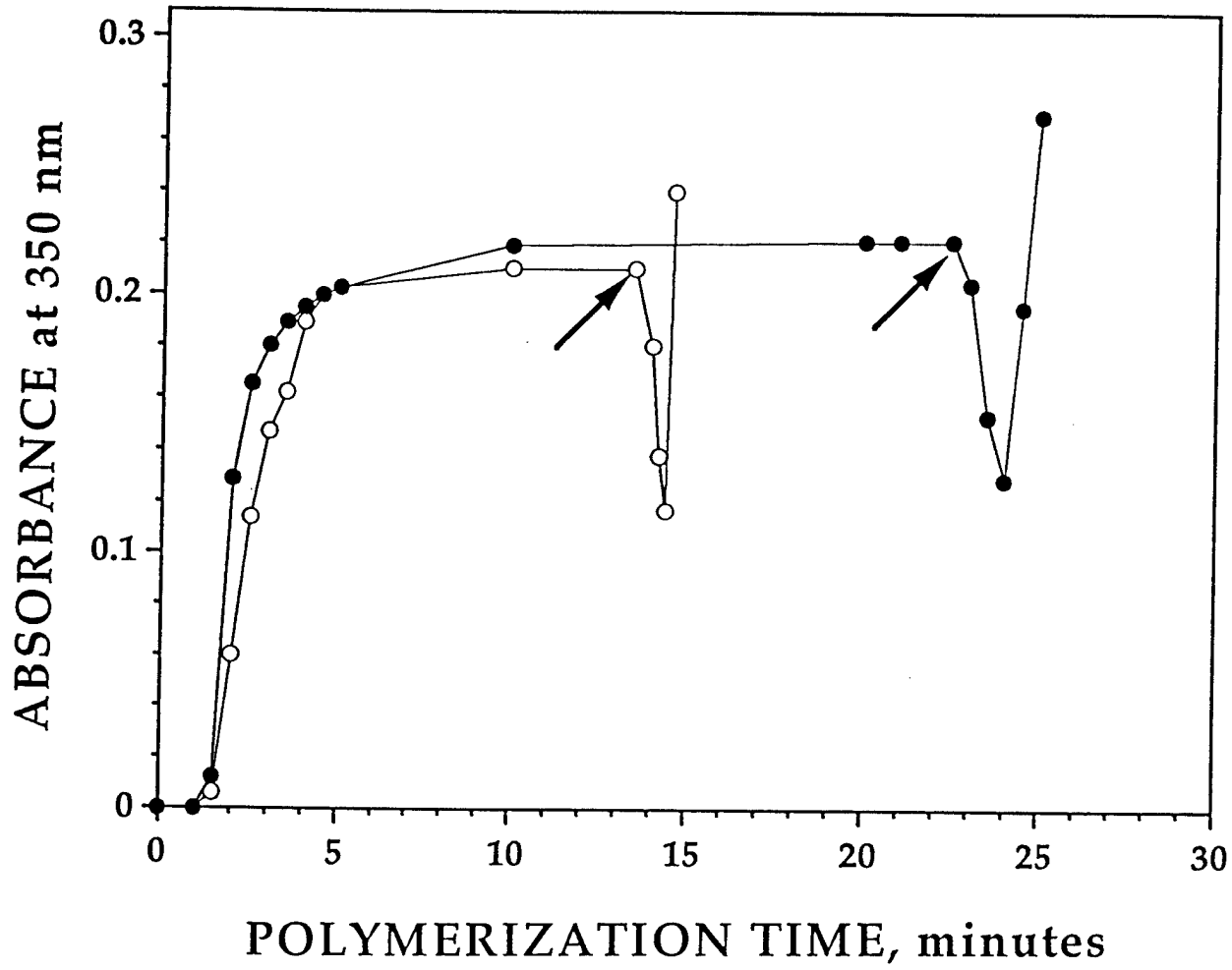
ABSORBANCE at 350 nm
0.3
0.2
0.1
0
0
5
10
15
20
25
30
POLYMERIZATION TIME, minutes

Figure 5

(1). (PCT + 0 μM VBL + Tau)

(2). (PCT + 1 μM VBL + Tau)

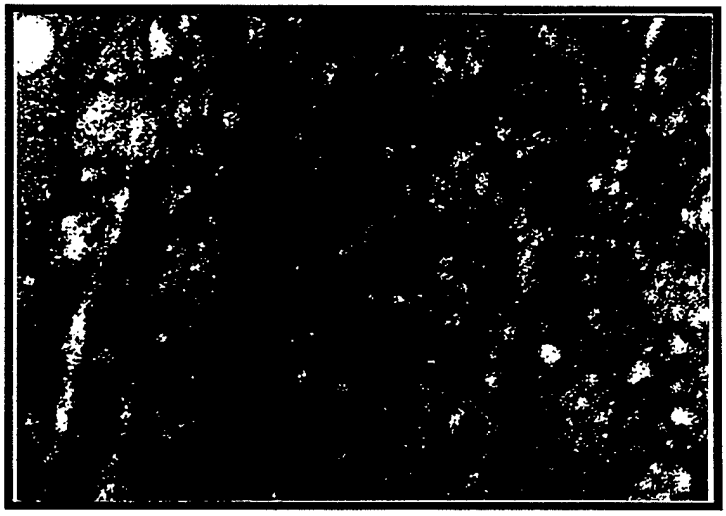

(3). (PCT + 20 μM VBL + Tau)

Figure 6a

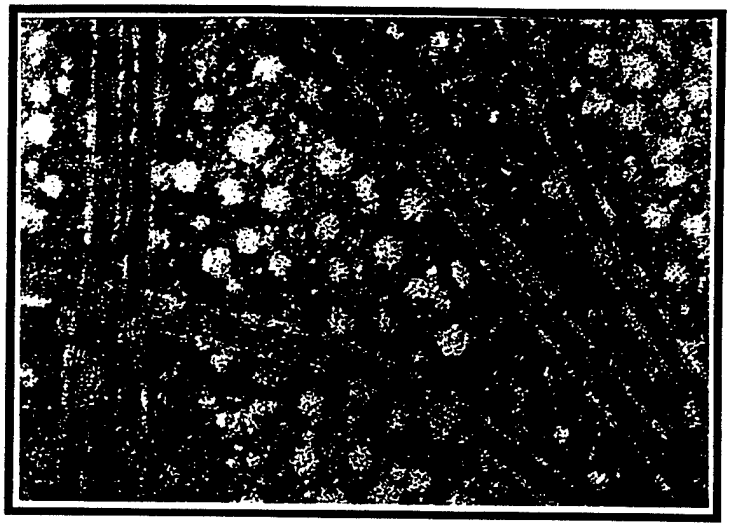

(1). ($\alpha\beta_{II}$ + 0 μM VBL + Tau)

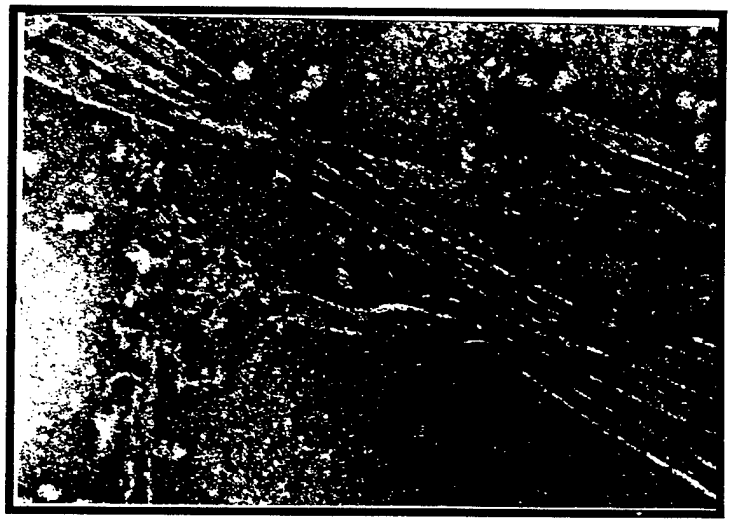

(2). ($\alpha\beta_{II}$ + 1 μM VBL + Tau)

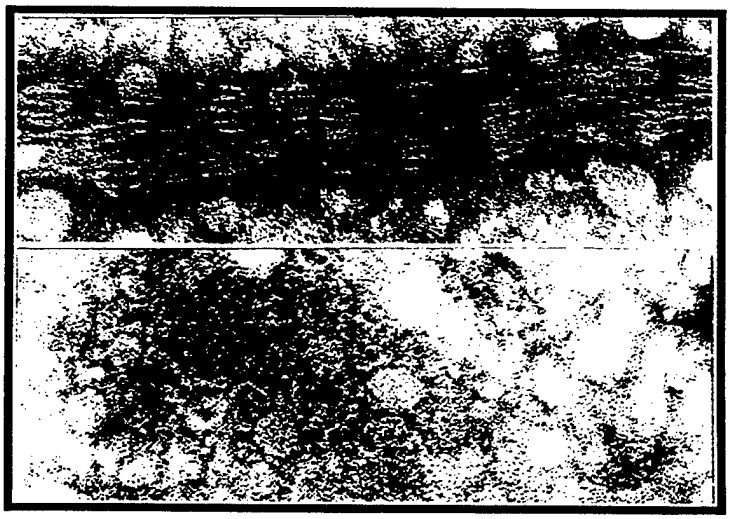

(3). ($\alpha\beta_{II}$ + 20 μM VBL + Tau)

Figure 6b

(1). ($\alpha\beta_{III}$ + 0 μM VBL + Tau)

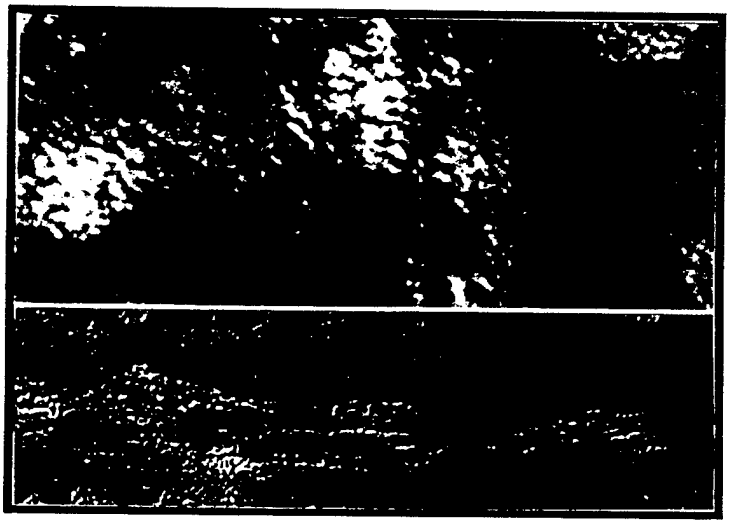

(2). ($\alpha\beta_{III}$ + 1 μM VBL + Tau)

(3). ($\alpha\beta_{III}$ + 20 μM VBL + Tau)

Figure 6c

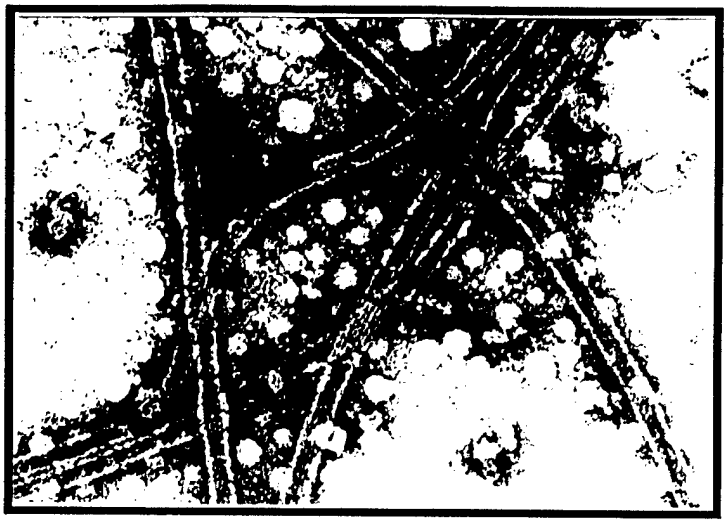

(1). ($\alpha\beta_{IV}$ + 0 μM VBL + Tau)

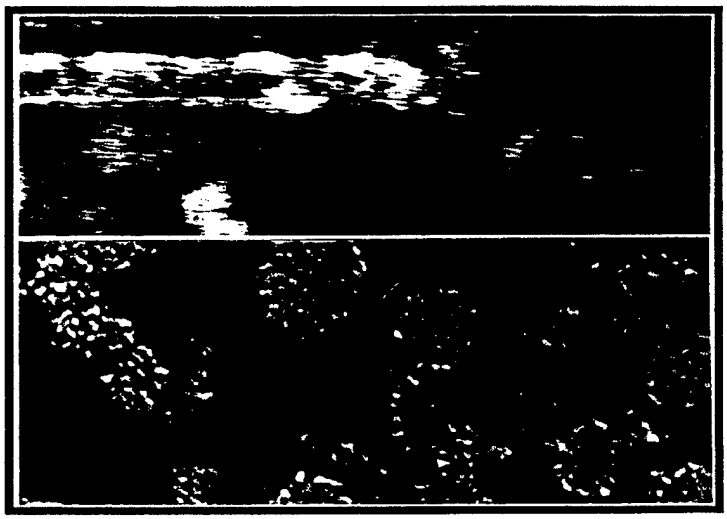

(2). ($\alpha\beta_{IV}$ + 1 μM VBL + Tau)

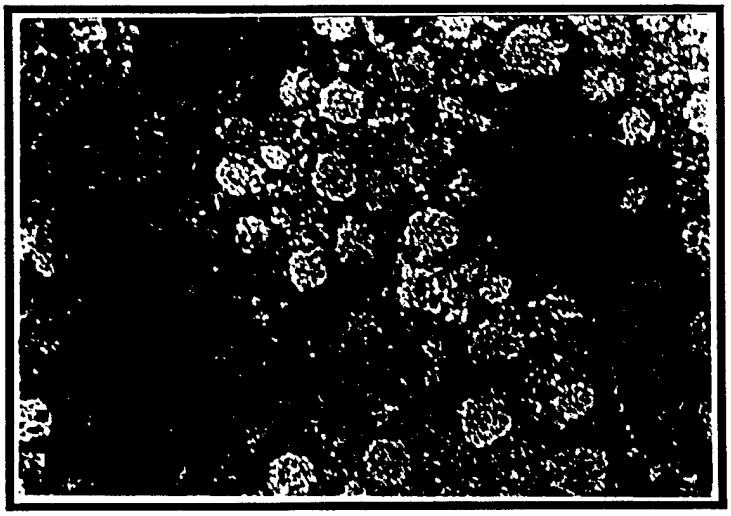

(3). ($\alpha\beta_{IV}$ + 20 μM VBL + Tau)

Figure 6d

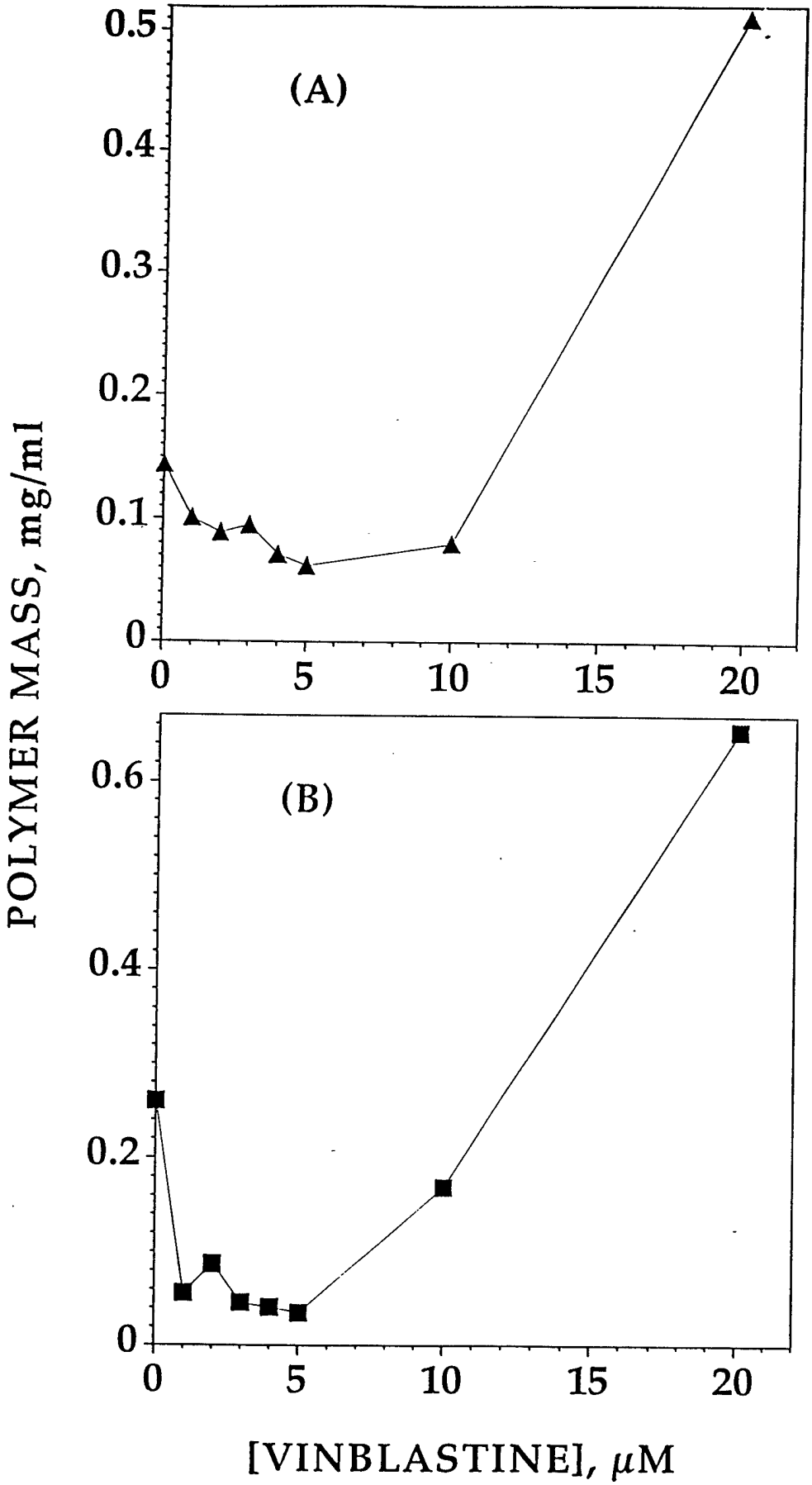

Figure 7a and 7b

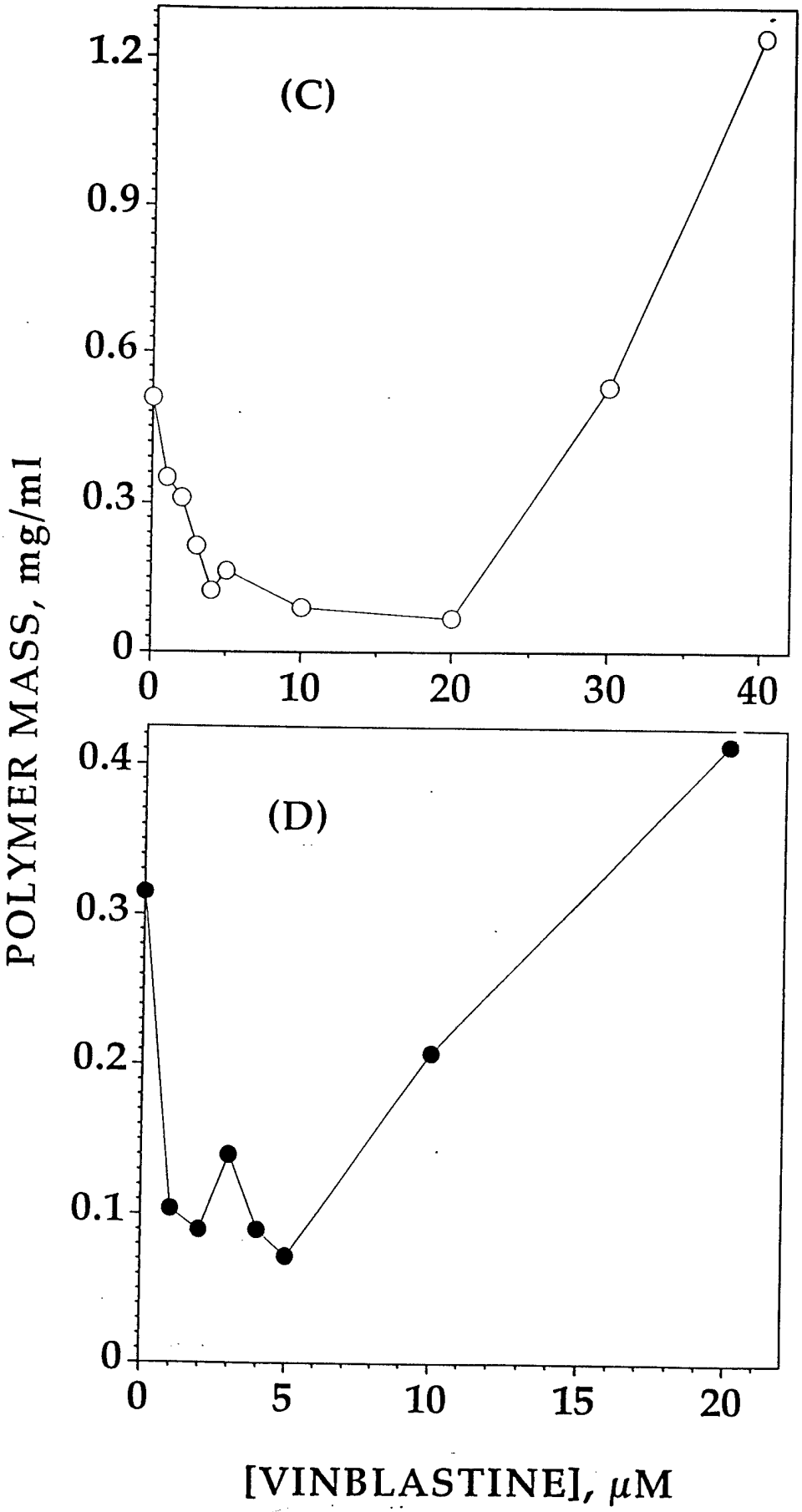

Figure 7c and 7d

Appendix 5

Effect of the Anti-Tumor Drug Vinblastine on Nuclear β_{II}-Tubulin in Cultured Rat Kidney Mesangial Cells

Consuelo Walss-Bass[1,2], Jeffrey I. Kreisberg[3] & Richard F. Ludueña[1,4]

Departments of [1]Biochemistry and [3]Surgery, University of Texas Health Science Center, San Antonio, Texas 78229, USA and the †The Research and Development Service Department of Veteran Affairs, San Antonio, Texas 78229, USA.

[2]Present address: Department of Psychiatry, University of Texas Health Science Center, San Antonio, TX 78229.

[4]To whom correspondence should be addressed.

Send correspondence to:

Dr. Richard F. Ludueña

Department of Biochemistry

University of Texas Health Science Center

San Antonio, TX 78229-3900

T: 210-5673732

F: 210-5676595

E-mail: luduena@uthscsa.edu

Running head: Effect of vinblastine on nuclear β_{II}-tubulin

Submitted to Investigational New Drugs

ABSTRACT

Tubulin, the main component of microtubules, is a major target for anti-tumor drugs such as vinblastine. We have recently discovered that the β_{II} isotype of tubulin is present in the nuclei of cultured rat kidney mesangial cells, smooth muscle-like cells present in the renal glomerular mesangium (Walss C, Kreisberg JI, Ludueña RF. 1999. Cell Motil Cytoskeleton 42:274-284). Here, we have investigated the effect of vinblastine on nuclear β_{II}-tubulin in these cells. We have found that, at concentrations of 15 nM and higher, vinblastine caused a reversible loss of β_{II}-tubulin from the nucleus. Our results raise the possibility that nuclear β_{II}-tubulin constitutes a population of tubulin that could be a novel target for anti-tumor drugs such as vinblastine.

Key words: tubulin isotypes, microtubules, vinblastine, nuclear localization, DNA fragmentation.

INTRODUCTION

Because of their crucial role in chromosome segregation during cell division, microtubules have long been a target for anti-tumor drugs [1]. These drugs inhibit microtubule dynamics by binding to tubulin, the structural subunit of microtubules [2]. Vinblastine, a member of the *Vinca* alkaloid family, is an anti-tubulin drug widely used in chemotherapy [3]. By binding to the β-subunit of tubulin, vinblastine inhibits microtubule dynamics [2]. At high concentrations, vinblastine causes microtubule depolymerization [4] and the formation of tubulin para-crystals [5]. Therefore, this drug is known as a microtubule destabilizing agent. At low, clinically relevant, concentrations, vinblastine is known to arrest cells in mitosis by suppressing the dynamics of spindle microtubules, without significantly changing the amount of polymerized tubulin [6]. The end result of this drug at low concentrations is to impede cell division and ultimately cause cell death.

We have previously reported the presence of a specific isotype of tubulin, β_{II}, in the nuclei of rat kidney mesangial cells [7]. Nuclear β_{II}-tubulin exists as an $\alpha\beta_{II}$ tubulin dimer and appears to be in non-microtubule form and, as such, it constitutes a novel population of cellular tubulin. Recently, we have found that β_{II} is present in the nuclei of a variety of human cancer cells, but seems to be absent from the nuclei of many normal human cells [8]. Since tubulin is a major target of certain anti-tumor drugs, it is of interest to examine the effects of these drugs on nuclear tubulin. Therefore, we have now investigated the effect of vinblastine on nuclear β_{II}-tubulin in rat kidney mesangial cells, smooth-muscle-like cells from the renal mesangium. We have found that, at concentrations higher than clinically relevant, these drugs appear to cause β_{II}-tubulin to

exit the nucleus. Loss of nuclear tubulin occurs after microtubule depolymerization caused by vinblastine. Removal of the drug allows β_{II} to re-enter the nucleus. Treatment of cells with anti-tumor drugs has been shown to induce apoptosis. The mechanism by which this occurs remains unclear [9]. Our results raise the possibility that vinblastine may act by binding to nuclear β_{II}-tubulin and preventing it from executing its as yet unknown function.

MATERIALS AND METHODS

Source of cells and antibodies. Rat kidney mesangial cells were obtained as follows. Glomeruli were isolated from 200 g male Sprague-Dawley rats (Harlan Sprague-Dawley, Inc, Indianapolis, IN) using a graded sieve technique and were plated for culture in RPMI 1640 (Gibco BRL, Grand Island, N.Y.) tissue culture medium with 20% FCS plus penicillin, streptomycin and fungizone (E.R. Squibb and Sons) for explant growth of mesangial cells [10, 11]. One hundred percent of the cells were identified as glomerular mesangial cells. Positive identification was obtained by ultrastructural examination, contractile responsiveness to vasopressin and angiotensin II, and shape change in response to cAMP-elevating agents [10, 11, 12]. For the experiments described below, cells were used between the 4th and 40th passage. The monoclonal antibodies SAP.4G5 and JDR.3B8 specific for the β_I and β_{II} isotypes of tubulin, were prepared as previously described [13, 14].

Immunofluorescence microscopy. Rat kidney mesangial cells were plated on glass coverslips in RPMI-1640 medium (Gibco BRL, Grand Island, N.Y.) containing 20% fetal calf serum (Atlanta Biologicals, Norcross, GA). After 24 h, cells were treated with various concentrations of vinblastine (Sigma Chemical Co., St. Louis. MO.), from a 1 mM stock solution prepared fresh in H_2O. After various periods of time, cells were washed twice with PBS (0.15M NaCl, 0.0027 M KCl, 0.00147M KH_2PO_4, 0.01M $NaHPO_4$, pH 7.2), fixed for 15 min with 3.7 % paraformaldehyde at room temperature and permeabilized for 1 min with 0.5% Triton X-100 in PBS. Cells were then incubated at 4 °C overnight with the respective isotype-specific monoclonal IgG mouse antibody (anti-β_I, 0.05-0.1 mg/ml; anti-β_{II}), diluted in PBS containing 10% normal goat serum

(Jackson Immunoresearch, West Grove, PA). After rinsing in PBS, coverslips were stained with a Cy3-conjugated goat anti-mouse antibody (1:100, Jackson Immunoresearch) for 1 hr at room temperature. For DNA detection, cells were stained with DAPI (4',6-diamidino-2-phenylindole, dihydrochloride) (Molecular Probes, Eugene, OR.) (2 μl/ml in PBS) during the last wash with PBS after incubation with the secondary antibody. Coverslips were mounted on glass slides and examined with an Olympus epifluorescence photomicroscope using a Plan-Neufluar 100x oil objective. For drug reversibility experiments, cells were incubated with vinblastine at various concentrations for 24 h, after which the drug was removed and cells were incubated in fresh media for 24 h. Cells were then fixed and treated as described above.

RESULTS

Because we were not interested in blocking cells in mitosis, we chose to use vinblastine concentrations higher than those clinically relevant. Therefore, rat kidney mesangial cells were incubated with vinblastine at concentrations of 15 to 50 nM for 1 to 6 h. Cells were then fixed and stained with monoclonal antibodies to β_I- and β_{II}-tubulin. The β_{II}-tubulin antibody has been reported previously to detect nuclear β_{II}-tubulin [7]. The β_I-tubulin antibody was used to observe the effect of vinblastine on cytosolic microtubules, since this isotype is present only in the cytosol [7]. Cells treated with anti-β_I in the absence of drug revealed a normal microtubule network in the cytosol (Fig. 1*A*). However, 1hr treatment with 15 nM vinblastine, the lowest drug concentration used, was enough to completely depolymerize the microtubules (Fig. 1*B*). No difference in the cytosolic fluorescence pattern was observed when cells were treated longer or with higher drug concentrations.

Staining of control, drug-free cells, with anti-β_{II} tubulin revealed that all cells contained β_{II}-tubulin in the nucleus, as had been previously reported [7] (Fig. 1*C*). Very little fluorescence was observed in the cytosol. After treatment with 15 nM vinblastine for 1 h, 3 out of 10 cells seemed to have lost their nuclear tubulin, as they contained no nuclear fluorescence (Fig. 1*D*). The nuclei of these cells appeared unaffected, as seen by DAPI staining (Fig. 1*E*). After 3 h of treatment with 15 nM vinblastine, 8 out of 10 cells had lost their nuclear tubulin (Fig. 1*F*) and, as before, DAPI staining revealed that the nuclei of these cells appeared intact (not shown). By increasing the vinblastine concentration to 30 nM, 1 h of treatment was enough to cause the loss of nuclear tubulin in 7 out of 10 cells (Fig. 1*G*). At this drug concentration, micro-nucleation, or DNA

fragmentation, was seen by DAPI staining in 3 out of 10 cells, indicating that these cells were probably undergoing apoptosis (Fig. 1*H*). Micro-nucleation appeared to occur regardless of whether β_{II}-tubulin was present in the nucleus or not. Furthermore, the nuclei of cells that had lost their nuclear tubulin, but had not entered apoptosis, appeared to be normal, as indicated by DAPI staining (Fig. 1*H*). After 3 h of treatment with 30 nM vinblastine, nuclear tubulin was absent in 9 out of 10 cells (Fig. 1*I*, *J*). Treatment of cells with concentrations of 40 to 60 nm vinblastine for 1 h caused the total disappearance of nuclear tubulin (Fig. 1*K*, *L*).

In order to determine if the effect of vinblastine on nuclear tubulin was reversible, cells were incubated with vinblastine at concentrations from 15 to 50 nM for 24 h and then incubated in media without drug for 24 h. Treatment of these cells with anti-β_{II} revealed that cells were able to recover form the effect of the drug, even at the higher concentrations used. Cells appeared nearly confluent, indicating that they were able to proliferate, and very few apoptotic cells were observed. Furthermore, β_{II}-tubulin was able to re-enter the nucleus of the cells, as appearance of nuclear fluorescence was seen in nearly all cells examined (Fig. 2).

DISCUSSION

The results shown here revealed that the anti-tumor drug vinblastine, when used at high concentrations, causes β_{II}-tubulin to exit the nucleus. The exit of β_{II}-tubulin from the nucleus may be due to vinblastine binding directly to nuclear tubulin, or, it may be an indirect result of the effect of this drug on cytoplasmic microtubules. It is possible that, in an effort to counteract the effect of vinblastine on microtubules, cells may translocate β_{II}-tubulin into the cytosol, where it may be needed more. However, our studies did not reveal an increase in cytosolic β_{II}-tubulin after treatment with vinblastine. This is most likely due to the fact that vinblastine causes microtubule depolymerization. In fact, vinblastine has been shown to inhibit the assembly of $\alpha\beta_{II}$ microtubules more than it does the assembly of $\alpha\beta_{III}$ and $\alpha\beta_{IV}$ microtubules [15].

The effect of vinblastine on nuclear tubulin was found to be reversible, since β_{II}-tubulin appeared to re-enter the nucleus after the drug was removed and cells were able to recover. This is consistent with the findings by Jordan *et al.* [16], who reported that vinblastine is effluxed from cells after the drug is removed from the media. The mechanism by which vinblastine and other anti-tumor drugs, trigger apoptosis remains unknown [17]. It is tempting to speculate that the effect of these drugs on nuclear tubulin may somehow be related to activation of the programmed cell death pathway. However, in our present studies we have found that vinblastine causes cells to enter apoptosis regardless of whether they contain nuclear β_{II}-tubulin or not. This suggests that activation of the apoptotic pathway is independent of the presence of β_{II}-tubulin in the nucleus.

Our studies on nuclear tubulin have revealed that β_{II}-tubulin is present in the nuclei of a variety of cultured human cancer cells, while it is absent from the nuclei of some cultured human normal cells [8]. Although the rat kidney mesangial cells used in the present experiments are considered normal, they grow extremely fast in culture [18] and in this sense resemble cancerous cells. These findings have led us to believe that β_{II}-tubulin may be somehow involved in assisting rapid cell proliferation. By blocking microtubule dynamics, the anti-tubulin drug vinblastine inhibits cell proliferation [6]. Therefore, it is possible that the function of β_{II}-tubulin in the nucleus is inhibited by this drug. Vinblastine has been shown to affect cellular processes such as DNA and RNA synthesis [19, 20]. The finding of β_{II}-tubulin in the nucleus, and the fact that vinblastine appears to cause this isotype to exit the nucleus, could explain the effect of this drug on these seemingly non-tubulin related functions. Further studies are necessary to determine whether nuclear β_{II}-tubulin is in fact involved in DNA and RNA synthesis.

In conclusion, our present studies on the effect of vinblastine on nuclear β_{II}-tubulin have revealed that anti-tubulin drugs may be useful tools to determine the exact role of β_{II}-tubulin in the nucleus. They also raise the possibility that these drugs may exert their anti-tumor activity through an interaction with nuclear tubulin.

Acknowledgments

This research was supported by grants CA26376 from the National Institutes of Health (R.F.L.), AQ-0726 from the Welch Foundation (R.F.L.), DAMD17-98-1-8246 from the U.S. Army Medical Research Program (R.F.L.) and VA Merit Review to J.I.K. We are grateful to Phyllis Smith, Asok Banerjee, Pat Schwarz, Asish Chaudhuri, and Veena Prasad for their assistance.

REFERENCES

1. Dustin P (ed): Microtubules, 2nd Ed., Springer-Verlag, Berlin, 1984
2. Wilson L, Jordan MA: 1994. Pharmacological probes of microtubule function. In: Hyams JS, Lloyd CW (eds), Microtubules. Wiley-Liss, New York,1994, pp 59-83
3. Gerzon K: Dimeric catharanthus alkaloids. In: Cassady JM, Douros JD (eds), Anticancer Agents Based on Natural Product Models Academic Press, New York, 1980, pp 271-317
4. Owellen RJ, Hartke CA, Dickerson RM, Haines FO: Inhibition of tubulin microtubule polymerization by drugs of the *Vinca* alkaloid class. Cancer Res 36: 3798-3802, 1976
5. Na GC, Timasheff SN: In vitro vinblastine-induced tubulin paracrystals. J Biol Chem 257:10387-10391, 1982
6. Jordan MA, Thrower D, Wilson L: Mechanism of inhibition of cell proliferation by *Vinca* alkaloids. Cancer Res 51:2212-2222, 1991
7. Walss C, Kreisberg JI, Ludueña RF: Presence of the β_{II} isotype of tubulin in the nuclei of cultured mesangial cells from rat kidney. Cell Motil Cytoskeleton 42:274-284, 1999
8. Walss-Bass C, Xu K, David S, Fellous A, Ludueña RF: Occurrence of nuclear β_{II}-tubulin in cultured cells. Cell Tiss Res 2002 (in press).
9. Tsukidate K, Yamamoto K, Snyder JW, Farber JL: Microtubule antagonists activate programmed cell death (apoptosis) in cultured rat hepatocytes. Am J Pathol 143:918-925, 1993

10. Ausiello DA, Kreisberg JI, Roy C, Karnovsky MJ: Contraction of cultured cells of apparent mesangial origin after stimulation with angiotensin II and arginine vasopressin. J Clin Invest 65: 754-760, 1980

11. Kreisberg JI, Venkatachalam MA, Patel PY: Cyclic AMP-associated shape change and its reversal by PGE_2. Kidney Int 25:874-879, 1984

12. Kreisberg JI, Venkatachalam MA: Vasoactive agents affect mesangial cell adhesion. Am J Physiol 251:C505-C511, 1986

13. Banerjee A, Roach MC, Wall KA, Lopata MA, Cleveland DW, Ludueña RF: A monoclonal antibody against the type II isotype of β-tubulin. Preparation of isotypically altered tubulin. J Biol Chem 263:3019-3034, 1988

14. Roach MC, Boucher VL, Walss C, Ravdin P, Ludueña RF: Preparation of a monoclonal antibody specific for the class I isotype of β-tubulin: the β isotypes of tubulin differ in their cellular distributions within human tissues. Cell Motil Cytoskeleton 39:273-285, 1998

15. Khan IA, Ludueña RF: Effect of vinblastine on the assembly of isotypically pure tubulins from bovine brain. Mol Biol. Cell 6:30a, 1995

16. Jordan MA, Wendell K, Gardiner D, Derry WB, Copp H, Wilson L: Mitotic block induced in HeLa cells by low concentrations of paclitaxel (taxol) results in abnormal mitotic exit and apoptotic cell death. Cancer Res 56:816-825, 1996

17. Sorger PK, Dobles M, Tournebize R, Hyman AA: Coupling cell division and cell death to microtubule dynamics. Curr Opin Cell Biol 9:807-814, 1997

18. Floege J, Topley N, Hoppe J, Barrett TB, Resch K: Mitogenic effect of platelet-derived growth factor in human glomerular mesangial cells: modulation and/or

suppression by inflammatory cytokines. Clin Exp Immunol 86:334-341, 1991

19. Creasey WA: Modifications in biochemical pathways produced by the Vinca alkaloids. Cancer Chemother Res 52:501-507, 1968

20. Bernstam VA, Gray RH, Bernstein IA: Effect of microtubule-disrupting drugs on protein and RNA synthesis in *Physarum polycephalum* Amoebae. Arch.Microbiol., 128:34-40, 1980

FIGURE LEGENDS

Fig. 1. Effect of vinblastine on nuclear tubulin in mesangial cells. (*A*), Control, drug-free cells, stained with anti-β_I. (*B*), Cells treated with 15 nM vinblastine for 1 h, stained with anti-β_I. Notice depolymerization of microtubules. (*C*), Control, drug-free cells stained with anti-β_{II}. Notice the strong nuclear fluorescence. (*D*), Cells treated with 15 nM vinblastine for 1 h, stained with anti-β_{II}. (*E*), Same cells as in *D*, stained with DAPI to reveal the nuclei. (*F*), Cells treated with 15 nM vinblastine for 3 h, stained with anti-β_{II}. (*G*), Cells treated with 30 nM vinblastine for 1 h, stained with anti-β_{II}. (*H*), same cells as in *G*, stained with DAPI to reveal the nuclei. (*I*), Cells treated with 30 nM vinblastine for 3 h, stained with anti-β_{II}. (*J*), Same cells as in *I*, stained with DAPI to reveal the nuclei. (*K*), Cells treated with 50 nM vinblastine for 1 h, stained with anti-β_{II}. (*L*), Same cells as in *K*, stained with DAPI, to reveal the nuclei. Arrows indicate micronucleation.

Fig. 2. The effect of vinblastine on nuclear tubulin is reversible. (*A*, *C*, *E*), Cells stained with anti-β_{II}. (*B*, *D*, *F*), Cells stained with DAPI. (*A*, *B*), Cells treated with 15 nM vinblastine for 6 h, then incubated in media without drug for 24 h. (*C*, *D*), Cells treated with 30 nM vinblastine for 6 h, then incubated in media without drug for 24 h. (*E*, *F*), Cells treated with 50 nM vinblastine for 6 h, then incubated in media without drug for 24 h.

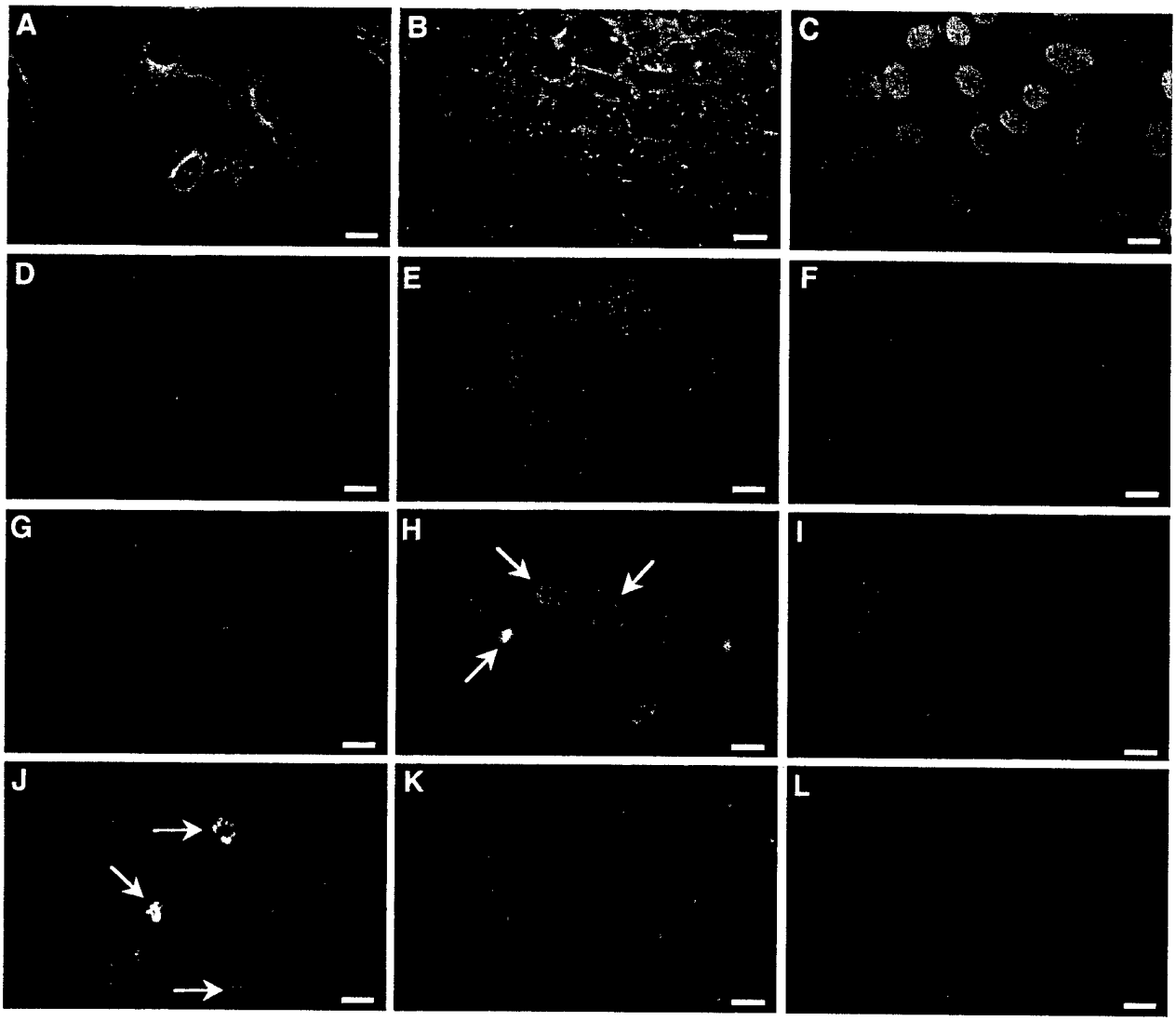

Figure 1

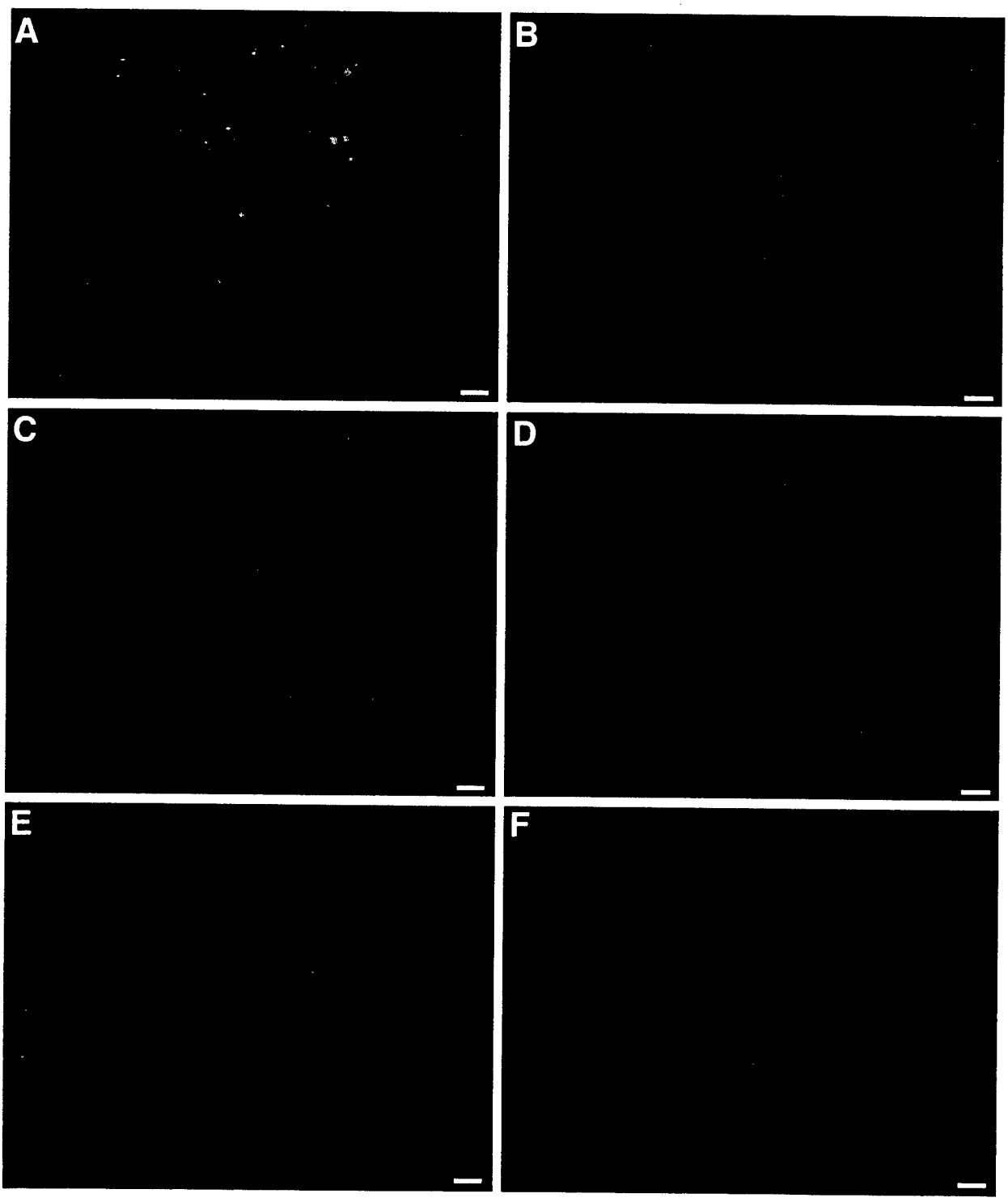

Figure 2

Appendix 6

Thursday, September 13, 2001

Submitted to JARO

Differential Expression of β Tubulin Isotypes In Gerbil Vestibular End Organs

BRIAN PERRY[1], HEATHER JENSEN[2], RICHARD F. LUDUEÑA[3], AND RICHARD HALLWORTH[2]

[1]Department of Pediatrics and [3]Department of Biochemistry, The University of Texas Health Science Center at San Antonio, San Antonio Texas 78229-3900, and [2]Department of Biomedical Sciences, Creighton University, Omaha, Nebraska 68178.

Running Head: βTubulin in the Vestibule
Target Journal: J.A.R.O.
Corresponding Author:
Richard Hallworth
Department of Biomedical Sciences
Creighton University
2500 California Plaza
Omaha, NE 68178
Phone: (402) 280-3057
FAX: (402) 280-2690
Email: hallw@creighton.edu

Abstract

The seven mammalian isotypes of β tubulin are strikingly similar in amino acid sequence. Nonetheless, the isotypic sequence differences are conserved in evolution, which suggests that they may have distinct functional roles. Such roles should be reflected in the selective expression of isotypes by cell type, or even in the sorting of isotypes to within-cell pools. The hair cells of the vestibular sensory epithelia each possess kinocilia, a microtubule-based organelle that could represent such a compartment, distinct from the extensive microtubule network in the hair cell soma. The afferent neurons that innervate the vestibular sensory epithelia may also be functionally divided into dendritic, somatic and axonal compartments, each with its own complement of microtubules. We have therefore examined the selective expression and possible intracellular sorting of β tubulin isotypes in gerbil vestibular sense organs using isotype-specific antibodies and indirect immunofluorescence. We find that, while hair cells and supporting cells express distinct ensembles of β tubulin isotypes, the isotypes are deployed uniformly throughout each cell. However, the dendritic compartment of vestibular afferent neurons exhibits a distinct isotype, β_{III}, that is different from the isotypes in other neuronal compartments. The implication of these findings is that β tubulin isotypes are sometimes, but not always, sorted within cells.

Introduction

Microtubules consist of heterodimers of α and β tubulin, both of which exist as numerous isotypes. Seven isotypes of mammalian β tubulin have been characterized, termed β_I, β_{II}, β_{III}, β_{IVa}, β_{IVb}, β_V and β_{VI} (Ludueña 1998). The β-tubulin isotypes are among the most highly conserved proteins known (Ludueña 1998). The multi-tubulin hypothesis (Fulton and Simpson 1976) proposes that the β tubulin have separate functional roles. A prediction of this hypothesis is that the isotypes will be selectively expressed in different tissues and may even be compartmentalized within the same cell. Consistent with the hypothesis, it has been found that different isotypes are expressed in different cell types of the same tissue (Roach et al. 1998; Hallworth and Ludueña 2000). However, little is known about the functional roles of these seven isotypes, except that the β_{IVb} isotype appears to be associated with axonemal microtubules (Renthal et al. 1993; Lu et al. 1998; Roach et al. 1998).

Vestibular sense organs consist of sensory hair cells, supporting cells, afferent neurons and efferent nerve endings. Hair cells bear multiple actin-based stereocilia and a single polarized kinocilium, a microtubule-based organelle that connects the stereocilia to an overlying membrane (the otolithic membrane in macula organs, the cupula in ampullary organs). The kinocilium has the 9+2 paired organization of microtubules characteristic of the axoneme, but is not motile. Other somatic microtubules in hair cells originate from the cuticular plate and nucleating centers near the epithelial apex (Jaeger et al. 1994), and have likely roles in intracellular trafficking and in the maintenance of cell shape. Each hair cell makes synaptic contact with the dendrites of one or more afferent neurons. In addition, a small number of small diamter efferent fibers, originating in the vestibular brainstem, make synaptic contact with hair

cells. The vestibular sensory organs are therefore an interesting test of the possibility of cellular sorting of β tubulin isotypes.

In this study we have examined the distribution of β tubulin isotypes in vestibular sensory organs and neurons. We have used a variety of approaches to preparation of tissue for examination, including frozen sections, whole mounts and dissociation of fresh sensory organs into isolated cells. Isotypes were detected using isotype-specific antibodies (Roach et al. 1998) and indirect immunofluorescence. We find that hair cells and supporting cells express different combinations of isotypes but do not sort them into separate compartments. However, vestibular afferent neurons express a single isotype in their dendritic compartment, but several isotypes in the somatic and axonal compartments, suggesting that β tubulin isotypes in vestibular neurons are sorted for functional reasons.

Materials and Methods

The distribution of β tubulin isotypes was examined in adult gerbil vestibular organs and nasal epithelium using indirect immunofluorescence in frozen sections and isolated cells. Adult gerbils (22 days old or older) were anesthetized with Nembutal and cardiac-perfused with 4% paraformaldehyde in phosphate buffered saline (PBS). For whole mounts, temporal bones were removed from the head, post-fixed, decalcified in EDTA, and the organs were dissected out. For vestibular sections, decalcified temporal bones were embedded in agar and bisected with a razor blade. The halves were then processed to equilibration in 30% sucrose in PBS as a cryoprotectant and were then quickly frozen in O.C.T. (Miles Labs) using methanol cooled by dry ice. 10 or 20 μm sections were cut on a cryostat (Leica). Some isolated organs were also processed for frozen sections when specific orientations were desired.

Organs for whole mount preparations and sections were blocked and permeabilized in PBS containing 1% bovine serum albumin (BSA), 0.25% Triton-X and 5% normal goat serum. The presence of β tubulin isotypes was detected with monoclonal antibodies raised in mouse as previously described (Banerjee et al. 1988, 1990, 1992; Roach et al. 1998). Each antibody was prepared to an epitope unique to the C-terminus of that isotype. The C-termini of β_{IVa} and β_{IVb} are virtually identical, and therefore the anti-β_{IV} antibody was unable to discriminate between them. The primary antibody was made visible by staining with goat anti-mouse IgG coupled to fluorescein isothiocyanate (Sigma) or Alexa 488 (Molecular Probes). Polymerized actin was made visible using Alexa 568 conjugated phalloidin obtained from Molecular Probes. The β_{III} antibody TUJ1 (Lee et al. 1990) was obtained from Research Diagnostics Inc. (Flanders, N.J.) and the same goat anti-mouse secondary antibodies were used. Sections and whole mounts were sealed under coverslips in 50% PBS: 50% glycerol containing 1% n-propylgallate. Negative

controls were performed by omitting the primary antibody. Positive controls were performed using the same procedures as above with a monoclonal primary antibody to β tubulin raised in mouse (Sigma).

Isolated vestibular cells were prepared as follows. A day prior to the experiment, #1 coverslips were coated in Concanavalin A (Sigma) as described by Maue and Dionne (1987) and stored in a humidified atmosphere. Adult gerbils (22 days old or older) were anesthetized with Nembutal and decapitated. Vestibular epithelia were quickly dissected from the temporal bones and placed in a low-calcium saline containing 1% papain (Worthington Enzyme). The mixture was gently agitated for 30 minutes, after which the enzyme was removed and replaced with artificial CSF containing 0.001% DNAase I (Sigma). After 5 minutes, the mixture was then triturated until turbid using a syringe. Cells from the resulting suspension were plated onto coated coverslips, which were maintained in a humidified chamber at room temperature. After allowing 30 minutes for the cells to settle and attach, the cells were fixed in PBS containing 0.25% paraformaldehyde for 10 minutes. The fixed cells were then processed for immunolabeling essentially as above, except that the labeling steps were only 10 minutes long and only two rinses were performed between labeling steps.

Specimens were photographed using a Zeiss Axioskop II microscope equipped with 40x and 100x objectives. Images were obtained using a Spot RT digital camera (Diagnostic Instruments) and were analyzed and prepared for presentation using Adobe Photoshop and N.I.H. Image. Confocal images were obtained on a Radiance 2000 confocal microscope (Bio-Rad, Hercules, CA) on a Nikon Eclipse 800 upright microscope equipped for epifluorescence.

For immunoblotting, vestibular sense organs removed from anesthetized gerbils were homogenized in 2x SDS sample buffer. A uniform amount of protein (18 μg) was loaded into

each lane of a 10% poly-acrylamide Tris-Glycine gel (Gradipore LTD, French's Forest, N.S.W., Australia). The lanes were run at 150 V for 90 m in SDS electrophoresis buffer. The proteins were then transferred from the gels to nitrocellulose sheets after soaking in chilled Tris/Glycine/Methanol transfer buffer (100 V for 1 h). The protein lanes were cut into individual strips for labeling with antibodies. The strips were rinsed in Tris-buffered saline (TBS) with 0.1% Tween, then were blocked in 2% powdered milk in TBS for 1 h. Fresh blocking buffer was added to each primary antibody solution and the nitrocellulose sheets were exposed to one of the five primary antibodies (all four β tubulin isotype-specific antibodies plus the β tubulin monoclonal antibody described earlier) overnight at 4°C. After rinsing in TBS with 0.1% Tween, the protein strips were incubated in anti-mouse IgG linked to horseradish peroxidase (HRP; Cell Signaling Technology, Beverly, MA) in 2% milk/TBS blocking buffer for 1 h at room temperature. The markers were labeled with HRP-conjugated anti-biotin antibodies (Cell Signaling Technology). All protein strips were rinsed again in TBS with 0.1% Tween and treated for 10 m with Luminol reagent (Santa Cruz Biotechnology, Santa Cruz, CA). After one final rinse in TBS with 0.1% Tween, the protein strips were wrapped in plastic and exposed to Kodak XAR5 scientific imaging film (Rochester, NY).

Animal care and handling was performed in conformance with approved protocols of the University of Texas Health Science Center at San Antonio and Creighton University School of Medicine Institutional Animal Care and Use Committees.

Results

Immunoblots

Western blots of ~~olfactory and sensory epithelia~~ vestibular tissue indicated that labeling for β tubulin isotypes is restricted to a single band of molecular at or near 50 kDaltons (Figure 1), which is close to the molecular weight of β tubulin. Labeling for β_{IV} tubulin was faint, indicating a low abundance. This is consistent with the results described below.

{insert Figure 1 near here}

Identification of Cell Types in Vestibular Organs

Microtubules are present in vestibular hair cells, supporting cells and neurons in both macula and canal organs. Hair cells were identified by their centrally placed nuclei. Type I hair cells have the highest concentration of microtubules, predominantly in the supranuclear neck region (Favre and Sans 1983; Kikuchi et al. 1991). According to Kikuchi et al., these number 130-230 microtubules per cell in the guinea pig. A similar concentration of label was observed in this study in the neck of some gerbil vestibular hair cells and therefore this was used as the criterion to identify type I hair cells. In contrast, the 100-160 microtubules in the supranuclear region of type II hair cells are more diffuse (Kikuchi et al. 1991). Similar but more diffuse labeling, distinct from the type I pattern, was observed in other vestibular hair cells. We therefore considered these to be type II hair cells. Supporting cells had nuclei located in the base of the epithelium and exhibited a microtubules bundle that extended from the basal epithelium to the apex, at the level of the hair cell cuticular plate. Kikuchi et al. (1991) described the microtubules in guinea pig supporting cells as being 100-160 in number, clustered into bundles of 20-30. Most of the above observations were confirmed in the gerbil using an antibody to β tubulin, although we did not see the bundling of supporting cell microtubules (data not shown).

However, the diameter and brightness of supporting cell label was highly variable, as discussed below.

β_{II}

Label for β_{II} tubulin in vestibular sensory organs consisted of the fine processes of supporting cells. In a cross section of a macula (Figure 2A)., they were distinguished by the fact that they spanned the sensory epithelium and that their apical ends possessed small tufts. In canal organs, theses tufts were much broader, as seen in a whole mount (Figure 2B). As is typical in such specimens, a few cells are much brighter labeled that the others. In between the tufts, unlabeled spaces were observed, corresponding to the positions of hair cells. In a lower focal plane (Figure 2C), label in supporting cells was seen to be condensed to bright spots, five or six surrounding each unlabeled space.

In cross section, little label is seen in primary afferent dendrites near the organs (Figure 2D). Some fine fibers, possibly representing efferents, were seen to enter the organ in two or three discrete groups. However, the somas of vestibular ganglion cells were strongly labeled (Figure 2E). Axons and dendrites were not labeled except as parallel tracks. These resembled those previously observed in the dendrites of cochlear afferents (Hallworth and Ludueña 2000) and are therefore thought to represent label in the Schwann cell investment of the dendrites, rather than in the dendrites themselves.

No hair cells figures were observed in any β_{II} cross section, nor was hair cell labeling observed in whole mounts. Likewise label was not observed in kinocilia in any sections or whole mounts or in isolated cell preparations.

{insert Figure 2 near here}

β_{III}

Label for β_{III} tubulin in vestibular sensory organs appeared in large calyceal endings that surrounded some, but not all, hair cells and was continuous with afferent fibers. These are illustrated in Figure 3A. Labeled calyceal nerve endings were found on both macula and ampullary organs. Many fine processes were also seen to make possible synaptic contacts in the organs (Figure 3B). These are likely to be afferents making bouton-like synaptic contacts on type I hair cells, but some fine fibers could also be efferent fibers. No hair cells figures were observed, nor were supporting cells labeled. Nor were kinocilia labeled.

Vestibular neurons were labeled not only in their dendritic processes, but also on their somas and axons (Figure 4C). It was not possible to determine if the myelination was also labeled.

{insert Figure 3 near here}

β_{IV}

Label for β_{IV} tubulin was found primarily in hair cells but also in supporting cells (Figure 4). In isolated cells (Figure 4A), both the soma and the kinocilium were labeled. In whole mounts, kinocilia could be seen to be labeled (Figure 4B). In a lower focal plane, label was seen in hair cells and supporting cells (Figure 4C). Especially prominent were the type I hair cells, which were evident from bright label in the supranuclear region as a consequence of the concentration of microtubules therein. However, type II hair cells were also labeled, though not as brightly, as were supporting cells. The fine processes of supporting cells were labeled weakly, which made them difficult to trace through the bright hair cell layers of the epithelium. In sections, (Figure 4D), bright label could be seen in the necks of type I hair cells, but also in type

II hair cells (upper part of epithelium) and weakly in supporting cells (lower part of epithelium). There was no label in neuron dendrites, somas, or axons.

{insert Figure 4 near here}

β_I

The labeling pattern for β_I appears as a combination of aspects of the previously described patterns. Isolated hair cells were labeled in the soma and kinocilium (Figure 5A, arrow). The single kinocilium is indicated by the arrow and is parallel to and adjacent to the stereocilia bundle. In cross section, hair cells and support cells were labeled by the antibody to β_I tubulin (Figure 5B). However, the most prominent label was seen in supporting cells, in contrast to the pattern seen for β_{IV}, which was most prominent in hair cells. However, hair cell label was detectable above background (Figure 5B, arrow). Supporting cell label resembled that observed for β_{II} and was distinguished by their tufted apical ends. In many preparations, supporting cell label obscured all sign of hair cell label, as in a whole mount preparation of a macula (Figure 5C). In Figure 5D, a section of a canal organ is shown. Label to β_I was present in supporting cells and hair cells and in the dendrites of primary afferents (Figure 5D, arrow). Label in afferent dendrites was in the form of parallel tracks probably representing label in myelination rather than in the dendrites themselves. As with β_{II}, the label appeared to stop well short of the organ. The parallel track nature of the dendritic label may be better seen in Figure 5F, which shows a section of dendritic label close to a utricular macula. Solid label was seen in the somas of vestibular ganglion cells but was not as bright as label in the dendritic and axonal myelination (Figure 5F). Some fine processes observed in the layer below the sensory epithelium could represent efferents.

{insert Figure 5 near here}

Discussion

The results of this study are summarized in Table 1 and depicted in Figure 6.

{insert Figure 6, Table 1 near here}

β Tubulin Isotypes Are Selectively Expressed in Vestibular Sensory Cells But Are Not Sorted Within Those Cells

In both types of hair cell, we observed β_I and β_{IV} in both the soma and the kinocilia. The distributions of the two isotypes are apparently entirely overlapping. In supporting cells, we observed β_I, β_{II} and β_{IV}, each extending from the soma in the basal layer of the epithelium to the apical tuft. Both vestibular hair cells and supporting cells, therefore, selectively express β tubulin isotypes but do not sort the isotypes into separate compartments. In that respect, these findings are consistent with those for hair cells and supporting cells in the cochlea (Hallworth and Ludueña 2000).

Our observation that β_{III} is not expressed in vestibular hair cells or supporting cells is also consistent with the previous observations that β_{III} is not expressed in hair cells or supporting cells of the mammalian cochlea (Hallworth and Ludueña 2000). The absence of β_{III} in any other cell type than neurons corresponds to previous observations, using other antibodies, that β_{III} is not expressed in other cell types (Burgoyne et al. 1988; Joshi and Cleveland 1989). Indeed, β_{III} has been termed the "neuron-specific" tubulin for that reason, although β_{III} has also been reported in colon (Roach et al. 1998). In contrast, Molea et al. (1999) observed β_{III} in mature and regenerating chick cochlea hair cells.

β Tubulin Isotypes Are Sorted Within Neurons

We have here shown that while vestibular afferent neurons express the β_I, β_{II} and β_{III} isotypes, only the β_{III} isotype is seen in the dendrites. Label for the other isotypes β_I and β_{II} was

restricted to the myelination around dendrites. The β_{IV} isotype was not observed in vestibular nerve, which is consistent with previous observations that β_{IV} makes up only a small percentage of β tubulin in brain (Bannerjee et al. 1988).

Thus we have shown good evidence that vestibular neurons are capable or sorting β tubulin isotypes to separate compartments with the cell. This represents a first observation of such sorting in auditory and vestibular organs and is one of relatively few such observations so far.

Function of Kinocilia Related to Isotype Distribution

The kinocilia of vestibular hair cells are an axoneme-like tubulin-based organelle. Unlike other axoneme-based structures, such as the kinocilia or sperm or respiratory epithelial cells, they are not motile. The function of vestibular kinocilia appears to be to connect the sensory bundle of stereocilia that each hair cell possesses to a detector membrane. For macular organs this is the otolithic membrane while in ampullary organs it is the cupula.

A previous study (Renthal et al. 1993) had reported that the β_{IV} isotype was specifically expressed in the cilium of the rod photoreceptor, a short-kinocilium-like organelle that connects the inner and outer segments. It should be noted that the β_I isotype antibody was not available at the time of that study. In this and a companion study (Woo et al. 2001) we have now add to the information available on the expression of β tubulin isotypes in kinocilia. Woo et al. (2001) found that all four isotypes were expressed in kinocilia of olfactory sensory neurons, while only two isotypes were expressed in the kinocilia or respiratory epithelial cells. These results and those in this paper are tabulated in Table 2. In both cases, as in the vestibular system, there was no difference in the isotype distribution in the kinocilia and the rest of the cell. Thus it appears that kinocilia are assembled in an indiscriminate fashion from whatever isotypes are expressed by the cell.

{insert Table 2 near here}

β Tubulin Isotypes Are Not Uniformly Expressed

Our observation that β tubulin isotypes are differentially expressed is not new. Hallworth and Ludueña (2000), using the same antibodies as in this study, showed that the β tubulin isotypes are differentially expressed in cochlear hair cells and supporting cells. More recently, Woo et al. (2001) demonstrated a striking differential expression of isotypes in the olfactory system. Olfactory sensory neurons express all four isotypes (albeit β_{IV} is weak) while the adjacent respiratory epithelial cells express only β_I and β_{IV}. Further, Roach et al. (1998), also using the same antibodies, demonstrated selective expression of isotypes in a variety of tissues.

Others have shown differential expression of isotypes in different systems. Burgoyne et al. (1988) found that in rat cerebellum some isotypes are expressed in neurons, others in supporting cells, still others in both cell types. Wang et al. (1986) studied two mouse isotypes Mβ1 and Mβ3. Expression of Mβ1 was restricted to tissues involved in hematopoeisis (bone marrow, liver, lung, and spleen) and was not found in brain. Hamelin et al. (1987) described *mec–7*, a β tubulin isotype in *C. elegans* that is expressed only in touch receptor neurons. Using reporter genes, Chu et al. (1998) showed that in *Arabidopsis* the β tubulins TUB1 and TUB8 have non-overlapping expression in various tissues. Thus selective expression of β tubulin isotypes is common in nature.

β Tubulin Isotypes Are Not Commonly Sorted Within Cells

The multi-tubulin hypothesis leads to the prediction that some tubulin isotypes may be sorted into different functional pools within the same cell. However, the most common finding is that β tubulin isotypes are not compartmentalized, that is, all cellular microtubules contain all available isotypes. Hallworth and Ludueña (2000) found no difference in the subcellular

localization of the various isotypes incorporated into microtubules of cochlea hair cells and supporting cells. The distributions of the two and sometimes three isotypes in each cell types were completely overlapping. Woo et al. (2001) found that the four isotypes in olfactory sensory neurons were present in all four compartments (olfactory cilia, dendrite, soma, and axon). Lewis and Cowan (1988) found that, in mammalian spermatids, the isotypes expressed were uniformly distributed throughout the two distinct microtubule compartments, the manchette and the flagellum. The same was observed for the spindle microtubules in dividing testis cells. In a study by Lopata and Cleveland (1987) using three different cultured cell types (3T3, CV1 and CEF), several isotype-specific antibodies were found to label the cells in overlapping distributions. Ectopic isotypes introduced into cells are incorporated uniformly into all microtubules. Joshi et al. (1987) transfected a chicken isotype (cβ6), normally found only in the marginal band of thrombocytes and erythroid cells, into COS cells, wherein it was freely incorporated into cytoplasmic microtubules and into astral and chromosomal microtubules during cell division. However, microtubules assembled with the cβ3 isotype are more sensitive to cold depolymerization, which may be interpreted as suggesting some functional differences, although what they might be is unclear.

Nonetheless, some evidence for subcellular partitioning of β tubulin isotypes does exist. Arai and Matumoto (1988) in squid neurons saw two isotypes in the cell body but only one in the axon. Joshi and Cleveland (1989) found that β_{II} and β_{III} tubulin accumulated consequent to stimulated neurite outgrowth in PC-12 cells. β_{II} was observed to accumulate preferentially in axons. Falconer et al. (1992) found that β_{II} tubulin is preferentially incorporated into colchicine-stabile microtubules during development of embryonal carcinoma cells into neurons and muscle cells, while β_{III} is preferentially incorporated into colchicine-labile microtubules. Armas-Portela

et al. (1999) found that, in two cultured cell types (HeLa and Vero), β_{II} was enriched in interphase cells in perinuclear microtubules and at the periphery. Renthal et al. (1993) found that the cilia of bovine rod outer segments and respiratory epithelia were enriched in β_{IV}, compared to β_{II} and β_{III} (β_I was not examined). Perhaps the most striking example of segregated expression is found in *Drosophila* spermatogenesis (Nielsen et al. 2001). Axonemes and basal bodies utilize the same α tubulin but the β1 isotype is found in the basal body while the β2 isotype is found in the axoneme.

INSERT # 2

Relation of Isotype to Function

The multi-tubulin hypothesis suggests that the sequences have been conserved for functional reasons. However, it has been difficult to ascribe specific functions to isotypes. β_{IV} appears to be prominent in cilia and flagella (Renthal et al., 1993)~~; but is far from exclusive~~. Changing the isotypes that a cell expresses should have functional consequences and sometimes this can shown to be true. In *Drosophila*, a moth testes-specific β2 isotype results in the 16 protofilament microtubules characteristic of the moth (Raff et al. 1997). Further, over-expression of the β1 in *Drosophila* results in axonemes with 10 doublets instead of nine (Raff et al. 2000). Thus the nature and quantity of isotypes available can influence microtubule architecture in an invertebrate. It remains to be demonstrated that isotypes may influence function in vertebrates.

Whatever that phrase means!

Acknowledgments

Supported by N.I.H. grant CA26376, U.S. Army grant DAMD17-98-1-8246, and Welch Foundation grant AQ-0726 to R.F.L., and N.I.H. grant DC02053 to R.H. We thank Joseph Kaeller for technical assistance, and Tom Adrian, Xinquan Li and Xianzhong Ding for assistance with the Western blots.

References

ARAI T, MATSUMOTO G. Subcellular localization of functionally differentiated microtubules in squid axons: Regional distribution of microtubule-associated proteins and β-tubulin isotypes. J. Neurochem. 51:1825-1838, 1988.

ARMAS-PORTELA R, PARRALES MA, ALBAR JP, MARTINEZ-A C, AVILA J. Distribution and characteristics of β tubulin-enriched microtubules in interphase cells. Exp. Cell Res. 248:372-380, 1999.

BANERJEE A, ROACH MC, WALL KA, LOPATA MA, CLEVELAND DW, LUDUEÑA RF. A monoclonal antibody against the type II isotype of β-tubulin. Preparation of isotypically altered tubulin. J. Biol. Chem. 263:3029-3034, 1988.

BANERJEE A, ROACH MC, TRCKA P, LUDUEÑA RF. Increased microtubule assembly in bovine brain tubulin lacking the type III isotype of β-tubulin. J. Biol. Chem. 265:1794-1799, 1990.

BANERJEE A, ROACH MC, TRCKA P, LUDUEÑA RF. Preparation of a monoclonal antibody specific for the class IV isotype of β-tubulin. Purification and assembly of $\alpha\beta_{II}$, $\alpha\beta_{III}$, and $\alpha\beta_{IV}$ tubulin dimers from bovine brain. J. Biol. Chem. 267:5625-5630, 1992.

BURGOYNE RD, CAMBRAY-DEAKIN MA, LEWIS SA, SARKAR S, COWAN NJ. Differential distribution of β-tubulin isotypes in cerebellum. E.MB.O. J. 7:2311-2319, 1988.

CHU B, WILSON TJ, MCCUNE-ZEIRATH C, SNUSTAD DP, CARTER JV. Two β-tubulin genes, TUB1 and TUB8, of *Arabidopsis* exhibit largely nonoverlapping patterns of expression. Plant Molec. Biol. 37:785-790, 1998.

FALCONER MM, ECHEVERRI CJ, BROWN DL. Differential sorting of beta tubulin isotypes into colchicine-stable microtubules during neuronal and muscle differentiation of embryonal carcinoma cells.

FAVRE D, SANS A. Organization and density of microtubules in the vestibular sensory cells in the cat. Acta Otolaryng. 96:15-20, 1983.

FULTON C, SIMPSON PA. Selective synthesis and utilization of flagellar tubulin. The multi-tubulin hypothesis. In: Goldman R, Pollard T, and Rosenbaum J (eds) Cell Motility, vol. 3. Cold Spring Harbor Laboratory Press, New York, pp. 987-1005, 1976.

GOLDBERG JM, LYSAKOWSKI A, FERNANDEZ C. Structure and function of vestibular nerve fibers in the chinchilla and squirrel monkey. Ann. N.Y. Acad. Sci. 656:92-107, 1992.

JAEGER RG, FEX J, KACHAR B. Structural basis for mechanical transduction in the frog vestibular sensory apparatus: II. The role of microtubules in the organization of the cuticular plate. Hear. Res. 77:207-215, 1994.

JOSHI H, CLEVELAND DW. Differential utilization of β-tubulin isotypes in differentiating neurites. J. Cell. Biol. 109:663-673, 1989.

HALLWORTH R, LUDUEÑA RF. Differential expression of β tubulin isotypes in the adult gerbil organ of Corti. Hear. Res. 148:161-172, 2000.

JOSHI HC, YEN TJ, CLEVELAND DW. In vivo coassembly of a divergent β tubulin subunit (cβ6) into microtubules of different function. J. Cell Biol. 105:2179-2190, 1987.

KIKUCHI T, TAKASAKA T, TONOSAKI A, WATANABNE H, HOZAWA K, SHINKAWA H, WADA H. Microtubules subunits of guinea pig vestibular epithelial cells. Acta Otolaryng. Suppl. 481:107-111, 1991.

LEWIS SA, COWAN NJ. Complex regulation and functional versatility of mammalian αand β-tubulin isotypes during the differentiation of testis and muscle cells. J. Cell Biol. 106:2023-2033, 1988.

LEE MK, TUTTLE JB, REBHUN LI, CLEVELAND DW, FRANKFURTER A. The expression and posttranslational modification of a neuron-specific β-tubulin isotype during chick embryogenesis. Cell Motil. Cytoskelel. 17:118-132, 1990.

LOPATA MA, CLEVELAND DW. In vivo microtubules are copolymers of available isotypes: Localization of each of six vertebrate β-tubulin isotypes using polyclonal antibodies elicited by synthetic peptide antigens. J. Cell Biol. 105:1707-1720, 1987.

LU Q, MOORE GD, WALSS C, LUDUEÑA RF. Structural and functional properties of tubulin isotypes. Adv. Struct. Biol. 5:203-227, 1998.

LUDUEÑA RF. The multiple forms of tubulin: Different gene products and covalent modifications. Int. Rev. Cytol. 178:207-275, 1998.

MOLEA D, STONE JS, RUBEL EW. Class III β-tubulin expression in sensory and nonsensory regions of the developing avian inner ear. J. Comp. Neurol. 406:183-198.

MAUE RA, DIONNE VE. Preparation of isolated mouse olfactory receptor neurons. Pflügers Arch. 409:244-250, 1987.

NIELSEN MG, TURNER FR, HUTCHENS JA AND RAFF EC. Axoneme-specific β-tubulin specializations: A conserved C-terminal motif specifies the central pair. Curr. Biol.11:529-533, 2001.

RAFF EC, FACKENTHAL JD, HUTCHENS JA, HOYLE HD, TURNER FR. Microtubule architecture specified by a β-tubulin isoform. Science 275:70-73, 1997.

RAFF EC, HUTCHENS JA, HOYLE HD, NIELSEN MG, TURNER FR. Conserved axoneme symmetry altered by a component β-tubulin. Curr. Biol.10:1391-1394, 2000.

RENTHAL R, SCHNEIDER BG, MILLER MA, LUDUEÑA RF. β_{IV} is the major β-tubulin isotype in bovine cilia. Cell Motil. Cytoskel. 25:19-29, 1993.

ROACH MC, BOUCHER VL, WALSS C, RAVDIN PM, LUDUEÑA RF. Preparation of a monoclonal antibody specific for the class I isotype of β-tubulin: The β isotypes of tubulin differ in their cellular distributions within human tissues. Cell Motil. Cytoskel. 39:273-285, 1998.

WANG D, VILLASANTE A, LEWIS SA, COWAN NJ. The mammalian β-tubulin repertoire: Hematopoietic expression of a novel, heterologous β-tubulin isotype. J. Cell. Biol. 103:1093-1910, 1986.

INSERT #3 WOO K, JENSEN H, LUDUEÑA RF, HALLWORTH R. Differential Expression of β-tubulin isotypes in nasal epithelia. Submitted.

Figures

Figure 1. Western blots showing immunolabeling of gerbil vestibular tissue with an antibody to β tubulin (second lane from left) and the isotype-specific anti-β tubulin antibodies used in this study (lanes 3 through 6). A protein ladder with the molecular weights indicated is in the leftmost lane.

Figure 2. β_{II} labeling in vestibular sense organs and neurons. A. Cross section of a macula showing label in supporting cells. Note the tufts at the apical ends. B. Apical view of a whole mount of an ampulla. The apical tufts in the supporting cell label are broader than those in macula organs. C. Apical view of a utricle whole mount in a plane below the cell apex showing the condensed label in the five or six supporting cells surrounding each (unlabeled) hair cell. D. Cross section of a macula, showing fine probably unmyelinated nerve fibers entering the organ (arrow). E. Vestibular ganglion cells in cross section, showing solid label in the soma and paired label in the dendrites (left) and axons (right). The scale bar represents 20 μm for A and B, 50 μm for C-E.

Figure 3. β_{III} labeling in vestibular sense organs and neurons. A. High magnification of view of calyceal nerve endings in an ampulla. B. Lower magnification view of calyceal endings showing coarse and fine fibers entering a macula. C. Solid label in somas and axons of vestibular afferents. The scale bar represents 14 μm for A, 20 μm for B and C.

Figure 4. β_{IV} labeling in vestibular sense organs. A. Isolated vestibular hair cell showing label for actin (phalloidin - red) in stereocilia and the cuticular plate, and label for β_{IV} tubulin (green) in the soma and in a solitary kinocilium. B. Apical confocal view of a utricle whole mount showing label in kinocilia and in hair cells and supporting cells. C. Confocal view of a similar untricula whole mount in a lower focal plane, showing bright label in type I hair cells and more

diffuse label in type II hair cells and supporting cells. Note the partial cross section of hair cells and supporting cells in the lower left portion of the image. C. Cross section of a utricle showing bright label in the necks of type I hair cells, and label in type II hair cells (upper part of macula) and supporting cells (lower part). The scale bar represents 20 μm for A and D, 50 μm for B and C.

Figure 5. β_I labeling in vestibular sense organs and neurons. A. Isolated vestibular hair cell showing label for actin for (phalloidin - red) in stereocilia and the cuticular plate and label for β_I tubulin (green) in the soma and in a solitary kinocilium (arrow). B. View of supporting cell label in a canal organ, showing faint label in a hair cell (arrow). C. Low magnification view of a section of a canal organ showing label in supporting cells, hair cells and in the Schwann cell investments of peripheral afferent dendrites (arrow). Note that the dendritic label stops well short of the organ. E. Cross section of peripheral dendrites showing label in myelination. F. Label in neuronal somas (faint) and their myelinated investments (bright - arrow). The scale bar represents 20 μm for A-C, E and F, and 100 μm for C.

Figure 6. Diagram of the distribution of β tubulin isotypes in vestibular epithelial cells and neurons, based on the results of this study.

Table 1. Summary Of The Results of This Study.

Cell Type/ Structure	β_I	β_{II}	β_{III}	β_{IV}
Hair cells - body	✓	x	x	✓
Hair cells - kinocilia	✓	x	x	✓
Supporting cell	✓	✓	x	✓
Neurons – dendrite	x	x	✓	x
Neurons – soma	✓	✓	✓	x
Neurons – axons	✓	✓	✓	x
Neurons – myelination	✓	✓	?	x

Table 2. Distribution of βTubulin Isotypes in Kinocilia.

Isotype/Cell type	β_I	β_{II}	β_{III}	β_{IV}	Function of kinocilium
Vestibular hair cells	✓	x	x	✓	Attach motion detection membrane (cupula, otolithic membrane) to the stereocilia bundle for transduction
Olfactory respiratory epithelial cells	✓	x	x	✓	Motile – move olfactory mucus
Olfactory sensory neurons	✓	✓	✓	✓	Bear olfactory receptor molecules for transduction

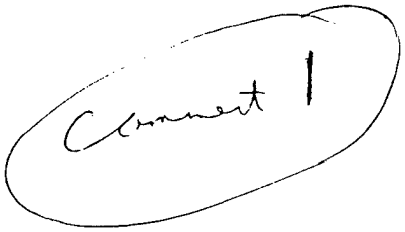

Figure 1

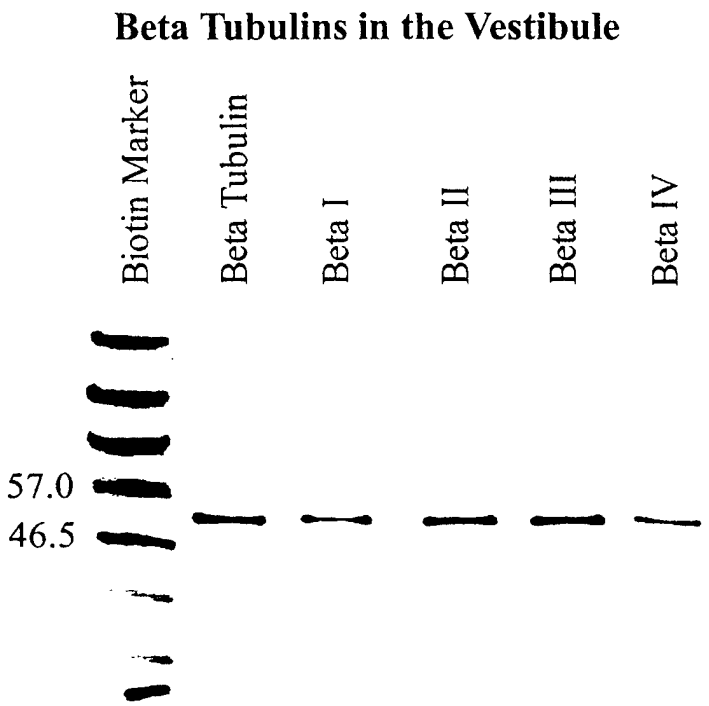
Beta Tubulins in the Vestibule
Biotin Marker
Beta Tubulin
Beta I
Beta II
Beta III
Beta IV
57.0
46.5

Figure 2

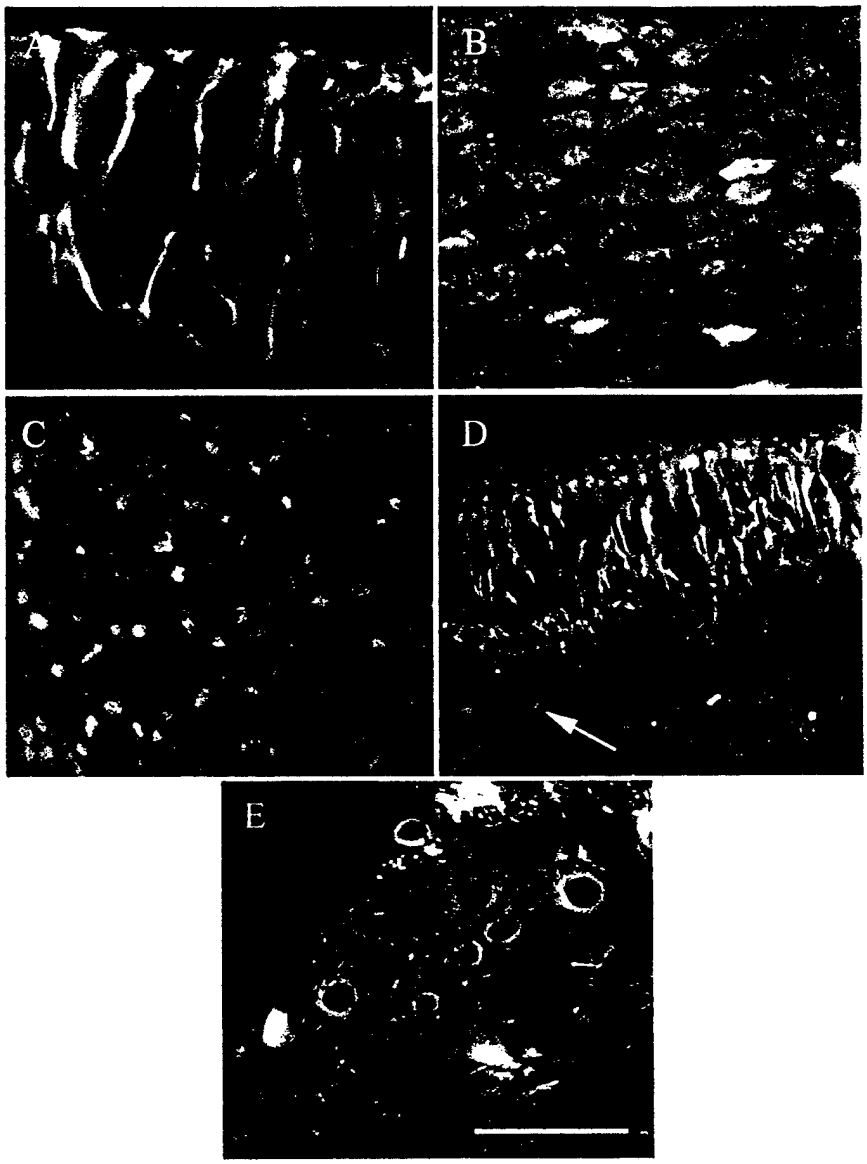

Figure 3

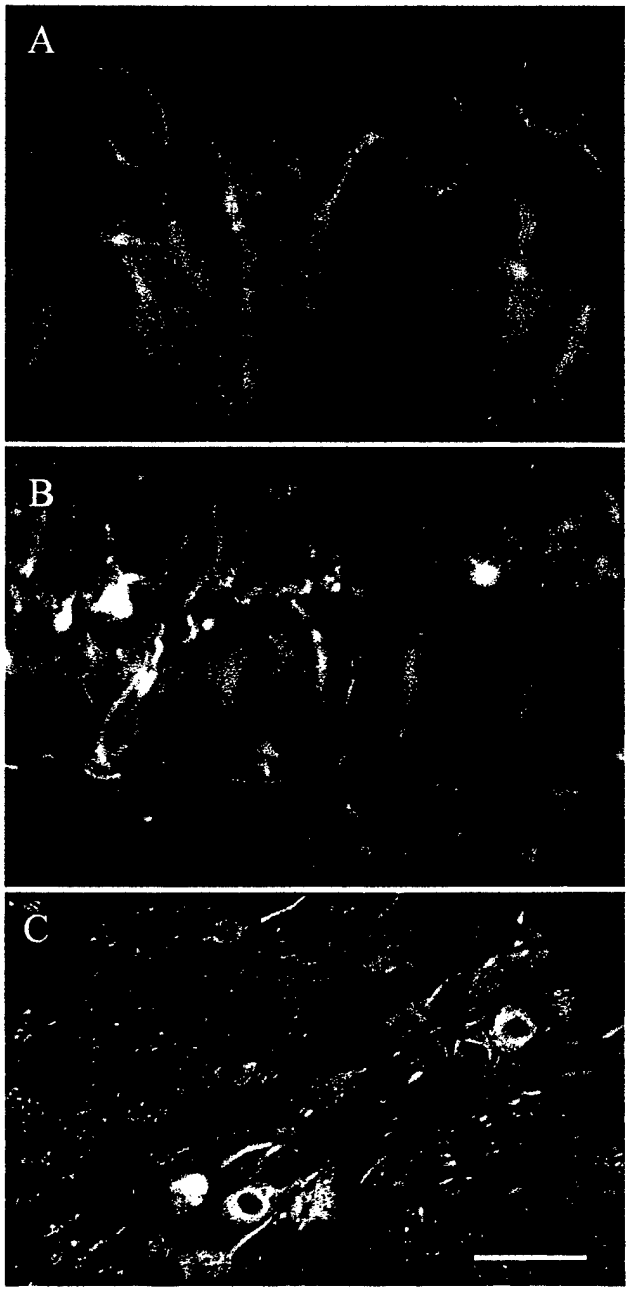

Figure 4

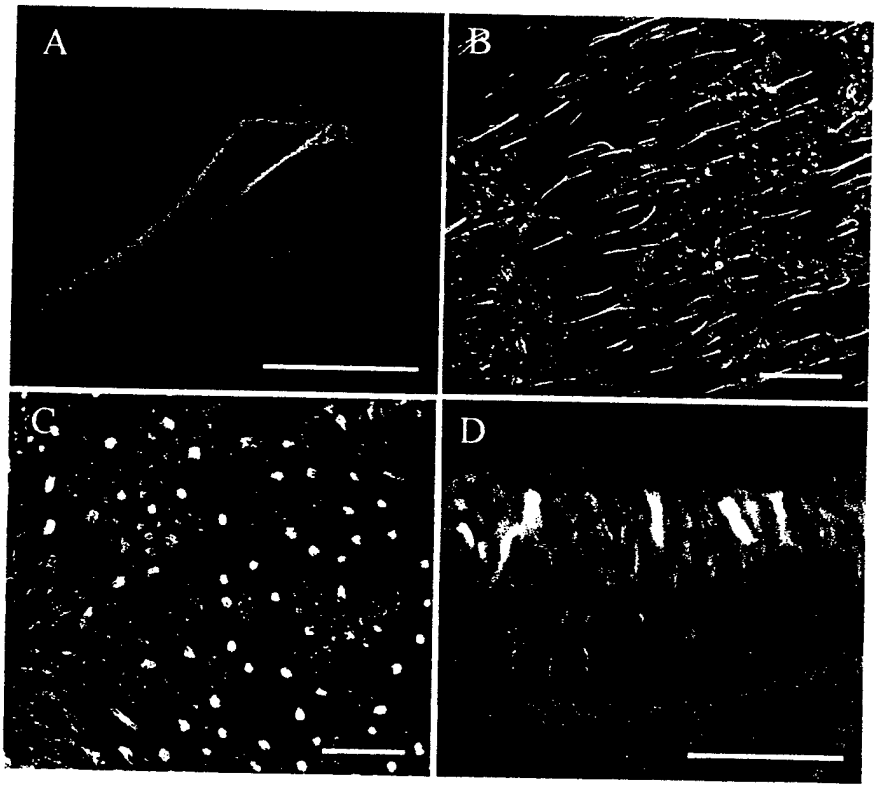

Figure 5

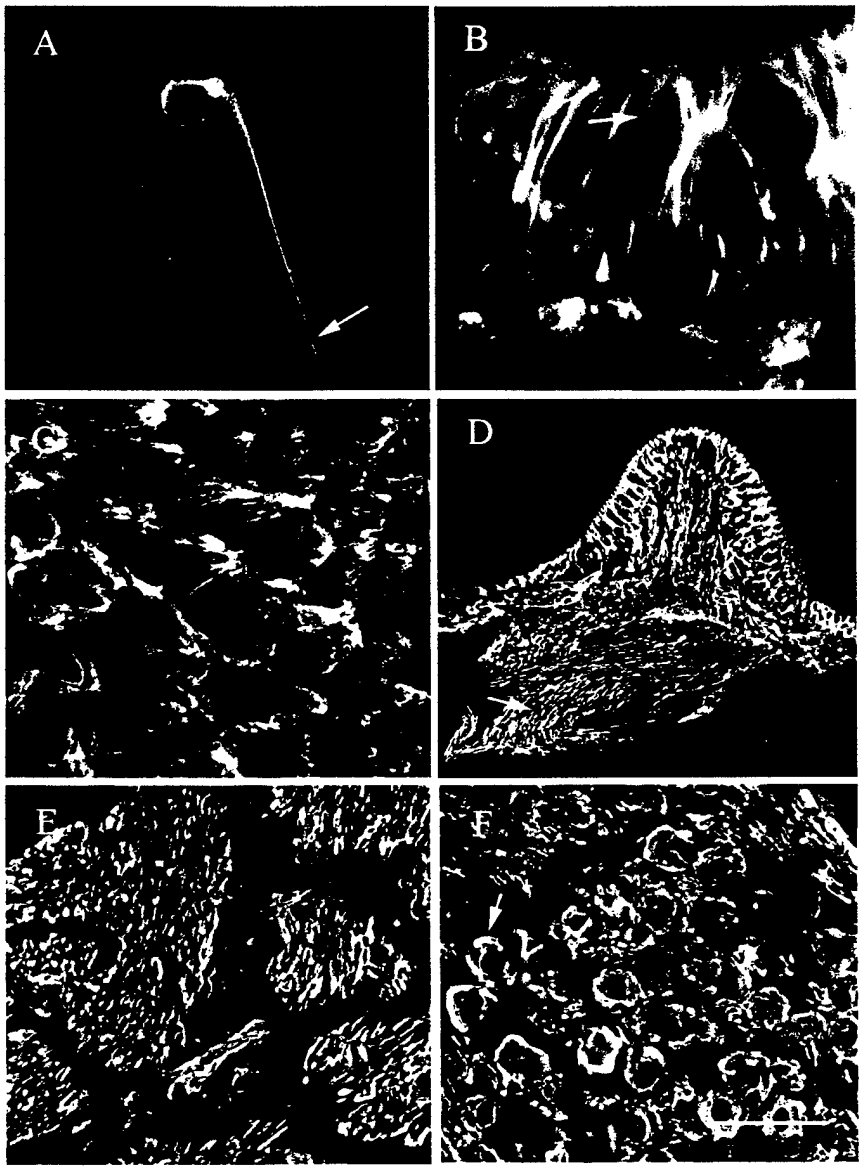

Figure 6

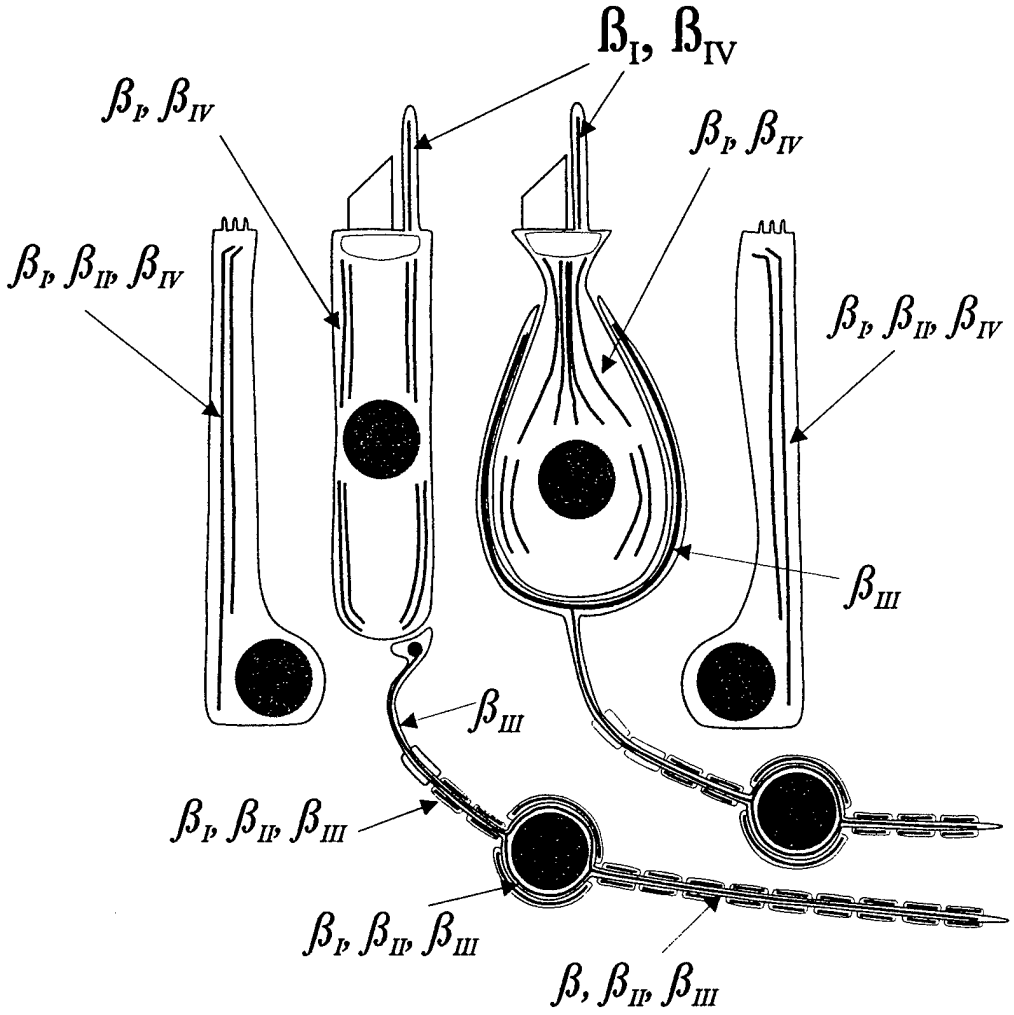
ß$_I$, ß$_{IV}$
β_I, β_{IV}
β_I, β_{IV}
β_I, β_{II}, β_{IV}
β_I, β_{II}, β_{IV}
β_{III}
β_{III}
β_I, β_{II}, β_{III}
β_I, β_{II}, β_{III}
β, β_{II}, β_{III}

Appendix 7

The β_{II} Isotype of Tubulin is Present in the Cell Nuclei of a Variety of Cancers

I-Tien Yeh[1] and Richard F. Ludueña[2,3]

Departments of [1]Pathology and [2]Biochemistry, University of Texas Health Science Center, San Antonio, TX 78229-3900

[3]To whom correspondence should be addressed.

Address correspondence to:

Dr. Richard F. Ludueña

Department of Biochemistry

University of Texas Health Science Center

San Antonio, TX 78229-3900

Tel: 210-5673732; FAX: 210-5676595; e-mail: luduena@uthscsa.edu

Keywords: Tubulin, β_{II}, nuclear, isotype

ABSTRACT

Tubulin, the subunit protein of microtubules. has generally been thought to be exclusively a cytoplasmic protein in higher eukaryotes. Recently, however, we found that cultured rat kidney mesangial cells contain the β_{II} isotype of tubulin in their nuclei in the form of an $\alpha\beta_{II}$ dimer (Walss et al., 1999). In contrast to β_{II}, the other β-tubulin isotypes examined in these cells are exclusively cytoplasmic. We have the immunoperoxidase method to look for nuclear β_{II} in a variety of tumors excised from 204 patients. We have found that 74% of the tumors we examined contain β_{II} in their nuclei. Distribution of nuclear β_{II} was highly dependent on the type of cancers, with 100% of the colon and prostate cancers, but only 12 % of the skin tumors, having nuclear β_{II}. In many cases, β_{II} staining occurred very strongly in the nuclei and not in the cytoplasm; in other cases, β_{II} was present in both. In many cases, particularly metastases, otherwise normal cells adjacent to the tumor also showed nuclear β_{II}, suggesting that cancer cells may influence nearby cells to synthesize β_{II} and localize it to their nuclei. Our results have implications for the diagnosis, biology and chemotherapy of cancer.

INTRODUCTION

An important target for anti-tumor drugs is the protein *tubulin*, the major subunit protein of microtubules, organelles involved in many critical functions inside cells (Hyams & Lloyd, 1994). Structurally, tubulin is an α/β heterodimer. Both α- and β-tubulin consist of a series of isotypes, differing in amino acid sequence, each one encoded by a different gene (Ludueña, 1998). Although there have been a few reports to the contrary, until very recently, tubulin has generally been thought to be exclusively a cytoplasmic protein. However, we have recently found that the β_{II} isotype of tubulin occurs in the nuclei of cultured rat kidney mesangial cells; in fact, in these cells, most of their β_{II} is located in the nuclei, with very little in the cytoplasm. This was shown with immunofluorescence and confirmed by immunoelectron microscopy, immunoblotting, and binding to fluorescein-colchicine. Nuclear β_{II} is in the form of an $\alpha\beta_{II}$ dimer and is not polymerized into microtubules. We also found that micro-injected fluorescently labeled $\alpha\beta_{II}$ enters the nuclei of these cells (Walss et al., 1999). The other two β-tubulin isotypes expressed (β_I and β_{IV}) are found exclusively in the cytoplasm (Walss et al., 1999). Nuclear β_{II} is often concentrated in the nucleoli (Walss et al., 1999). The phenomenon appears to be specific for the β_{II} isotype. In these cells, the β_I and β_{IV} isotypes are found exclusively in the cytoplasm. In contrast to $\alpha\beta_{II}$, fluorescently labeled $\alpha\beta_{III}$ and $\alpha\beta_{IV}$, when micro-injected into these cells, remain in the cytoplasm and do not enter the nuclei (Walss et al., 1999, 2001).

More recently we have examined a variety of cultured cells, both transformed and non-transformed. The transformed cell lines included breast, glial, prostate, and cervical cancers. We have found that β_{II} occurs in the nuclei of some normal cells and in all of the cancer cell lines; in many cases, there is more β_{II} in the nuclei than in the cytoplasm. In contrast to β_{II}, the β_{I}, β_{III}, and β_{IV} isotypes are located exclusively in the cytoplasm. We have also found nuclear β_{II} in a breast cancer excision (Walss-Bass et al., 2002). In the work described here, we performed a preliminary survey of a variety of cancers excised from 204 patients; we have examined these excisions by immunoperoxidase staining for β_{II}. We have found that 74 % of the tumors examined contain β_{II} in their nuclei. This is true even in cases where the normal tissue does not appear to synthesize β_{II}. In addition, we find that some adjacent non-cancerous cells also contain β_{II} in their nuclei, as if the presence of a nearby tumor induced the appearance of β_{II} in the nuclei of the adjacent cells. Our results suggest the possibility that nuclear β_{II} could be a useful diagnostic agent in cancer and also raise the question of the biological function of nuclear tubulin in cancer cells.

MATERIALS AND METHODS

Preparation of Reagents

The monoclonal antibody to the β_{II} isotype of tubulin (JDR.3B8) was prepared as previously described (Banerjee et al., 1988).

Sources of tumors

Tumors were randomly selected from the San Antonio Cancer Institute Tumor Bank to represent a variety of tumor types, grades and stages. Benign tissues adjacent to the tumor were examined when possible. In addition to malignant tumors, selected benign lesions were also examined. All tissues were formalin-fixed and paraffin-embedded.

Immunohistochemistry.

Standard immunohistochemical techniques were utilized (Hsu et al., 1981). The monoclonal antibody to the β_{II} isotype of tubulin (JDR.3B8) was at an initial concentration of 2 mg/mL an diluted 1:2000, for a final concentration of 1 μg/mL. No antigen retrieval step was used. Slides were incubated at room temperature with the primary antibody for one hour. The sections were then exposed to a secondary biotinylated rabbit anti-mouse antibody (DAKO, cat #E354, 1:100), then Streptavidin horseradish peroxidase was applied, followed by diaminobenzidine and 0.2 % OsO_4. Slides were counter-stained with methyl green.

Microscopy

Slides were visualized using an Olympus BX-40 microscope, equipped with PlanFluorite objectives. The pattern and location of cells staining with the antibody to β_{II}-tubulin were recorded. Intensity and proportion of cells stained were recorded in a semiquantitative manner, as previously described (Allred, 1998).

RESULTS

We examined a variety of tumors excised from a total of 204 patients. Cytoplasmic β_{II} was visualized in many normal tissues, with particularly strong staining in nerves, and to a slightly lesser degree in smooth and skeletal muscle. Nuclear β_{II} was also visualized in normal tissues; distribution exhibited variability at many levels. It was widespread in certain tumors and rare or absent in others. Within a single sample, there were areas that were rich in nuclear β_{II} and others that lacked it. In the nuclei the pattern of staining varied from very intense to very faint. Occasionally, the staining was particularly prominent in the nucleoli. In other cases, there were round well-defined areas within the nuclei that did not stain for β_{II}. The different tumors are discussed more specifically below, arranged by site.

Stomach

A total of 14 excisions of gastric adenocarcinomas were examined. These consisted of 8 poorly differentiated, 4 moderately differentiated, and 2 well-differentiated adenocarcinomas. Classified according to stages, they consisted of 2 stage I, 2 stage II, 6 stage III, and 4 stage IV. All of the tumors expressed the β_{II} isotype of tubulin. Of the 14 tumors, 13 contained β_{II} in their nuclei(Figure 1). The intensity of nuclear staining was variable, ranging from strong to very weak. Six of the 14 tumors examined appeared to stain for β_{II} more intensely in the nuclei than in the cytoplasm. Four stained more strongly in the cytoplasm. The remaining 4 cases stained equally between cytoplasm and nuclei. There was no significant correlation between the presence or intensity of nuclear β_{II} and either the stage of the cancer or the degree of differentiation. A signet ring

adenocarcinoma showed strong nuclear β_{II} staining and no visible β_{II} in the cytoplasm. Nucleoli did not stain in any of the tumors.

Metastases to lymph nodes were examined from 8 of these patients. All of them showed nuclear β_{II}.. In three there was more staining for β_{II} in the nuclei than in the cytoplasm; in one the cytoplasm stained more strongly and in 4 it was about equal. The distribution of β_{II} in the nuclei versus the cytoplasm in the metastatic cells corresponded with that in the parent tumor in 6 cases, and in 2 cases, the distribution was split, with one showing greater nuclear positivity in the primary, and the other showing greater nuclear staining in the metastases.

Many of the cases showed area of nuclear and cytoplasmic staining in adjacent benign glandular cells, with only a few cases showing more nuclear staining than cytoplasmic staining for nuclear β_{II}..

Colon

A total of 15 excisions of colon adenocarcinomas were examined. These consisted of 3 well-differentiated adenocarcinomas, 11 moderately differentiated adenocarcinomas and an adenocarcinoma *in situ* arising in a villous adenoma. The distribution of stages included 1 stage 0, 2 stage I, 6 stage II, 3 stage III, and 3 stage IV tumors. All cancers showed β_{II} in the nuclei, often staining very strongly. Nine of the tumors had more intense staining of β_{II} in the nucleus than in the cytoplasm. Only one showed the reverse pattern. Focal nucleolar β_{II} staining was seen. There was no significant correlation between nuclear staining and the stage of the cancer. Five of the cases had metastases to lymph nodes, and one to liver, and all showed nuclear β_{II} staining. Of the benign tissues, smooth muscle showed strong cytoplasmic staining, as

did nerves. Lymphocytes showed scattered weak nuclear β_{II}. Benign glandular cells showed weak nuclear and cytoplasmic staining, with occasional cells demonstrating more intense nuclear staining.

Pancreas

A total of 12 excisions were examined. Nine of these were adenocarcinomas, consisting of one borderline tumor, 2 well-differentiated, 4 moderately differentiated, and 2 poorly differentiated. One was a papillary cystic tumor, one an acinar cell carcinoma, and one was a neuroendocrine tumor, arising from the Islets of Langerhans. Tumors were staged as follows: 1 stage 0, 4 stage II, 4 stage III, and 1 stage IV. Of the 9 adenocarcinomas, 7 had nuclear staining for β_{II} and 6 had stronger staining in the nuclei than in the cytoplasm. The papillary cystic tumor, acinar cell carcinoma and neuroendocrine tumor appreaed to have β_{II} only in the cytoplasm.

Of three metastases examined, two had β_{II} only in the cytoplasm and the third only in the nuclei. In the latter, some of the adjacent lymphocytes had β_{II} in the nuclei as well. In one tumor, some of the adjacent exocrine cells stained weakly for nuclear β_{II}. Nerves and normal Islet cells stained strongly for β_{II}, but only in the cytoplasm.

Liver

We examined a total of 11 tumors involving the liver, including 7 hepatocellular carcinomas, a cholangiosarcoma a sarcoma, and two metastatic tumors (colon adenocarcinoma and melanoma). Of the seven hepatocellular carcinomas, two were well-differentiated and four were moderately differentiated. Stages ranged from II to IV with 5 stage II, 2 stage III and 4 stage IV cases. Tumor cells in general contained β_{II} only in the cytoplasm (Figure 4). Two of the hepatocellular carcinomas stained weakly for β_{II}

in the nuclei in addition to β_{II} in the cytoplasm. The cholangiocarcinoma contained β_{II} largely in the cytoplasm with light staining in the nuclei. Smooth muscle and nerves included in the excisions stained strongly for β_{II}, but only in the cytoplasm. There was little or no staining for β_{II} in normal hepatic tissue included in the excisions. The epithelial cells of the bile duct exhibited weak cytoplasmic β_{II} staining.

Bone

A total of 17 bone tumors were examined: 13 osteosarcomas and 4 giant cell tumors. One of he osteosarcomas was low grade and the remaining 12 cases were high grade. Giant cell tumors were not graded. Stage was not available in most of the cases. All tumors had nuclear β_{II}, with weak staining in many cases, but in others very strong. All 13 osteosarcomas and all 4 giant cell carcinomas had nuclear β_{II}. In many cases nuclear β_{II} staining is weak but in others it is very strong. In 10 of the osteosarcomas, β_{II} stained more intensely in the nuclei than in the cytoplasm, as was the case with one of he giant cell tumors. β_{II} was also seen in the cytoplasm of adjacent osteoclasts, adipocytes, fibroblasts, endothelial cells and skeletal muscle cells. The sarcomeres of skeletal muscle stained strongly for β_{II} as did some of the Z-lines. It is seen in the nuclei of some of the osteocytes and very strongly in the nuclei of endothelial cells. In most of the giant cell tumors, the nuclear β_{II} staining is weak. Spindle cells also show faint nuclear β_{II} staining with most of the β_{II} in the cytoplasm.

Brain

A total of 17 tumors were examined, including 12 astrocytomas, two meningiomas, one ependymoma, one chordoma and one medulloblastoma. Astrocytomas were graded as low grade in one case, anaplastic astrocytoma in three cases, and

glioblastoma multiforme in 8 cases. The other tumors are not graded. No staging information was available. All the tumors had strong cytoplasmic β_{II} (Figure 2). However, five showed weak nuclear β_{II}. including the two meningiomas, the chordoma, and two of the gliobastoma multiforme cases. The adjacent normal brain tissue showed strong cytoplasmic β_{II} staining, particularly in glial processes, with focal nuclear localization in neurons (Figure 3).

Lung

Fourteen lung tumors were examined including 11 non-small cell lung carcinomas, 1 small cell lung carcinoma, 1 carcinoid tumor and 1 fibrosarcoma. Of these cases, 1 was well differentiated, 4 were moderately differentiated, and 9 were poorly differentiated. Tumors were stage I in 7 cases, stage II in 1 case, stage III in 4 cases and stage IV in one case. No staging information was available on the fibrosarcoma case. A total of nine tumors showed nuclear β_{II} (Figure 4), but only in 7 did β_{II} stain more strongly in the nucleus than in the cytoplasm; in 7 the cytoplasm stained more strongly. There was no β_{II} visible in the nuclei of two of the non-small cell carcinomas, the small cell carcinoma, the fibrosarcoma and the carcinoid.

In tumor excisions where normal alveolar tissue was visible, some normal alveolar lining cells contained β_{II} in their nuclei, even if the tumor had no nuclear β_{II} (Figure 5). Cytoplasmic localization of β_{II} also occurred in scattered cells. In one case, the normal bronchial epithelia contained nuclear β_{II}.

Lymph Nodes and Related Organs

Fifteen tumors were examined, including six Hodgkins lymphoma, three follicular center cell lymphomas, three B-cell lymphomas, two thymomas, and one spleen in a

patient with myelofibrosis. The stage was unknown in the majority of cases. Grading is not applicable in these cases. Extremely weak nuclear β_{II} was seen in the lymphocytes in the majority of cases, and no staining of either nuclei or cytoplasm was noted in several of the cases. Interestingly, the Reed-Sternberg cells in the Hodgkins lymphoma cases were characterized by strong cytoplasmic staining for β_{II} (Figure 6). One of the B-cell lymphomas also had strong cytoplasmic staining for β_{II}; the other two had little or no β_{II}. In some samples, otherwise normal lymphocytes stained very faintly for nuclear β_{II}.

Skin

Seventeen cases were examined including 9 melanomas (including 4 metastatic tumors), 5 basal cell carcinomas, 2 squamous carcinomas and one dermatofibrosarcoma protuberans (DFSP). Of these tumors, 8 were stage I, 4 stage II, 2 stage III and 3 stage IV. Except for the squamous carcinomas, these tumors are generally not graded; both squamous carcinomas were grade 2. Of these skin lesions, only three had weak nuclear β_{II} including two basal cell carcinomas and one melanoma. Most of the cases showed cytoplasmic staining without significant nuclear staining. The melanomas showed moderate intensity cytoplasmic β_{II} staining, including both primary and metastatic tumors. The squamous carcinomas both showed strong intensity cytoplasmic staining. The basal cell carcinomas and the DFSP showed very weak cytoplasmic staining. One of the two squamous carcinomas had β_{II} only in the cytoplasm. The other one had low levels of β_{II} in the nuclei of the undifferentiated cells. The fibroblastic tumor had β_{II} only in the cytoplasm.

As with some of the other tumors examined here, small amounts of β_{II} were visible in the nuclei of lymphocytes close to two of the metastatic tumors, one melanoma and one squamous carcinoma.

Ovary

Fourteen tumors were examined including 11 carcinomas, one adenosarcoma, one Sertoli-Leydig tumor, and one carcinosarcoma. Breaking the cases down according to stage, there were 5 stage I, 3 stage II, 2 stage III, and 4 stage IV. All but two of the tumors had nuclear β_{II} (Figure 7). Of these, 7 appeared to have β_{II} only in the nuclei and not in the cytoplasm (all carcinomas). In addition, 2 tumors had β_{II} only in the cytoplasm, including the adenosarcoma and the carcinosarcoma. The adjacent cells showed strong cytoplasmic staining. The relative distribution of β_{II} between the nucleus and cytoplasm did not appear to be correlated with either the stage or type of the tumor.

Other Gynecological Sites

Twelve tumors were examined including 9 uterine tumors, two cervical tumors, and one fallopian tube carcinoma; 4 metastases were included. These tumors included 5 stage I, one stage II, 4 stage III, and 2 stage IV lesions. Grades of the tumors included 2 grade 1, 3 grade 2, and 6 grade 3. One tumor was not graded (adenosarcoma of the uterus). Eleven tumors showed nuclear β_{II} (Figure 8). The exception was an endometrial carcinoma that had β_{II} only in the cytoplasm of neoplastic cells. The carcinosarcoma contained β_{II} both in the carcinoma and the sarcoma, but primarily in the carcinoma. Four metastases that were examined showed nuclear β_{II} in the tumor cells; two of them also had nuclear β_{II} in some of the adjacent lymphocytes.

Some of the adjacent tissues were examined as well. Nuclear β_{II} was seen in some benign glandular epithelia adjacent to the tumor (Figure 9). Nuclear β_{II} was also seen in some lymphocytes and stromal cells. As with other tissues, smooth muscle stained strongly for β_{II}, but only in the cytoplasm.

Two normal placentas were also examined. The villous trophoblast had some nuclear β_{II}. In contrast, the non-villous trophoblast had intense cytoplasmic β_{II}. The maternal decidua also had only cytoplasmic β_{II}.

Prostate

Sixteen prostatic adenocarcinomas were examined. These included one stage I, 7 stage II, 7 stage III and one stage IV. There was one well differentiated carcinoma, 9 moderately differentiated carcinomas, and 5 poorly differentiated carcinomas. All tumors showed nuclear β_{II}, in some cases very intensely (Figure 10). There did not appear to be any correlation between cancer stage or grade and the intensity of nuclear β_{II} staining. In general, there was relatively little β_{II} in the cytoplasm, but four tumors had more intensely staining β_{II} in the cytoplasm than in the nuclei. Adjacent areas of benign prostate hyperplasia showed nuclear β_{II} staining, sometimes very intense. Smooth muscle and nerves were intensely positive for cytoplasmic β_{II}.

In addition to the prostate cancers, eighteen samples of benign prostate hyperplasia were examined, taken by transurethral prostatic resections in individuals with no evidence of cancer. All but one of these cases showed nuclear β_{II}. The staining was often quite variable, both in intensity and in localization, with some areas of hyperplasia having no nuclear β_{II} and others having intense staining.

Breast

Thirty-three breast cancers were examined, including 26 invasive ductal carcinomas (including 3 with prominent mucinous differentiation), 3 ductal carcinomas *in situ*, 1 invasive lobular carcinoma, 1 lobular carcinoma *in situ*, 1 metaplastic carcinoma, and 1 medullary carcinoma. These tumors were staged as follows: 4 stage 0, 10 stage I, 8 stage II, 10 stage III, and 1 stage IV. The distribution of grades in the invasive carcinomas included 4 well-differentiated, 9 moderately differentiated, and 15 poorly differentiated. Nuclear β_{II} was present in 31 cancers, sometimes staining very intensely, especially in the mucinous carcinomas (Figure 11). However, nuclear staining was greater than cytoplasmic staining in only 13 cases. In some samples, the β_{II} was concentrated in the nucleoli; in others, it was absent from round discrete bodies in the nuclei. Staining for cytoplasmic β_{II} was variable. Metastases generally had the same pattern of β_{II} staining as did the primary tumor in 11 of the 17 cases; if, in the primary tumor, β_{II} was strong in the nuclei and weak in the cytoplasm, the same was true for the metastasis. In every metastases, the lymphocytes close to the metastatic cells also had nuclear β_{II} (Figure 12).

We also examined 14 samples of benign breast tissue, including 9 with fibrocystic changes, 4 fibroadenomas and 1 radial scar. Nuclear β_{II} staining was relatively minimal, generally not as intense as in the cancer. Cytoplasmic β_{II} staining was very strong in the myoepithelial cells. In apocrine metaplasia, the cytoplasm stained strongly for β_{II} and the nuclei only weakly. Two of the fibroadenomas had prominent nuclear β_{II} staining.

DISCUSSION

Our preliminary survey of cancers excised from patients indicates that the β_{II} isotype of tubulin is present in the nuclei of many cancers. Nearly three quarters (74 %) of the cancers we examined contained nuclear β_{II} (Table 1). The frequency of occurrence of nuclear β_{II} was greatly dependent on the type of cancer involved. Every sample of colon and prostate cancer we examined was very rich in nuclear β_{II}, while few of the lymphomas and none of the skin tumors had nuclear β_{II}. Ranganathan et al. (1997) previously reported the presence of β_{II} in the nuclei of prostate tumors and of benign prostate hyperplasia. There may be a correlation with epithelial origin. Epithelial tumors more frequently contain nuclear β_{II} than tumors of mesenchymal origin, such as brain tumors, or those of neuroendocrine derivation, such as small cell carcinoma and carcinoid tumors.

Even in tumors that were rich in nuclear β_{II}, its distribution was variable, occurring widely in certain portions of the section and not in others; in some cases, one group of cells would stain intensely for nuclear β_{II}, while an adjacent tumor cell had none. The intracellular distribution of β_{II} was quite variable. In some cases, almost all of the β_{II} occurred in the nuclei with barely any in the cytoplasm, as we have previously observed in cultured mesangial cells and some cancer cells (Walss et al., 1999; Walss-Bass et al., 2002). In other cases, β_{II} occurred in both the nuclei and the cytoplasm and in others almost entirely in the cytoplasm. The intensity of nuclear staining was also rather variable. Distribution of β_{II} within the nuclei also varied, ranging from intense to faint, sometimes being concentrated in the nucleoli as we have previously reported (Walss et

al., 1999; Walss-Bass et al., 2002) and sometimes being clearly absent from round well-defined bodies that could be nucleoli or another intra-nuclear structure.

An interesting finding is that nuclear β_{II} occurs in some cells, adjacent to the tumor, that are otherwise normal in appearance. When this occurs in the same type of cell from which the cancer originated, one could argue that the presence of nuclear β_{II} is a reflection of a pre-cancerous change. However, it is very clear that this is not always the case (Table 2). A very striking example is the occurrence of nuclear β_{II} in lymphocytes close to metastatic cells. This was seen with metastases of several kinds of cancer including breast, colon, pancreas and skin cancers. In contrast, lymphocytes more distant from the metastatic focus did not stain as well for nuclear β_{II}. It is possible, therefore, that cancer cells containing nuclear β_{II} are able to influence nearby non-cancerous cells to synthesize β_{II} and localize it to their nuclei. The mechanism for this process is unknown.

We do not yet know the extent to which normal tissue from normal individuals contains nuclear β_{II}. We have seen intense nuclear β_{II} in placenta, specifically in the villous trophoblast. However, a previous survey (Roach et al., 1998) suggests that nuclear β_{II} does not occur in normal tissues.

Occasionally, the excisions included sections of normal tissue. β_{II} occurred strongly in the cytoplasm of various cells, including nerves, smooth muscle and skeletal muscle. This is consistent with previous observations (Havercroft and Cleveland, 1984) and an indication that the staining procedure is working normally.

Our results raise three issues that have implications for cancer and its treatment. First, it is conceivable that nuclear β_{II} could be developed as a marker, either for diagnosis, prognosis or detection. Particularly intriguing in this respect is the presence of

β_{II} in otherwise normal cells adjacent to the tumor. One could imagine a biopsy that could miss the actual tumor but collect some of the adjacent cells; presence of nuclear β_{II} may indicate that there is a tumor nearby. Alternatively, presence of nuclear β_{II} in cells obtained from blood or lavage may also indicate the presence of a tumor. The fact that nuclear β_{II} occurs in benign hyperplasia, however, indicates that this will not be a simple story.

The second question is the function, if any, of nuclear β_{II}. At present, this is unknown. It is conceivable that it may play a part in proliferation. The fact that it occurs strongly in normal placenta is consistent with that hypothesis. Elucidation of its role may reveal more information about the biology of cancer cells.

Third, the nuclear $\alpha\beta_{II}$ dimer constitutes a novel population of tubulin. It is clearly not in the form of microtubules; it may be in the form of a novel aggregate (Walss et al., 1999). Tubulin is already a major target in cancer chemotherapy (Hardman & Limbird, 1996). If nuclear β_{II} should have an important function in cancer cells, it would be interesting to explore the possibility of using nuclear β_{II} as a chemotherapeutic target.

ACKNOWLEDGMENTS

We thank Oredius Pressley and Guadalupe Castillo for their skilled assistance in tissue preparation and immunohistochemistry. We appreciate the help of Phyllis Smith and Veena Prasad in producing the JDR.3B8 antibody. This research was supported by grants to R.F.L. from the National Institutes of Health (CA 26376), the US Army BCRP (DAMD17-01-1-0411), the US Army PCRP (DAMD17-02-1-0045) and the Welch Foundation (AQ-0726) and by grant P30 CA54174 from the NIH to the San Antonio Cancer Institute.

REFERENCES

Allred DC, Harvey JM, Berardo M, Clark GM. 1998. Prognostic and predictive factors in breast cancer by immunohistochemical analysis. Mod. Pathol. 11:155-168.

Banerjee A, Roach MC, Wall KA, Lopata MA, Cleveland DW, Ludueña RF. 1988. A monoclonal antibody against the type II isotype of β-tubulin. Preparation of isotypically altered tubulin. J. Biol. Chem. 263:3029-3034.

Bryan J, Wilson L. 1971. Are cytoplasmic microtubules heteropolymers? Proc. Natl. Acad. Sci. USA 68:1762-1766.

Hardman JG & Limbird LE (1996) *Goodman & Gilman's The Pharmacological Basis of Therapeutics*, 9th Ed., pp. 1228, 1257-1261, 1603, McGraw-Hill, New York.

Havercroft JC & Cleveland DW (1984) Programmed expression of β-tubulin genes durign development and differentiation of the chicken. *J. Cell Biol.* **99**, 1927-1935.

Hsu SM, Raine L & Fanger H (1981) The use of antiavidin antibody and avidin-biotin-peroxidase complex in immunoperoxidase technics. *Am. J. Clin. Pathol.* **75**, 816-821.

Hyams JS & Lloyd CW, eds..(1994) *Microtubules*. Wiley-Liss, New York.

Ludueña RF (1998) The multiple forms of tubulin: different gene products and covalent modifications. *Int. Rev. Cytol.* **178**, 207-275.

Ranganathan S, Salazar H, Benetatos CA, Hudes GR. 1997. Immunohistochemical analysis of β-tubulin isotypes in human prostate carcinoma and benign prostatic hypertrophy. Prostate 30:263-268.

Roach MC, Boucher VL, Walss C, Ravdin PM & Ludueña RF (1998) Preparation of a monoclonal antibody specific for the class I isotype of β-tubulin: the β isotypes of tubulin differ in their cellular distributions within human tissues. *Cell Motil. Cytoskeleton* **39**, 273-285.

Walss C, Kreisberg JI, Ludueña RF. 1999. Presence of the β_{II} isotype of tubulin in the nuclei of cultured mesangial cells from rat kidney. Cell Motil. Cytoskeleton 42:274-284.

Walss C, Barbier P, Banerjee M, Bissery MC, Ludueña RF, Fellous A. 2000. Nuclear tubulin as a possible marker for breast cancer cells. Proc. Amer. Assoc. Cancer Res. 41:553.

Walss-Bass C, Kreisberg JI., Ludueña RF. 2001. Mechanism of localization of β_{II}-tubulin in the nuclei of cultured rat kidney mesangial cells. Cell Motil. Cytoskeleton 49:208-217.

Walss-Bass C, Xu K, David S, Fellous A, Ludueña RF. 2002. Occurrence of nuclear β_{II}-tubulin in cultured cells. Cell Tissue Res., in press.

Table 1. Occurrence of the β_{II} Isotype of Tubulin in Cancer Cell Nuclei

Type of Cancer Examined	Fraction of Cancers with Nuclear β_{II}
Stomach	14/14
Colon	14/14
Pancreatic	8/12
Liver	4/9
Bone (total)	18/18
Brain (total)	5/17
Lung	9/14
Lymphoid	7/15
Skin	2/18
Ovary	12/12
Other gyn sites	11/12
Prostate	16/16
Breast	31/33
TOTAL	151/204 = 74 %

Table 2. Nuclear β_{II} in non-cancerous cells adjacent to tumors with nuclear β_{II}

Tumor	Adjacent tissue	"Normal" Cells with Nuclear β_{II}
Stomach	Glands	Epithelial cells
Colon	Glands	Epithelial cells
Liver	Bile duct	Epithelial cells
Bone	Fatty tissue	Osteocytes
Brain	Brain	Neurons
Lung	Alveoli, bronchioles	Epithelial cells
Uterus	Endometrium	Epithelial cells
Prostate	Hyperplastic glands	Epithelial cells
Lymph node	Lymphocytes	Lymphocytes
Breast	Glands	Myoepithelium

FIGURE LEGENDS

Figure 1. Adenocarcinoma of Stomach. Cytoplasmic and nuclear staining is seen for β_{II}.

Figure 2. Glioblastoma multiforme, brain. Prominent cytoplasmic staining is seen in tumor cells for β_{II}-tubulin. Little or no nuclear β_{II} staining is seen. Note vessel in center of field is essentially negative (original magnification 400X).

Figure 3. Brain, normal neurons. There is intense staining in the background by glial processes. Most neurons do not demonstrate nuclear β_{II}, however, a few neurons are seen here that show nuclear as well as cytoplasmic staining.

Figure 4. Lung, non-small cell carcinoma. Nuclear β_{II} is evident in this lung carcinoma. Note that nucleoli are accentuated by the anti-β_{II} antibody.

Figure 5. Lung, normal alveoli. In this area of lung adjacent to tumor, there is nuclear β_{II} in alveolar lining cells.

Figure 6. Hodgkin's Lymphoma. Reed Sternberg cells show evident cytoplasmic staining for β_{II}-tubulin, whereas background normal lymphocytes are negative. There is little or no nuclear staining.

Figure 7. Carcinoma of Ovary. Note prominent nuclear staining for β_{II}. Not all the nuclei stain for β_{II} (400X).

Figure 8. Uterus, adenosarcoma. This sample shows benign epithelium of the adenosarcoma with nuclear β_{II}, as well as spindle cells of the tumor staining for β_{II}.

Figure 9. Atrophic endometrium. This area of endometrium shows cystic atrophy of endometrium and foci of tubal metaplasia (left). The tubal metaplasia demonstrates cytoplasmic β_{II}, whereas the endometrial-type glands demonstrate nuclear β_{II}.

Figure 10. Prostate carcinoma. The nuclei in this prostatic adenocarcinoma shows moderate nuclear and slight cytoplasmic β_{II}.

Figure 11. Colloid carcinoma of breast. Malignant cells are present in a background of colloid (mucin). Note nuclear staining for β_{II}.

Figure 12. Lymph node with metastatic breast carcinoma. Cytoplasmic and nuclear staining is seen for β_{II} in tumor cells. Adjacent lymphocytes also show weak nuclear staining (bottom left).

Figure1.

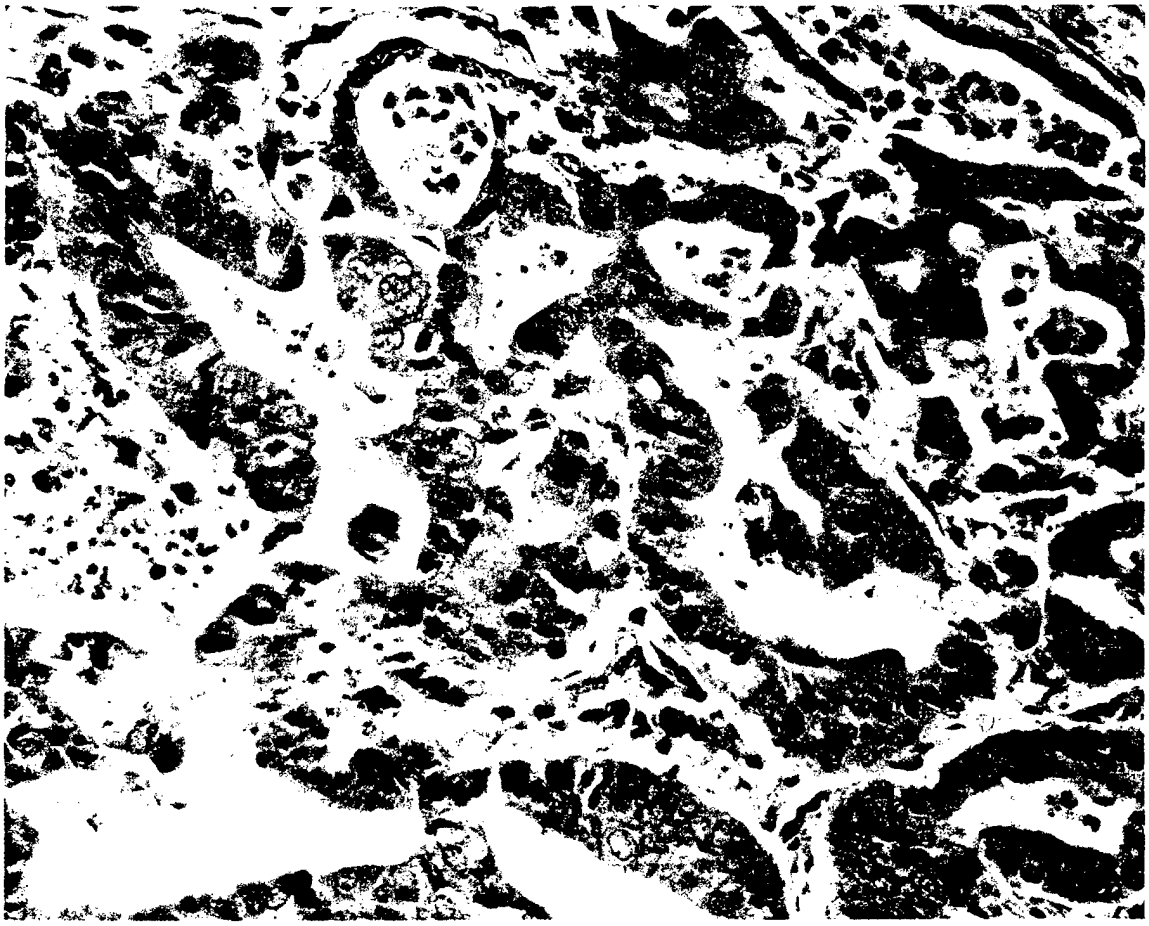

Figure 2.

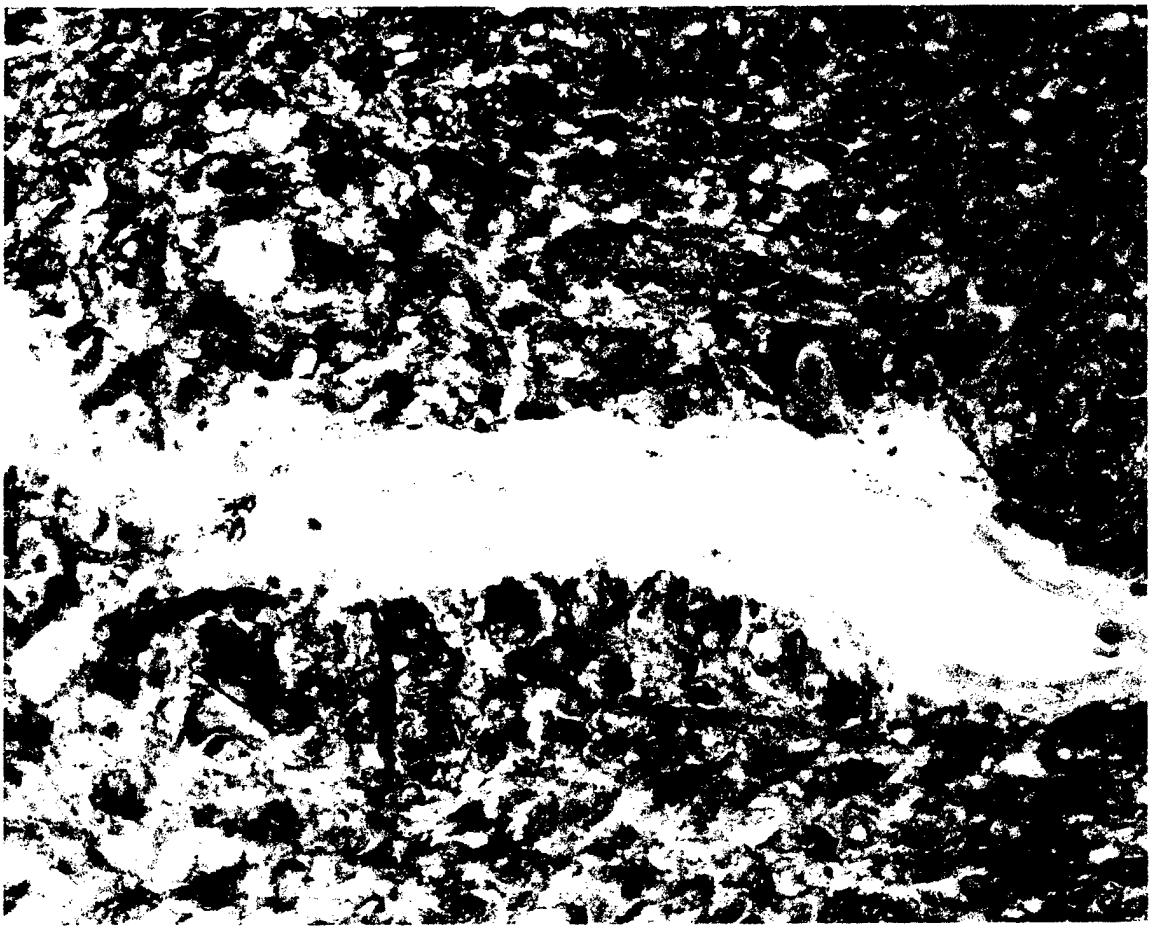

Figure 3.

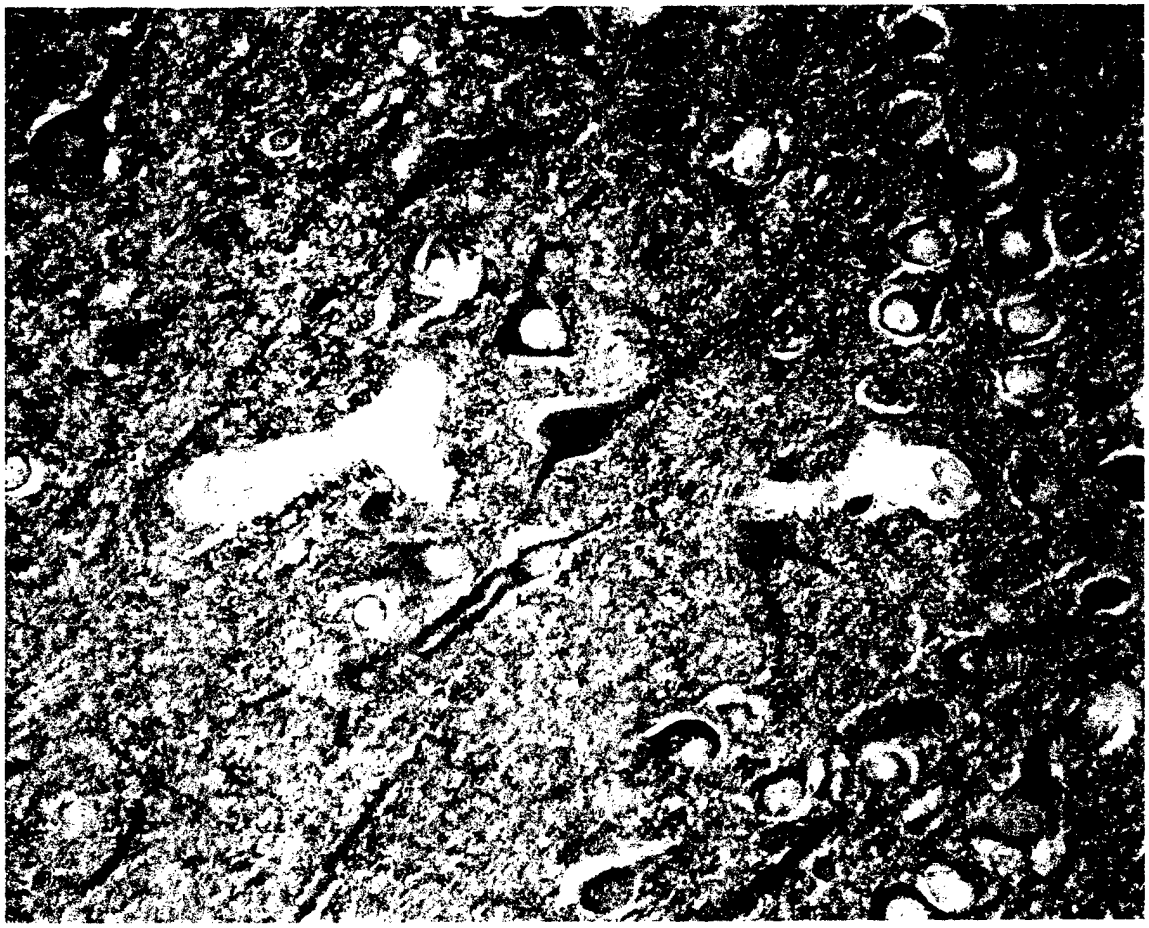

Figure 4.

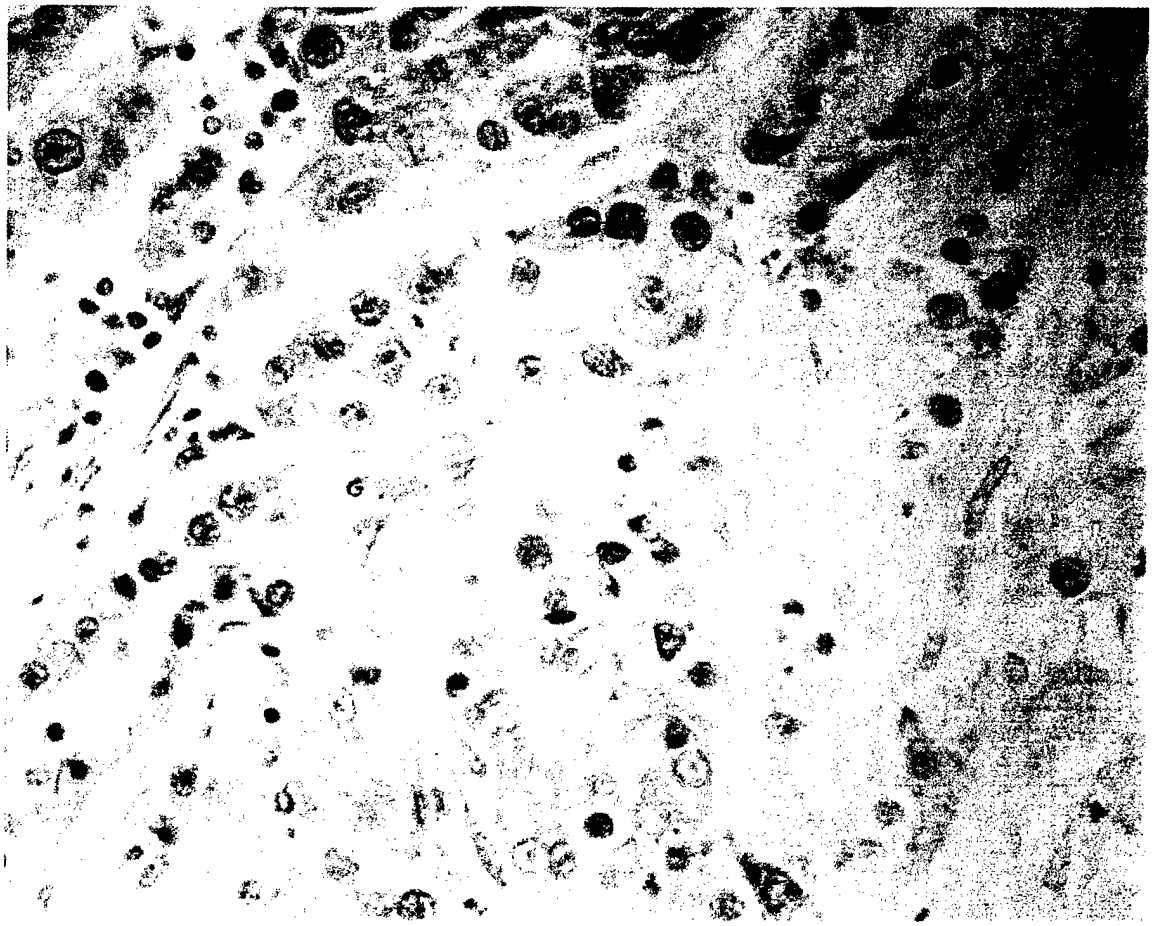

Figure 5.

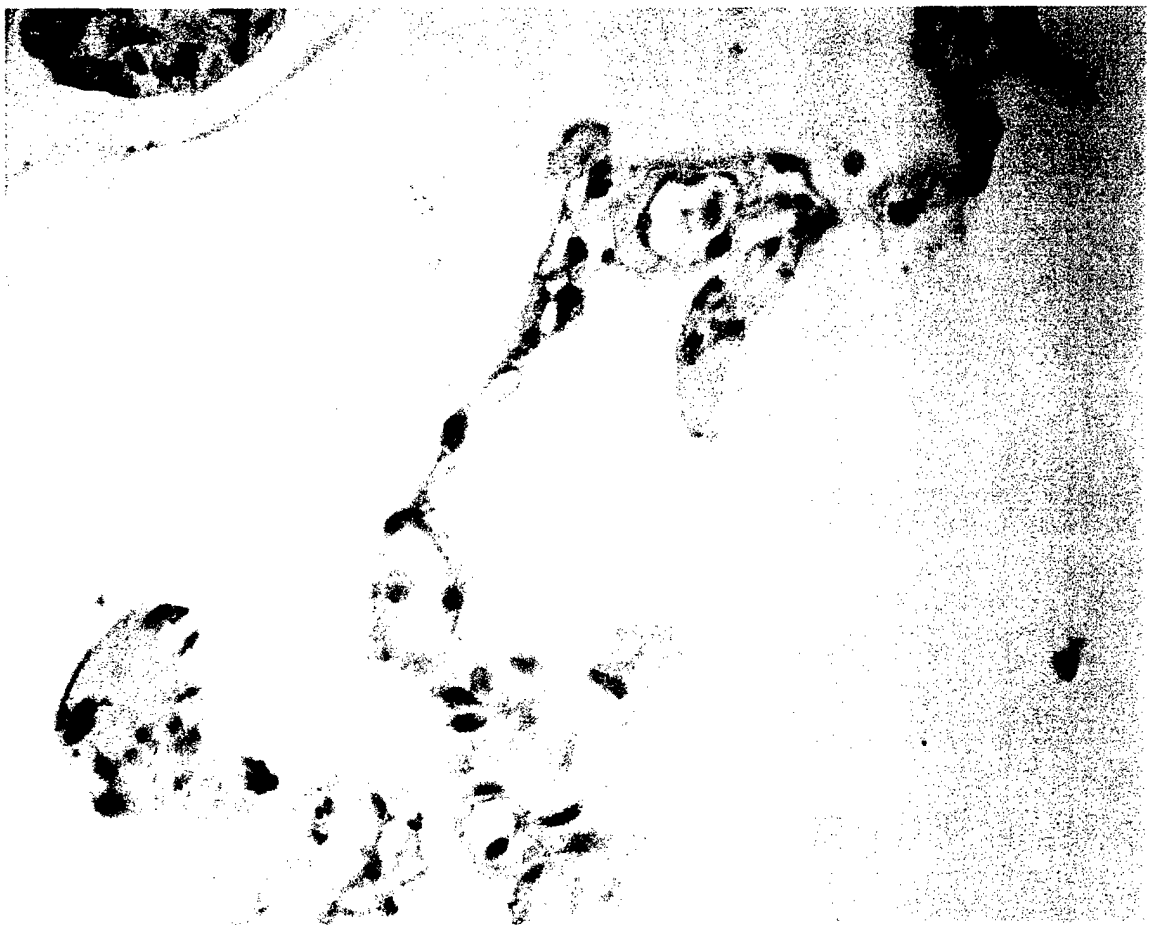

Figure 6.

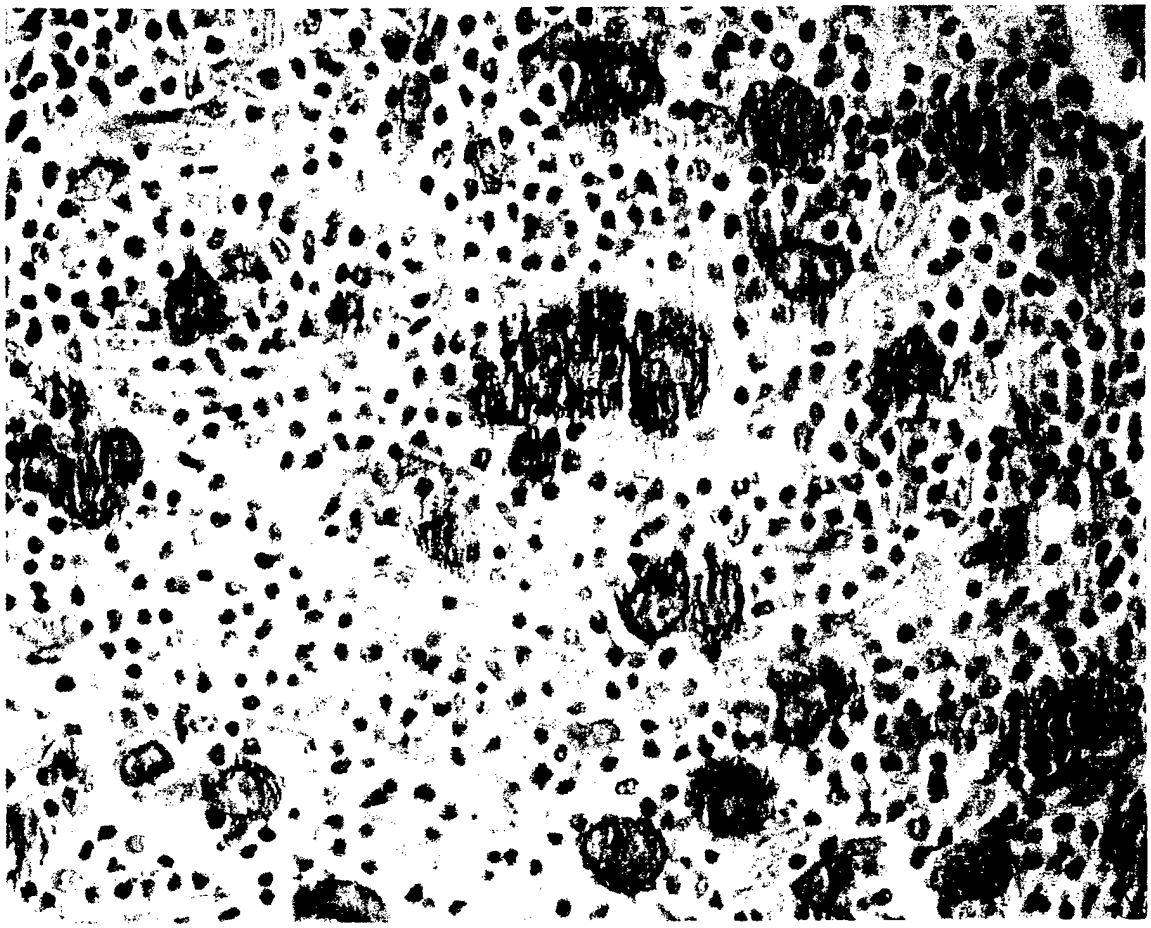

Figure 7.

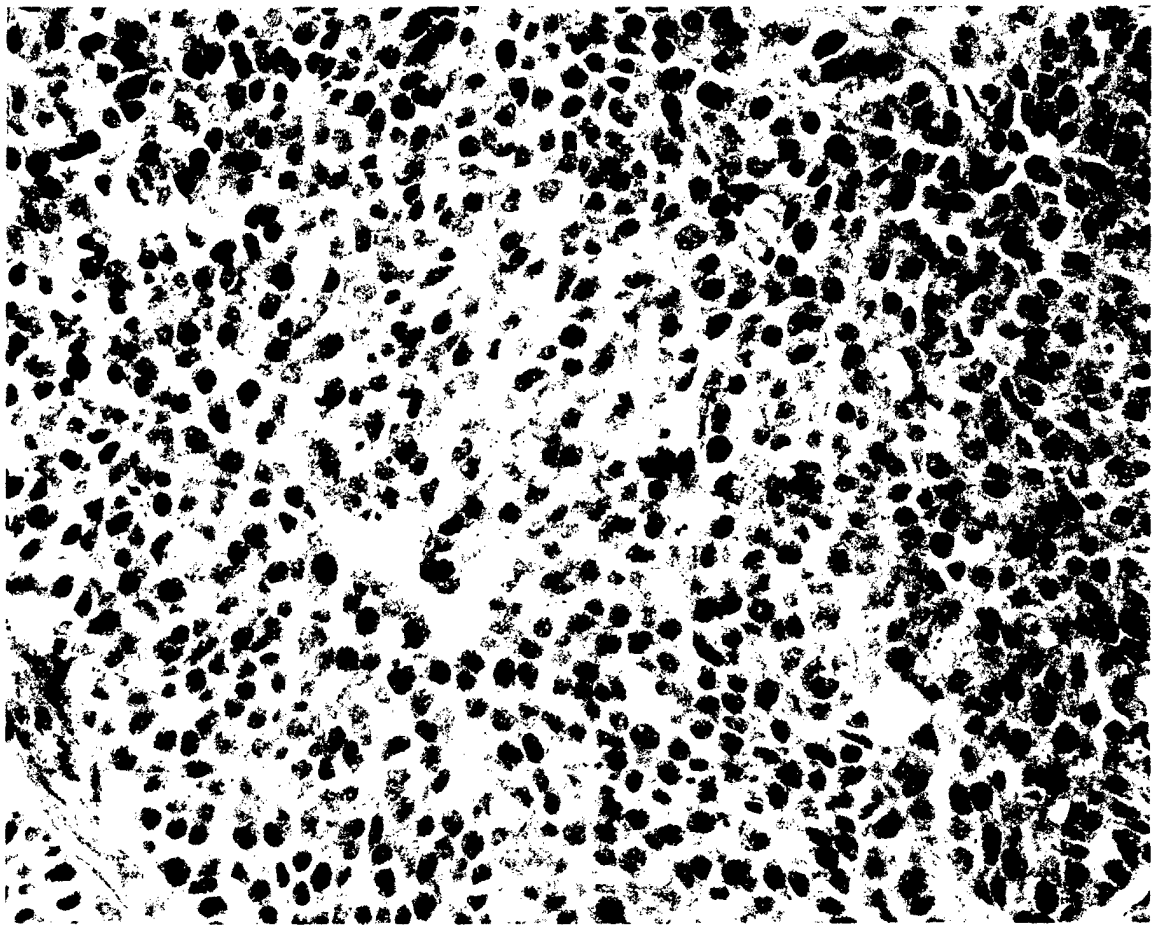

Figure 8.

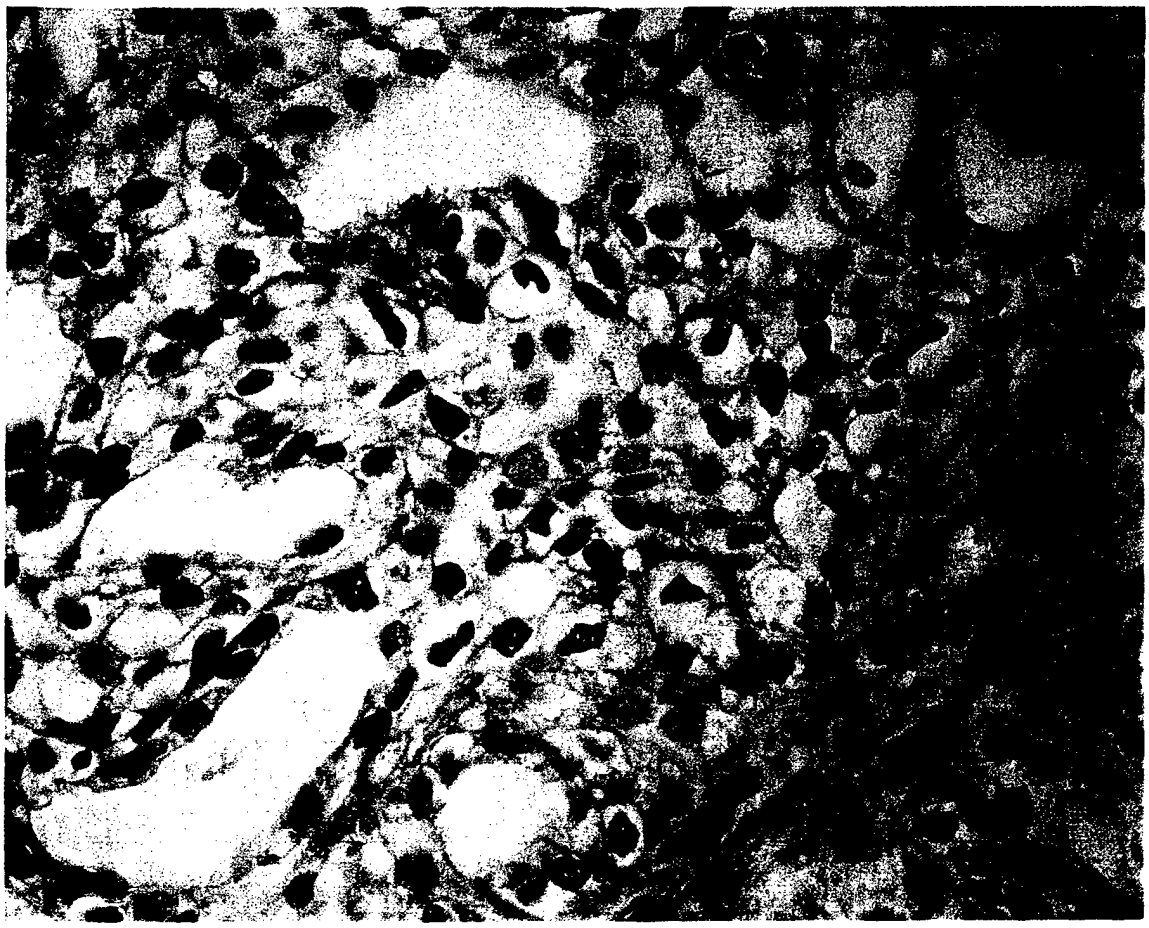

Figure 9.

Figure 10.

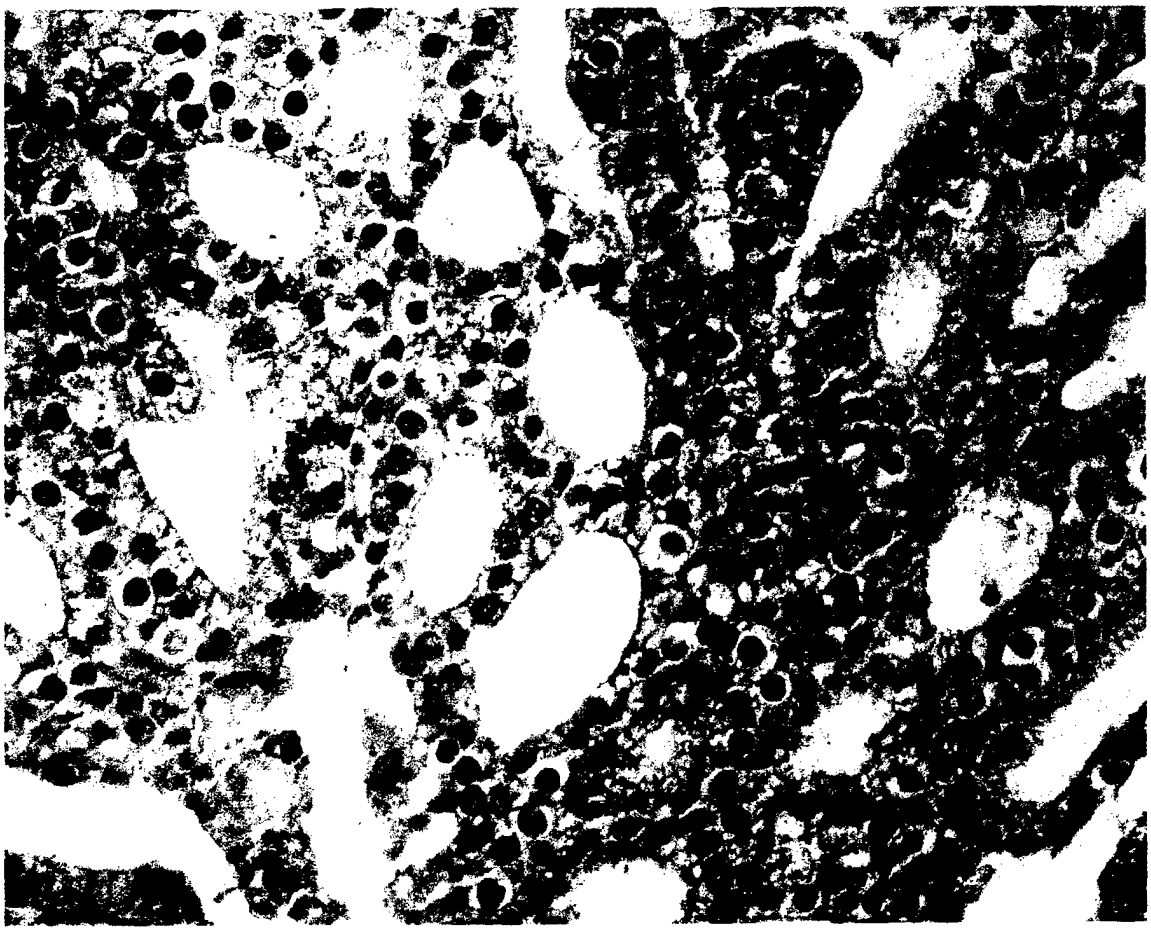

Figure11.

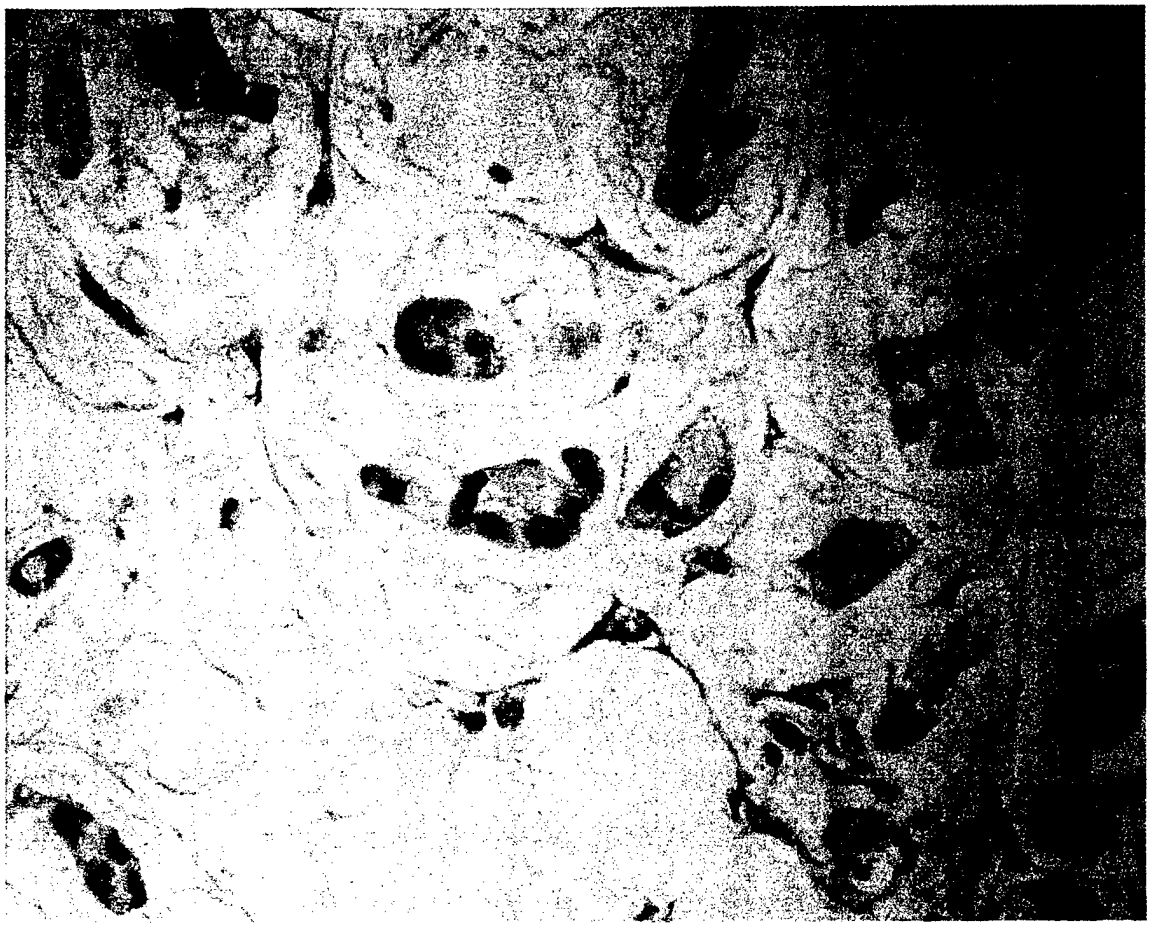

Figure 12.

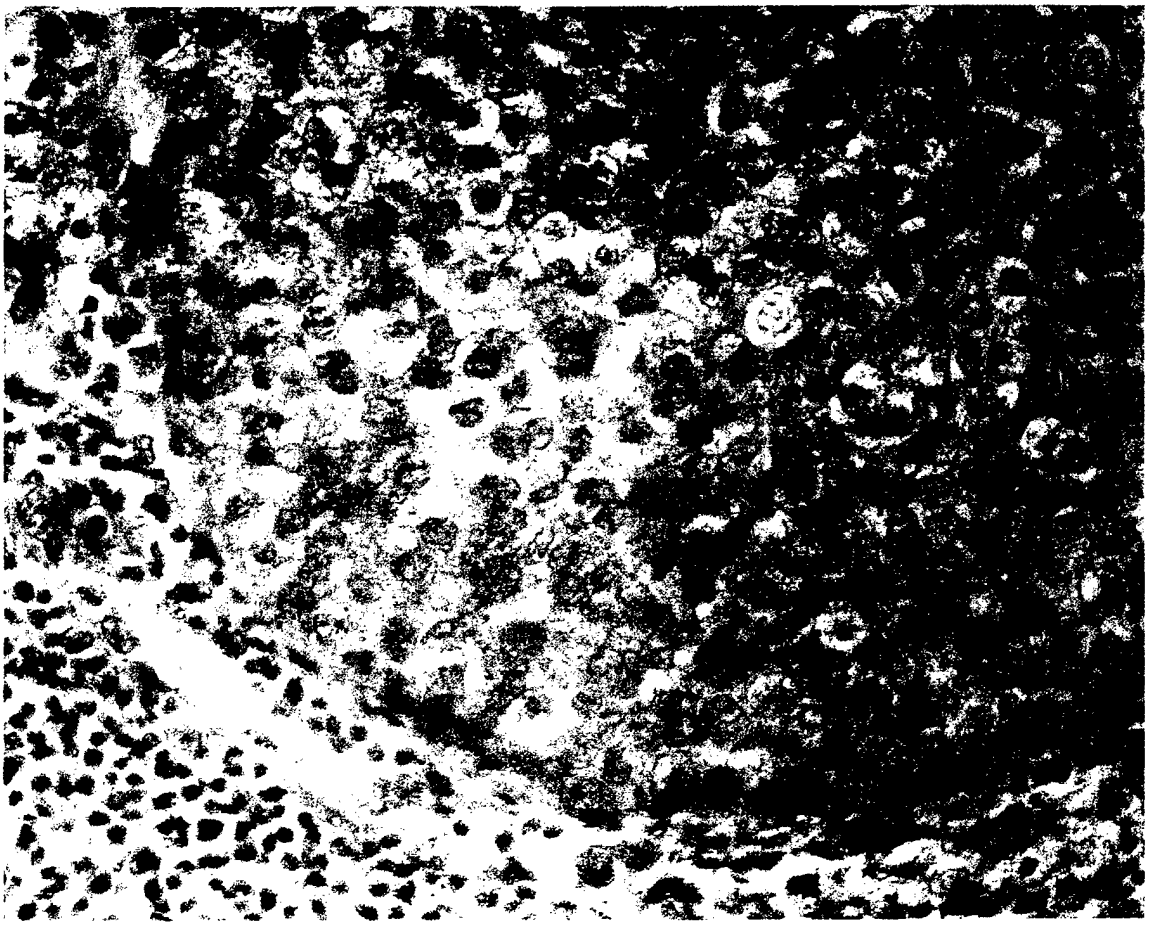

Appendix 8

This dynamic behavior was found in Z-rings in any part of the cell cycle, newly formed rings to rings in the process of septation. ZipA, an *E* membrane protein involved in cell division that colocalizes with FtsZ, r equally dynamic behavior. An isodesmic assembly model derived from studies (Romberg et al., J Biol. Chem. 276:11743) predicts t protofilaments fragment and reanneal upon each GTP hydrolysis eve whether in vivo assembly dynamics are coupled to GTP hydr examined the mutant *ftsZ84*, which has 1/10 the GTPase activity FtsZ in vitro. The FtsZ84 ring showed a 9-fold slower turnover in v that assembly dynamics are determined primarily by GTP hydroly the greatly reduced assembly dynamics, the *ftsZ84* cells divide cell cycle time. This study is the first time that fluorescence photobleaching has been used on bacterial cells.

st
ve
ype
ying
ite of
ormal
y after

2366

Interphase Microtubules Are Stiffer Than Mitotic Cytoplasmic Extracts of *Xenopus* Eggs

abules in

Gaudenz Danuser[1], Phong T. Tran[2], E D Salmo Biomechanics, ETH Zurich, Wagistrasse, Schlieren [2]Department of Microbiology, Columbia University, [3]I University of North Carolina - Chapel Hill

oratory for Switzerland, nt of Biology,

We developed an assay for standardized measureme rigidity by thermal vibration analysis. Microtubule g the ends of *Lytechnicus pictus* sperm flagellar ax surface of a slide-coverslip perfusion chamber. Mi mixtures of pure mammalian brain tubulin (v associated proteins, MAPs) or from clarified *Xe* the interphase or mitosis state of the cell cycle. nucleation site was spatially fixed while the gre vibrate freely. Lateral vibration was rec microscopy and tracked with specialized sof quantify deflection changes as small as *Microscopy*). Based on a model of therr stiffness was calculated from second orde Several positions along the microtubule points. Because of the high degree of au subsequent detection of outlier trajecto for robust distinction between variou follow. Microtubules nucleated from stiffer than those grown in mitoti Nm^2). Our current interphase re *Xenopus* mitotic extracts and p stiffness (both 29×10^{-24} Nm^2). M MAPS were almost threefold taxol depends on the presence microtubules (13×10^{-24} Nm microtubules assembled with NIH GM24364 to EDS.

rotubule flexural as nucleated from fixed to the inner es were grown from without microtubule ytoplasmic extracts in cedure ensured that the d of a microtubule could y video-enhanced DIC ne program allowed us to Danuser et al., 2000, *J.* ing of polymeric rods, the s of the vibration trajectories. ked in order to detect pivotal , not only in tracking but also in were able to pool large data sets ions. The most important results se extracts appear about five times s (158×10^{-24} Nm^2 versus 29×10^{-24} preliminary and will be updated. n tubulin microtubules will have similar les assembled with tubulin plus brain p to 81×10^{-24} Nm^2). The influence of s. Addition of taxol softens pure tubulin le addition of taxol to pure tubulin ad no effect (78×10^{-24} Nm^2). Supported by

2367

Immune Characterizat - and β- Tubulin Isoelectric Variants

Anna Maria Zambito[1], Maria della Misericor lff[2], [1]DPMSC, University of Udine, P.le Santa e, 33100 Italy, [2]NIDDK/LBG, NIH

In higher eukaryotic genes. However, m genes. Previously tubulin from 45-3 isoelectric focus tubulin (more i This yields sh most part, se charge. To developed membran β tubuli more b antibo are u the

and β tubulin monomers are codified by several isoforms exist than can be accounted for by these as 21 variants have been detected using amounts of 6.3 µg in a pH range of 4-7. We have adapted a new od that yields at least 30 isoelectric variants of rat brain α) using only 1 µg of tubulin in the 4.5-5.4 pH range. s and no background on silver staining that are, for the by ~0.02 pH units, equivalent to a difference of a single e isoelectric variants to either α- or β- tubulin, we have d that efficiently transfers the focused variants to PVDF ing identification with N- and C- terminus-directed anti α and onal antibodies. C-terminus directed antibodies detect the ants (4 in α and 6-8 in β), while more N-terminus-directed many more variants but not the most acidic ones. These methods en very small amounts of protein need to be visualized as e.g. in bulin (or other proteins) extracted from membranes.

2

ion of the Tubulin Dimer Is Extremely Slow, Thermodynamically rable and Reversible in the Absence of An Energy Source

l Caplow, Lanette Fee, Department of Biochemistry, University of North na, Campus Box 7260, Chapel Hill, NC 27599-7260

finding that exchange of tubulin subunits between tubulin dimers (αβ + α'β'> + αβ') does not occur in the absence of protein cofactors and GTP hydrolysis ian et al., J. Biol. Chem. 274, 24054, 1999) conflicts with the assumption that ure tubulin dimer and monomer are in rapid equilibrium. This assumption underlies the many physical chemical measurements of the Kd for dimer dissociation. To resolve this important discrepancy we used surface plasmon resonance (SPR) to determine the rate constant for dimer dissociation. The half-time for dissociation of the dimer at 25° was 9.6 hours (h) when the E-site contained GTP, 3.0 h with GDP and 1.3 h with no nucleotide. The effect of nucleotides on the intradimer bond parallels the effect on the interdimer bond in microtubules. Dimer stability was also demonstrated with size exclusion chromatography in which about 80% of 0.2 µM tubulin-GDI d as dimer after 20 h at 25°; tubulin oligomers were also formed. Since 2' esponds to 6.7 half-times for dissociation, only monomer would be presen ciation were an irreversible reaction. The persistence of dimer proves that ion is reversible and that dimerization does not require GTP hydrolysis. T ity of the tubulin dimer indicated by SPR was confirmed with gel exclusi atography of 0.2-2 nM tubulin-GDP; the amount of dimer dissociation sistent with a Kd equal to 1 E-11 M. Finally, assuming that dissociation from the tubulin N-site requires dimer dissociation, our results are in reasc greement with the 16 h half-time for N-site GTP dissociation in vitro (Z nd Caplow, J. Biol. Chem., 252, 1978), and with the 33 h half-life for N-site dissociation in CHO cells (Spiegelman et al., Cell, 12: 587, 1978). 59231.

2369

Interactions of Antimitotic Peptides with T Oligomerization and Polymerization Reaction

Induction of Aberrant

Zobeida Cruz-Monserrate[1], George R Pettit[2], V [1]Screening Technologies Branch, DTP, DC Frederick, [2]Cancer Research Institute, Arizc California at San Diego, Scripps Institution of

I Fenical[3], Ernest Hamel[1], tional Cancer Institute at University, [3]University of graphy

A highly diverse family of naturally occurri tubulin and cause cells to arrest in mitosis. that they all contain modified and/or unusi in their interaction with tubulin, induce oligomers and/or polymers of tubulin. demonstrated by high-performance liq centrifugation, and/or turbidimetry. In (depsi)peptides: the peptide hemias including *Hemiasterella minor*, the dolastatin 15, isolated from the depsipeptide cryptophycin 1, isola cyclic peptide phomopsin A isolate and the bicyclic peptide diazon *angulata*. Most notably, the mul be structurally distinct and to h These differences will be des temperature for initiation of 22°C, for the diazonamide cryptophycin 1 polymers, 0°C

les and depsipeptides bind to ly common structural feature is acids. Typically these agents, mation of structurally aberrant multimeric complexes can be natography, electron microscopy, es we have focused on six of these olated from a number of sponges dolastatin 10 and the depsipeptide *Dolabella auricularia*, the cyclic the cyanobacterium *Nostoc* sp., the ne fungus *Phomopsis leptostomiformis*, , isolated from the ascidian *Diazona* med with each (depsi)peptide appears to rent optimal conditions for its formation. n detail. As an example, the optimum of the dolastatin 10-induced polymer is ner, 37°C, and for the hemiasterlin and

2370

Mutagenesis of Cystei Decreases Microtubule I

in *Saccharomyces cerevisiae* β-Tubulin s *In Vivo* and *In Vitro*

Mohan L. Gupta, Jr.[1], C Richard H. Himes[1], [1]De Sunnyside Ave, Lawre Carolina, Chapel Hill,

Bode[1], Douglas A. Thrower[2], Kerry S. Bloom[2], olecular Biosciences, University of Kansas, 1200 66045, [2]Dept. of Biology, University of North

Previously, we used residues in *Sacchar* found that mutatior phenotypes charac whether this was measure microtu microtubule dyn and *in vitro*. In by a factor of microtubules modulation c wild-type ar microtubul single mic bud site

ted mutagenesis to investigate the roles of cysteine *erevisiae* β-tubulin (Tub2p) (Gupta et al., 2001). We 4 in Tub2p to a serine or alanine residue produced f microtubules with increased stability. To determine the case, we used a GFP-Tub1p fusion construct to namics *in vivo* and purified yeast tubulin to measure *vitro*. The mutations severely dampen dynamics *in vivo* d cells catastrophe and rescue frequencies were decreased amicity was only 1 to 2% of that in wild-type cells, and greater than 90% of the time attenuated. In addition, ubule dynamics throughout the cell cycle was different in it cells. In contrast to wild-type cells which contain 3 to 6 ast majority of unbudded Tub2p-C354 mutant cells contain a that, with very low dynamic character, is still able to locate the slocate the nucleus to the bud neck in the mutants. Proper progression through the cell cycle does require some degree of microtubule dynamicity, however, because the alanine mutant, with even lower microtubule dynamics than the serine mutant, is aneuploid and has decreased viability. Microtubules prepared *in vitro* from Tub2p-C354S tubulin had a catastrophe frequency that was 6% that of wild-type microtubules. Rescue events, which were not observed in wild-type microtubules, occurred in 75% of Tub2p-C354S microtubules. In addition, the shrinkage rate was reduced by a factor of 17 and dynamicity by a factor of 9. Thus, the effects of the mutations on microtubule dynamics are intrinsic to the mutated tubulin molecule.

2371

Occurrence of the β_{II} Isotype of Tubulin in the Nuclei of Cancer Cells

Richard F. Luduena[1], Guadalupe T. Perez[2], I-tien Yeh[2], [1]Biochemistry, Univ. Texas Health Science Center, 7703 Floyd Curl Drive, San Antonio, TX 78229-3900, [2]Pathology, Univ. Texas Health Science Center

We have previously demonstrated that the β_{II} isotype of tubulin is present in the nuclei of rat kidney mesangial cells and several cultured cancer cell lines. We have therefore examined 150 cancers excised from patients, including breast, ovarian, brain, liver, bone, prostate, stomach, colon, pancreatic and other cancers. We have found nuclear β_{II} in 80% of the cancers, including 14% of liver, 29% of brain, 67% of pancreas, 77% of ovarian, 89% of bone, 93% of stomach, 94% of breast, and 100% of prostate and colon cancers. Nuclear β_{II} occurs in varying intensities, ranging from very weak to very strong staining. A single cancer in a given patient can demonstrate more than one pattern. Metastases often contain nuclear β_{II}. Nuclear β_{II} also occurs in otherwise normal cells that are adjacent to the tumor. For example, in colon cancer, one group of normal epithelial cells may be very rich in nuclear β_{II} while an adjacent group of these cells has none. In stomach and breast cancer metastases to lymph nodes, the lymphocytes adjacent to the metastatic tumor cells are often very rich in nuclear β_{II} while those more distant have none. These findings imply that tumor cells may induce adjacent cells to localize β_{II} to their nuclei. Our results suggest that nuclear β_{II} may be useful in cancer diagnosis and that it may play an important role in the biology of tumor cells. (Supported by grants DAMD17-98-1-8246 from the U.S. Army Breast Cancer Research Program and AQ-0726 from the Welch Foundation to RFL).

2372

Nuclear β_{II}-Tubulin in Cultured Cancer Cells: Subnuclear Localization and the Effects of Anti-Tubulin Drugs

Keliang Xu, Richard F. Luduena, Biochemistry, Univ. Texas Health Science Center, 7703 Floyd Curl Drive, San Antonio, TX 78229-3900

We have previously shown that the β_{II} isotype of tubulin is located in the nuclei of cultured rat kidney mesangial cells. We have investigated its cellular and subcellular localization in the following cancer cell lines: MCF-7 and MDA breast cancer, C6 and T98G glioma, and HeLa. We find that nuclear β_{II} in these cells is in the form an $\alpha\beta_{II}$ dimer capable of binding to fluorescent derivatives of both colchicine and taxol. Co-localization of β_{II} with the nucleolar marker nucleolin indicates that β_{II} is largely localized in the nucleoli of these cells. Taxol causes expulsion of β_{II} from the nuclei of C6 cells in a dose-dependent manner, often with apoptosis. β_{II} also forms microtubule bundles in the cytoplasm. Pre-treatment of C6 cells with cycloheximide, an inhibitor of protein synthesis, does not inhibit, but rather augments, the taxol-induced expulsion of β_{II} from the nuclei. This indicates that the β_{II} that appears in cytoplasmic bundles in these cells comes from the nuclei rather than from de novo synthesis. Treatment of C6 cells with either colchicine or nocodazole causes apoptosis but no expulsion of nuclear β_{II}. Colchicine favors binding to the $\alpha\beta_{IV}$ dimer. We measured binding of nocodazole to the $\alpha\beta_{II}$, $\alpha\beta_{III}$ and $\alpha\beta_{IV}$ dimers and found that the Kd's for the primary binding site were, respectively, 0.52, 1.54, and 0.29 μM, indicating a higher affinity for $\alpha\beta_{IV}$. It may be that drugs (such as taxol) that favor interaction with $\alpha\beta_{II}$ are more able to expel β_{II} from the nucleus. (Supported by grants DAMD17-98-1-8246 from the US Army Breast Cancer Research Program and AQ-0726 from the Welch Foundation).

2373

Elevated βIII Tubulin In Cancer And Drug-Resistant Cells And Selective Conformational Effect Of Phomopsin A On The αβIII Tubulin Dimer

Asish R. Chaudhuri[1], Patricia M. Schwarz[1], Gilberto R. Carrizales[2], Susan L Mooberry[2], Richard F Luduena[1], [1]Biochemistry, Univ. TX. Hlth. Sci. Ctr. at San Antonio, 7703 Floyd Curl Drive, San Antonio, TX 78229, [2]Physiology and Medicine, Southwest Foudation for Biomedical Research

Both α and β-subunits of tubulin exist in several isoforms that are expressed differently in our tissues; αβII and αβIV are widespread while αβIII is restricted mainly to neurons although it is elevated in cancer and drug-resistant cells. Thus an ideal anti-tumor drug would be one that would bind selectively to αβIII. Unfortunately, drugs such as taxol and vinblastine bind strongly to αβII and αβIV and least well to αβIII. Here, we have studied the expression of βII and βIII in eight cell lines including normal and cancer cells and have searched for the drug that has a major effect on αβIII. We find that βIII is expressed in all the cancer cells but not in normal smooth muscle (A-10) cells, while βII is expressed in most of these cell lines. We examined the binding of phomopsin A to αβIII and αβII using footprinting. We found a specific cysteine-containing domain in both α- and β-subunits of αβIII that allows phomopsin A to bind selectively to that site. We also found that phomopsin A increased the affinity of colchicine for αβII and αβIII 4-fold and 12-fold, respectively. These data suggest that phomopsin A has a much larger effect on the conformation of αβIII than it has on that αβII. Mapping of the binding sites of phomopsin A as well as the domains affected by conformational changes will help in designing more specific and potent drugs against αβIII. (Supported by NIH grant CA26376 (RFL), US Army BCRP grant DAMD 17-98-1-8246 (RFL) and NIH grant CA70743 (SLM)).

2374

Interaction of actin and the βIV isotype of tubulin in normal and transformed cells

Veena Prasad[1], Vivek Kasinath[1], Ross B Clements[1], Rachel Leal[2], Susan L Mooberry[3], Richard F Luduena[1], [1]Biochemistry, UTHSC at San Antonio, 7703 Floyd Curl Drive, San Antonio, TX 78229, [2]Southwest Foudation for Biomedical Research, [3]Physiology and Medicine, Southwest Foudation for Biomedical Research

The tubulin molecule is an α/β heterodimer. Both α and β consist of numerous isotypes that have been highly conserved in vertebrate evolution, suggesting that they may perform specific functions. We have previously shown that, when cultured rat kidney mesangial cells are treated so as to disrupt the microtubules, the βIV isotype, but not the βI or βII isotypes, co-localizes with actin filaments. Here we show that in non-extracted cells, the βIV isotype co-localizes with actin stress fibers. In cultured A10 smooth muscle cells, the βIV isotype is in a configuration resembling that of actin stress fibers. We have also examined the distribution of tubulin isotypes and actin in three cancer cell lines: HeLa, C6 glioma, and MCF-7 breast cancer cells. We have found no co-localization of actin with either βI, βII, or βIII. However, there is limited co-localization of βIV and actin, particularly in mitotic cells, where co-localization is seen in mitotic spindles and mid-bodies. It appears that βIV may interact with actin filaments in certain normal cells, but this interaction is less likely to happen in transformed cells. (Supported by grants DAMD17-98-1-8246 from the U.S. Army Breast Cancer Research Program and AQ-0726 from the Welch Foundation to RFL and NIH grant CA70743 to. SLM).

2375

A Quantitative Evaluation of the Effects of Inhibitors of Tubulin Assembly on Assembly Induced by Discodermolide, Epothilone B, and Paclitaxel

Donnette A Dabydeen[1], Gordon J Florence[2], Ian Paterson[2], Ernest [1]Screening Technologies Branch, DTP, DCTD, National Cancer In Frederick, [2]Department of Chemistry, University of Cambridge, United K

Although a number of investigators have shown that paclitaxel-ind ilin assembly can be inhibited by various inhibitors of assembly, there h ittle systematic evaluation of these inhibitory effects. Moreover, there en no significant studies with discodermolide and epothilone B, two cently described natural products that are even more potent than paclit hancers of assembly. We have selected five inhibitors of assemb amine in combination with the assembly inducers. These are nocodazole tastatin A-4, maytansine, halichondrin B, and dolastatin 15, all selecte e they that have little tendency to cause aberrant tubulin polymerizatio is associated with increased turbidity. We are obtaining IC_{50} values for ents with and without the three inducing drugs at 30°C and with the in ugs at 0°C. In initial experiments at 30°C, much higher IC_{50} values for astatin A-4 than for maytansine were obtained with inducing drugs as c with the reaction condition without inducing drug. One possibility that ial results seem to exclude is that a constant inhibitor IC_{50} value wou ained if drugs were evaluated under reaction conditions with identical tu cal concentrations.

2376

Analysis of the Antitubulin Activities of Thi Benzofuran and Indole Derivatives

M. Katherine Jung[1], Karl O. Hessian[2], Jason n[2], Pascal Verdier-Pinard[3], Bernard L. Flynn[2], Ernest Hamel[3], [1]SAIC-Fr National Cancer Institute at Frederick, Frederick, MD 21702, [2]Dept emistry, Australian National Univeristy, Australia, [3]Screening Techno anch, DTP, DCTD, National Cancer Institute-Frederick

Pinney and collaborators synthesized a ophene compound with structural similarity to known antimicrotubule with the goal of identifying more potent antitumor agents (Bioorganic dicinal Chemistry Letters 9, 1081-1086, 1999). This initial compound nly a low affinity for tubulin, but was cytotoxic to human solid tumor cell n an effort to improve on the antitumor potential of this agent, we synthes ries of analogs, in some cases replacing the benzothiophene moiety wit rent aromatic group. Several of these compounds proved to be more an the initial compound both as inhibitors of tubulin polymerization an otoxic agents against human tumor cells. These compounds have struc ogy to the natural product combretastatin A-4. In the newly synthesized ids, the simple two-carbon bridge between the phenyl rings of combretast was replaced by an aromatic moiety consisting of a benzothiophene, thic enzofuran or indole group. The activities of the new agents were therefc ared to those of combretastatin A-4. Several were as active as, or more han, combretastatin A-4 as inhibitors of tubulin polymerization. How e of the compounds in this series of analogs was as active as combretast either as an inhibitor of colchicine binding to tubulin or as a cytotoxic These data allow us to carry out a structure-activity analysis that may our understanding of the interactions of inhibitory agents with tubulin.

2377

Characteriz a Fluorescent Vinca Alkaloid (Bodipy-Vinblastine) to Probe Drug and Apoptosis

Sharon Lo n J. Correia[2], [1]School of Nursing and Dept. of Biochemistry, University ssippi Medical Center, 2500 N. State St., Jackson, MS 39216, [2]Dept. B ry, University of Mississippi Medical Center

Antimi gs share a common mechanism of action, suppressing microtubule dynar arresting cells in metaphase, processes that frequently lead to apor though vinca alkaloids induce tubulin heterodimers to form spiral pol ey also preferentially interact with microtubule (MT) ends, induce

Appendix 9

APPENDIX 9

Figure 1. RT-PCR analysis of the expression of β–tubulin isotypes in breast cancer cells. Aliquots of total RNA (1μg) from MCF-7 breast cancer cells were incubated with AMV reverse transcriptase in the presence of oligo (dT) primer at 37 ^{0}C for 1 h. Samples were subsequently subjected to 30 cycles of PCR reaction using primers specific for β_I, β_{II}, β_{III}, β_{IVa}, and β_{IVb} as described in the preliminary studies section. The PCR products were run on a 1% agarose gel. The gel was stained with ethidium bromide for visualization. Lane 1, Markers; lane 2, β_I ; lane 3, β_{II}; lane 4, β_{III} ; lane 5, β_{IVa}; lane 6, β_{IVb}.

Figure 2. Co-localization of β_{IV}-tubulin and actin stress fibers in cultured MCF-7 breast cancer cells. MCF-7 cells were fixed in paraformaldehyde, blocked, and β_{IV} visualized (**A**) by indirect immunofluorescence. **B**. Actin stained with Bodipy-phalloidin. **C**. Superimposition of A and B. Note that almost the only localization between actin and β_{IV} is in the mitotic spindle.

Figure 3. Co-localization of β_{II}-tubulin and actin stress fibers in cultured MCF-7 breast cancer cells. MCF-7 cells were fixed in paraformaldehyde, blocked, and β_{II} visualized (**A**) by indirect immunofluorescence. **B**. Actin stained with Bodipy-phalloidin. **C**. Superimposition of A and B. Note very little overlap between actin and β_{II}.

Figure 4. Effect of β_I transfection on adhesion in MCF-7 cells. One group of MCF-7 cells were transfected with β_I-tubulin. Another group (mock-transfected) was transfected with the vector lacking the gene for β_I. At the indicated times, cells were plated in wells on a 96-well plate. The wells were washed with phosphate-buffered saline and then fixed with formaldehyde prior to staining with methylene blue. Excess stain and loose cells were removed by four washes with borate buffer. Methylene blue is a marker for cells. The better the cell adherence to the substrate, the greater the methylene blue staining. The absorbance at 630 nm, due to methylene blue, was determined in a 96-well plate reader. Note that at 480 and 540 minutes, the β_I-transfected cells demonstrated much greater adherence than did the mock-transfected cells.

Figure 5. Effect of combretastatin A 4-phosphate (CA-4-P) on adhesion in β_I-transfected and mock-transfected MCF-7 cells. MCF-7 cells were either transfected with β_I-tubulin or mock-transfected as in Figure 4. One aliquot of each group of cells was treated with 500 nM CA-4-P. Cell adhesion was measured as in Figure 4.

Figure 6. Presence of free radicals in cultured cells. Cell extracts were treated with the indicated concentrations of 2,7-dichlorofluorescein diacetate, which fluoresces in the presence of H_2O_2; the latter is produced from superoxide anion ($O_2^{-}\bullet$) by the action of superoxide dismutase. The fluorescence was determined.

Figure 7. Lymph node with metastatic breast carcinoma. A lymph node excision was treated with antibody to β_{II} and stained with immunoperoxidase. Methyl green was used as the counter-stain. Cytoplamic and nuclear staining is seen for β_{II}-tubulin in tumor cells. Adjacent lymphocytes also show weak nuclear staining. Note that normally lymphocytes stain hardly at all for β_{II} (original magnification 400X)

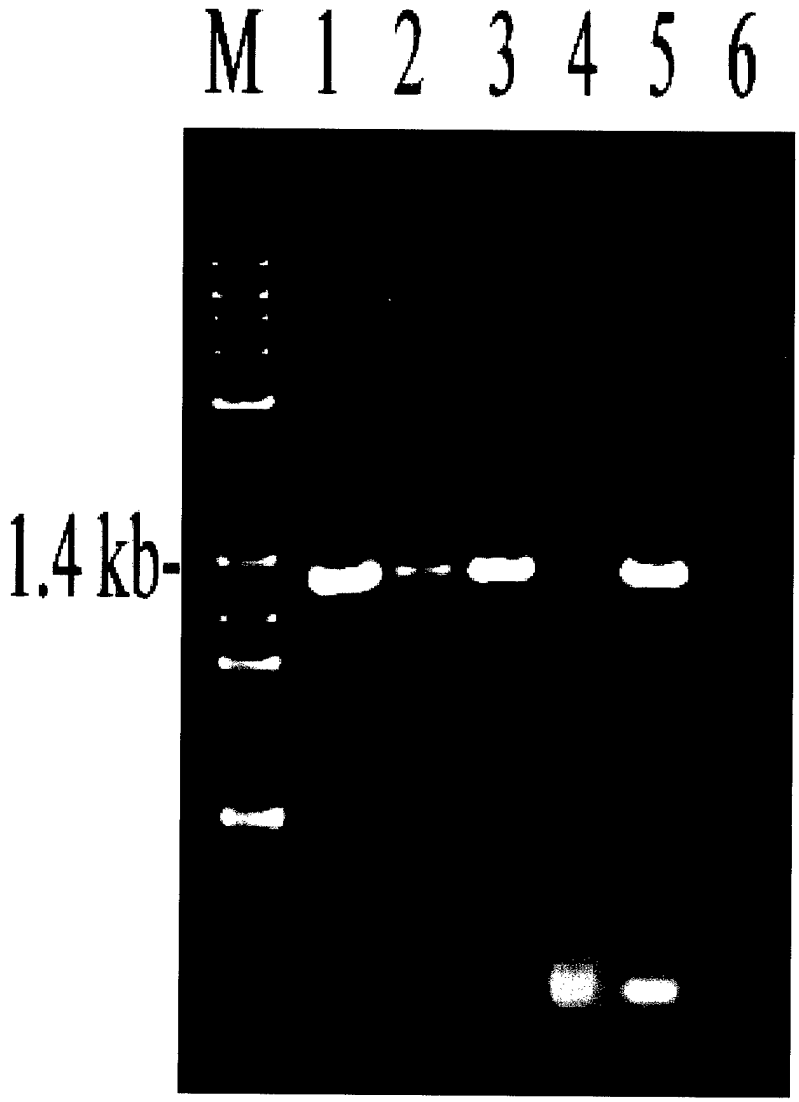

Figure 1

Figure 2

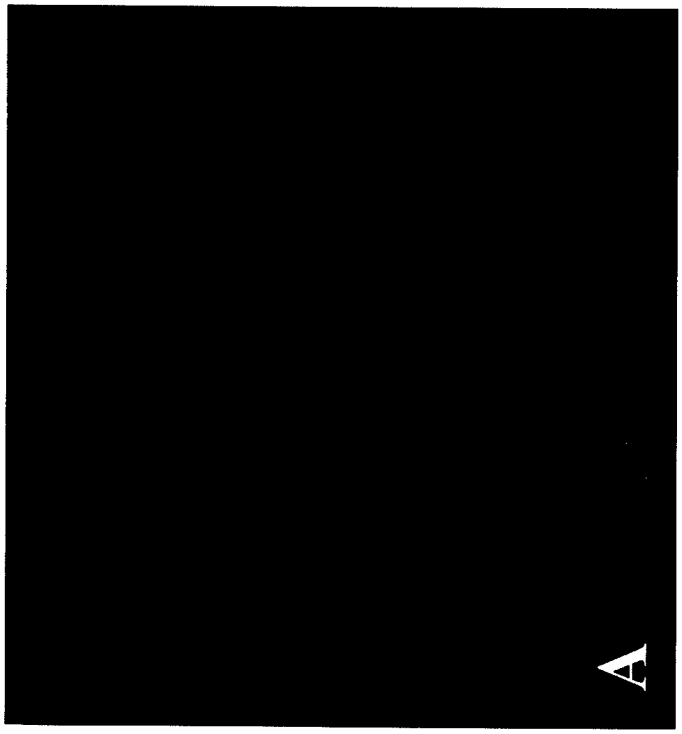

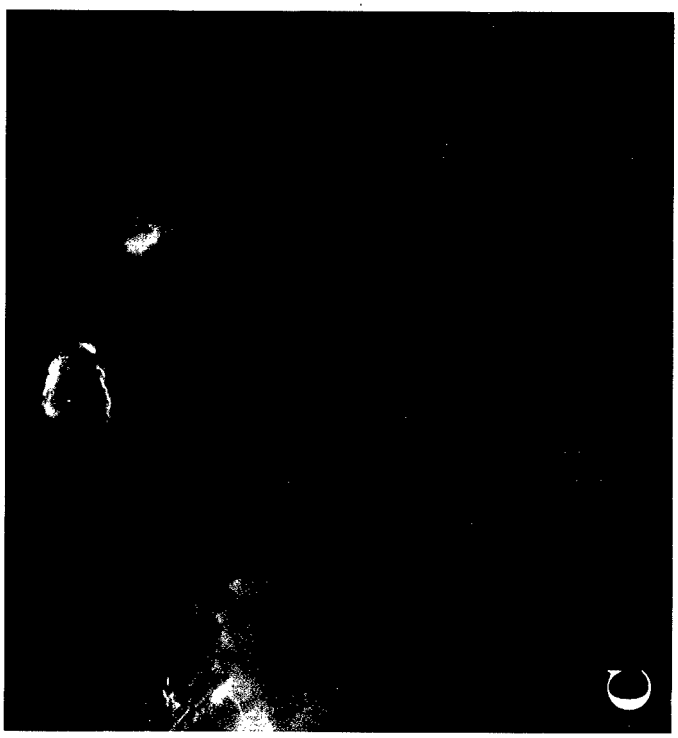

Figure 3

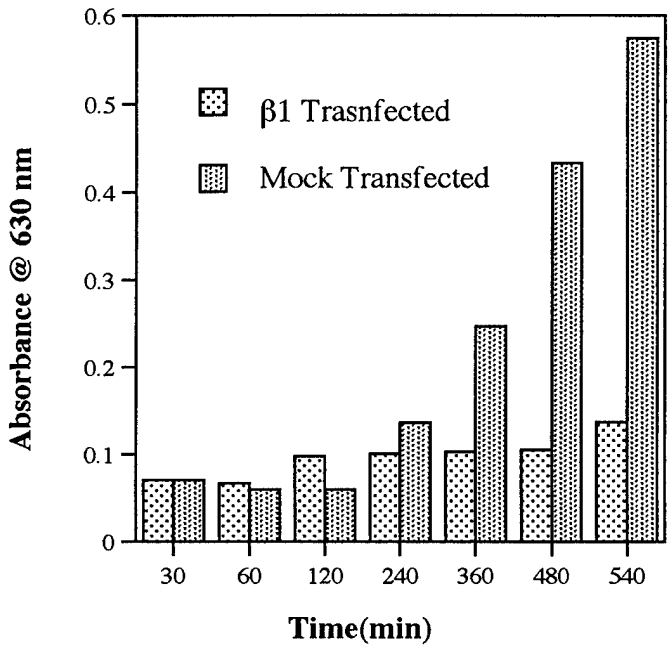
0.6
0.5
0.4
0.3
0.2
0.1
0
β1 Trasnfected
Mock Transfected
Absorbance @ 630 nm
30
60
120
240
360
480
540
Time(min)

Figure 4

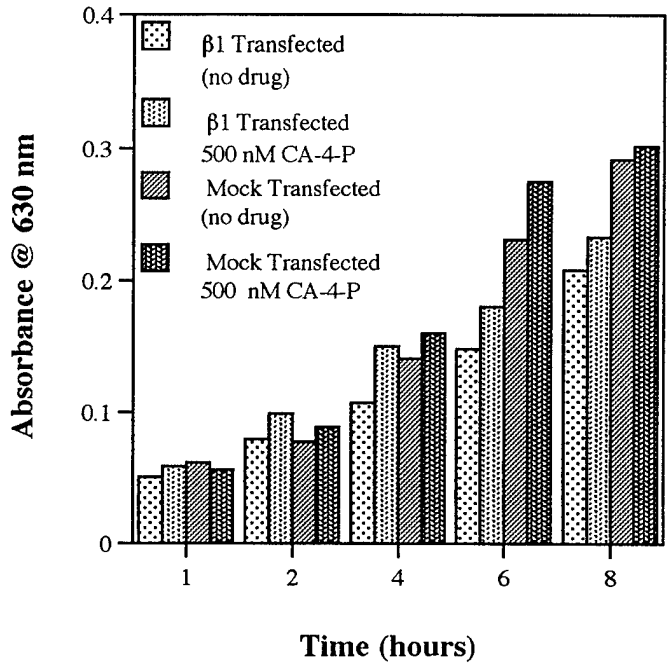
0.4
0.3
0.2
0.1
0
Absorbance @ 630 nm
β1 Transfected
(no drug)
β1 Transfected
500 nM CA-4-P
Mock Transfected
(no drug)
Mock Transfected
500 nM CA-4-P
1
2
4
6
8
Time (hours)

Figure 5

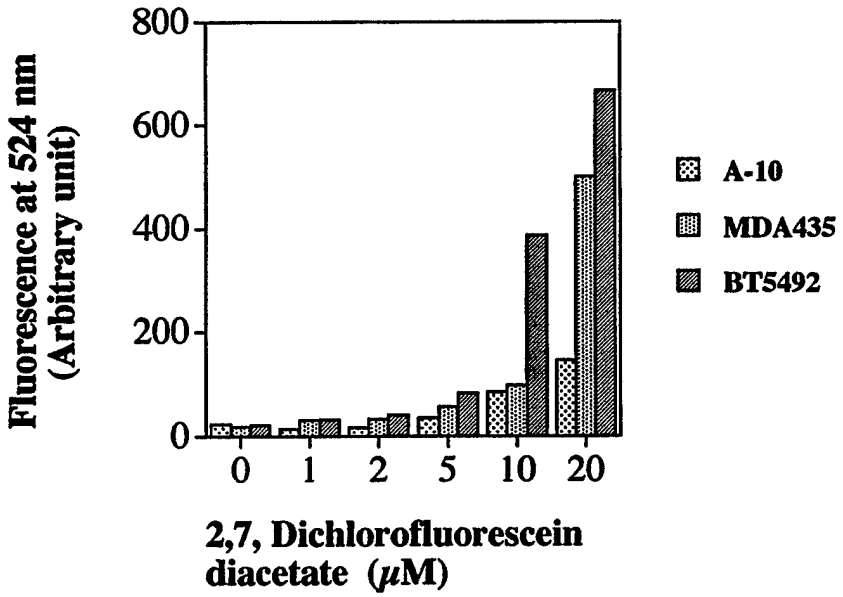
Fluorescence at 524 nm
(Arbitrary unit)
800
600
400
200
0
0
1
2
5
10
20
2,7, Dichlorofluorescein
diacetate (μM)
A-10
MDA435
BT5492

Figure 6

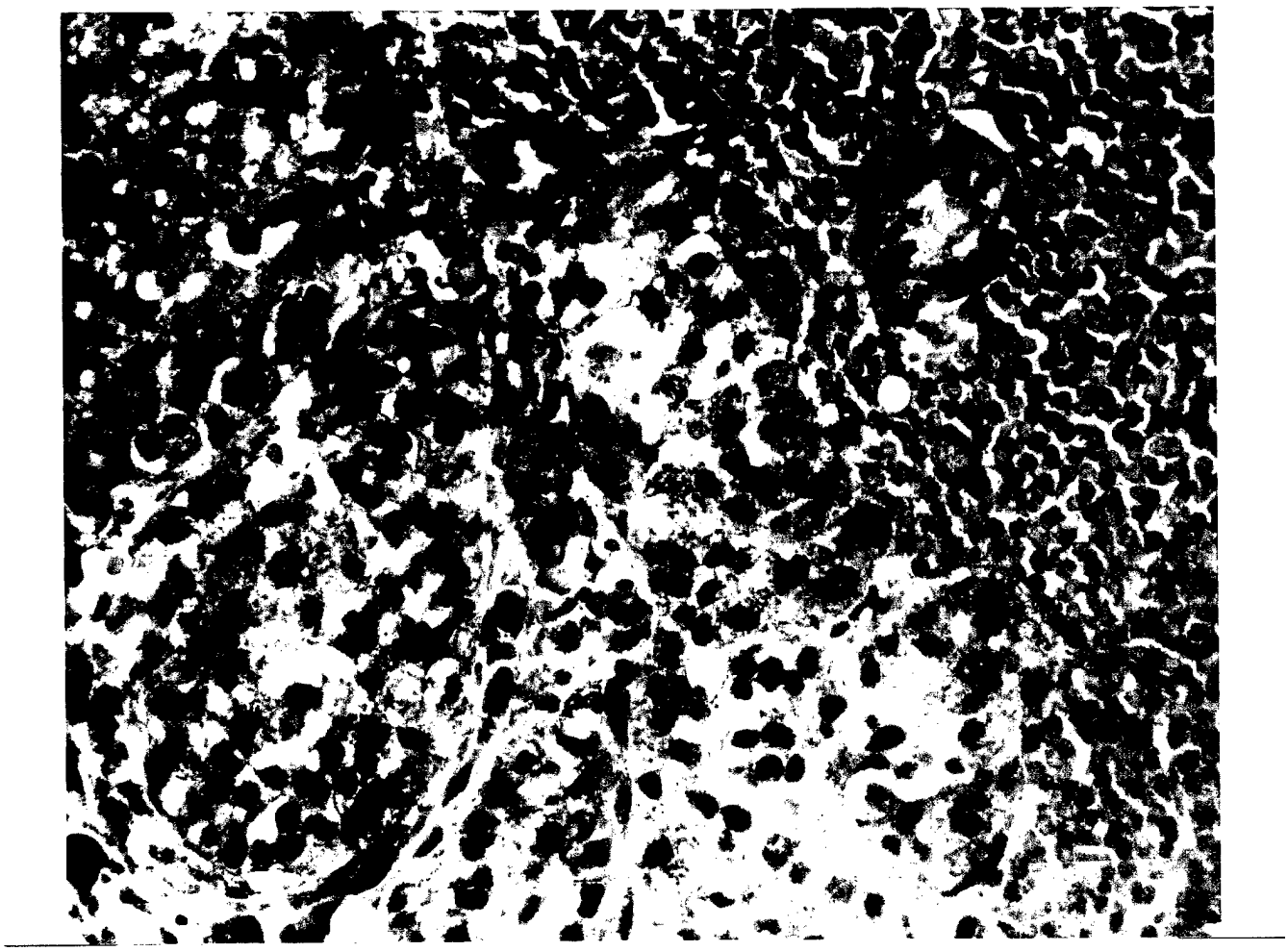

Figure 7